FACHBEREICH PHYSIK
JOHANNES GUTENBERG-UNIVERSITÄT MAINZ

# Monte Carlo Simulations of Potts Glasses

DISSERTATION
ZUR ERLANGUNG DES GRADES
"DOKTOR DER NATURWISSENSCHAFTEN"

vorgelegt von
**Claudio Brangian**

Januar 2002

# Abstract

A complete understanding of the glass transition is still a challenging problem. Some researchers attribute it to the (hypothetical) occurrence of a static phase transition, others emphasize the dynamical transition of mode coupling-theory from an ergodic to a non ergodic state. A class of disordered spin models has been found which unifies both scenarios. One of these models is the $p$-state infinite range Potts glass with $p > 4$, which exhibits in the thermodynamic limit both a dynamical phase transition at a temperature $T_D$, and a static one at $T_0 < T_D$. In this model every spins interacts with all the others, irrespective of distance. Interactions are taken from a Gaussian distribution. In order to understand better its behavior for finite number $N$ of spins and the approach to the thermodynamic limit, we have performed extensive Monte Carlo simulations of the $p = 10$ Potts glass up to $N = 2560$. The time-dependent spin-autocorrelation function $C(t)$ shows strong finite size effects and it does not show a plateau even for temperatures around the dynamical critical temperature $T_D$. We show that the $N$-and $T-$dependence of the relaxation time for $T \geq T_D$ can be understood by means of a dynamical finite size scaling Ansatz. The behavior in the spin glass phase down to a temperature $T = 0.7$ ($\approx 60\%$ of the transition temperature) is studied. Well equilibrated configurations are obtained with the parallel tempering method, which is also useful for properly establishing static properties, such as the order parameter distribution function $P(q)$. Evidence is given for the compatibility with a one step replica symmetry breaking scenario. The study of the cumulants of the order parameter does not permit a reliable estimation of the static transition temperature. The autocorrelation function at low $T$ exhibits a two-step decay, and a scaling behavior typical of supercooled liquids, the time-temperature superposition principle, is observed. In this region the dynamics is governed by Arrhenius relaxations, with barriers growing like $N^{1/2}$. We analyzed the single spin dynamics down to temperatures much lower than the dynamical transition temperature. We found strong dynamical heterogeneities, which explain the non-exponential character of the spin autocorrelation function. The spins seem to relax according to dynamical clusters. The model in three dimensions tends to acquire ferromagnetic order for equal concentration of ferro- and antiferromagnetic bonds. The ordering has different characteristics from the pure ferromagnet. The spin glass susceptibility behaves like $\chi_{SG} \propto 1/T$ in the region where a spin glass is predicted to exist in mean-field. Also the analysis of the cumulants is consistent with the absence of spin glass ordering at finite temperature. The dynamics shows multi-scale relaxations if a bimodal distribution of bonds is used. We propose to understand it with a model based on the local spin configuration. This is consistent with the absence of plateaus if Gaussian interactions are used.

# Contents

# Chapter 1

# Introduction

A complete understanding of the glass transition of a fluid and what structural features really distinguish the solid glass from the liquid from which it was formed, are still challenging problems. If a liquid can be cooled below its melting temperature $T_m$ without the occurrence of crystallization, it becomes metastable with respect to the crystalline phase. A substance that remains liquid below its melting temperature is called supercooled (a recent comprehensive review can be found in (Debenedetti, 1996)). Good glass formers can be kept supercooled and their properties can be studied over a large temperature range. Upon further cooling, in a rather narrow temperature range, the viscosity $\eta(T)$ and other measures of the structural relaxation increase typically by several orders of magnitude. The relaxation time then exceeds the timescale of the experiment. The fluid falls out of (metastable) equilibrium and the structure gets arrested in an amorphous solid state. This phenomenon goes under the name of glass transition (Jäckle, 1986). A glass transition temperature $T_g$ can be defined when the viscosity reaches a certain value, before the supercooled fluid vitrifies (see the schematic representation in Fig. 1.1). The phenomenology in glass forming materials is general.

However it is yet not clear how to interpret these observations within a general theoretical framework. One theory (Gibbs and DiMarzio, 1958) postulates the existence of a genuine static phase transition at a temperature $T_0$, located extrapolating to zero the excess of entropy in the supercooled region with respect to the one of the corresponding crystalline state (the latter is essentially due to vibrational excitations). This theory has been formulated for polymer melts, but has been taken as general for the phenomenology of glasses. The entropy difference $\Delta S$ has been named configurational entropy. The theory has been further developed (Adam and Gibbs, 1965) to link static and dynamical properties through the concept of cooperatively rearranging regions. These are a group of molecules that can rearrange into a different configuration independently of the environment and as a result of an energy fluctuation. The relaxation time $\tau$ is related to the timescale associated to the rearrangement of these regions. The theory of Adam and Gibbs connects $\tau$ to the configurational entropy, leading to the result $\tau \propto \exp(C/T\Delta S)$. A functional form $\Delta S \propto (1 - T_0/T)$, valid from calorimetric measurements in many simple liquids, produces then $\tau \propto \exp[A/(T - T_0)]$. This formula has the same structure of the empirical Vogel-Fulcher law, which is a popular description of the slowing down near $T_g$. There is up to now no direct evidence for the occurrence of this static phase transition, and experimentally the configurational

entropy cannot be followed completely to zero because vitrification occurs.

Probably the most successful approach is mode coupling theory (MCT) (Götze, 1989). This microscopic description for the dynamics of density fluctuations in supercooled fluids in its idealized form leads to a sharp transition from an ergodic to a non-ergodic behavior at a critical temperature $T_c > T_g$, as it seems the case for realistic models. It is found that the predicted power law divergence of $\eta \propto (T/T_c - 1)^{-\gamma}$ is not completely in agreement with experiment since usually $\eta(T)$ remains finite even a bit below $T_c$. Therefore it is argued that this divergence occurs only when the atoms are strictly arrested in cages formed by their neighbors, but gets rounded off when hopping "processes" (i.e., thermally activated crossings of barriers in configuration space) are included. But MCT does not make any predictions about a further transition at $T < T_c$. These two theoretical scenarios are sketched in Fig. 1.1.

The Potts glass is a possible prototype model for the structural glass transition. A class of disordered spin models has been found which exhibit both the scenarios mentioned above, and has a lot in common with the structural glass phenomenology (Kirkpatrick and Thirumalai, 1995). One of these models is the $p$-state infinite range Potts glass with $p > 4$ (Kirkpatrick and Wolynes, 1987; Kirkpatrick and Thirumalai, 1988), which presents both, a dynamical phase transition, and a static one at a lower temperature. In this model every spin interacts with all the others, irrespective of distance. Interactions are taken from a Gaussian distribution. The spins are discrete variables that can take one out of $p$ values and an energy is gained if two interacting spins are in the same state. It is well established that one has both a dynamical transition where the relaxation time of the spin autocorrelation function diverges at a temperature $T_D$ and a static transition at a lower temperature $T_0$ where a glass order parameter appears discontinuously, and both the internal energy and the entropy as functions of the temperature present a kink. The equations of motion for the autocorrelation function $C(t)$ have the same structure of those describing the structural arrest in the mode-coupling theory.

The Potts model can also be considered as a coarse-grained model for orientational glasses (Binder and Reger, 1992). Experimentally these systems are created by random dilution of molecular crystals (which otherwise are characterized by a low temperature long range orientational order of the quadrupole moments). The dilution has the effect that at low temperatures the quadrupole moments of the molecules freeze in random orientations (Höchli et al., 1990). Long range quadrupolar order, in fact, gets severely disturbed by dilution of the material with atomic species that have no quadrupole moment (e.g. KCN diluted with KBr, or $N_2$ diluted with Ar, or ortho (o)-$H_2$ diluted with para (p)-$H_2$). Another possibility to create orientational glasses is by considering mixed crystals with different types of orientational order (e.g. KCN mixed with NaCN). If the crystal anisotropy singles out $p$ discrete preferred orientations (e.g. the 4 diagonal directions in a cubic crystal), a Potts glass model with $p$ states may give a qualitatively correct description of the system. This is further corroborated by the similarities, at least at the mean-field level, between models for the Potts glass and for orientational glasses (Goldbart and Sherrington, 1985). And, last but not least, the Potts glass model of course completes our knowledge about the different types of phase transitions and ordered phases that spin glasses can have (Binder and Young, 1986; Fischer and Hertz, 1991; Stein, 1992; Young, 1998), which provides an additional motivation for the large activity in this field.

In this work, we use Monte Carlo simulations to study the ten state Potts glass model. We

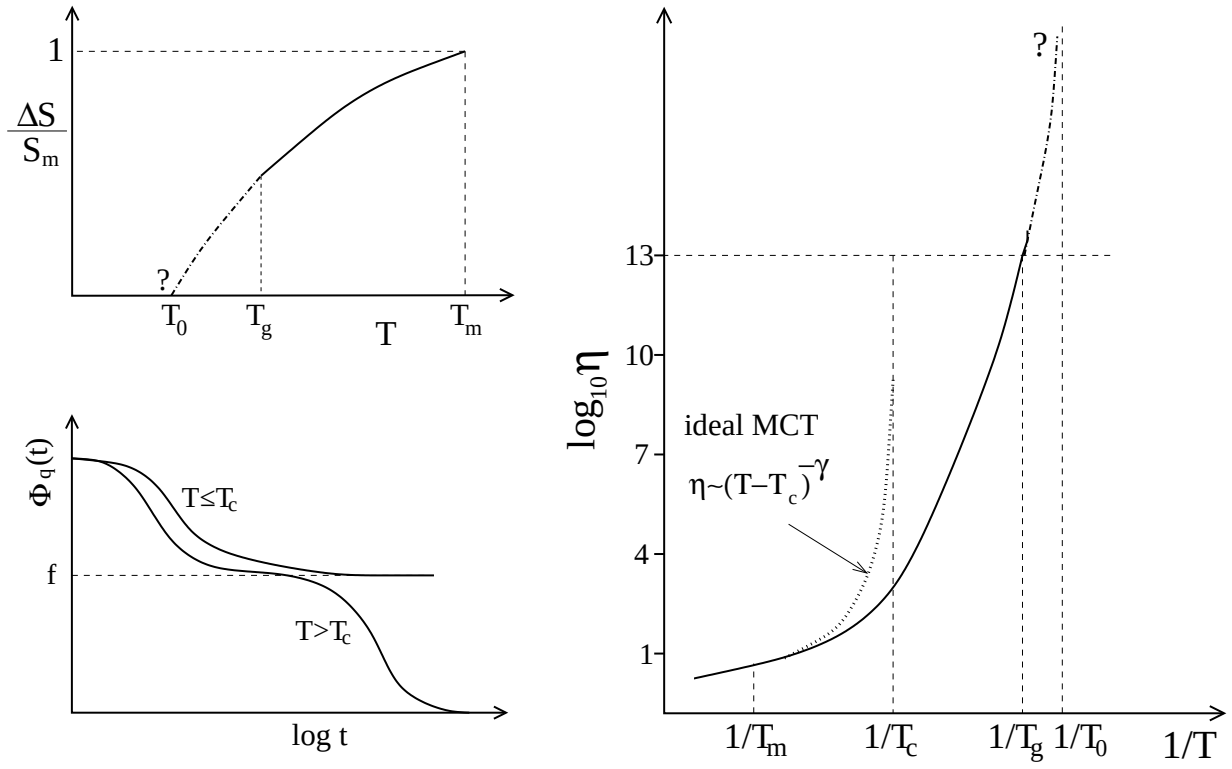


**Figure 1.1:** On the right, schematic plot of the viscosity $\eta(T)$ of a fluid vs inverse temperature $1/T$. Characteristic temperatures are indicated: melting temperature $T_m$, critical temperature $T_c$ of mode coupling theory (MCT), glass transition temperature $T_g$-defined via $\eta(T = T_g) = 10^{13}$ Poise - and Vogel-Fulcher temperature $T_0$, respectively. Upper left inset shows $\Delta S/S_m$, with $\Delta S$ the entropy difference between fluid and crystal, and $[S_m = \Delta S(T_m)]$, as a function of $T$: often these data are compatible with a linear extrapolation according to which $\Delta S$ vanishes at $T_0$. Dot-dashed lines represent a possible extrapolation. Lower left inset shows the schematic behavior of the Fourier transform of the density correlation $\phi_q(t)$ for wave-vector $q$ according to the idealized MCT. For $T > T_c$ this correlator decays to zero as function of time $t$, in two steps ($\beta$-relaxation, $\alpha$-relaxation). For $T < T_c$ only the first steps remains, the system is frozen at a plateau value $f$ ("non-ergodicity parameter").

are motivated by several aims. It is not clear, in fact, to what extent the interesting and nontrivial mean-field behavior which is known exactly in the thermodynamic limit, $N \to \infty$, can be seen for *finite* $N$. In thermodynamic limit the breaking of ergodicity in this model is induced by the divergence of free energy barriers between the various states. This divergence will be always avoided using finite systems, all the transitions will be rounded off, and the dynamical transition temperature will play the role of a crossover temperature between different physical behaviors. From this point of view, finite-size Potts glasses might be viewed as better a description of what happens in realistic structural glasses (Crisanti and Ritort, 2000). In addition, we want to elucidate the dynamical behavior of the model in greater detail than has been done so far. Simulations give access to a lot of quantities difficult to investigate analytically, such for instance the single spin autocorrelation function. This can help to clarify the reasons for non-Debye relaxation in glassy systems, in analogy to similar studies in glasses (Ediger, 2000). An open question is also the survival of all the characteristics of the mean-field solution in three dimensions. Previous studies on a $p = 3$ Potts glass seem to state the absence of a finite temperature transition to a glass phase (Scheucher and Reger, 1993).

Chapter 2 is devoted to the presentation of the known rich features of Potts glasses. We concentrate on the physical picture emerged from the solution of the infinite range model in thermodynamic limit, and we give a short description of the methods used to investigate such systems analytically. In chapter 3 we give an overview of standard Monte Carlo methods, discuss their application to the problem under investigation, and present also an optimized Monte Carlo algorithm, known as *parallel tempering* (Hukushima and Nemoto, 1996), that permits to improve the performances with respect to traditional implementations, and let us explore the otherwise unaccessible low temperature region of the fully connected Potts glass. Our original results on the fully connected version of the model are presented in chapter 4. We characterize both its static and dynamical properties, concentrating on the region of the two transitions and on the low temperature regime. We analyze the strong role played by finite-size effects, compare our findings with the mean-field solution, and discuss to what extent all the interesting temperatures can be obtained by finite-size scaling techniques. The single spin dynamics at high and low temperature, and the presence of dynamical heterogeneities are investigated and discussed. Chapter 5 presents the results regarding the investigation of the three dimensional version of the model, again regarding static and dynamical properties. Attention is paid also to the role of the ferromagnetic bond concentration and its effect on the phase diagram of the system.

# Chapter 2

# The known mean field scenario

## 2.1 The Potts model and the phase diagram of the Potts glass

In a $p$-state Potts model with $N$ sites each spin $\sigma_i$ ($i \in \{1, \cdots, N\}$) is a variable that can be in one of $p$ discrete states, $\sigma_i \in \{1, 2, \ldots, p\}$. A coupling constant $J_{ij}$ is assigned to every couple of interacting spins $\sigma_i$ and $\sigma_j$ , and the model is defined in such a way that an energy proportional to $-J_{ij}$ is gained (or lost, depending on the sign of $J_{ij}$) if the two spins are in the same state. Therefore ferromagnetic bonds (with positive $J_{ij}$) are energetically favored. The general Hamiltonian can therefore be written as

$$\mathcal{H} = -\frac{1}{2} \sum_{i,j} J_{ij}(p\delta_{\sigma_i\sigma_j} - 1). \tag{2.1}$$

The sum runs on every couple of interacting spins. For instance, in a three dimensional lattice with simple cubic geometry, every spin interacts with its six nearest neighbors. In the limit of very high temperatures every Potts state is randomly distributed among the spins (the interactions play no role) with probability equal to $1/p$, so that the thermal average $\langle \delta_{i,j} \rangle_{T=\infty}$ is equal to $1/p$, and therefore $\langle \mathcal{H} \rangle_{T=\infty} = 0$ irrespective on the choice of the $J_{ij}$'s.

A better representation of this Hamiltonian is obtained by making use of the simplex representation of the Potts spins (Zia and Wallace, 1975), in which the $p$ possible states of $\sigma_i$ correspond to vectors in a $(p-1)$ dimensional space, each of them pointing towards a corner of a $p$-simplex, with the constraint:

$$\vec{e}_l \cdot \vec{e}_m = (p\delta_{lm} - 1) \quad \text{with} \quad l, m = 1, \ldots, p. \tag{2.2}$$

These vectors $e_l^\nu$ with $\nu \in (1, \cdots, p-1)$ can be constructed explicitely using the following relation (Kirkpatrick and Wolynes, 1987)

$$e_l^\nu = \begin{cases} 0 & \nu < l \\ \left[\frac{p(p-l)}{p+1-l}\right]^{1/2} & \nu = l \\ - \left[\frac{p}{(p-l)(p+1-l)}\right]^{1/2} & \nu > l. \end{cases} \tag{2.3}$$

The mapping is then

$$\sigma_i \in \{1, \cdots, p\} \longmapsto \vec{S}_i \in \{\vec{e}_1, \cdots, \vec{e}_p\}. \tag{2.4}$$

Using the simplex representation the Hamiltonian (2.1) can be rewritten as

$$\mathcal{H} = -\frac{1}{2} \sum_{\langle i,j \rangle} J_{ij} \vec{S}_i \cdot \vec{S}_j. \tag{2.5}$$

This is formally analogous to a vector model, only the components of the vectors are not continuous but belong to the set (2.3). The Potts model, both in its ferromagnetic ($J_{ij} = 1$) and antiferromagnetic ($J_{ij} = -1$) version, is a "workhorse" in the study of critical phenomena, and shows a very rich behavior in mean-field and as a function of the dimensionality. A comprehensive review can be found in (Wu, 1982). The Potts model is also widely studied as a general model for coarsening (i.e. domain-growth) dynamics (Grest et al., 1988).
As it is customary in spin glasses, the exchange interactions $J_{ij}$ are quenched random variables taken from a Gaussian distribution $P(J_{ij})$

$$P(J_{ij}) = \frac{1}{\sqrt{2\pi}\Delta J} \exp\left[-\frac{(J_{ij} - J_0)^2}{2(\Delta J)^2}\right]. \tag{2.6}$$

Since it is an infinite range model, a proper scaling of these variables is needed in order to have a finite thermodynamic limit of the energy, so the first two moments are given by

$$J_0 = [J_{ij}]_{av} = \int J_{ij} P(J_{ij}) dJ_{ij} = \frac{\tilde{J}_0}{N-1} \tag{2.7}$$

$$(\Delta J)^2 = \left[J_{ij}^2\right]_{av} - [J_{ij}]_{av}^2 = \frac{(\tilde{\Delta J})^2}{N-1}. \tag{2.8}$$

These two formulae define the quantities $J_0$ and $\Delta J$, important to fix the temperature scale and the range of occurrence of the various phases.

The problem is now, given the Hamiltonian and the ensemble of the interaction, to calculate the main thermodynamical quantities, like the free energy, and other physical observables. The solution of this problem already at the level of the Ising spin glass model (that is $p = 2$) has proven extremely difficult, but also shed light, at least at the mean field level, on a very rich structure of the phase space. We will quote only the main results, outlining the general idea of the various steps for the solutions. Detailed calculations and discussions of the range of validity of the methods can be found in the papers we refer to.

The problem of dealing with disordered systems is that, in addition to the usual canonical (thermal) average, which we denote with $\langle \cdots \rangle$, one has to perform also an average over the disorder (that is over the distribution $P(J_{ij})$), which we denote with $[\cdots]_{av}$. For every realization $J_{ij}$ of the disorder there is a partition function

$$Z_J = \sum_{\vec{S}} \exp\left[-\beta H_J(\vec{S})\right] \tag{2.9}$$

and a free energy per spin

$$f_J = -\frac{k_B T}{N} \ln Z_J \tag{2.10}$$

with $\beta = (k_B T)^{-1}$. Usually in standard statistical mechanics, in order to obtain the main thermodynamical quantities, it is sufficient to calculate $f_J$, since the $J_{ij}$'s form a set of known interactions. When investigating disordered systems, $J_{ij}$ is taken from a given distribution, so the correct physics is given by a further average

$$f = [f_J]_{av} = \int dJ_{ij} P(J_{ij}) f_J = -\frac{k_B T}{N} \int dJ_{ij} P(J_{ij}) \ln \sum_{\vec{S}} \exp\left[-\beta H_J(S)\right]. \tag{2.11}$$

The difficulty with eq. (2.11) is that first one has to perform the sum over the variables $\vec{S}$, inside the logarithm, and only afterwards the averaging over $P(J_{ij})$. The first approach to the problem is to use the replica trick. It is based on the following result

$$\begin{aligned} &y^x \approx 1 + x \ln y \quad \text{for} \quad x \approx 0 \\ &\lim_{x \to 0} \frac{y^x - 1}{x} = \ln y. \end{aligned} \tag{2.12}$$

One can then try to use an analytical continuation procedure for the partition function of $n$ non interacting realizations (replicas) of the system under investigation. This partition function is given simply by $Z_J^n$, and it is well defined for every integer $n \geq 1$:

$$Z_J^n = \prod_{\alpha=1}^{n} \sum_{\{\vec{S}_\alpha\}} \exp\left[-\beta H_J(\{\vec{S}_\alpha\})\right]. \tag{2.13}$$

The analytical continuation consists in taking $n$ real and performing the following limit

$$[\ln Z_J]_{av} = \lim_{n \to 0} \frac{[Z_J^n]_{av} - 1}{n}. \tag{2.14}$$

This permits to perform calculations based on eq. (2.11) in a more direct way, since a disordered problem is converted into a non-disordered one, to the price of multi-spin interactions that in some cases can be handled. To show how the method works we use as example the Ising version, since it simplifies the use of indices. The vectors $\vec{S}_i$ are then substitute by the variables $S_i$ that can take values $\pm 1$. We do not perform all the steps of the calculation, but only sketch what happens. A pedagogic derivation can be found in (Fischer and Hertz, 1991). At first one has to calculate $[Z_J^n]_{av}$. Starting from the definition and performing the Gaussian average one has

$$\begin{aligned} &[Z_J^n]_{av} = \int dJ_{ij} P(J_{ij}) Z_J^n = \cdots = \\ &\sum_S \exp\left[\frac{1}{N} \sum_{ij} \left( \frac{1}{4} (\beta \tilde{\Delta J})^2 \sum_{\alpha,\beta} S_i^\alpha S_j^\alpha S_i^\beta S_j^\beta + \beta \tilde{J}_0 \sum_\alpha S_i^\alpha S_j^\alpha \right)\right]. \end{aligned} \tag{2.15}$$

We see then explicitly that the disorder is now integrated out, but there is the presence of $4-$ spin interactions $\sum_{\alpha,\beta} S_i^\alpha S_j^\alpha S_i^\beta S_j^\beta$. However, using special properties of the spin variable and of the Gaussian functions we can rewrite eqn. (2.15) like

$$[Z_J^n]_{av} = \exp\left[nN\frac{1}{4}(\beta\tilde{\Delta}J)^2\right]\int_{-\infty}^{+\infty}\prod_{(\alpha\beta)}\frac{\beta\tilde{\Delta}JN^{1/2}}{\sqrt{2\pi}}dy^{\alpha\beta}\prod_\alpha\left(\frac{\beta J_0 N}{2\pi}\right)^{1/2}dx^\alpha\exp(-NG) \tag{2.16}$$

with

$$G = \frac{1}{2}(\beta\tilde{\Delta}J)^2\sum_{(\alpha\beta)}(y^{\alpha\beta})^2 + \frac{1}{2}\beta J_0\sum_\alpha(x^\alpha)^2 -$$
$$\ln\sum_{S^\alpha}\exp\left[\frac{1}{2}(\beta\tilde{\Delta}J)^2\sum_{(\alpha\beta)}y^{\alpha\beta}S^\alpha S^\beta + \beta\sum_{S^\alpha}J_0 x^\alpha S^\alpha\right]. \tag{2.17}$$

With $(\alpha\beta)$ we intend the summation over $(\alpha \neq \beta)$. The sum $\sum_{S^\alpha}$ extends over all states of a single replicated spin $S^\alpha$, and everything is reduced to a Gaussian-averaged single site problem. The integral in eq. (2.16) can be done by means of the steepest descents method which, schematically, consists in the following

$$\int dy\exp[-NG(y)] \approx \int dy\exp[-NG(y_0) - \frac{1}{2}NG''(y_0)(y-y_0)^2 + \cdots] \tag{2.18}$$

where $G'(y_0) = 0$ defines the saddle point $y_0$. It is also essential that $G''(y_0) > 0$ otherwise the integral diverges and the procedure is no longer correct.

This approach implicitly assumes a permutation symmetry of the index $\alpha$ eq. (2.13), meaning that this equation is unchanged if two replica indices are permuted. One is able to calculate by means of statistical mechanics $[Z_J^n]$ only for every integer $n$ and to give it a physical interpretation. This permutation symmetry (that is the equivalence of the physics given by each replica) may be broken when $n \to 0$, as it turns out to be the case for infinite range spin glass models. The replica solution turns out valid only for temperatures above the spin-glass transition. The tentative (and up to now widely accepted) solution of this problem gave rise to a new method in theoretical physics, the so-called replica-symmetry-breaking, carrying also a physical picture (Mézard et al., 1984). As we said, we will quote only the relevant results; general references and discussions about the problem can be found in (Edwards and Anderson, 1975; Sherrington and Kirkpatrick, 1975; Binder and Young, 1986; Mézard et al., 1987; Fischer and Hertz, 1991; Stein, 1992; Parisi, 1992; Young, 1998). The spin glass phase is characterized by the absence of magnetic ordering, but spins are frozen in random orientations. For the Potts model the usual magnetic ordering is measured by the magnetization

$$\vec{m}_i = \langle\vec{S}_i\rangle$$
$$\vec{M} = \frac{1}{N}\sum_i^N\vec{m}_i. \tag{2.19}$$

The Potts model is symmetric under global rotations of the spins, that is the Hamiltonian (2.5) is invariant if we rotate all the spins $\vec{S}_i$ by the same angle. There are $p$ possible rotations, so every microstate is $p$ times degenerate. In a Potts ferromagnet in the thermodynamic limit $N \to \infty$ this symmetry is broken, that is the system chooses only one of the possible rotations, so the average in eq. (2.19) has to be intended not as a conventional Gibbs average over all configurations, but only over part of the configuration space, not allowing symmetry operations. This is a standard problem in statistical mechanics (Binder and Young, 1986; Fischer and Hertz, 1991). The same effect of a restricted average can be obtained imposing to the system for every finite $N$ an external field $\vec{h}$ (to select one of the possible rotations) and then letting $h \to 0$ only after taking the thermodynamic limit.
In a spin glass $M = 0$, but $\langle \vec{S}_i \rangle \neq 0$, so the proper spin-glass order parameter is (Binder and Reger, 1992)

$$q^{\mu\nu} = \frac{1}{N} \sum_i \left[ \langle S_i^\mu \rangle \langle S_i^\nu \rangle \right]_{av} . \tag{2.20}$$

Assuming isotropy in the spin orientations we can write it in the special form

$$q^{\mu\nu} = q\delta_{\mu\nu} \tag{2.21}$$

where $q$ is a scalar quantity and $\delta_{\mu\nu}$ is the Kronecker delta. We can also introduce a spin-glass susceptibility, related to the second moment of the order parameter (Chen and Lubensky, 1977; Fisch and Harris, 1977; Binder and Young, 1986; Kirkpatrick and Wolynes, 1987)

$$\chi_{SG} = N^{-1} \sum_{ij}^{N} \left[ \left( \left\langle \vec{S}_i \cdot \vec{S}_j \right\rangle - \left\langle \vec{S}_i \right\rangle \cdot \left\langle \vec{S}_j \right\rangle \right)^2 \right]_{av} . \tag{2.22}$$

The replica-symmetric solution (Erzan and Lage, 1983; Elderfield and Sherrington, 1983a) gives the following high-temperature (i.e. valid when $q = 0$) results, in units of $k_B = 1$:

$$\text{free energy per spin} \quad \beta f = \frac{\beta^2 (1-p)}{4} - \ln(p) \tag{2.23}$$

$$\text{energy per spin} \quad e = \frac{\beta (1-p)}{2} \tag{2.24}$$

$$\text{entropy per spin} \quad s = \frac{\beta^2 (1-p)}{4} + \ln(p) \tag{2.25}$$

$$\text{spin glass susceptibility} \quad \chi_{SG} = \frac{p-1}{1 - \frac{\tilde{\Delta} J^2}{T^2}}. \tag{2.26}$$

The replica approach predicts the occurrence of a paramagnet-to-spin glass transition. For $p < 6$ this transition is continuous (second-order) and occurs at a temperature $T_s = \tilde{\Delta} J$. For $p > 6$ the transition is discontinuous (first-order). It has also been shown that in the Potts glass for

$p > 2$ there is a strong tendency towards ferromagnetism. The temperature $T_f$ below which conventional ferromagnetism appears is (Elderfield and Sherrington, 1983b)

$$\frac{1}{T_f}\left(\tilde{J}_0 + \frac{(p-2)(\tilde{\Delta J})^2}{2T_f}\right) = 1. \tag{2.27}$$

It is then important to set the parameters $J_0$ and $\Delta J$ to proper values, so as to enter the spin-glass phase at a temperature higher than $T_f$.

It is already clear from eq. (2.25) that the replica symmetric solution cannot be correct for every temperature, since it predicts a negative entropy for $T < \sqrt{(p-1)/(4\ln(p))}$. The entropy must be positive, since it is the logarithm of the number of microstates. It is then necessary to allow a breaking of this symmetry and explore the consequences. The detailed treatment can be found in (Gross et al., 1985; Cwilich and Kirkpatrick, 1989; Cwilich, 1990). The solution for $p = 2$, the Ising case, has been widely investigated and reviewed (Mézard et al., 1984; Binder and Young, 1986; Mézard et al., 1987; Fischer and Hertz, 1991; Young, 1998). We will review what happens for $p \geq 3$.

The spin-glass phase is characterized by a novel behavior with respect to standard critical phenomena. Below the transition temperature, the phase space splits into an infinite number of pure states. A popular way to describe this is by means of the so-called many-valley picture. To every spin $i$ we associate its magnetization $m_i$, and consider the total free energy $F(m_1, m_2, \cdots, m_N)$. $F$ describes a hypersurface in the $N+1$-dimensional space. The physically relevant states correspond to the minima of this function, that is solutions of $\partial F/\partial m_i = 0$ with the eigenvalues of the matrix $\partial^2 F/\partial m_i \partial m_j$ all positive. In infinite range spin glasses below the phase transition temperature one has many of this minima, and they are not related by simple symmetry operations like global rotations. In the limit $N \to \infty$ the barriers between these minima diverge, and the phase space can be partitioned into mutually inaccessible valleys. Each of them correspond to a thermodynamically stable state, like the magnetized state of a ferromagnet (with the only difference that, as we already remarkered, all the stable states of a ferromagnet are related by rotations, and they can be all mapped onto a single one). The picture suggested is like a mixture of equilibrium-also called pure- Gibbs states (Mézard et al., 1987). This phenomenon of coexistence of many stable states not related by symmetry properties goes under the name of *broken ergodicity* (Palmer, 1982; Palmer, 1983). Due to the coexistence of states, the role of order the parameter is played by the distribution function of the overlap between them. Given two states, labeled with index $a$ and $b$, the overlap between them is defined as

$$q_{ab}^{\mu\nu} = \frac{1}{N}\sum_i \langle S_{ia}^{\mu}\rangle\langle S_{ib}^{\nu}\rangle = q_{ab}\delta_{\mu\nu}. \tag{2.28}$$

Since the indices $a$ and $b$ run over a large number of states, many values of $q_{ab}$ will be found, and for each realization of disorder we can define a distribution function (Fischer and Hertz, 1991)

$$P_J(q) = \langle \delta(q - q_{ab})\rangle = \sum_{ab} \mathcal{P}_a \mathcal{P}_b \delta(q - q_{ab}) \tag{2.29}$$

where $\mathcal{P}_a$ is the probability to sample the state $a$

$$\mathcal{P}_a = \frac{\exp(-\beta F_a)}{\sum_s \exp(-\beta F_s)}. \tag{2.30}$$

The general distribution function is the average over the disorder, that is

$$P(q) = [P_J(q)]_{av}\,. \tag{2.31}$$

The replica-symmetry-breaking approach makes predictions for this function, that is not accessible in experiments but can be obtained in a numerical simulation. To introduce a simple reference, in an Ising ferromagnet below the phase transition temperature one has two possible states, with magnetization $\pm M$, related by a global spin-flip symmetry. The possible value of the overlap then, getting rid of the symmetries, is only $M^2$. The same is true also for Potts ferromagnets. The distribution function of the overlap has a single delta-peak, and this explains also the analogy of $q$ with the standard concept of order parameter. In the Potts glass for every $p \geq 3$ and below the spin-glass transition the distribution function of $q$, which we indicate with $P(q)$, assumes a double-delta structure, with a first peak centered at $q = 0$ and another one, temperature dependent, at $q_0 = q_0(T)$. Also in the replica-symmetry-broken approach a phase transition from a paramagnet to a spin-glass transition is found at a temperature which we denote by $T_0$. The distribution function $P(q)$ goes for every $p \geq 3$ from a single-delta function (Gross et al., 1985; Kirkpatrick and Wolynes, 1987; Cwilich and Kirkpatrick, 1989) centered around $q = 0$ for $T > T_0$ to a double-delta function

$$\begin{aligned} P(q) &= \delta(q) && T > T_0, N \to \infty \\ P(q) &= [1 - w(T)]\delta(q) + w(T)\delta(q - q_0(T)) && T \leq T_0, N \to \infty. \end{aligned} \tag{2.32}$$

This implies that below $T_0$ the phase space splits into an infinite number of pure Potts-glass states that do not overlap (Gross et al., 1985). The value $q_0$ is the glass order parameter inside each pure state. For $p = 3, 4$ $q_0$ is continuous throughout the transition, which takes place at $T_0 = \tilde{\Delta} J$, and $w(T \lesssim T_0) = (4 - p)/2 + O(1 - T/T_0)$. For $p > 4$ it is no longer possible to calculate analytically the interesting quantities systematically as a function of $p$. An expansion in the limit $\epsilon = p - 4 \to 0$ (Cwilich and Kirkpatrick, 1989) gives

$$T_0 \simeq \tilde{\Delta J} + \frac{(p-4)^2}{3(p^2 - 18p + 42)} \tag{2.33}$$

$$q_0(T_0) \simeq \frac{2(p-4)}{(p^2 - 18p + 42)} \tag{2.34}$$

$$w(T \lesssim T_0) \propto (1 - T/T_0) \tag{2.35}$$

To have a quantitative estimation of these quantities a numerical solution of the replica-symmetry-breaking equation is needed (De Santis et al., 1995). For $p = 10$, the value we adopted for our simulations, we have $T_0 = 1.131$ and $q_0(T_0) = 0.432$. This value $p = 10$ has a rather large

discontinuity in the order parameter, which would be easier to detect in a simulation. This discontinuity grows as $p$ is increased, but one also has to keep in mind that it will be always more difficult to equlibrate the system as the $p$ increases, since we have to sample more states. The weight $w(T_0)$ is always proportional to $1-T/T_0$. We show the complete temperature dependence in Fig. 2.1.

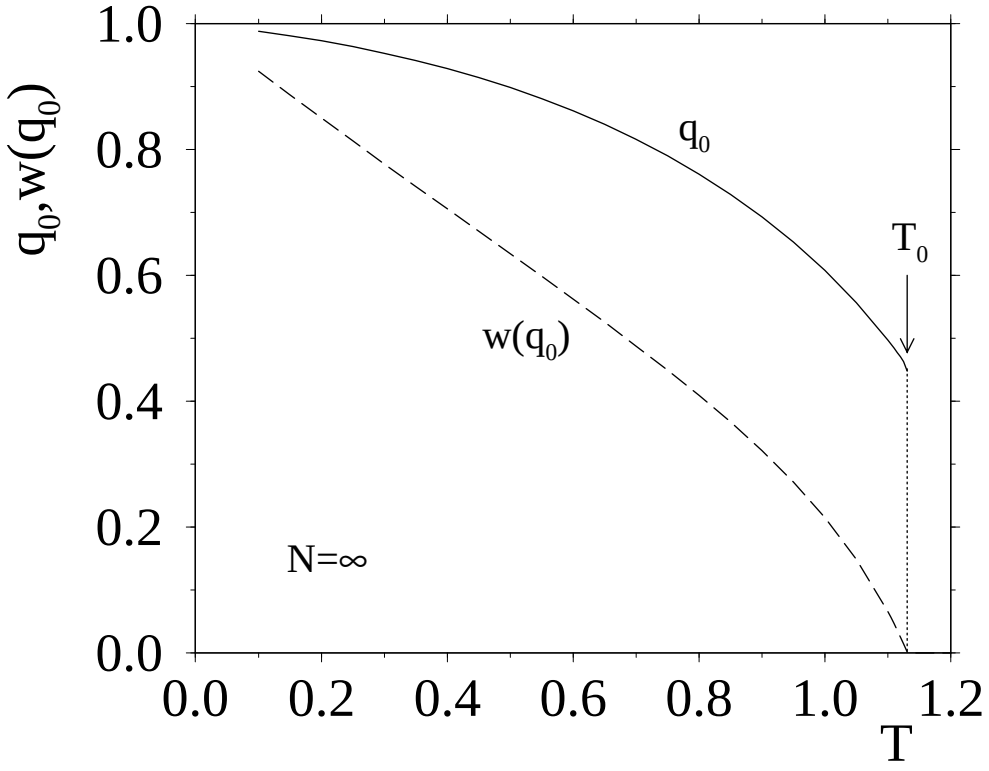


**Figure 2.1:** Temperature dependence of $q_0$ and $w(T)$ for $p = 10$, as obtained from the one-step replica-symmetry-breaking solution (De Santis et al., 1995).

Despite the fact that the order parameter jumps discontinuously at $T_0$ for $p > 4$, this is not an ordinary first order phase transition. Only *second derivatives* of the free energy with respect to temperature and static external fields are discontinuous at $T_0$, and in particular there is no latent heat of transition, appearing when there is a discontinuity in the energy (Gross et al., 1985). This is a novel behavior in the realm of critical phenomena, and up to now has only been found for certain classes of infinite-range spin-glass models (for a review concerning these models, see (Kirkpatrick and Thirumalai, 1995)).

Also this replica-broken solution becomes unstable at low temperatures for every $p \geq 3$, giving negative values of the entropy for finite temperatures, and a spin-glass to spin-glass transition takes place (Gross et al., 1985; Gardner, 1985). It is very difficult to study this second transition analytically, since it involves coupling between the glass order parameter and the spontaneous magnetization. It seems that the new phase is mixed ($M \neq 0,\ q \neq 0$) and goes under the name of

"canted random ferromagnet" (Elderfield and Sherrington, 1983b). Every pure Potts state splits into an infinite number of partially correlated states (Gross et al., 1985). A lower bound for the occurrence of this transition has been established at a temperature

$$T_2 = (p/2 - 1)/(1 - \tilde{J}_0). \tag{2.36}$$

## 2.2 The dynamics

Spin Hamiltonians like (2.1) do not have an intrinsic dynamics. We need then to couple the system to a thermal reservoir, in order to allow for spin flips and relaxations. Two approaches are mostly used to do that, one more suitable for analytical work and based on a continuum picture, the other based on a master equation and more used in numerical (Monte Carlo) studies [1]. We will discuss this second technique in the chapter devoted to numerical methods, since it is the basis of our investigation about the dynamics of the *finite size* system. Here we concentrate more to give a review of the results obtained analytically (Kirkpatrick and Wolynes, 1987; Kirkpatrick and Thirumalai, 1988). The quantity studied is the spin autocorrelation function

$$C(t) = \frac{1}{N(p-1)} \sum_{i=1}^{N} \left[ \langle \vec{S}_i(t') \cdot \vec{S}_i(t'+t) \rangle \right]_{av} \quad . \tag{2.37}$$

Every element of the Potts vectors must obey a Langevin equation, describing a relaxation process (Fischer and Hertz, 1991), so soft spins versions of (2.3) are used. Every $S_i^\nu$ can assume values between $-\infty$ and $+\infty$, and the Hamiltonian (2.5) is consequently modified (Kirkpatrick and Thirumalai, 1988). The Langevin equation is given by

$$\Gamma_0^{-1} \partial_t S_i^\nu(t) = -\frac{\delta(\beta H)}{\delta S_i^\nu(t)} + \xi_i^\nu(t). \tag{2.38}$$

$\Gamma_0$ is a coefficient setting the microscopic time-scale, and $\xi_i^\nu(t)$ a Gaussian random noise with zero mean and variance

$$\langle \xi_i^\nu(t) \xi_i^\mu(t') \rangle = \frac{2}{\Gamma_0} \delta_{ij} \delta_{\nu\mu} \delta(t - t'). \tag{2.39}$$

This equation can be solved in the limit $N \to \infty$. The results for $p = 3, 4$ are typical for the dynamics close to a static second order phase transition, in analogy to what happens in the infinite-range Ising spin glass (Binder and Young, 1986). The relaxation time $\tau$ diverges like $\tau \propto (T - T_0)^{-\Delta}$, the temperature $T_0$ is the static transition temperature. For $p > 4$ a temperature $T_D > T_0$ appears at which the system loses ergodicity, that is

$$\lim_{t \to \infty} \lim_{N \to \infty} C(t) = q_{EA} \neq 0. \tag{2.40}$$

[1] For general reviews see (Hohenberg and Halperin, 1977; Cardy, 1996); for applications to the spin glass problem, see (Fischer and Hertz, 1991).

This fact is rather surprising, since it is believed that the long time limit of $C(t)$ gives the (static) order parameter (Edwards and Anderson, 1975), which is, as we have seen from the static approach, zero for every $T > T_0$. The relaxation time diverges again as a power law, but now as $(T - T_D)^{-\Delta}$, with $T_D > T_0$. $T_D$ goes under the name of dynamical transition temperature. What is also interesting is that the equations describing the behavior of $C(t)$ for $p > 4$ are formally analogous to those introduced to describe the phenomenon of structural arrest taking place close to the glass transition in the so-called mode coupling theory (Götze, 1989; Götze, 1999). This led to the speculations that certain classes of spin glass models, like the Potts glass with $p > 4$, are spin models to describe the statistical physics of the glass transition (Kirkpatrick et al., 1989).

A connection can be made between statics and dynamics, that apparently predicts two different results, using an approach to the Hamiltonian (2.5) which is alternative to the replica method. Thouless, Anderson and Palmer introduced a set of nonlinear coupled equations for the single-spin magnetizations $\vec{m}_i$ (Thouless et al., 1977). Every set of these equation refers to a fixed set of bonds $J_{ij}$, so the thermal average has to be performed at the end. Again for simplicity, in order to understand the idea behind it, we discuss the case of Ising spins, where magnetizations are scalar quantities $m_i$. The equations for the Potts case can be found in (Kirkpatrick and Wolynes, 1987). A free energy functional $F\{m_i\}$ can be written down using mean-field arguments (Fischer and Hertz, 1991). Every spin $i$ experiences the presence of a field $\sum_j J_{ij} m_j$ due to all the others magnetizations $m_j$. In addition to it, which is the base of mean field theory in non-disordered model, one has also to take into account the presence of a reaction term, that is the local magnetization $m_i$ at site $i$ induces a mean field $J_{ij} m_i$ at site $j$, which induces a magnetization[2] $J_{ij}\chi_{jj} m_j$ at site $j$, and hence a mean-field $J_{ij}^2 \chi_{jj} m_i$ at site $i$. It turns out then that the ordering of spin $S_i$ is induced by the internal fields of all the spins $S_j$ in the absence of $S_i$, so this reaction term has to be subtracted from the full mean-field $\sum_j J_{ij} m_i$ in computing $m_i$ (Fischer and Hertz, 1991). In usual mean-field theories $J_{ij} \sim N^{-1}$ and the reaction term can be neglected, but in spin glasses $J_{ij} \sim N^{-1/2}$ and this fluctuation contribution is needed for consistency (Kirkpatrick and Wolynes, 1987). The so-called TAP equations are then derived by variation of the free energy functional, $\partial F / \partial m_i = 0$. Their solution is consistent with the replica approach, in the sense that the same spin-glass phase transition is predicted at $T_0$, but they reveal more about the structure of the phase space. The replica formalism gives for every $T > T_0$ a paramagnetic solution that minimizes the free energy of the system. The TAP approach, surprisingly, shows that in the range $T_0 < T < T_D$ the same replica free energy can be obtained considering an ensemble of *exponentially* large (in $N$) solutions, with a higher free energy (Kirkpatrick and Wolynes, 1987). We denote the total number of solutions $m_s$ to the TAP equations with $K^*$. When many solutions appear, their weighted total free energy is given by

$$\bar{F} = \sum_s F(m_s)\mathcal{P}_s \tag{2.41}$$

$$\mathcal{P}_s = \frac{e^{-\beta F(m_s)}}{\sum_s e^{-\beta F(m_s)}}. \tag{2.42}$$

[2] $\chi_{ij} = \partial m_i / \partial \tilde{h}_j$ is the local magnetic susceptibility, and describes the answer of $m_i$ to a small change of the (effective) field $\tilde{h}_j$

$F(m_s)$ is the free energy inside each solution, $\mathcal{P}_s$ is the canonical probability to be in that state. However, since there is a (exponential) number of solutions $K^*$, we have to take into account the contribution to the free-energy coming from their total number, which defines the so-called *complexity* $I$:

$$I = k_b \ln K^* \tag{2.43}$$

so that the true free energy of the system is given by

$$F = \bar{F} - TI. \tag{2.44}$$

$F$ is then the same calculated within the replica formalism for $T_0 < T < T_D$.

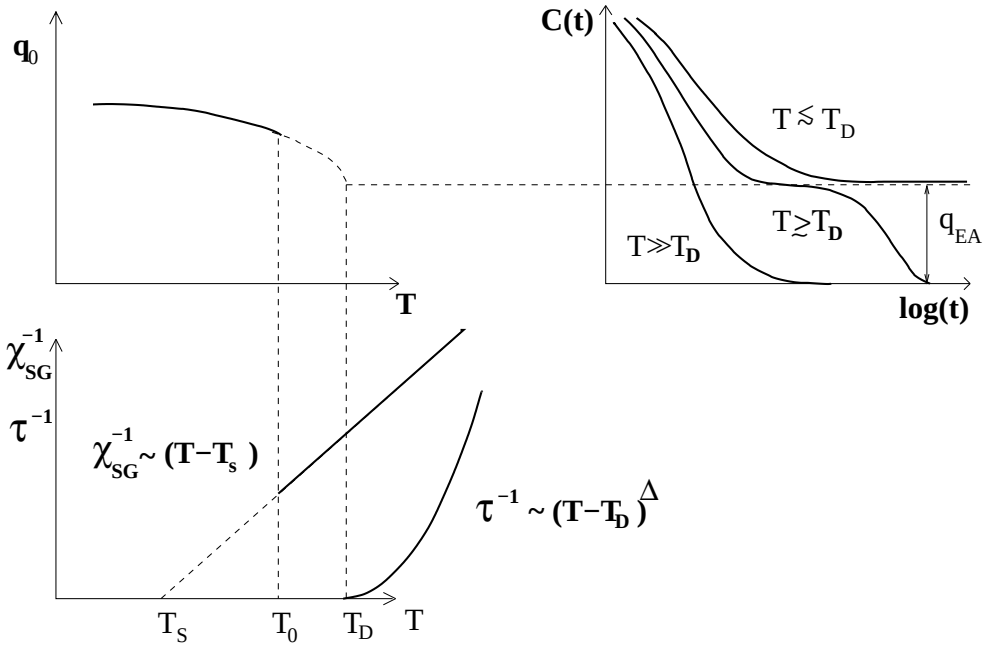


**Figure 2.2:** Qualitative sketch of the mean-field predictions for the $p$-state Potts glass model with $p > 4$. The spin glass order parameter, $q_0$, is nonzero only for $T < T_0$ and jumps to zero discontinuously at $T = T_0$. The spin glass susceptibility $\chi_{SG}$ follows a Curie-Weiss-type relation with an apparent divergence at $T_s < T_0$. The relaxation time $\tau$ diverges already at the dynamical transition temperature $T_D$. This divergence is due to the occurrence of a long lived plateau of height $q_{EA}$ in the time-dependent spin autocorrelation function $C(t)$.

The proposed connection (Kirkpatrick et al., 1989) with the dynamical transition obtained solving the dynamical problem (2.38) (Kirkpatrick and Thirumalai, 1988) is based on the appearance of these metastable solutions. They are metastable because in the range $T_0 < T < T_D$ each of them has a higher free energy than the paramagnet. However, in the course of its time evolution the system can visit a local free energy minimum, and , in the mean-field limit $N \to \infty$, become trapped since activated processes that would permit the relaxation cannot take place because barriers diverge (Kirkpatrick and Thirumalai, 1988), that is in mean-field limit metastable

states can have infinite lifetime. So these $K^*$ spin-glass-like states lead to a dynamical freezing of the system, but no static phase transition still takes place because the free energy remains the same as the one of the paramagnetic state. A physical picture to describe what happens is (Kirkpatrick and Wolynes, 1987): "*two temperatures - $T_D$ and $T_0$ - appear in the theory. The first one is associated with the appearance of well-defined free-energy minima, the latter with their ultimate thermodynamic stability*". The fact that the correlation function $C(t)$ does not decay any longer to zero (its expected value in the paramagnetic state) but gets stuck to $q_{EA}$ is related to the infinite-range character of the forces and to the limit $N \to \infty$, since free-energy barriers diverge. In finite dimensions or for every $N$ finite, it is expected that $T_D$ plays the role of a crossover temperature, above which $C(t)$ starts to show a long-lived plateau structure and the relaxation time $\tau$ changes from a power-law behavior $(T - T_D)^{-\Delta}$ for $T \geq T_D$ to an Arrhenius behavior $\exp(c/T)$ for $T < T_D$.

A summary of the rich behavior of $p > 4$ Potts glasses is shown in Fig. 2.2 . We give the connections between statics (represented by the order parameter $q_0$ and the associated susceptibility $\chi_{SG}$) and dynamics, represented by a qualitative picture of $C(t)$. Note also the role of $T_s$, the temperature at which the extrapolation of the high-temperature susceptibility diverges. In a standard first order transition (*with* latent heat) $T_s$ would play the role of the spinodal temperature, the lowest temperature at which paramagnetic metastable states can still appear in the region of the ordered phase. However, due to the particular nature of the spin-glass transition, the paramagnetic state is completely unstable for every $T < T_0$, so that $T_s$ does not have a physical meaning (Gross et al., 1985).

# Chapter 3

# Monte Carlo Methods

## 3.1 Methods to sample the configuration space

Statistical mechanics teaches us how to derive equilibrium properties of a system knowing its microscopic states. A key quantity is the partition function

$$Z = \sum_{s=1}^{\mathcal{N}} e^{-\beta H(X_s)}. \tag{3.1}$$

The sum [1] is over all $\mathcal{N}$ microscopic states accessible to a system ($\mathcal{N} = p^N$ in the case of a $p$-state Potts model with $N$ spins), and $\beta = (k_B T)^{-1}$. With $X$ we indicate a microscopic configuration, $X = \{\vec{S}_1, \cdots, \vec{S}_N\}$. The free energy is then given by

$$F = -k_B T \ln Z \tag{3.2}$$

and the important thermodynamic quantities follow by differentiating the free energy. The equilibrium mean value of any observable $\mathcal{O}$ is given by

$$\langle \mathcal{O} \rangle = \frac{\sum_{s=1}^{\mathcal{N}} \mathcal{O}(X_s) e^{-\beta H(X_s)}}{Z}. \tag{3.3}$$

The goal, from a theoretical point of view, is then to compute sums like (3.1) and (3.3). This is, in most cases, not possible analytically. Computers can help in computing exactly the partition function, but the sizes accessible are rather small. In the case of infinite range spin glasses, the Ising system was investigated up to $N = 20$ (Young and Kirkpatrick, 1982), and the Potts model with $p = 3$ and $p = 6$ up to $N = 15$ (Peters et al., 1996). To investigate bigger sizes, one has to resort on approximate methods, making certain *Ansätze* on the structure of the phase space (introducing theories), or finding certain ways, again numerically, to restrict the sums over a smaller and accessible number of representative states. The scope of this chapter is to illustrate

[1] If the system has continuous degrees of freedom, the sum is replaced by an integral, but conceptually the treatment remains the same.

how to realize this latter purpose by using suitable methods to sample the phase space. They go under the name of Monte Carlo methods, since they contain stochastic elements. They were implemented just after the second world war, when the first computers became available, and have gained continued popularity in the scientific community. These methods are now standard, and the range of problems they can treat is rather large, regarding both lattice and off-lattice systems. Two recent references are (Newman and Barkema, 1999; Landau and Binder, 2000). As we saw, when the number of spins $N$ starts to grow, it is no longer possible to treat numerically all the states exhaustively. We can consider a subset of $\mathcal{M}$ different states out of the $\mathcal{N}$ total. Every state $X_s,\ s \in \{1, \ldots, \mathcal{M}\}$ is chosen according to a certain probability $p(X_s)$. Then (3.3) is approximated by

$$\mathcal{O}_{\mathcal{M}} = \frac{\sum_{s=1}^{\mathcal{M}} \mathcal{O}(X_s) p(X_s)^{-1} e^{-\beta H(X_s)}}{\sum_{s=1}^{\mathcal{M}} p(X_s)^{-1} e^{-\beta H(X_s)}}. \tag{3.4}$$

The factor $p(X_s)^{-1}$ is present since (3.3) is an unweighted sum, while the $\mathcal{M}$ states are chosen according to $p(X_s)$, so one needs to correct. Clearly $\lim_{\mathcal{M}\to\infty} \mathcal{O}_{\mathcal{M}} = \langle \mathcal{O} \rangle$. This is true in the limit when all states are sampled. We need then a good recipe to sample the states, in order to make (3.4) a good estimate. A constant $p(X_s)$ is a poor choice. Every state is sampled with the same probability, and in a reasonable computer time we are able to access only a small part of them. The problem is dramatic at low temperature, when only a small fraction of states dominate the sum, and the probability to pick them at random is very small. The way to solve this problem is to choose

$$p(X_s) = e^{-\beta H(X_s)} \tag{3.5}$$

and goes under the name of importance sampling. With this choice (3.4) becomes a simple arithmetic average over the $\mathcal{M}$ states

$$\mathcal{O}_{\mathcal{M}} = \frac{1}{\mathcal{M}} \sum_{s=1}^{\mathcal{M}} \mathcal{O}(X_s) \tag{3.6}$$

In this way we sample more often the states that the real system would visit at a selected temperature.

The problem is then reduced to find a suitable way to pick up states according to the proper Boltzmann weight. This is done by realizing a Markov process. A detailed treatment of this problem can be found in the above mentioned books and in the reference they give also to the mathematical literature. A concise but very informative treatment is given in (Wang, 1999), and we will follow it here. We just give an idea how to arrive to the solution. We want to generate states according to the Boltzmann probability. We do it following a chain process. Given a first state $X_0$, we generate $X_1$, and so on. This is done according to a transition probability, encoded in the matrix $W(X_1, X_0)$. This matrix has two properties, $W(X_1, X_0) \geq 0$ and $\sum_s W(X_s, X_0) = 1$. We indicate with $p_0(X)$ the probability of the initial configurations. Then the probability of sampling $X$ after $n$ steps is given by

$$p_n(X) = \sum_s W^n(X, X_s) p_0(X_s) \tag{3.7}$$

The power $W^n = W \cdot W \cdot \ldots \cdot W$ means a repeated action of the matrix $W$, $n$ times. It can be shown that a unique distribution

$$p(X) = \lim_{n\to\infty} p_n(X) = \lim_{n\to\infty} W^n(X, X_s) \tag{3.8}$$

exists and is independent of the initial distribution, provided that $W^k(X, X_s) > 0$ for every $X$ and $X_s$ and for all $k$ for sufficiently large $k$. This condition means:

1. starting from any initial state $X_s$, it is possible to reach any other state $X$ with nonzero probability in an arbitrary but finite number $k$ of steps (this is known as ergodicity);

2. starting from $X_s$, the probability that the system comes back to $X_s$ in $k$ steps is nonzero for all $k$ greater than a threshold value.

All is needed now is to be sure that the limit $p(X)$ is the Boltzmann distribution. It is then sufficient to impose the *detailed balance* condition:

$$\begin{aligned} W(X_s, X)p(X) &= W(X, X_s)p(X_s) \quad \text{for all } X \text{ and } X_s \\ \Rightarrow \frac{W(X_s, X)}{W(X, X_s)} &= e^{-\beta[H(X_s)-H(X)]}. \end{aligned} \tag{3.9}$$

There is some freedom on the choice of $W$. The first to be proposed, and most commonly used is given by the so-called Metropolis criterion (Metropolis et al., 1953)

$$W(X_s, X) = \begin{cases} \tau_0^{-1} e^{-\beta[H(X_s)-H(X)]} & \text{if} \quad H(X_s) - H(X) > 0 \\ \tau_0^{-1} & \text{otherwise.} \end{cases} \tag{3.10}$$

The factor $\tau_0$ is arbitrary, and for our purposes it can be set to unity. In the dynamical interpretation of the Monte Carlo method, it plays the role of a microscopic time. The Metropolis algorithm is our choice for the simulation of the infinite range Potts glass. The algorithm is the following:

1. choose a starting configuration;

2. choose randomly and uniformly a site $i \in \{1, \ldots, N\}$;

3. choose randomly and uniformly a new state $l \in \{1, \ldots, p\}$ for $i$;

4. calculate the energy difference $\Delta E$ between the proposed configuration and the old one;

5. if the energy difference is non positive, accept $l$ as new state; Otherwise generate a random number $0 < r < 1$ and accept the state only if $r < \exp(-\beta\Delta E)$. If the new state in not accepted, the new configuration will be identical to the old one.

6. repeat from point 2.

The heat-bath method provides another algorithm that satisfies detailed balance. The acceptance criterion is no longer based on the energy difference between old and proposed state, but on the relative energy weight of all the possible states of the spin we want to update. So, once we choose a spin $i$ at random, we have $p$ different values of the energy of the system, depending on the state of spin $i$. We then select the new state for the chosen spin according to the probability $p_l$

$$p_l = \frac{e^{-\beta E_l}}{\sum_{m=1}^{p} e^{-\beta E_m}} \tag{3.11}$$

where $E_l$ is the energy of the system if $\sigma_i = l$. This algorithm is more efficient than the Metropolis one in finding energetically desirable states, especially when $p$ is large and at low temperatures. As a drawback it implies the calculation of $p$ exponential functions at every Monte Carlo step, an operation that is computationally expensive. Our choice was to use this algorithm in the short range case, because we adopted for the most part of the simulations a bimodal distribution of bonds instead of a Gaussian one. In this way the values of the exponentials can be tabulated in advance, saving the computations. Details are given in the chapter devoted to the short range version of the model.

## 3.2 Dynamical interpretation

Although Monte Carlo methods have been introduced to study the static properties of a system, through the calculation of statistical averages like in eq. (3.3), they are essentially dynamical in nature. This is because the chain process creating new configurations can be considered as the evolution of the system in time. If we label as $t$ the number of steps per spin performed after the chain program starts, the distribution probability for the states obeys the following master equation

$$\frac{d}{dt}p(X,t) = -\sum_{X_s} W(X_s, X)p(X,t) + \sum_{X_s} W(X, X_s)p(X_s,t). \tag{3.12}$$

In analogy to the Langevin equation given in eq. (2.38), it also describes the relaxation dynamics of a system in contact with a thermal bath (Landau and Binder, 2000). Of course, given the fact that a single spin flip Monte Carlo simulation realizes eq. (3.12), we can measure also time-dependent quantities like correlation function. Time units can be normalized such that, on average, $N\tau_0^{-1}$ single particle transitions are performed in unit time. One Monte Carlo sweep (MCS), measure unit for $t$, corresponds then to $N$ Monte Carlo steps for the system. Gibbs averages over states can also be seen as averages over the stochastic time trajectory. In order to measure equilibrium properties, a certain number of states $M_0$ has to be omitted from the average. They are the first states to be sample, and they do not represent yet typical equilibrium configurations, since the system has still to be thermalized. In other terms, before starting to measure we have to wait a time $t_0$ before the system thermalizes.

## 3.3 Equilibration

Spin glasses are characterized by a very slow dynamics, and this effect becomes stronger decreasing the temperature. Simulations also reflect this property, and if the system is not properly thermalized, it will show "aging" effects, that is quantities that in equilibrium should be constant, like the energy per spin, show weak time dependence, and correlation functions do not show time-translation invariance, but their shape depend on the time at which the measurement start (a review of this effects specialized to spin glasses and simulation can be found in (Rieger, 1994)). To avoid these effects, a careful thermalization procedure is needed. In a Monte Carlo simulation we investigate finite systems, which by definition are always ergodic. So equilibrium will be achieved if, after a perturbation (i.e. a change of temperature), we let the system evolve for a time $t_0$ longer than the longest relaxation time. Different observables (e.g. the energy or the spin autocorrelation function) in fact tend to relax to their equilibrium value after different times. To every configuration, at a given time, we can associate an energy: $e$ is therefore an example of a *one-time* quantity. To measure the spin autocorrelation function,as we have seen from the definition in section 2.37, we need for every point of this function two different configurations corresponding to two different times, therefore $C(t)$ is a *two-time* quantity. We found in our simulations that two-times quantities have longer relaxation times, and are usually more affected by out-of-equilibrium effects. They are good indicators to test thermalization. We give now some definitions for the observables. The energy per spin is given by

$$e = \frac{[\langle H \rangle]_{av}}{N}. \tag{3.13}$$

With $[\cdots]_{av}$ we indicate the average over different realizations of disorder. When we refer to quantities for a single sample, it is of course omitted from the definition. The order parameter has to be considered as a distribution, $P(q)$ (we explained the fact in chapter 2). In order to calculate this distribution, one needs the value of the overlap between independent states visited at a certain temperature. It is customary in Monte Carlo simulations, to improve the statistic and to assure a better de-correlation, to use states belonging to two different replicas (Young, 1983). This means that the same realization of bonds is simulated according to two independent sequences of random numbers, which we label with $\alpha$ and $\beta$. Given then two states $\{\vec{S}_\alpha\}$ and $\{\vec{S}_\beta\}$ we calculate their overlap as

$$q = \sqrt{\frac{1}{p-1}\sum_{\mu,\nu=1}^{p-1}\left(q^{\mu\nu}\right)^2} \qquad q^{\mu\nu} = \frac{1}{N}\sum_{i=1}^{N} S_{i\alpha}^{\mu} S_{i\beta}^{\nu}. \tag{3.14}$$

This quantity is invariant under complete rotations of the spins in the configurations, since it involves scalar products inside each replica. In fact, with a bit of algebra, it can be shown that

$$q = \sqrt{\frac{1}{N^2(p-1)}\sum_{i,j=1}^{N}\left(\vec{S}_{i\alpha}\cdot\vec{S}_{j\alpha}\right)\left(\vec{S}_{i\beta}\cdot\vec{S}_{j\beta}\right)}. \tag{3.15}$$

The results of the overlaps between different states are then collected in a histogram. This is done for every realization of disorder, so we get a $P_J(q)$. The total distribution is simply given by the disorder average of them, $P(q) = [P_J(q)]_{av}$. The moments are then obtained according to the definitions

$$q^{(n)} = \int q^n P(q) dq. \tag{3.16}$$

The spin autocorrelation function is calculated according to

$$C(t) = \frac{1}{N(p-1)} \sum_{i=1}^{N} \left[ \langle \vec{S}_i(t') \cdot \vec{S}_i(t'+t) \rangle \right]_{av} \quad . \tag{3.17}$$

The symbol $t'$ refers to a time origin, and in this case the average $\langle \cdots \rangle$ is more easily understood as an average over different $t'$ (usually $4$ at high temperature and $10$ at low temperature in our simulations, equally spaced). Another useful correlation function is the rotational invariant one

$$C_{RI}(t) = \left[ \frac{\langle \tilde{q}(t) \rangle}{\langle \tilde{q}(0) \rangle} \right]_{av} \tag{3.18}$$

$$\tilde{q}(t) = \left[ \frac{1}{p-1} \sum_{\mu,\nu=1}^{p-1} \left( \tilde{q}^{\mu\nu}(t) \right)^2 \right]^{1/2} \qquad \text{and} \quad \tilde{q}^{\mu\nu}(t) = \frac{1}{N} \sum_{i=1}^{N} (\vec{S}_i)^{\mu}(t'+t)(\vec{S}_i)^{\nu}(t'). \tag{3.19}$$

It is particularly interesting because, in equilibrium, its long time limit must give exactly the first moment of the order parameter distribution. This is true for every realization of the disorder. It follows directly from the definition. It is important for the order parameter distribution to calculate overlap between decorrelated thermalized configurations, as is indeed the case in equilibrium when $t \to \infty$. We call two configurations decorrelated when the time separating them is of the order of the time it takes the correlation function to decay, say, to $1/e$. This value is somewhat arbitrary, and one has to be sure actually that long time processes have already occurred. When making a simulation, it is wise to start at high temperature. Relaxation times are short, and usually one has also an idea of the values to be expected (we can, e.g., compare with the replica solution in the infinite range case.). To have an idea of the time-scales involved, starting from completely random configurations we let the system evolve and monitor one-time quantities, typically the energy. We simulate two replicas of the bond configurations which evolve independently (for a Monte Carlo simulation this means that the initial configurations and the random numbers used in the Metropolis criterion are independent). After our initial guess of $t_0$, which is usually much longer ($2$ orders of magnitude) than the time needed to $e$ to thermalize, we start to measure for every replica two time quantities, such as $C(t)$ and $C_{RI}(t)$, and look at their long-time behavior. We expect from this second run that $C(t_0) = 0$ and $C_{RI}(t_0) = q^{(1)}$, the first moment of the order parameter distribution. $q^{(1)}$ is also calculated by making the average of the overlap between configurations of the two replicas. This last test is particularly good, since we compare quantities obtained in different ways. If they do not agree, a full equilibrium is not yet achieved, and we have to thermalize the system for a longer $t_0$. We used always this criterion

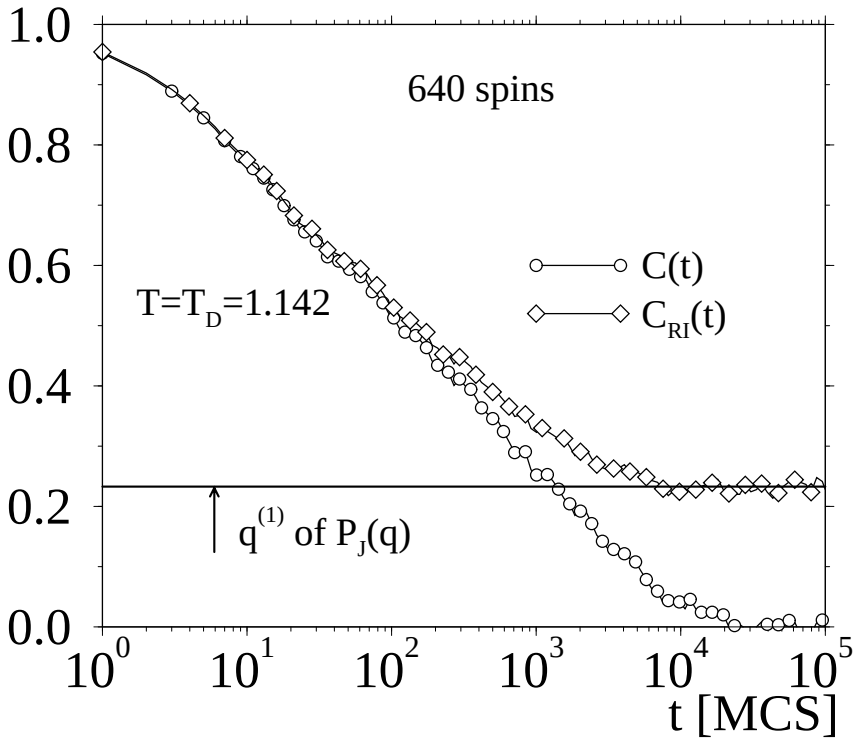


**Figure 3.1:** Correlation functions for a single sample. The results refer to the infinite range model with $640$ spins at $T = T_D = 1.142$. We have let the system thermalized for a time $t_0 = 10^5\ MCS$ and then started to record the functions. We show also the comparison of the long-time limit of $C_{RI}(t)$ with the first moment of the order parameter distribution for the sample, obtained from the overlap of two replicas configurations. The agreement is indicative of reached thermalization.

(Bhatt and Young, 1988) self-consistently for every sample and at every temperature, checking the properties of the correlation functions at the end of the equilibrium run after a thermalization run of the same length as the observation time. If convergence and de-correlation are not found, we thermalize the system for longer times and repeat the procedure. As an example we show $C_{RI}(t)$ for a single sample of $640$ spins at $T = T_D = 1.142$ in Fig. 3.1. The system has been equilibrated for a time $t_0 = 10^5 MCS$. We see that the long time limit falls directly onto the line representing the value of $q^{(1)}$ obtained from the overlap of two replicas of the system. Also shown is the spin autocorrelation function $C(t)$. Its relaxation is slower. In checking for equilibrium, we always waited also for a complete de-correlation of $C(t)$. When lowering the temperature we pay attention to use as starting configurations, for the thermalization run, equilibrium configurations obtained at a higher temperature. This makes thermalization easier to achieve with respect to the use of random initial configurations (corresponding to $T \to \infty$).

## 3.4 The parallel tempering method

The conventional Metropolis and Heat-Bath schemes suffer the problem that they slow down upon decreasing the temperature. This means that the equilibration time grows, for a fixed system size, as a power law (in a system where a phase transition is expected). For the infinite-ranged Potts model we found that $\tau \propto (T - T_D)^{-2}$. Moreover, close to the phase transition temperature, [2] the relaxation times grow as a function of the system size as $N^{1.5}$. Below the region where we expect a dynamical transition in the thermodynamic limit, relaxation times start to grow exponentially as a function of the inverse temperature and of the square root of the system size. This makes it impossible to equilibrate a system of $320$ spins below $T = 0.9$ in a reasonable computer time. It takes, at that temperature and system size, about $12$ hours on a Pentium II processor ($400$ MHz) to equilibrate a single sample (this number must then be multiplied by $4$ in order to study the dynamics and the statics in equilibrium).

New numerical methods have recently been developed that permit to improve the efficiency of Monte Carlo simulations in spin glasses and disordered systems with slow dynamics. Although the problem of getting rid of slowing down in disordered system has not yet been solved, progresses have been made in developing optimized methods. For a recent review see (Marinari, 1996). We decided to implement the one that up to now proved to be quite effective, the *parallel tempering* method (Hukushima and Nemoto, 1996).

At low temperature, in spin glasses and other disordered systems, a lot of local energy minima appear in the phase space, separated by barriers, as we have seen in section 2.1. In order to properly thermalize the system, all these regions have to be visited. But the characteristic time needed by the system to escape from a local minimum increases very rapidly upon lowering the temperature. We need therefore to "help" the system escaping local minima, avoiding in this way long relaxations. One possible way is to make use of an extended canonical ensemble. A collection of replicas of the sample is considered. To each of them we attribute a different temperature, in such a way to span a range including high and low temperature values. We let then evolve the replicas canonically and independently for a few Monte Carlo steps, and then try to exchange the temperature between replicas (with small temperature difference) according to an energetic Boltzmann criterion. We hope in this way to let the system explore more easily the phase space, by introducing additional possibilities of warming and cooling through the exchanges, so that escaping from minima is facilitated. Alternatively, one can look at this process as an exchange of configurations, that is configurations instead of temperatures, of a pair of replicas are exchanged. The two representations are equivalent.

This is just a naive interpretation of the method, whose formalism (Hukushima and Nemoto, 1996) is rather general and clarify the two interpretations. The extended ensemble is made of $M$ different replicas of the sample we want to simulate, which is described by a Hamiltonian $H(X)$. With $X$ we denote, for simplicity, all the microscopic spin variables, $X = \{\vec{S}_1, \cdots, \vec{S}_N\}$. $N$ is the total number of spin. To the $m$-th replica $X_m,\ m \in \{1, \ldots, M\}$ we associate an inverse temperature $\beta_m = (k_B T_m)^{-1}$. The state of the extended system is specified by the set

[2] This specific results will be discussed in more detail in the chapter devoted to the simulation of the infinite ranged model. We anticipate them here to give an idea of the difficulty we encountered facing these relaxation times.

$\mathbf{X} = \{X_1, \cdots, X_M\}$. With $\boldsymbol{\beta} = \{\beta_1, \cdots, \beta_M\}$ we indicate the set of temperatures, and for simplicity we assume $\beta_m > \beta_{m+1}$. The partition function is given by

$$\mathcal{Z}(\boldsymbol{\beta}) = \prod_{m=1}^{M} e^{-\beta_m H(X_m)} = \prod_{m=1}^{M} Z(\beta_m) \tag{3.20}$$

where $Z(\beta)$ refers to the original system. Once the set $\boldsymbol{\beta}$ is specified, the probability distribution of $\mathbf{X}$ is

$$\begin{aligned} \mathcal{P}(\mathbf{X}, \boldsymbol{\beta}) &= \prod_{m=1}^{M} P(X_m, \beta_m) \\ P(X, \beta) &= \frac{e^{-\beta H(X)}}{Z(\beta)}. \end{aligned} \tag{3.21}$$

The detailed balance is satisfied for the normal Monte Carlo spin-flip moves between attempts to exchange configurations between replicas. To prove it also for the global exchanges, we can introduce a transition matrix $W(X, \beta | X', \beta')$, which defines the probability of exchanging temperatures between two replicas, with configurations $X$ and $X'$ and temperatures $\beta$ and $\beta'$. Then, the detailed balance condition requires

$$\begin{aligned} &\mathcal{P}(\ldots; X, \beta; \ldots; X', \beta'; \ldots) W(X, \beta | X', \beta') = \\ &\mathcal{P}(\ldots; X', \beta'; \ldots; X, \beta; \ldots) W(X', \beta' | X, \beta). \end{aligned} \tag{3.22}$$

Combining eqs. (3.21) and (3.22) one obtains the condition

$$\frac{W(X, \beta | X', \beta')}{W(X', \beta' | X, \beta)} = e^{-\Delta} \qquad \text{with} \qquad \Delta = (\beta' - \beta) \left[ H(X) - H(X') \right]. \tag{3.23}$$

In this way, adopting the usual Metropolis criterion, the transition probability for the exchange is

$$W(X, \beta | X', \beta') = \begin{cases} 1 & \text{for} \Delta \leq 0 \\ e^{-\Delta} & \text{for} \Delta > 0. \end{cases} \tag{3.24}$$

The canonical thermal average for an observable $\mathcal{O}$, at the inverse temperature $\beta$ is given by

$$\langle \mathcal{O} \rangle_\beta = \frac{1}{t_{MAX}} \sum_{t=1}^{t_{MAX}} \sum_{m=1}^{M} \mathcal{O}\left(X_m(t)\right) \delta_{\beta, \beta_m(t)} \tag{3.25}$$

where we introduce, for the $m$-th replica, time dependent configuration $X_m(t)$ and temperature $\beta_m(t)$; $t_{MAX}$ is the total number of Monte Carlo sweeps.
As we already said, we can look at the algorithm as an exchange of configurations instead of temperatures. The same derivation applies, and for every $m \in \{1, \ldots, M\}$ the thermal averages are then computed as

$$\langle \mathcal{O} \rangle_{\beta_m} = \frac{1}{t_{MAX}} \sum_{t=1}^{t_{MAX}} \mathcal{O}\left(X_m(t)\right). \tag{3.26}$$

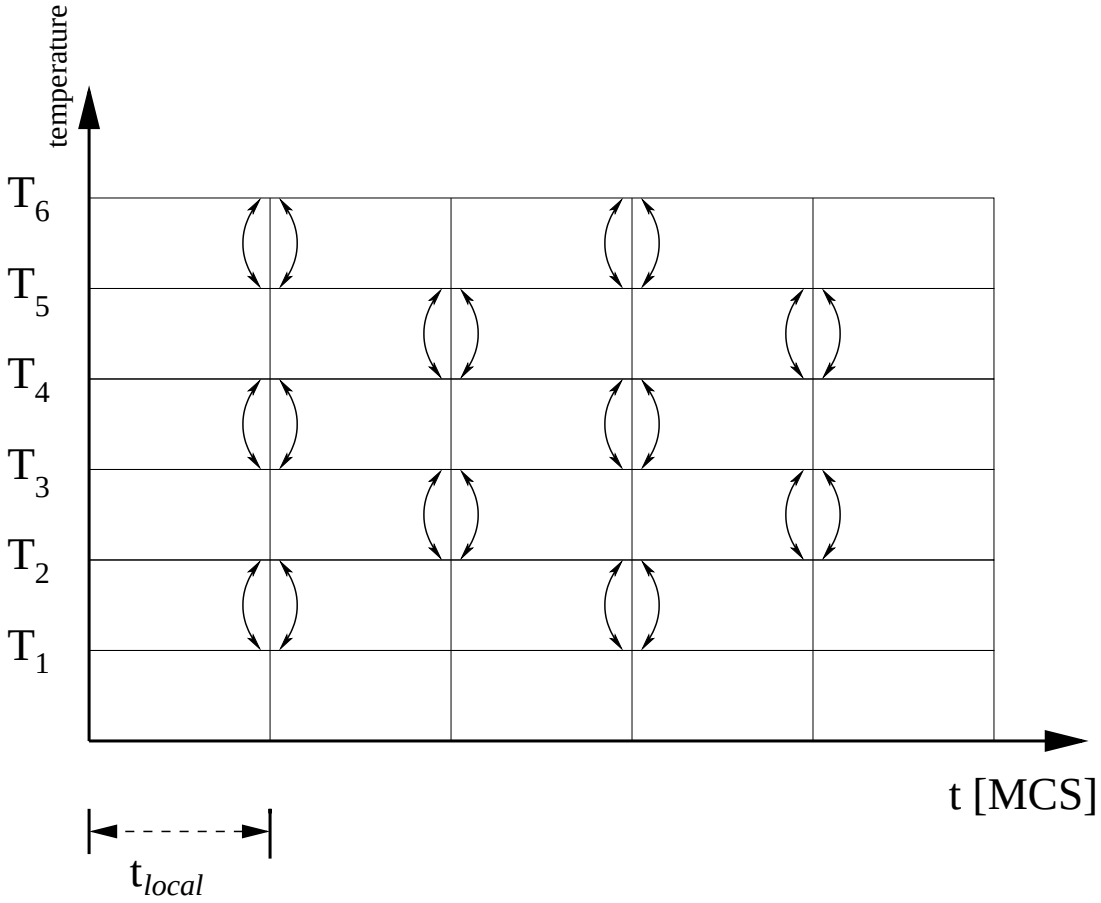


**Figure 3.2:** Representation of the exchange scheme for the parallel tempering method. A system of $6$ replicas is considered here, and the picture shows the alternating scheme used to attempt to exchange temperatures between different systems.

We describe now the actual Monte Carlo procedure we adopt to realize the described algorithm. Two types of steps are performed:

1. every replica is updated with standard Metropolis algorithms for a number of $t_{local}$ sweeps; an exchange of temperature is attempted between the replicas having inverse temperatures $\beta_i$ and $\beta_{i+1}$, with $i = 2n-1,\ n \in \{1, 2, \ldots, M/2\}$. We use always adjacent values in order to maximize the acceptance rate of the move;

2. the replicas are then again updated locally for $t_{local}$ sweeps; an exchange of temperature is attempted between the replicas having inverse temperatures $\beta_i$ and $\beta_{i+1}$, with $i = 2n,\ n \in \{1, 2, \ldots, M/2-1\}$.

The scheme of this exchange process is illustrated in Fig. 3.2. For simplicity, we show an example with six replicas. The horizontal axis gives the Monte Carlo time, and in the vertical axis the various temperatures are indicated. Here they are equally spaced, but in principle they

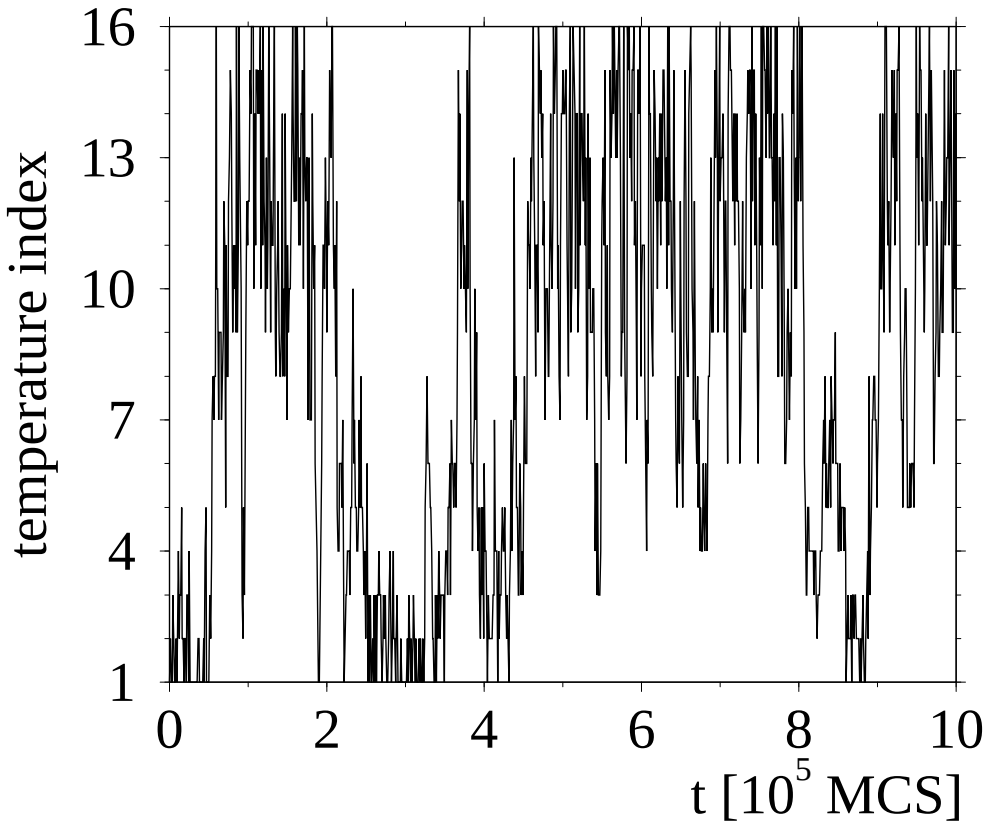


**Figure 3.3:** Random walk of a replica of the system in the temperature space. The extended ensemble consists of $16$ different replicas and the temperature range is $[0.7, 1.964]$. The size of the system is $320$ spins.

need not to. Every $t_{local}$ moves, temperature exchanges between the various replicas are proposed as in the algorithm described above, alternating the pairs involved [3].

During the Monte Carlo run, every replica will visit the various temperatures, making in this way a random walk in temperature space. In order to obtain a proper thermalization, every replica has to spend on average the same amount of time in every temperature, avoiding to be trapped only at low temperatures. Looking at a random walk, this means that each replica has to travel up and down visiting each temperature level.

Up to now we did not comment about the choice of the temperature set. Much freedom is given, the important thing is to select them in order to have significant probability of actually performing the exchange, improving in this way the efficiency of the algorithm. The exchange probability is given by energy difference multiplied the inverse temperature difference. In the canonical ensemble, the total energy distribution of a system at a temperature $T$ can be well approximated

[3] This is only one of the possible realization of the temperature exchange. Other possibilities could be to try to involve all the pairs after the local update, or to select randomly a pair every local update.

by a Gaussian distribution

$$P_T(E) = \frac{1}{\sqrt{2\pi}\sigma(T)} \exp\left[-\frac{(E(T) - \langle E(T)\rangle)^2}{2\sigma(T)}\right]. \tag{3.27}$$

Both $\langle E(T)\rangle$ and $\sigma(T)$ are functions of the temperature. In order to have a good probability

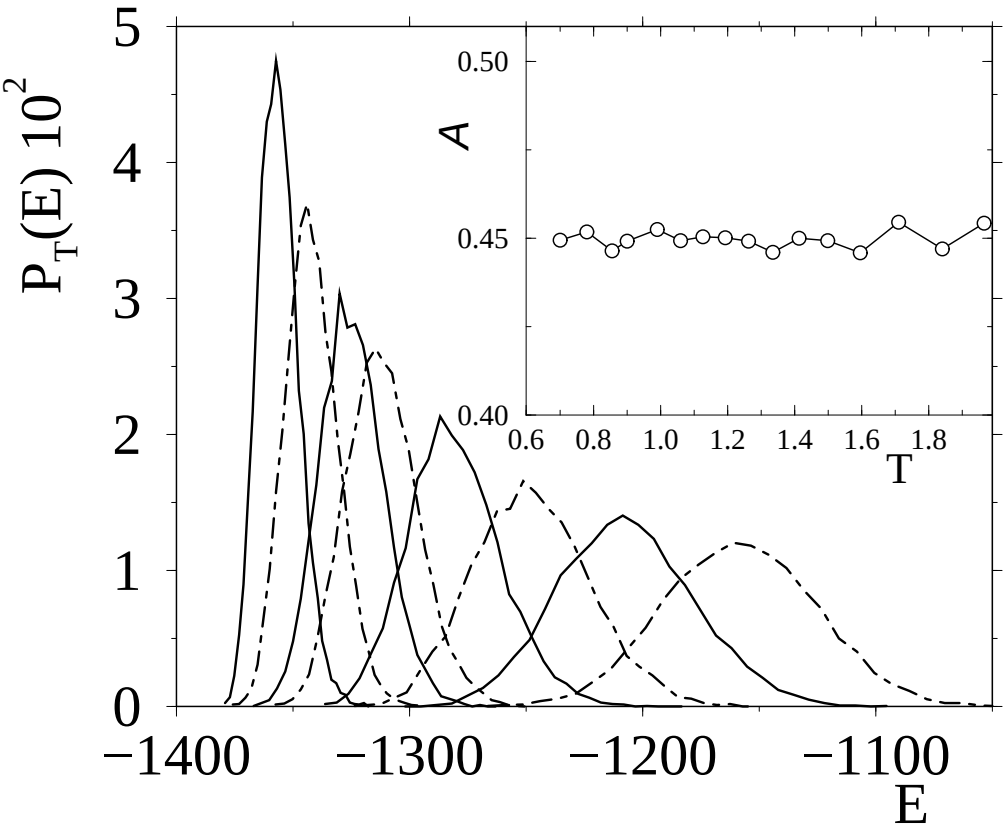


**Figure 3.4:** Energy distribution for s system of $320$ spins. This is the result of a parallel tempering run with $16$ replicas. Here we show the results for $8$ temperatures in the range $[0.7, 1.193]$. In the inset we show the acceptance rate during the same run. It is practically constant in the whole temperature range. The $16$ temperatures used in the $N = 320$ simulations are obtained making use of formula (3.28).

of exchange, the Gaussian distributions of the energy at the two temperatures have to overlap considerably, otherwise the Metropolis factor will be small. Therefore the first condition for an efficient algorithm is to take a set of temperatures with good overlapping of the energy distributions between neighboring values. This can be verified also *a posteriori*, calculating the acceptance rate at every temperature. The temperatures can be equally spaced. The problem with this choice is that, for low temperatures, the acceptance rate will be small, since $\sigma_i$, and consequently the overlap between temperatures, tends to decrease with the temperature. One

should then try to make it uniform. Suppose we have a good knowledge of the temperature dependence of $\langle E_T \rangle$ and $\sigma_T$. We could then reconstruct the distribution (3.27). We could then, given two temperatures $T_i$ and $T_{i+1}$, guess in advance the acceptance rate $\mathcal{A}(T_i, T_{i+1})$ through the formula

$$\begin{aligned} \mathcal{A}(T_i, T_{i+1}) &= \int\int dxdy g(x,y) P_{T_i}(x) P_{T_{i+1}}(y) \\ g(x,y) &= \min\left\{1, \exp\left[-(y-x)(\beta_i - \beta_{i+1}]\right\}\right. . \end{aligned} \tag{3.28}$$

In this way, we could set up a numerical procedure, starting from the lower temperature and the acceptance rate we would like to have, calculating step by step the successive temperature through a numerical integration of (3.28). All we need to know then is the temperature dependence of the average energy and its variance. To do so in a wide range of temperatures, we can just use a preliminary parallel tempering run with equally spaced temperatures. In this way we will obtain a plot for both $E(T)$ and $\sigma(T)$. We can then use a polynomial fit to interpolate between them, and use the results for the calculations of $\mathcal{A}$. In spin glasses simulations the advantage is that one can use for every realization of disorder the parameters calculated for one sample, since for quantities related to the energy the sample-to-sample fluctuations are not strong. We show the results of such a method in the inset of Fig. 3.4. The acceptance rate is presented for the same system of $320$ spins, with a set of temperatures optimized according to (3.28). This is the measured accepted rate, that is number of exchanges divided the total number of attempts. The same procedure has been used successfully in parallel tempering simulations of supercooled liquids (Stühn, 2000).

We discuss now how to actually check the thermalization of the system.

As we said, a rapid first check is to control the random walk performed by each replica in the temperature space. If the system is not thermalized, the replica can get stuck in one of the temperature levels. An example of well-behaved random walk is given in Fig. 3.3. Every replica has to visit each temperature in the set with a similar frequency, on the order of the inverse number of total Monte Carlo steps divided by the total number of temperatures. It is then also important to check that no observable is drifting in time, after a sufficient equilibration time. This is analogous to what we already explained referring to standard spin flip algorithms, see section 3.3. Again, we concentrate on the energy per particle, easy to check during a run, and the order parameter $q$. Looking at the results on a logarithmic time scale helps better in locating drifts.

The use of fluctuation dissipation relation also helps in checking thermalization. We employ the following formula, relating the specific heat $c$ to the fluctuations of the energy

$$\frac{d\langle e \rangle}{dT} = c = \frac{N\left(\langle e^2 \rangle - \langle e \rangle^2\right)}{(k_B T)^2}. \tag{3.29}$$

The right hand side of this equation can be calculated for every temperature, the left hand side requires to do the derivative numerically once we have the value of $e$ at every temperature. The results for the parallel tempering algorithm are shown in Fig. 3.5a. If non equilibrium effects are present, the fluctuation dissipation theorem would be violated and the two curves would show significant drifts (Yamamoto and Kob, 2000).

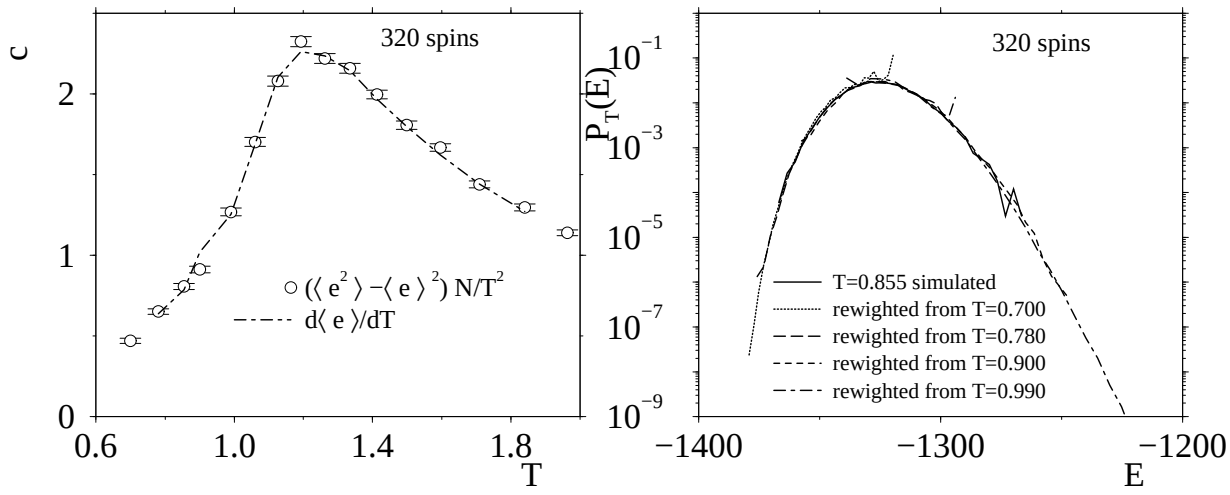


**Figure 3.5:** (a) Specific heat as a function of temperature calculated in two different ways, as derivative of the energy per spin and as a function of the energy fluctuation. The compatibility of the two results is an indication that thermalization is achieved. (b) Reweighting of the energy distribution. The chosen temperature is $T = 0.855$. Four other curves are shown, the distributions reweighted produced with data at different temperatures, as indicated.

In the same spirit, one can also check the possibility of reweighting, that is to obtain information about static quantities at a temperature $T$ making use of those obtained for a $T^*$, provided that the overlap of the energy distribution between them is appreciable. For a general discussion of the method and its applications see (Newman and Barkema, 1999; Landau and Binder, 2000). We concentrate here on the possibility of obtaining $P_T(E)$ from the knowledge of $P_{T^*}(E)$. The relation between them is

$$P_T(E) = \frac{P_{T^*}(E)\exp(\beta E)}{\int dE' P_{T^*}(E')\exp(\beta E')}. \tag{3.30}$$

We can obtain them for all the temperatures from the simulation, and then try to reweight each of them to other temperatures, in order to compare. This is also a good test for equilibrium. In case of non proper thermalization, the system does not explore fully and properly all the energy spectrum at a certain temperature, and reweighting does not work properly. An example concerning the properties of low-temperature results is given in Fig. 3.5b.
Note that we can define a time autocorrelation function also for the parallel tempering dynamics, which is not realistic because the system visits different temperatures, but can help to check the de-correlation of the configurations. It is defined as

$$C_{PT}(t,\beta) = \frac{1}{NM(p-1)} \sum_{m=1}^{M}\sum_{i=1}^{N} \langle \left(p\delta_{\sigma_i(t'),\sigma_i(t+t')} - 1\right)\rangle_{\beta}^{(m)}. \tag{3.31}$$

The superscript $(m)$ refers to the fact that each thermal average has to be computed separately between configurations belonging the same replica, and the subscript refers to the fact that $\{\sigma_i(t')\}$

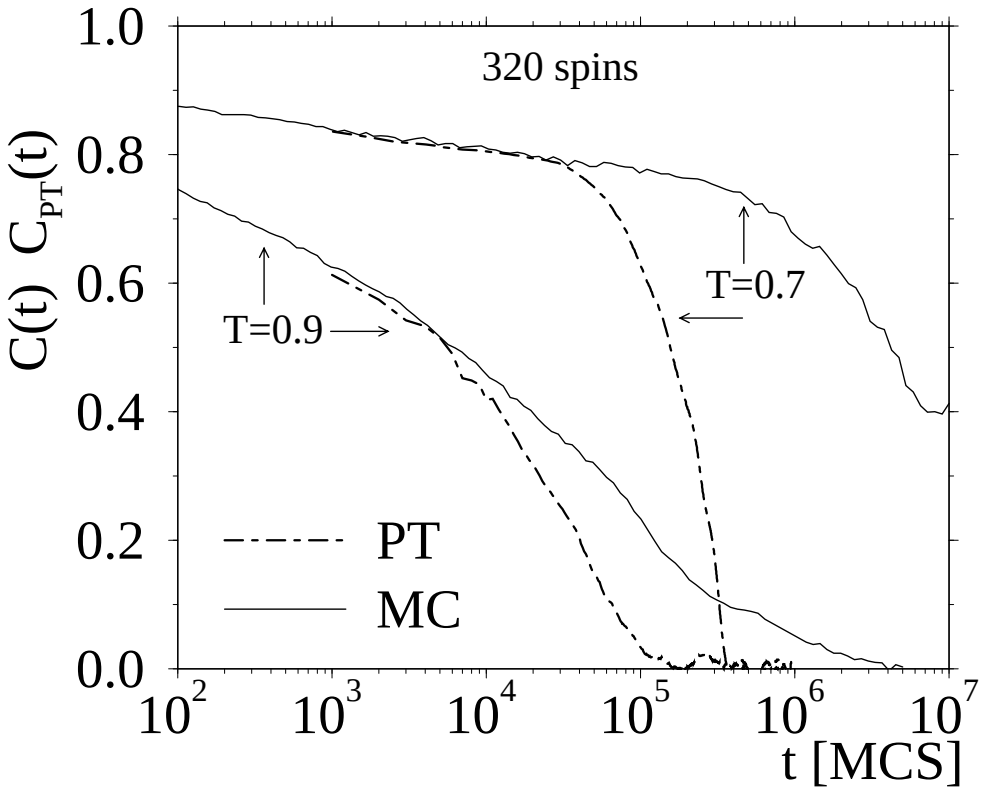


**Figure 3.6:** Spin autocorrelation functions for the standard spin flip Metropolis algorithm (MC) and parallel tempering method (PT), for a single sample of $320$ spins, at two different temperatures $T = 0.7$ and $T = 0.9$.

and $\{\sigma_i(t + t')\}$ must be at the same temperature $\beta$. As usual, before starting to measure this correlation function, we always let the system equilibrate for the same amount of Monte Carlo sweeps that constitutes our observation time. De-correlation is achieved when this autocorrelation function goes to zero. We can then also compare the efficiency of the parallel tempering algorithm with respect to the standard Metropolis. In Fig. 3.6 we show the spin autocorrelation functions of the two methods at two different temperatures. The curves regarding the Metropolis case have been produced with runs having as starting point thermalized configurations produced with parallel tempering. From the different curves we recognize that at the higher temperature the PT method leads to a relaxation which is more than one decade faster than the one of the standard Monte Carlo procedure. This factor has increased to more than 100 at the lower temperature and we see that at this temperature the equilibration of the system with the standard Monte Carlo method becomes hardly feasible. We have also checked that this type of speedup is typical in that it does not depend on the realization of the disorder, i.e. the bonds $J_{ij}$ in the Hamiltonian.

As last remark, we discuss the dependence of the algorithm on the time $t_{local}$, that is the number of standard Monte Carlo sweeps occurring between successive attempts to exchange temper-

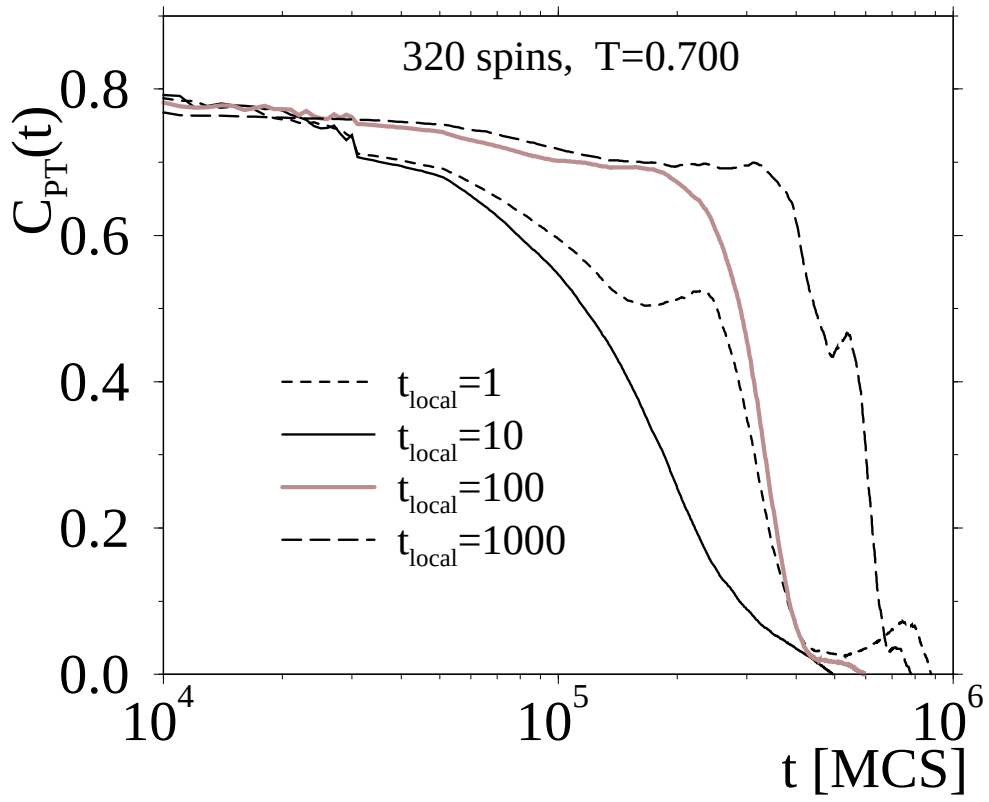


**Figure 3.7:** Spin autocorrelation functions for the parallel tempering method, for different values of $t_{local}$.

atures between replicas. We found that for the system sizes investigated ($N = 160, 320, 640$), $t_{local} = 10$ was a good choice. Other values, smaller or larger, lead to a slower de-correlation, although this effect is really strong for $t_{local} \geq 100$. A possible explanation is that the individual replicas need to relax a bit at the new temperature after the exchange, so that then the successive exchange process can be successful. A too short $t_{local}$ cannot permit that, while if it is too long the system spend lot of time inside each temperature and the exchange process is not effective. An example is shown in Fig. 3.7. This quantity $t_{local}$ is also a lot dependent on the way the algorithm is actually set up, so that a preliminary observation is always needed.

## 3.5 The random number generator

The essential point in every Monte Carlo simulation is the generation of a sequence of uniformly distributed random numbers, which are used in the part of the algorithm concerned with the acceptance of moves. Random numbers are also used in choosing which spin in the lattice we should try to flip, and in our particular case which Potts state we try to assign, if we use the Metropolis criterion. Using spin glass models, we face also the need of producing different realizations of disorder, that is for every different sample the interactions are taken according to

a particular distribution.

Numbers in itself are not random, is the sequence that has to be such. However, these sequences are produced by deterministic algorithms, and so, correctly speaking, are pseudo-random sequences. These algorithms produce sequences of numbers uniformly distributed in a chosen interval, and a good-quality generator must not produce correlation between numbers over a long period, since extensive simulations require very long uncorrelated sequences. Just to refer to our case, we made runs as long as $10^8$ MCS with $1000$ spin in the short range case, and this imply the use of $10^{11}$ random numbers per single run.

The method commonly used to generate a sequence is to apply a certain function to the element number $n$ of the sequence in order to produce the next one, that is $i_{n+1} = f(i_n)$. The first number of the sequence is called seed, and even though one uses the same function $f$ one can generate different sequences by changing seed. This is essential, otherwise one would need a different algorithm for every run. Operations are performed between integers, and eventually all the numbers are normalized to the biggest producible number (we are considering here, as general example, the generation of numbers in the interval (0,1)). The most widely used functions are part of a class called *linear congruential generators*:

$$i_n = (\mathrm{a} i_{n-1} + \mathrm{c}) \bmod m. \tag{3.32}$$

In this case, a,c, and m are "magic" numbers, in the sense that choosing them appropriately will produce sequences of good quality. With good quality one usually means ergodicity, i.e. all the numbers must occur, and "randomness", i.e. as little correlation as possible. This statement is unavoidable since these numbers are created by means of an algorithm. A discussion along these lines can be found in (Newman and Barkema, 1999) and references therein. However a drawback is that linear congruential generators produce sequences that have a period of at most $2 \cdot 10^9$, using $31$-bit integers, so it is very likely that if we use to produce longer sequences, we would introduce correlations that would affect the results. One must also keep in mind that the period we mention is the theoretical maximum, so it can also happen to have sequences with even shorter periods.

Various strategies have been found to overcome the problem, see (Newman and Barkema, 1999; Landau and Binder, 2000). We adopted a recently developed generator (Blöte et al., 1995). We give just a short description of it. Details as well as references to the mathematical literature upon which the generator is based can be found in the article cited and references therein. Using the idea of shift-register generator, one generates bit strings $a_i$ with standard methods. A new series $a_i^{'}$ is produced out of them, by performing shifting operation on the previous one, $a_i^{'} = a_{i-9218} \oplus a_{i-9689}$, where $\oplus$ represents the bitwise modulo-2 addition of two integers. Again there is the presence of magic numbers. In the same way, another sequence is produced, $b_i^{'} = b_{i-97} \oplus b_{i-127}$. At the end, these two sequences are used to produce the final sequence, $r_i^{'} = a_i^{'} \oplus b_i^{'}$. This random number generator has been tested successfully on the three dimensional regular Ising model giving excellent results (Blöte et al., 1995).

## 3.6 Details of the simulations

We give now some technical details of the simulations we have done. In the next tables, 3.1, 3.2, 3.3, we show for the various models and algorithms used the longest runs we have made. The first two regard the single spin flip Monte Carlo, both in the infinite range and in the short range case. We indicate the lowest temperature we could investigate and the corresponding length of the run. This latter number must be multiplied by two, since it is the time it takes to the system to equilibrate. After that, we let it evolve for the same time, performing the measurements. We indicate also the total number of different realization of disorder investigated. As we said in fact, in spin glass simulations one has to perform also average on disorder, in addition to the usual thermal average. The third table is devoted to the parallel tempering algorithm, used only in the infinite range case. Here we indicate also the total number of replicas used for every run (remember that the parallel tempering algorithms simulate more replicas simultaneously). Other runs, e.g. the dynamics at very low temperatures produced starting from equilibrated PT configurations, or the Gaussian interactions in the three dimensional case, are described in the related chapters.

**Table 3.1:** Infinite range system with the single spin flip Metropolis algorithm (Gaussian interactions). We show, for every system size, the minimum temperature investigated, the time it takes to equilibrate, and the number of different realizations of disorder.

| Size $N$ | $T_{min}$ | lenght of the run (MCS) | number of samples |
|---|---|---|---|
| 160 | 0.9 | $10^7$ | 500 |
| 320 | 0.9 | $10^7$ | 100 |
| 640 | 1.0 | $5 \cdot 10^6$ | 100 |
| 1280 | 1.142 | $6 \cdot 10^5$ | 100 |
| 2560 | 1.2 | $10^5$ | 20 |

**Table 3.2:** Short range system with the single spin flip Heat Bath algorithm. We show, for every system size, the minimum temperature investigated, the time it takes to equilibrate, and the number of different realizations of disorder.

| Size $N$ | $T_{min}$ | lenght of the run (MCS) | number of samples |
|---|---|---|---|
| 216 | 1.5 | $10^8$ | 100 |
| 1000 | 1.5 | $10^8$ | 100 |
| 4096 | 1.6 | $10^7$ | 50 |

**Table 3.3:** Infinite range system with the parallel tempering algorithm. We show, for every system size, the minimum temperature investigated, the time it takes to equilibrate, the number of different realizations of disorder, and the number of replicas used.

| Size | $T_{min}$ | lenght of the run (MCS) | number of samples | replicas |
|---|---|---|---|---|
| 160 | 0.7 | $10^6$ | 400 | 16 |
| 320 | 0.7 | $10^6$ | 200 | 16 |
| 640 | 1.0 | $5 \cdot 10^5$ | 100 | 16 |

# Chapter 4

# The infinite range Potts glass

## 4.1 Static properties

In this chapter we investigate the fully connected Potts glass with $p = 10$. The Hamiltonian is given by

$$\mathcal{H} = -\frac{1}{2}\sum_{i,j} J_{ij}(p\delta_{\sigma_i\sigma_j} - 1). \tag{4.1}$$

The sum is on every couple of different spins. All the spins are therefore connected though the coupling $J_{ij}$. They are taken from a Gaussian distribution

$$P(J_{ij}) = \frac{1}{\sqrt{2\pi}\Delta J}\exp\left[-\frac{(J_{ij} - J_0)^2}{2(\Delta J)^2}\right]. \tag{4.2}$$

Since it is an infinite range model, as we explained in chapter 2 a proper scaling of these variables is needed to ensure a finite thermodynamic limit. So the first two moments are given by

$$J_0 = \frac{3-p}{N-1} \tag{4.3}$$

$$(\Delta J)^2 = \frac{1}{N-1}. \tag{4.4}$$

Using these parameters eliminates the problem of the tendency to ferromagnetism above the spin glass transition temperature. Also the second transition temperature is not close to the spin glass transition temperature, since with this choice of parameters it occurs at $T_2 = 1/2$. In this way we pay attention not to mix different behaviors so as to concentrate only on the paramagnet-to-spin glass transition. We recall that, in these units, the expected dynamical transition temperature in the thermodynamic limit is at $T_D = 1.142$ and the static transition temperature at $T_0 = 1.131$ (De Santis et al., 1995). We always use units in which $k_B = 1$.

### 4.1.1 Energy and entropy

We present the results of our simulation of the $10-$state Potts glass with infinite range interactions, starting from the discussion of the internal energy of the system. Fig. 4.1a shows a plot of the energy per spin versus inverse temperature, over the whole range of temperatures investigated ($0.7 \leq T \leq 2$). As we said, in the choice of the parameters of our Hamiltonian (eq. 4.1) we paid attention to stay away from every possible ordering of ferromagnetic type, so the temperatures $T_F$ and $T_2$, discussed in chapter 2 and calculated above for this model, are outside of this range (in fact $\beta_F \equiv 1/T_F \approx 1.88$, $\beta_2 \equiv 1/T_2 = 2.0$). We choose to plot the energy as a function of $\beta$ because a linear dependence is predicted in the thermodynamic limit above the static transition temperature (replica symmetric theory) (Elderfield and Sherrington, 1983a). Also the theoretical prediction for $N \to \infty$ obtained within the one-step replica symmetry breaking solution (De Santis et al., 1995), is included in the plot. This figure reveals unexpectedly large finite size effects over a broad temperature regime: only for $\beta \lesssim 0.6$ the energy coincides with the asymptotic result, starting from $N = 640$. For $\beta \gtrsim 0.6$ clear deviations from the asymptotic solution are visible, which are larger for smaller $N$. Our numerical data for finite $N$ reveal only a smooth crossover from the disordered (paramagnetic) high temperature phase to the low temperature spin glass-like phase: no indication of the kink at $\beta_0$, predicted by the one-step replica symmetry breaking theory and signaling the occurrence of the phase transition is yet visible; furthermore, as expected, there is no effect of the presence of the dynamical transition on static quantities like the energy. It is interesting to discuss further the size dependence of the convergence of the energy to the thermodynamic limit. The calculation of finite size corrections to the thermodynamic behavior for various quantities in the Ising spin glass has been carried out analytically (Parisi et al., 1993a; Parisi et al., 1993b); it was found that, at the critical temperature $T_c$

$$e_c = e_c^{\infty} + e_c^{'} N^{-2/3} + e_c^{''} N^{-1} + \cdots \tag{4.5}$$

(analogous formulae can be obtained also for the order parameter and its moments, as we will discuss in section 4.1.2). Although this result is based on an infinite level of replica-symmetry-breaking, the exponents can be understood phenomenologically for analogous second-order transitions, in particular in the $p = 3$ Potts glass (at the heart of the reasoning in fact is the Landau expansion of the free energy close to the critical temperature) (Dillmann et al., 1998). However such a phenomenological understanding cannot be directly applied to the $p = 10$ case, being the phase transitions of different nature, and an extension of eq. (4.5) to the case of first order transition without latent heat is still lacking at the moment. A finite size scaling analysis of our data is presented in Fig. 4.1b, where we plot $e(N,T) - e(\infty,T)$ for three different temperatures and various system sizes. We see that well above (as expected) but also below the region of the phase transition the data are compatible with a $N^{-1}$ leading correction; however in the vicinity of $T_0$ a different exponent, compatible with $-2/3$ comes into play (see inset of Fig. 4.1b). It seems then that also in the $p = 10$ case the leading order correction of eq. (4.5) is valid; we will see an analogous behavior also for the moments of the order parameter [1].

[1] Note that we plot here data for $T_D$ instead of $T_0$ since we have simulated more system sizes at this temperature. Actually such a different "critical" exponent should be correct only at $T_0$ exactly, and even at $T_D$ only a crossover

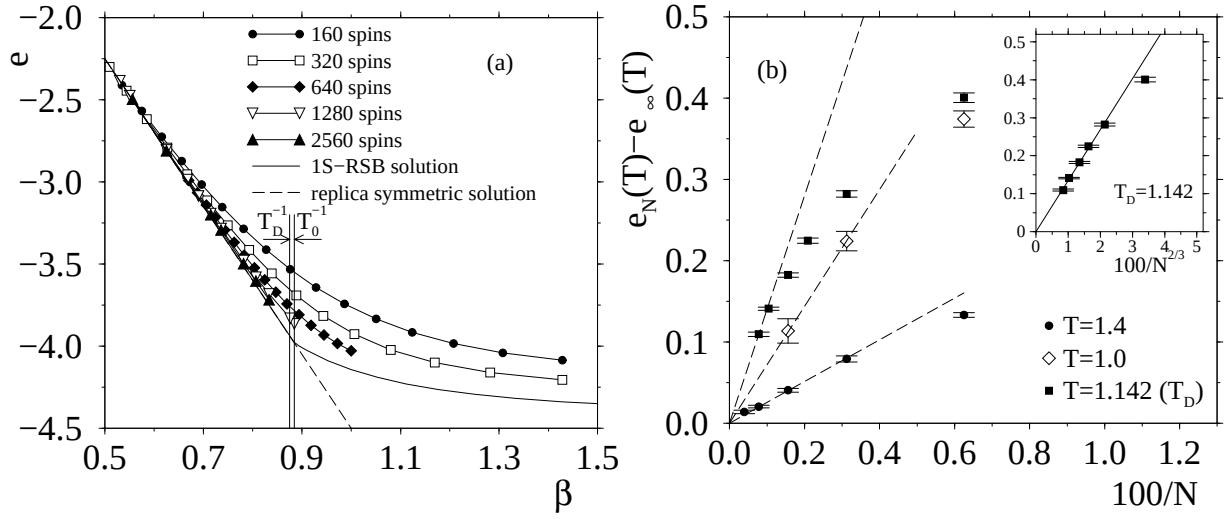


**Figure 4.1:** (a) Energy $e$ per spin as a function of the inverse temperature $\beta = 1/T$ for different system sizes (curves with symbols). The bold solid curve shows the one step replica symmetry breaking solution (De Santis et al., 1995), the broken curve - which coincides with the former for $T \geq T_0$ - is the replica symmetric solution, eq. (2.24). The thin vertical lines indicated the inverse temperatures $\beta_D$ (left) and $\beta_0$ (right) of the dynamical transition and the static transition, respectively. (b) Analysis of the size dependence of the energy difference $e_N(T) - e_\infty(T)$, using the one-step replica symmetric solution (De Santis et al., 1995) to calculate $e_\infty(T)$. The inset shows the data at $T = T_D = 1.142$ plotted versus $N^{-2/3}$ instead of $N^{-1}$.

The energy is related to the first derivative of the free-energy: given the fact that the spin glass transition in this model is expected to have no latent heat of transition (although the order parameter jumps discontinuously at the static transition), it does not show any singularity or discontinuity (Stanley, 1971). A discontinuity is instead expected in the specific heat (Gross et al., 1985), which we plot together with the solution obtained in the framework of 1S-RSB, for different system sizes in Fig. 4.2. We recall that a direct calculation of the specific heat from the simulation for every temperature can be obtained (without having to calculate derivatives of the energy) by using

$$c = \frac{\left[\langle \mathcal{H}^2 \rangle - \langle \mathcal{H} \rangle^2\right]_{av}}{NT^2}. \tag{4.6}$$

Again the convergence to the thermodynamic limit is clear, especially for temperatures above the static transition one; close to $T_0$ the height of the maximum is particularly affected by the rounding off of the transition, and below not much can be said, only the qualitative behavior seems to be the same also for finite $N$. A standard way to locate phase transition of standard type is to locate the maximum of the specific heat (due to the tendency to a divergence in the thermodynamic limit, or to the developing of a discontinuity). We can also analyze the maximum

towards the high temperature $N^{-1}$ behavior should be present for $N$ very large. However, since the two temperatures are so close to each other this does not matter for the system sizes investigated here.

for the different curves, trying in this way to extrapolate the position of the expected discontinuity in the thermodynamic limit, which is alway rounded off for finite systems. This procedure has been employed in previous studies of similar models with small system sizes but a high statistics regarding the realizations of disorder (Peters et al., 1996; Dillmann et al., 1998), finding a leading size correction to both the position and the height of the maximum scaling like $N^{-1/2}$. We show the results of such extrapolation, done interpolating the points and locating the region of the maximum, in the insets of Fig. 4.2. Since we do not have many points, we just took the $N^{-1/2}$ dependence to see the compatibility with our data: although affected by relatively large error bars, they are compatible, and also a value compatible with $T_0 = 1.131$ can be obtained. The extrapolation of the data gives $1.13 \pm 0.02$, since the points themselves are affected considerably by uncertainties. In order to make a careful study, one should perform a high statistics (in this case reweighting procedures can be useful) study close to the region of the maximum; however, it does not seem that this is a practical procedure, since one should go to rather large value of $N$ and very close to $T_0$, a purpose that is at present simply not feasible for $N \gtrsim 2000$. Besides, one should also note that this pronounced discontinuity is typical only of mean-field models; experimental systems and also lattice models in finite dimensions show usually a very broad and flat region of maximum around the phase transition temperature (Fischer and Hertz, 1991).

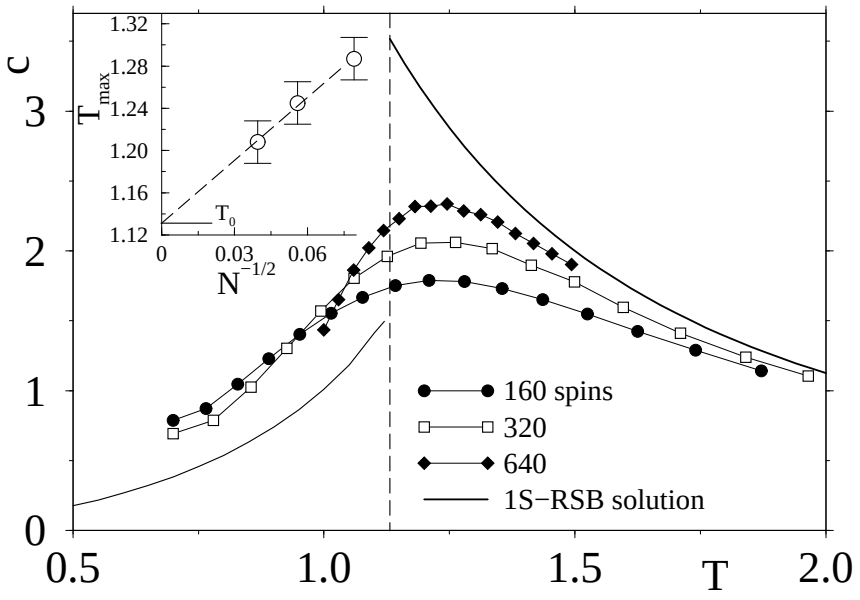


**Figure 4.2:** Specific heat as a function of the temperature for system sizes $N = 160, 320, 640$; the solid line shows the solution in the thermodynamic limit (De Santis et al., 1995). In the inset the size dependence of the position of the maximum of the three curves, plotted as a function of $N^{-1/2}$; see text for more details. The data for $N = 1280,\ 2560$ are not reported here since they are rather noisy and do not display a maximum in the temperature region investigated.

We can now discuss the temperature dependence of the entropy $e(T)$, shown in Fig. 4.3. The entropy cannot be directly estimated during a canonical Monte Carlo simulation: methods based

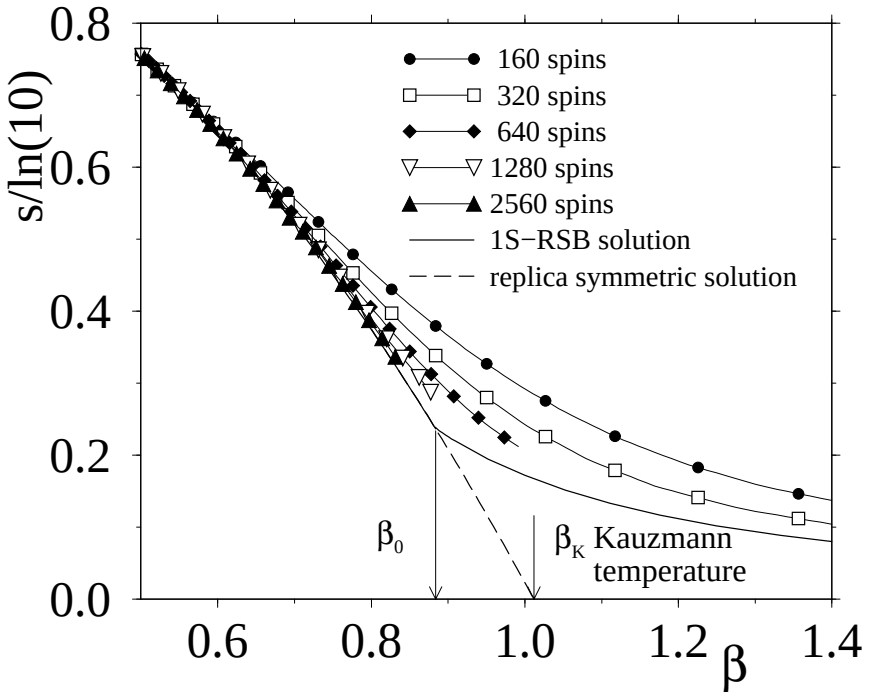


**Figure 4.3:** Entropy $s$ per spin, normalized by its high temperature value $\log(10)$ plotted vs. inverse temperature for different system sizes (curves with symbols). The bold dashed and the bold solid curves are the replica symmetric solution and the one-step replica symmetry breaking solution, respectively. Vertical arrows indicate the static inverse transition temperature $\beta_0$ and the inverse of the "Kauzmann temperature" $\beta_K$, where the entropy of the replica symmetric solution vanishes.

on importance sampling permit to generate various configurations $X_\nu$ of the system under investigation with a probability $a_\nu$ proportional to

$$p_\nu = Z^{-1} \exp\left[-H(X_\nu)/(k_B T)\right], \tag{4.7}$$

$Z$ being the partition function. The proportionality constant relating $a_\nu$ and $p_\nu$ is not known, and not needed to evaluate quantities that can be expressed as thermal averages of suitable operators (as we explained in the section devoted to numerical methods). However the partition function $Z$, the free energy per spin $f = -(k_B T \ln Z)/N$ and the entropy $s = (e - f)/T$ cannot be obtained in this way. One can access these quantities by making use of thermodynamic integration, starting from a reference temperature $T_R$ (that can be also $T_R = \infty$) at which the behavior of the system is known. References to this method applied to the analysis of Monte Carlo data can be found in (Landau and Binder, 2000). One has then

$$\beta f(T) = -\frac{s(T_R)}{k_B} + \int_{\beta_R}^{\beta} e(\beta) d\beta \tag{4.8}$$

$$\frac{s(T)}{k_B} = \frac{s(T_R)}{k_B} + \beta e(T) - \int_{\beta_R}^{\beta} e(\beta) d\beta \tag{4.9}$$

We have used $T_R = 2$, a temperature at which our data are no longer sensitive to finite size effects and the replica symmetric solution is fulfilled, so that we can use as reference $s(T_R)$ the mean-field value $-9/16 + \ln(10)$, given in eq. (2.25). We just recall that we are using units in which $k_B = 1$. The integral over $e$ was done by using a spline interpolation of our data, with $180$ points for $N = 160, 320, 640$ and $100$ points for $N = 1280, 2560$. From eq. (2.25) we note that the entropy at the static transition is

$$s(T_0) = \ln 10 - \frac{9}{4}\left(\frac{T_s}{T_0}\right)^2 \approx 0.54424, \quad \text{i.e. } \frac{s(T_0)}{s(\infty)} \approx 0.23636. \tag{4.10}$$

Thus we see that while at the static transition temperature $T_0$ the entropy has decreased to less than a quarter of its high temperature value it is clearly nonzero (and nonnegative, of course); in analogy to the energy, finite size effects do no permit to see the kink at $T_0$ present in the thermodynamic limit.

The entropy is a crucial quantity in the study of supercooled liquids (Debenedetti, 1996); it is, in the supercooled region, bigger that in the underlying crystal phase, but decreases faster towards zero; due to the fact that eventually supercooled liquids fall out of equilibrium (vitrification), it is not possible to measure their entropy up to low temperatures, but an extrapolation can be done. If one then accept the validity of this extrapolation (that would correspond to an infinitely slow cooling of the system) , a crossing of the entropy of the crystal and of the supercooled liquid is found [2]. Continuing to extrapolate would lead to a situation that seems paradoxical, since there would be an entropy of the amorphous state lower than that of the crystal at the same temperature (this is known as "Kauzmann paradox" (Kauzmann, 1948)). The temperature at which the extrapolated supercooled entropy equals the one of the crystal is called "Kauzmann temperature $T_K$". A possible solution to this is to view this plausible entropy crisis as a manifestation of a genuine phase transition to a glass phase at $T_K$. A theoretical calculation has been carried out for a *lattice model* for polymers (Gibbs and DiMarzio, 1958). Gibbs and DiMarzio assumed that in the supercooled regime the entropy of the polymer can be decomposed into vibrational (due to phonons) and configurational; since a lattice model was used, lacking by definition a vibrational contribution to thermodynamics, the total entropy was identified with the configurational one; under some specific assumptions, they calculated the partition function for the model, and found that the entropy vanishes at a nonzero temperature $T_K$. A simulation study of the glass transition in the framework of the bond fluctuation model found a decrease of $s$ from its high temperature value to about 1/4 of this value, when $T$ is lowered, but then the curve $s(T)$ vs. $T$ bends over and a well-defined $T_k$ does not exist - (also the high temperature results does not coincide with the analytical predictions of (Gibbs and DiMarzio, 1958), indicating probably an error in the calculation of the partition function in their approach)- (Wolfgardt et al., 1996).

If one proceeds in the same way with the current (lattice) model to obtain a Kauzmann temperature $T_K$ where the entropy of the (meta)stable high temperature phase vanishes, one gets from eq. (4.10)

$$\frac{T_K}{T_s} = \frac{3}{2}(\ln 10)^{-1/2} \approx 0.9885 \tag{4.11}$$

[2]Note that in the case of o-terphenil, a good glass former, the cooling rate necessary to reach this crossing point would require a waiting time on the order of $10^5$ times the age of the universe, see the discussion in (Jäckle, 1986)

which is even below the "true" stability limit $T_s = 1$ of the disordered phase, where the (extrapolated) static glass susceptibility is divergent [3]. Also a strictly linear extrapolation of $s(T)$ from $T_s$ or $T_0$ down to a temperature where this extrapolation would vanish does not give a meaningful result.

These results show that the idea to locate the static glass transition temperature by an extrapolation of the (configurational) entropy function $s(T)$ in the disordered high temperature phase to $s(T = T_K) = 0$ can be misleading, even for a mean-field model that does indeed exhibit both a dynamical transition (at $T_D$) and a static transition (at $T_0$). While $T_K$ is always lower than $T_0$, it does not coincide with the stability limit of the metastable high temperature phase, and thus lacks any physical significance.

The proper quantity to deal with in the case of spin glasses is the "complexity", which signals the splitting of the phase space into disjunct valleys, and is a more suitable quantity to locate the spin-glass transition rather than the configurational entropy, that can be ill-defined in the case of lattice models. The definition of complexity is strongly connected to the concept of broken ergodicity (Palmer, 1982; Monasson, 1995). It can be shown that in the mean-field limit spin glasses with an discontinuous order parameter at the phase transition presents a very large (exponentially) number of *metastable* states in the range $T_0 < T < T_D$; the logarithm of this number is called complexity; it starts to be extensive, coming from high temperature, at $T_D$, and vanishes as $T_0$ is approached. The vanishing is due to the fact that the number of relevant states is no longer exponential in $N$, but algebraic, i.e. $N^a$ (Kirkpatrick and Wolynes, 1987). The complexity can be calculated from the solutions so-called TAP equations, introduced for the Ising case by Thouless, Anderson and Palmer (Thouless et al., 1977), for the mean-field local magnetizations (Kirkpatrick and Wolynes, 1987). We have discussed this approach in chapter 2, section 2.2. This cannot be done analytically for the present model with $p = 10$, so a numerical solution is needed. Since they are $N$ coupled non-linear equations with an exponential (in $N$) number of solutions, the task is rather difficult. Recently also another approach has been presented to extract it from simulations, based on the decomposition of the phase space in inherent structures, that is the local minima of the energy in the configuration space (Crisanti et al., 2001). Due again to the large number of minima, and also to the fact that a rather exhaustive search has to be done, the method is restricted to rather small sizes. However in our case, since $T_0$ and $T_D$ so close to each other, and due to the presence of large finite size effects close to the transition region, a quantitative estimation of the complexity would be rather difficult.

### 4.1.2 The order parameter distribution and its cumulants

For defining a spin glass order parameter, we follow the standard method used in simulations of Potts glasses (Scheucher and Reger, 1993; Dillmann et al., 1998; Hukushima and Kawamura, 2000) to consider two replicas $\alpha$ and $\beta$ of the system, i.e. two systems that have identical bond configurations, and to make for each of them an independent Monte Carlo simulation. We have discussed the calculation of the order parameter in chapter 3 devoted to the numerical methods,

[3] Note that the proximity of $T_K$ and $T_s$ happens accidentally for $p = 10$. E.g. for $p = 5$ the general result (Elderfield and Sherrington, 1983a; De Santis et al., 1995) $T_K/T_s = \left[\frac{1}{4}(p-1)/\ln p\right]^{1/2}$ implies $T_K/T_s \approx 0.7882$.

section 3.3. We just recall here the definition of overlap:

$$q = \sqrt{\frac{1}{p-1}\sum_{\mu,\nu=1}^{p-1}\left(q^{\mu\nu}\right)^2} \qquad q^{\mu\nu} = \frac{1}{N}\sum_{i=1}^{N} S_{i\alpha}^{\mu} S_{i\beta}^{\nu}. \tag{4.12}$$

In the investigation of spin glass systems a great role is played by the order parameter *distribution* $P(q)$, that is the distribution of the overlaps between different equilibrium configurations at a certain temperature. Below the spin glass transition the mean field theory predicts for this function a nontrivial behavior, and for the model under investigation a double-delta function is expected, with two peaks at $q = 0$ and $q = q_0(T)$.

Numerically $P(q)$ is calculated by making a histogram of the values of $q$ resulting from the analysis of the overlaps between configurations thermalized at the temperature of interest. The $n$-th moment of the order parameter is then given by

$$q^{(n)} = [\langle q^n \rangle]_{av} = \int q^n P(q) dq. \tag{4.13}$$

The second moment is related to the *reduced* spin glass susceptibility through

$$\tilde{\chi}_{SG} = \frac{N}{p-1}[\langle q^2 \rangle]_{av}. \tag{4.14}$$

The difference with the ordinary spin glass susceptibility defined in eq. (2.22) is just the factor $(p-1)^{-1}$ used to normalized it to 1 for $T \to \infty$. $\tilde{\chi}_{SG}$ diverges in the limit of infinite system in presence of a spin-glass phase. Sometimes in the literature is also known as "overlap susceptibility" (Marinari et al., 1998b) .

We start now to discuss our results, starting from the order parameter distribution. Fig. 4.4 is the order parameter distribution for many different temperatures for $N = 320$: we see indeed the appearance of a second peak, at low temperatures, at a value $q_0 \neq 0$, distinct from the first one at small but finite $q$ and present also at high temperatures $T > T_0$.
The position of the first peak at $q \neq 0$ is however a finite size effect. We must keep in mind that, by definition, $q$ is a sum of all positive element (the matrix element of the overlap tensor) and is never equal to zero, so finite size effects are quite pronounced even in the paramagnetic phase (this is typical when using rotational invariant order parameters (Landau and Binder, 2000)). Increasing the system size will bring thus the position of first peak always closer to $q = 0$. This statement is proven in Fig. 4.6b, a finite size scaling analysis of the first moment of $P(q)$. We see that for temperatures well above $T_0$ the first moment vanishes like $N^{-1/2}$. However, close to $T_0$ this type of extrapolation would give a *finite* value of the moment, inconsistent with the solution in the thermodynamic limit, according to which all the moments goes to zero for $T \geq T_0$ (Gross et al., 1985). If instead an extrapolation with $N^{-1/3}$ is done, see inset, one finds again as expected that the moment vanishes. Note that, according to this results, for the second moment of $P(q)$ we have at $T = T_0$ again a scaling of the type $N^{-2/3}$, consistent with the values we found for the energy, see Fig. 4.1b: the same notes and remarks we made are still valid in this case.
The size dependence of $P(q)$ at low temperatures ($T = 0.7 \approx 0.6T_0$) is plotted in Fig. 4.5. The vertical dotted line represents the value of the second peak expected in the thermodynamic

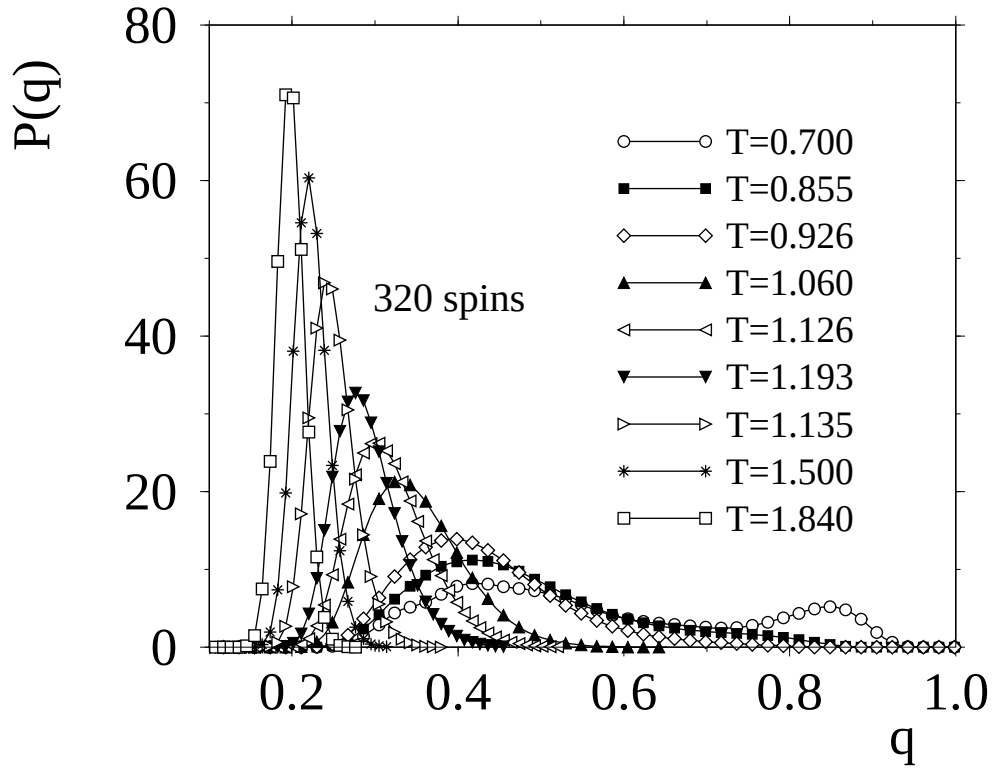


**Figure 4.4:** Order parameter distribution $P(q)$ versus $q$ for $N = 320$ and various temperatures down to $T = 0.7 \approx 0.6T_0$

limit $q_{EA}(T = 0.7) \approx 0.82$ (De Santis et al., 1995). The agreement is rather good, and shows that this peak is less affected by finite size effect as the first one. The shape of $P(q)$ at low temperature then is consistent with the one step-replica symmetry breaking scenario, different from the continuous one realized in the Ising mean-field spin glass, whose Monte Carlo evidence appeared in (Young, 1983). The complete temperature dependence of the first moment $q^{(1)}$ is in Fig. 4.6a: it starts to grow quickly in the low temperature region, where the size effects are weaker; the inset shows a scaling plot of $q^{(1)}$ versus temperature, and again gives a rather good idea of the separation between the paramagnetic region, where the curves collapse, and the spin glass phase, where $q^{(1)}$ acquires a finite weight.

The discussion of the second moment $q^{(2)}$ comes together with the one of the spin glass susceptibility $\tilde{\chi}_{SG}$, since they are connected through eq. (4.14).

Fig. 4.7 shows the reduced spin glass susceptibility as a function of the squared inverse temperature. This representation is adapted to the theoretical temperature dependence of this quantity, see eq. (2.26), which predicts at $T^{-2}$-law at high temperatures. As expected already from the behavior of the internal energy, even far above $T_s$ and $T_0$ the convergence to the thermodynamic limit is rather slow. Unfortunately the analysis of the finite size behavior of $\tilde{\chi}_{SG}$ is not straightforward, as we will show in the following. For $T < T_0$ and $N \to \infty$ eqs. (4.14), (2.32)

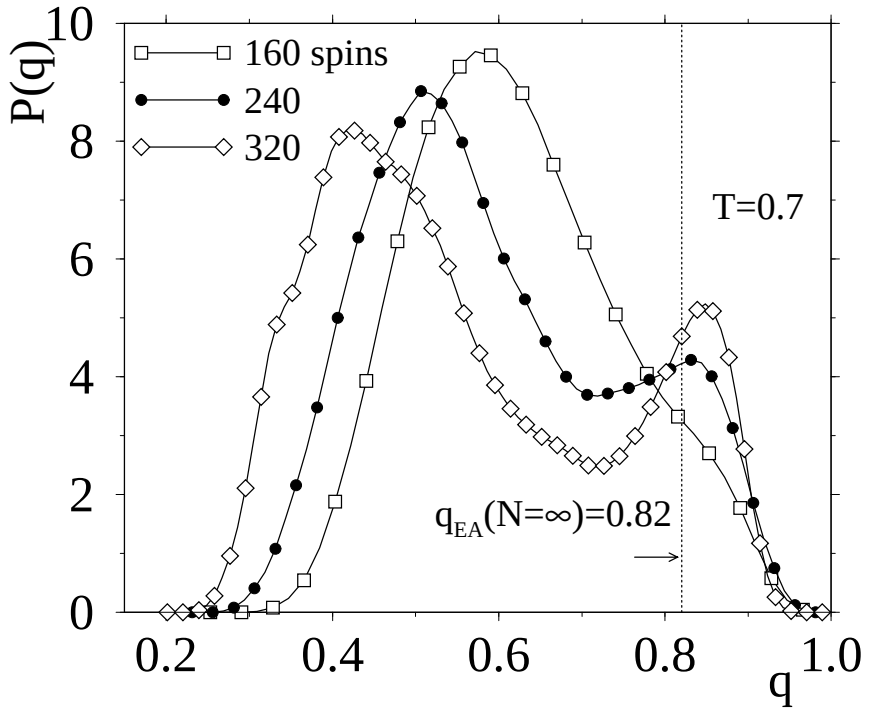


**Figure 4.5:** Order parameter distribution $P(q)$ versus $q$ for $T = 0.7$ and the three system sizes $N = 160, 240$ and $320$. The asymptotic value of the order parameter $q_{EA} \approx 0.82$ (De Santis et al., 1995) is included by a vertical line.

and (2.35) imply

$$\tilde{\chi}_{SG}^{-1} = \frac{p-1}{Nq_0^2} \frac{1}{(1 - T/T_0)}, \tag{4.15}$$

since for $T < T_0$ our definition for $\tilde{\chi}_{SG}$, eq. (4.14), simply picks up a contribution due to the nonzero spin glass order parameter $q_0$. As a result, $\tilde{\chi}_{SG}^{-1}$ for $N \to \infty$ should follow the straight dashed line in Fig. 4.7 that represents the replica-symmetric solution for all $T^{-2} < T_0^{-2}$, while for $T^{-2} > T_0^{-2}$, $\tilde{\chi}_{SG}^{-1}$ simply converges towards the abscissa: this discontinuity is sharp in the thermodynamic limit, since the following expected two limits are different (Kirkpatrick and Wolynes, 1987):

$$\tilde{\chi}_{SG}^{-1}(T \to T_0^+) = 1 - (1/T_0)^2 \qquad \tilde{\chi}_{SG}^{-1}(T \to T_0^-) = 0. \tag{4.16}$$

This singular behavior of $\tilde{\chi}_{SG}^{-1}$ is explained further in the inset, where we have added to $\tilde{\chi}_{SG}^{-1}$ the term $(T_s/T)^2$. This sum is thus supposed to give unity for $T > T_0$ and $(T_s/T)^2$ for $T < T_0$ in the thermodynamic limit, as can be seen from eq. (2.26). For very large but finite $N$, $\tilde{\chi}_{SG}^{-1}$ for $T < T_0$ exhibits a Curie-Weiss type divergence at $T_0$, coming from low temperature, but the amplitude of this effect is only of order $1/N$, as results from eq. (4.15). In order to analyze the finite size rounding of this singularity one should need a better understanding of the finite size rounding

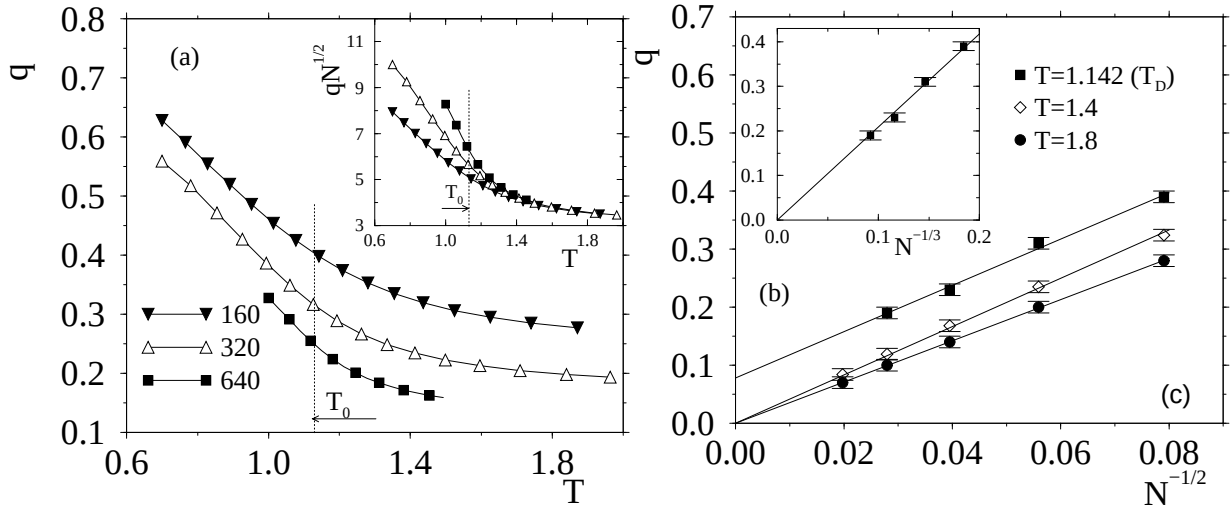


**Figure 4.6:** (a) Temperature dependence of the first moment of the order parameter distribution for different system sizes, as shown in the legend. In the inset we show the scaling with $N^{-1/2}$, which is satisfied at high temperatures. (b) Value of the first moment $\int qP(q)\,dq$ of the order parameter distribution vs. $N^{-1/2}$. The inset shows that close to the transition temperature $T_0 \approx T_D$ this moment scales like $N^{-1/3}$.

of the delta-peaks predicted for $N \to \infty$ into peak of finite height and nonzero width [4]. As we already showed in Fig. 4.4, our simulation results for $P(q)$ do indeed give evidence that a second peak at $q_0 \neq 0$ develops, distinct from the peak at small $q$ that exists also in the high temperature phase. However, the statistical accuracy of $P(q)$ is not very high due to the well known fact that in the ordered phase this quantity is not self-averaging (Binder and Young, 1986; Mézard et al., 1987; Fischer and Hertz, 1991), and the number of realizations of the random couplings that we were able to study is insufficient to overcome this problem. Hence we are currently not able to do a proper analysis of the finite size effects of $P(q)$, see Fig. 4.5, and thus cannot make a finite size analysis of $\tilde{\chi}_{SG}$.

The results so far for the statics are definitely all in qualitative agreement with the mean-field scenario. We find also quantitative agreement with the value of the Edwards-Anderson order parameter at low temperature, and it seems therefore clear that the phase transition and the low temperature phase are compatible with what is expected in the thermodynamic limit. Now it would be good also to see if we are able to get a quantitative estimation of the spin glass transition temperature without relying explicitly on the knowledge of the mean-field solutions. As already discussed, this is usually a matter of the analysis of the cumulants.

A further interesting quantity related to the distribution $P(q)$ is the reduced fourth-order

[4] A phenomenological attempt to describe the finite size behavior for the glass transition of Potts models has been made in (Dillmann et al., 1998), but this approach is not followed up here, since it is not compatible with a vanishing of the height of the second peak like $1 - T/T_0$ in the thermodynamic limit, see eq. (2.35).

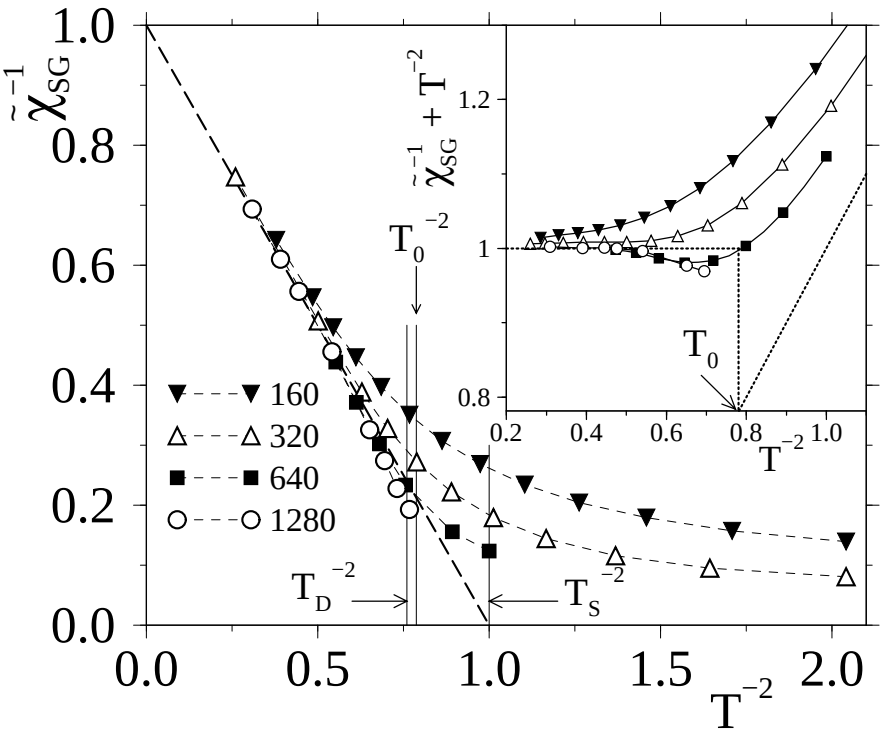


**Figure 4.7:** Inverse of the reduced spin glass susceptibility $\tilde{\chi}_{SG}$ versus the square of inverse temperature for different system sizes (curves with symbols). The solid line shows the result of the replica-symmetric theory, eq 2.26). Inset: Plot of $\tilde{\chi}_{SG}^{-1} + (T_s/T)^2$ to illustrate the non-monotonic convergence towards eq. (2.26). See text for more details.

cumulant (Binder and Young, 1986; Binder and Reger, 1992; Hukushima and Kawamura, 2000)

$$g_4(N,T) = \frac{(p-1)^2}{2}\left(1 + \frac{2}{(p-1)^2} - \frac{[\langle q^4\rangle]_{av}}{[\langle q^2\rangle]^2_{av}}\right) \tag{4.17}$$

This ratio of moments was found to be valuable in the context of finite size scaling analysis of phase transitions (Binder, 1981; Privman, 1990), both of first (Vollmayr et al., 1993) and second (Binder, 1992) order, also for spin glass systems (Binder and Young, 1986; Kawashima and Young, 1996). In ordinary second order phase transitions $g_4(N,T)$ goes to zero in the disordered phase and assumes a non-zero value in the ordered phase, approaching the value $1$ at $T = 0$ if the ground state of the system is non-degenerate. This result based on a the idea of a Gaussian shape of the order parameter distribution, which is smeared out from finite size effects. However, what makes $g_4$ so valuable is that, at leading order in finite size corrections, it takes a universal value at the critical temperature $T = T_c$. This is particularly suitable for a simulation. Usually one plots $g_4(N,T)$ as a function of the temperature for different system sizes, and the crossing point of all the curves locates the phase transition temperature.

For first order phase transitions the situation is different: $g_4$ goes always to zero in the high temperature phase, but shows a minimum at a certain temperature $T_{min}$, with $T_{min} - T_c \propto N^{-1}$ and a value of the cumulant $g_4(T_{min})$ scaling like $g_4(N, T_{min}) \propto N^{-1}$ and negative. All cumulants $g_4(N, T)$ approximately intersect at a common crossing point, scaling like $T_{cross} \propto N^{-2}$, with a universal value $g_4(N, T_{cross}) = 1 - n/(2q)$, where $n$ is the order parameter dimensionality and $q$ the degeneracy of the ordered state. This phenomenology has been tested and verified for Potts ferromagnets (Vollmayr et al., 1993). As far as numerical studies of spin glasses, a great effort was devoted to the search of a phase transition in the three dimensional Edward-Anderson model (that is an Ising system with random interactions (Edwards and Anderson, 1975)). There is now agreement that a second order phase transition takes place; the $g_4$ cumulant behaves as in ordinary critical phenomena, and is usually taken as the best evidence for the existence of a spin glass phase transition (see (Marinari et al., 1998b; Ballesteros et al., 2000) for the most up to date results).

Another quantity has been proposed (Marinari et al., 1998a) especially for spin glasses, which is a measure for the onset of lack of self-averaging [5], and goes under the name of Guerra parameter

$$G(N,T) = \frac{[\langle q^2 \rangle^2]_{av} - [\langle q^2 \rangle]^2_{av}}{[\langle q^4 \rangle]_{av} - [\langle q^2 \rangle]^2_{av}}. \tag{4.18}$$

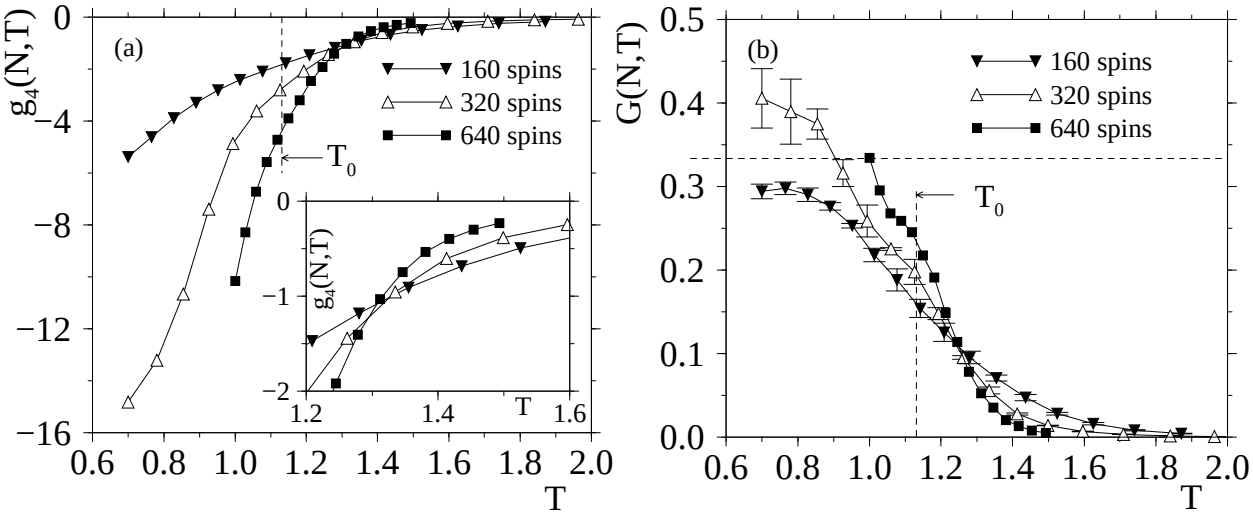


**Figure 4.8:** (a) Fourth order cumulant $g_4$ plotted versus temperature, for three values of $N$, $N = 160, 320$ and $640$. The vertical straight line highlights the predicted static transition temperature $T_0$. (b) Same as (a) but for the Guerra parameter. The horizontal dashed line is the theoretical expectation for $T < T_0$.

[5] Self-averaging means that a quantity is independent on the microscopic realization of the quenched disorder. In spin glasses the order parameter lack this property in the low temperature phase. We will come back to this point discussing the dynamics close to the dynamical transition, see section 4.2.1.

Again, the idea behind it comes from the fact that it has been shown (Guerra, 1996) that sample to sample fluctuations of the cumulants of the order parameter distribution $P_J(q)$ are Gaussian distributed in the thermodynamic limit. In mean field spin glass transitions $G(N,T)$ goes to zero like $N^{-1}$ at high temperature ($T > T_c$) but converges to a finite value $1/3$ for $T < T_c$. Therefore it is expected that a crossing of the various $G(N,T)$ for different lattice sizes locates the spin glass transition, whether of first or second order.

From the point of view of the order parameter, the phase transition in this model is first-order like. The $g_4(N,T)$ cumulants are presented in Fig. 4.8a. The presence of a minimum can only be inferred because all the curves have to go to a positive value for $T = 0$, although it cannot yet be seen explicitly. Moreover, the lines for different $N$ seem to cross around $T = 1.3$, which is still far from the real transition temperature. A more careful look however, see the inset, gives good reason to believe that the crossing of the curves is rather spurious, since the temperature at which the line cross is shifting towards lower values as $N$ is increased. From this point of view, it seems that correction to scaling are still big, if a crossing point is to be expected at all. The behavior of $g_4$ is nevertheless reminiscent of a first order phase transition. In this particular case, one has to keep in mind that the second peak in $P(q)$ appears discontinuously (that is $q_0(T)$ is a discontinuous function of the temperature) but with a weight proportional to $1 - T/T_0$, see eq. (2.35). If we take the expression for the $g_4$ cumulant given in eq. 4.17 and insert the expression for $P(q)$ expected in the thermodynamic limit, we see clearly that the cumulant has to go to minus infinity as $T_0$ is approached

$$g_4(N \to \infty, T \approx T_0) \approx \frac{1}{1 - \frac{T}{T_0}}. \tag{4.19}$$

This feature seems also to be consistent with the data. However a naive look at the crossing can lead to an overestimation of the spin glass transition. We would like to state that it also cannot completely be ruled out that the crossing we see is analogous to the crossing expected in normal first order phase transitions, since in that case the crossing happens at $T$ values lower than $T_0$, as we already said in the discussion at the beginning of this subsection.

Problems are also present for the Guerra parameter, Fig. 4.8b. A crossing of the temperature is present, but again the temperature we read off is $T = 1.24$, bigger than the true one. The Guerra cumulant has been used up to now only in few investigations (see (Marinari et al., 1998a; Hukushima and Kawamura, 2000; Picco et al., 2001)) and usually a bigger value with respect to the real one is found, although it has also been found that correction to scaling are important (Ballesteros et al., 2000). Anyway in the present range of system sizes these intersection points of the cumulants cannot be taken as accurate estimates of $T_0$. This already is obvious from the data alone, because the two quoted temperatures are not in mutual agreement. It is also highly probable that in reality neither the three curves for $g_4(N,T)$ nor those for $G(N,T)$ intersect at a unique temperature: given the relatively large error bars of the data, they only can define temperature intervals $\Delta T_{g4}$, $\Delta T_G$, in which the three intersection points fall. As $N \to \infty$, presumably all temperatures of these intersections converge (slowly!) towards $T_0$. Since $T_0$ falls distinctly outside the above intervals, this method of searching for intersection points, which is so successful for locating phase transitions in pure systems is not reliable here.

Recently also another class of cumulants has been introduced (Picco et al., 2001). They make use of the so-called "connected" order parameter, that is $q - \langle q \rangle$. We denote the correspondent cumulants with $g_{4c}(N,T)$ and $G_c(N,T)$. They are extensions of the former definitions:

$$g_{4c}(N,T) = \frac{(p-1)^2}{2}\left(1 + \frac{2}{(p-1)^2} - \frac{[\langle (q-\langle q\rangle)^4\rangle]_{av}}{[\langle (q-\langle q\rangle)^2\rangle]^2_{av}}\right) \tag{4.20}$$

$$G_c(N,T) = \frac{[\langle (q-\langle q\rangle)^2\rangle^2]_{av} - [\langle (q-\langle q\rangle)^2\rangle]^2_{av}}{[\langle (q-\langle q\rangle)^4\rangle]_{av} - [\langle (q-\langle q\rangle)^2\rangle]^2_{av}}. \tag{4.21}$$

The use of these cumulants linked to the order parameter fluctuations (since they are defined through $q - \langle q \rangle$) has been found to give good results in locating the phase transition in a $p$-spin model, exhibing the same replica-symmetry-breaking pattern as the Potts glass (Picco et al., 2001). There are however drawbacks, since in order to obtain good data about fluctuations one needs a very good statistics, difficult to obtain for medium-large system sizes. We show our data in Figs. 4.9. Also the use of this cumulants does not seem to bring advantages in the location of the phase transition in our case. The $g_{4c}$ is expected to go towards $-\infty$ at the static transition temperature, but we see again the presence of a probably spurious crossing point, since it is not present in the data for the $p$-spin model. The connected Guerra parameter also shows in analogy with the normal one a crossing point that does not correspond to $T_0$.

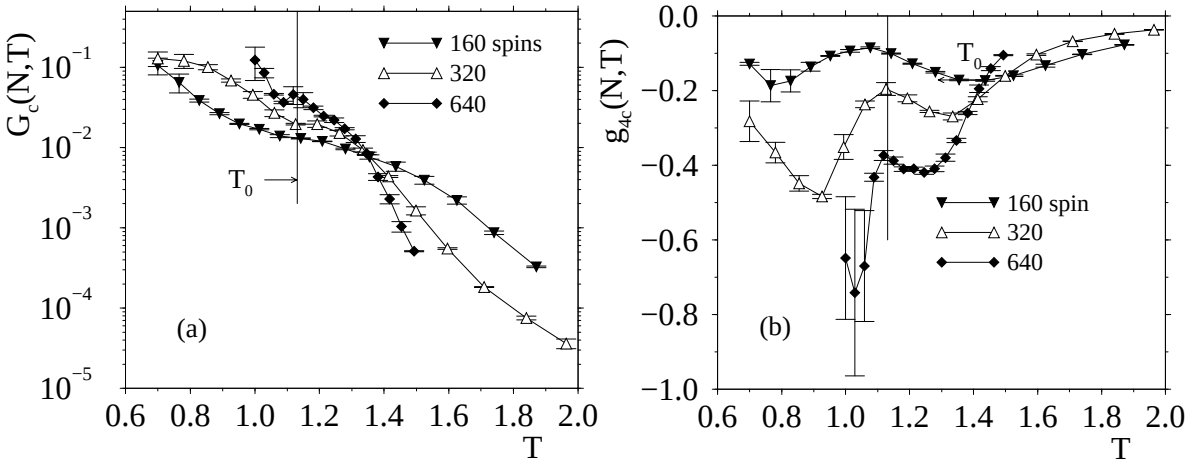


**Figure 4.9:** (a) Guerra cumulant $G_c(N,T)$ for the connected order parameter, see eq. (4.21). Three system sizes are shown: $N = 160, 320$ and $640$. The vertical straight line highlights the predicted static transition temperature $T_0$. (b) Same as (a) but for the $g_{4c}(N,T)$ parameter.

## 4.2 Dynamical properties

Before presenting and discussing our results concerning the dynamics of the system, we give a short reminder of the scenario expected in the thermodynamic limit (Kirkpatrick and Wolynes,

1987; Kirkpatrick and Thirumalai, 1988), as discussed in the introductory chapter. The theoretical results of Kirkpatrick *et al.* show that the Potts glass with $p > 4$ states has a "dynamical transition" at a temperature $T_D > T_0$, where non-ergodicity sets in. For $T \leq T_D$, the spin autocorrelation function $C(t)$ does not decay to zero anymore, but gets stuck for $t \to \infty$ at a nonzero value $q_{EA}(T)$, with (De Santis et al., 1995)

$$T_D = 1.142, \quad q_{EA}(T = T_D) = 0.328. \tag{4.22}$$

The details of this transition from ergodic (for $T > T_D$ where $C(t \to \infty) = 0$) to non-ergodic behavior (for $T < T_D$), as well as the time dependence of $C(t)$ for temperatures around $T_D$ are in fact described by equations formally analogous to those proposed for the structural glass transition by the so called "idealized mode-coupling theory" (Götze, 1989). The qualitative behavior of various quantities expected for $N \to \infty$ is sketched in Fig. 2.2. Note that for $T > T_D$ and $T < T_0$ we have $q_0 = q_{EA}$. In the temperature range $T_0 < T < T_D$ we have, however $q_0 = 0$ and $q_{EA} > 0$.

In the following we will discuss the general phenomenology of the dynamics of a fully connected $10-$state Potts glass with a finite number $N$ of spins, where no sharp dynamical transition is expected but rather a changing in the relaxation properties; we will then introduce a method to rationalize our results, comparing to the mean field limit with the dynamic finite size scaling. The approach to broken ergodicity will also be quantified, and some insights on the dynamics in the low temperature phase, where little is known, are presented. To conclude, we will discuss the behavior of single spin relaxations, found to be extremely heterogeneous.

### 4.2.1 Dynamics in the high temperature phase

In Fig. 4.10a we show the time dependence for the spin auto-correlation function $C(t)$ for $N = 1280$ and all temperatures investigated. We remind that, using the simplex representation (Wu, 1982), the spin autocorrelation function $C(t)$ is defined as

$$C(t) = \frac{1}{N(p-1)} \sum_i \left[ \left\langle \vec{S}_i(t') \cdot \vec{S}_i(t'+t) \right\rangle \right]_{av}. \tag{4.23}$$

Here and in the following we will measure time in units of Monte Carlo Steps (MCS), i.e. the average number of updates per spin. One of the features predicted in the thermodynamic limit is the appearance of a plateau in $C(t)$ approaching the dynamical transition temperature. It is also common in supercooled liquids to observe such behavior ((Kob, 1999)). Surprisingly we see that even for this rather large system size there is not yet any clear evidence for the development of a plateau for temperatures around $T_D$. Note that in the thermodynamic limit this function should, at $T = T_D$, decay to $q_{EA}$, i.e. to the horizontal line, loosing therefore ergodicity. In contrast to this our system with a *finite size* is always ergodic, since the free energy barriers separating the various "valleys" in phase space remain finite at all nonzero temperature. Of course every finite system is in principle ergodic (only hard core interactions can inhibit the system from reaching certain configurations of the phase space, and this can give broken ergodicity with finite size systems). However, for instance in structural glasses it is found that even a few hundred

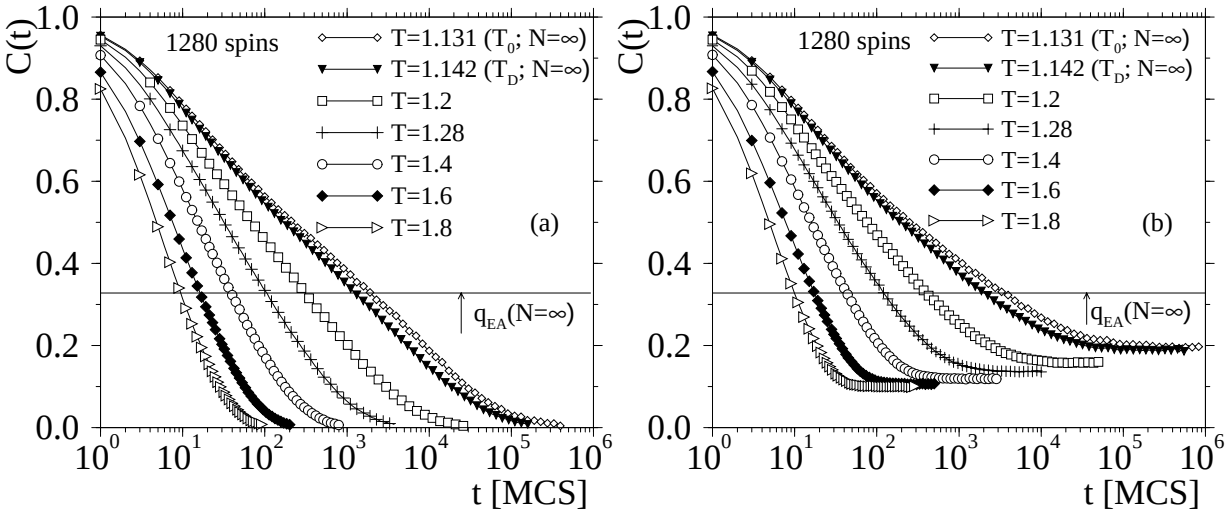


**Figure 4.10:** (a) Time dependence of the correlation function $C(t)$, eq. (4.23), for $N = 1280$ and various temperatures. Also included are the data for the predicted values of the static, $T_0$, and dynamic, $T_D$, transition temperature for $N \to \infty$. The horizontal straight line shows the theoretical prediction (De Santis et al., 1995) for the Edwards-Anderson order parameter at $T_D$, $q_{EA} = \lim_{t\to\infty} C(t)$. (b) Same as (a) but for the rotationally invariant correlation function $C_{RI}(t)$ defined in eq. (4.24).

particles are sufficient to show a pronounced (effective) ergodic to non-ergodic transition. Thus it is rather astonishing that for the present model the finite size effects are so strong that even for $N = 1280$ and at $T = T_D$ the existence of a plateau can hardly be seen. We have also considered a rotationally invariant order parameter time correlation function $C_{RI}(t)$ which is defined as

$$C_{RI}(t) = \left[\frac{\langle\tilde{q}(t)\rangle}{\langle\tilde{q}(0)\rangle}\right]_{av} \tag{4.24}$$

with

$$\tilde{q}(t) = \left[\frac{1}{p-1}\sum_{\mu,\nu=1}^{p-1}(\tilde{q}^{\mu\nu}(t))^2\right]^{1/2} \qquad \text{and} \quad \tilde{q}^{\mu\nu}(t) = \frac{1}{N}\sum_{i=1}^{N}(\vec{S}_i)^\mu(t)(\vec{S}_i)^\nu(0). \tag{4.25}$$

Note that $\tilde{q}^{\mu\nu}$ is not the same quantity as $q^{\mu\nu}$ defined in eq. (4.12), since for defining the latter one needs two replicas $\alpha$ and $\beta$ evolving independently in the phase space. However, for $t \to \infty$ the thermodynamic averages of the two quantities are the same. This means that in this limit also $\tilde{q}$ and $q$, from eq. (4.12), are the same. Furthermore we mention that the expectation value $\langle\tilde{q}(0)\rangle$ occurring in eq. (4.24) is equal to 1, as long as there is no ferromagnetic ordering of the system and the system remain isotropic. Also the time dependence of $C_{RI}(t)$, eq. (4.24), shows strong finite size effects, as can be seen from Fig. 4.10b. We see that, contrary to naive expectation, the long time limit of $C_{RI}(t)$ is different from zero, dependent on temperature and below we will discuss the origin of this effect and its dependence on system size in more detail. We see that

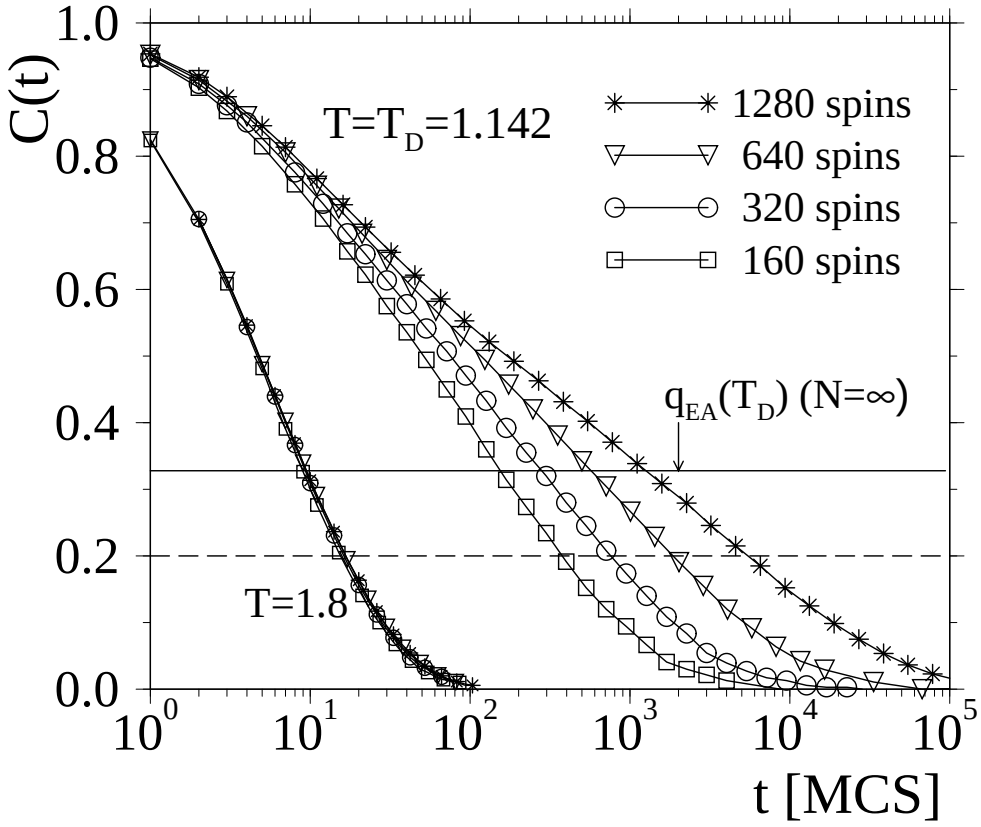


**Figure 4.11:** Time dependence of the correlation function $C(t)$ for $T = 1.8$ and for $T = T_D = 1.142$ for several values of $N$. The solid line is the theoretical value of the Edwards-Anderson order parameter $q_{EA}(T_D)$ for $N \to \infty$ (De Santis et al., 1995). The dashed line shows the value we use to define the relaxation time $\tau$.

also this correlation function does not show a plateau on intermediate time scale, before the total relaxation, even if $T$ is close to $T_D$ and hence we conclude that also $C_{RI}(t)$ converges only very slowly to its behavior in the thermodynamic limit.

In order to discuss the system size dependence of the correlation functions in more detail we show in Figs. 4.11 and 4.12 $C(t)$ and $C_{RI}(t)$ for different systems sizes and two temperatures.

We see from Fig. 4.11 that, at high temperatures, $C(t)$ shows basically no system size dependence, since all the curves collapse on each other. For low $T$, however, the relaxation becomes quickly slower with increasing system size and also the shape of the curves changes noticeably. But even at the largest system sizes accessible at this temperature we are not able to see a clear two step relaxation as one would expect for a sufficiently large *but finite* system. A somehow different behavior is observed in the case of $C_{RI}(t)$, Fig. 4.12a. Here, even at high temperatures the correlation function depends on the system size. This is in agreement with the arguments given in the context of eqs. (4.24) and (4.25) that $C_{RI}(t \to \infty)$ should scale like $1/\sqrt{N}$, since it behaves like the first moment of the order parameter distribution. That

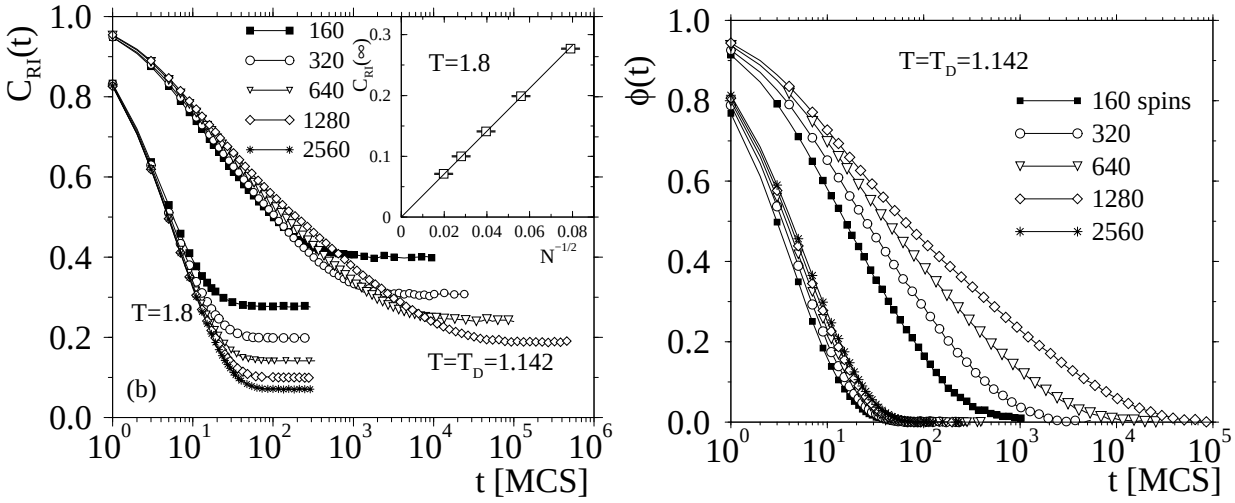


**Figure 4.12:** (a) Time dependence of the correlation function $C_{RI}(t)$ for $T = 1.8$ and for $T = T_D = 1.142$ for several values of $N$. The inset shows the scaling of the long-time limit of this function as a function of $N^{-1/2}$. (b) Time dependence of the reduced normalized function $\phi(t)$ for $T = 1.8$ and for $T = T_D = 1.142$ for several values of $N$.

one actually finds this size dependence is shown in the inset of Fig.4.12a. Instead of studying the function $C_{RI}(t)$ one could of course try to consider the reduced normalized function $\phi(t) = [C_{RI}(t) - C_{RI}(t \to \infty)]/[C_{RI}(0) - C_{RI}(t \to \infty)]$. However, also this type of correlation function has its problems since on one hand the final asymptote $C_{RI}(t \to \infty)$ is only known to within a certain statistical error, and on the other hand it shows finite size effects at high temperatures at *short* times, i.e. where $C_{RI}(t)$ is independent of $N$, see Fig. 4.12b. In view of these problems with $C_{RI}(t)$ we will in the following focus on $C(t)$ only. However, this is not a serious restriction, since in the thermodynamic limit these two functions should show at low temperatures the same time dependence anyway. That this is indeed the case for the simulations can be inferred from Fig. 4.13 where we show a parametric plot of $C_{RI}(t)$ versus $C(t)$ exactly at $T_D$. We see that with increasing system size the curves do approach the diagonal, as expected.

We now address the temperature and $N$ dependence of the relaxation time $\tau$ of the system. The definition of relaxation time is natural in a correlation function that decay exponentially, since then $\tau$ is the time it takes to decay to the value $1/e$ (this is the definition entering the formula of the normal exponential decay, $C(t) = \exp(-t/\tau)$). This argument can be extended if the correlation function is a stretched exponential $C(t) = \exp(-(t/\tau)^\beta)$. As we have seen however it is not clear which function to use for the system under study, so one possibility to define $\tau$ is

$$C(t = \tau) = 0.2. \tag{4.26}$$

This choice is indicated in Fig. 4.11 by the long-dashed line. Although the value $0.2$ is somewhat arbitrary, it is a reasonable choice: the only important thing is that it is significantly less than the

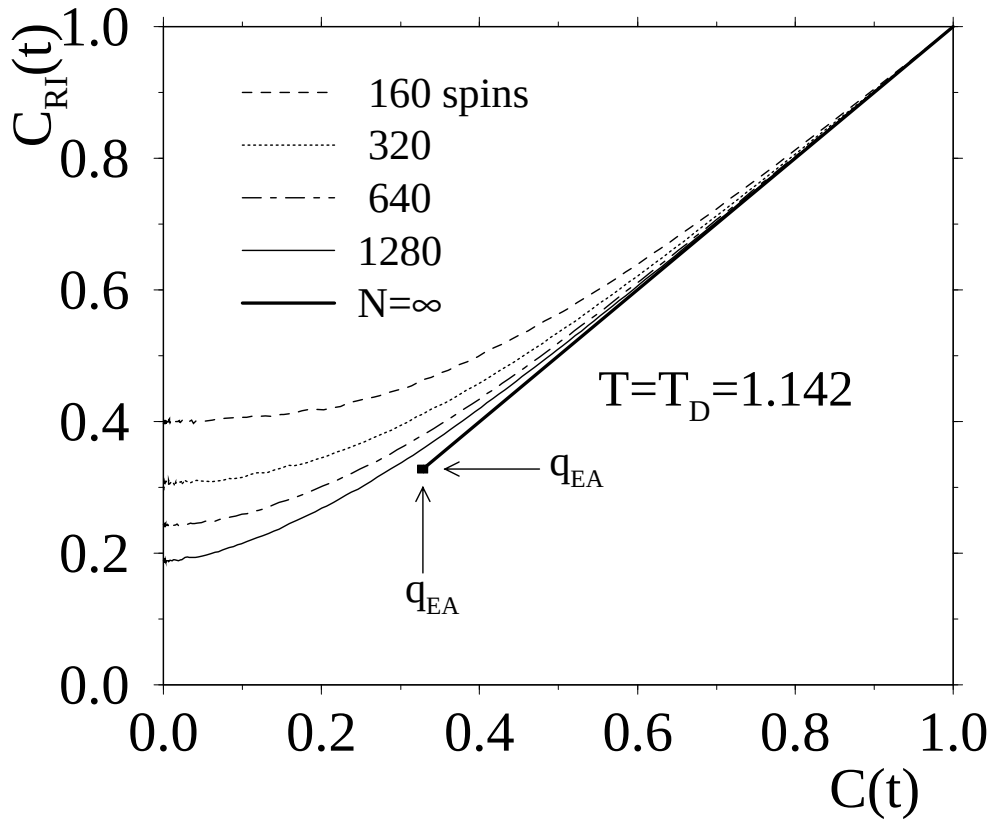


**Figure 4.13:** Parametric plot of $C_{RI}(t)$ vs. $C(t)$ at $T = T_D$ for different values of $N$. The square indicates the plateau value obtained for $N \to \infty$. The bold straight line describes the relation $C_{RI}(t) = C(t)$, believed to hold for $N \to \infty$.

height of the plateau [6] in the thermodynamic limit, $q_{EA}(T = T_D)$, cf. eq. (4.22). There is also no evidence for the development of further structures, like a plateau, in the dynamics below this reference value.
Another possibility would be to define

$$\tau_{av} = \int_0^\infty C(t)dt. \tag{4.27}$$

This is common in studies of the dynamics of critical systems and also of spin glasses (Ogielski, 1985; Binder and Young, 1986; Reuhl et al., 1998), and $\tau_{av}$ goes under the name of average relaxation time; we find however that this quantity, especially when the dynamics starts really to slow down, is much more affected by statistical errors (being important in $\tau_{av}$ the contribution coming from the long-time part of $C(t)$). However we can see also from Fig. 4.14 that for intermediate temperature the two definitions are practically equivalent, and start to deviate at

[6] If we would define a time $\tau'$ as $C(t = \tau') = 0.5$, on the other hand, $\tau'$ would be finite also below $T_D$, and even below $T_0$, until $q_{EA}(T)$ has increased up to $q_{EA} = 0.5$, due to the temperature dependence of the order parameter.

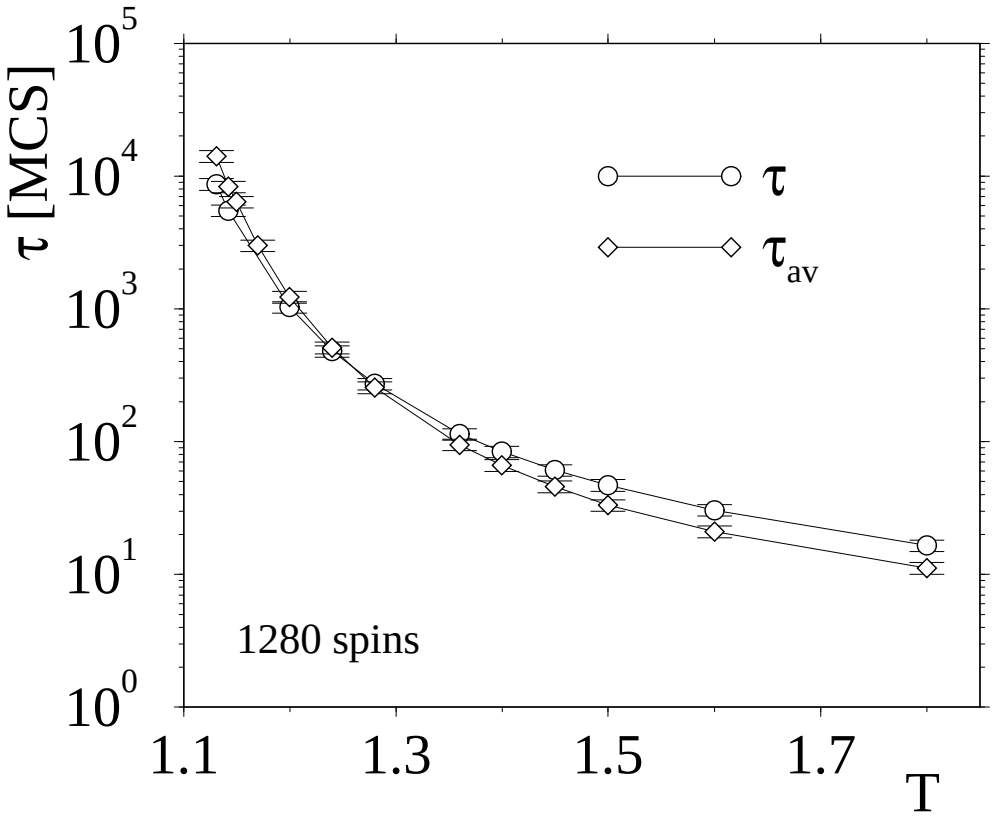


**Figure 4.14:** Comparison of the relaxation times $\tau$ and $\tau_{av}$ defined according to formula (4.26) and (4.27) respectively, for a system of $1280$ spins.

high temperatures where relaxation times are very fast and on the order of few Monte Carlo sweeps.

Since for $N \to \infty$ the dynamics of the model should be described by (idealized) mode-coupling theory (Kirkpatrick and Thirumalai, 1988), we expect that $\tau(T)$ shows a power law divergence at $T_D$ (Götze, 1989),

$$\tau \propto (T/T_D - 1)^{-\Delta}, \quad N \to \infty \quad , \tag{4.28}$$

where $\Delta$ is an exponent which is non-universal (i.e. model dependent), but typically not very different from $\Delta \approx 2$. In order to test the validity of eq. (4.28), one can plot $\tau^{-1/\Delta}$ vs. $T$ for a reasonable trial value of $\Delta$: if eq. (4.28) holds, a straight line should be seen over a reasonable range of temperatures, and the value of $T_D$ can be obtained by extrapolating the data towards $\tau^{-1/\Delta} = 0$. Fig. 4.15 shows that for $\Delta = 2$ indeed a series of straight lines are obtained, for $1.1 \leq T \leq 1.4$, while outside of this temperature range the curves bend, because the singularity is avoided due to the ergodicity in the finite size system, and another relaxation mechanism

comes into play (see below in the part devoted to the dynamics in the low temperature phase)[7]. In all cases it is difficult to use the estimates for $T_D$ for finite $N$ to extrapolate to the value of $T_D$ in the thermodynamic limit since the $N$-dependence is rather weak and the error bars of $T_D(N)$ are, due to the mentioned extrapolation, quite substantial. For the case of $\Delta = 2.0$ a dependence of the form $T_D(N) - T_D(\infty) \propto 1/N$ seems, however, to be compatible with the data, as can be seen in the inset of Fig. 4.15. A more quantitative method to investigate exponents and dynamical temperature will be presented in the next subsection. From the analysis of the

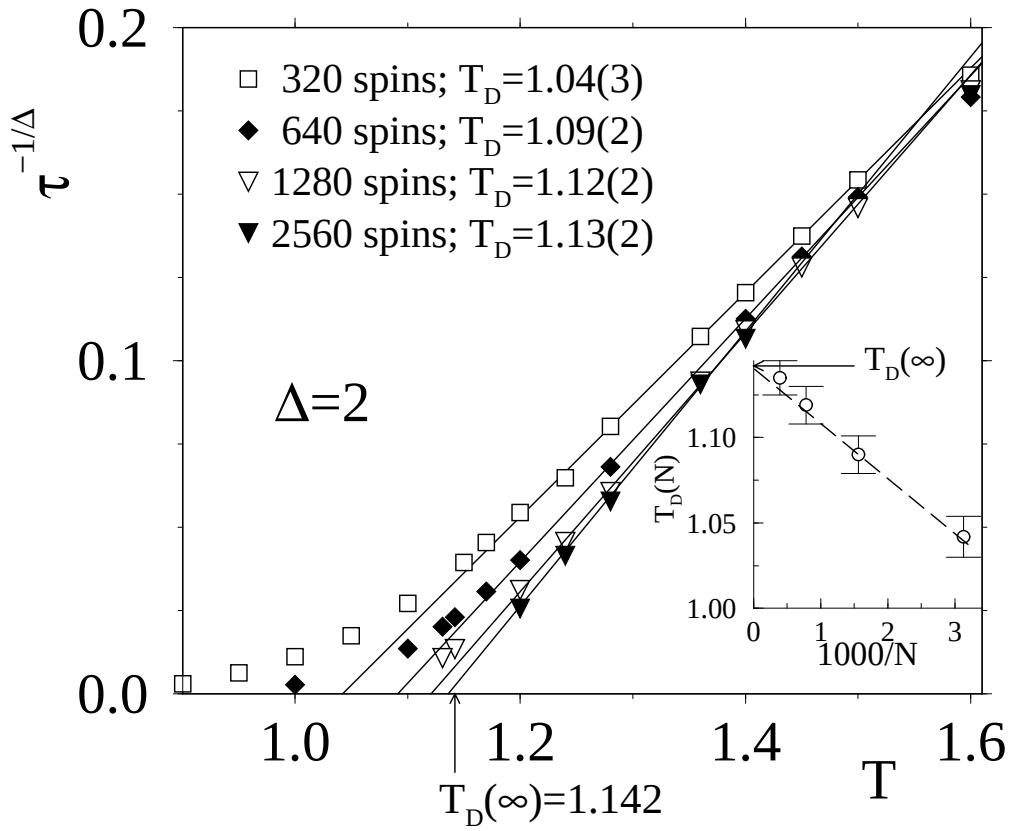


**Figure 4.15:** Temperature dependence of $\tau^{-1/\Delta}$ for different system sizes, using $\Delta = 2.0$ as a trial value. The bold straight lines are fits on a proper subset of point. The resulting extrapolated values for $T_D(N)$ are quoted in the figure. The inset show the various $T_D(N)$ as a function of $1000/N$, together with the thermodynamic limit signalled by the arrow.

dynamical equations it is possible also to extract information about the shape of the correlation functions, and properties they have to obey. Approaching the dynamical transition temperature from above, the correlators should be approximated well with the Kohlrausch-Williams-Watts function, $\exp(-(t/\tau)^\beta)$, a functional form that has been found to work very well in many glassy systems (Jäckle, 1986; Binder et al., 1999; Götze, 1999; Kob, 1999): this function describes the

[7]We have to remark that similar plots work also with exponents $1.9 \leq \Delta \leq 2.5$. The particular choice of $\Delta = 2$ is taken here because it turns out to be the best one also using a dynamic finite size scaling Ansatz, see section 4.2.2.

decay of the correlators to zero in the long time limit ($\alpha$-relaxation), the long-time region under the plateau structure . We find, however, that even close to $T_D$ and in the largest system used, this functional form does not give a good fit to the data. The second prediction of the theory concerning the $\alpha$-relaxation is the so-called time-temperature superposition principle. This principle implies that the correlator $C(t)$ can be written as

$$C(t,T) = \tilde{C}(t/\tau(T)), \tag{4.29}$$

where $\tilde{C}(x)$ is a temperature independent scaling function.

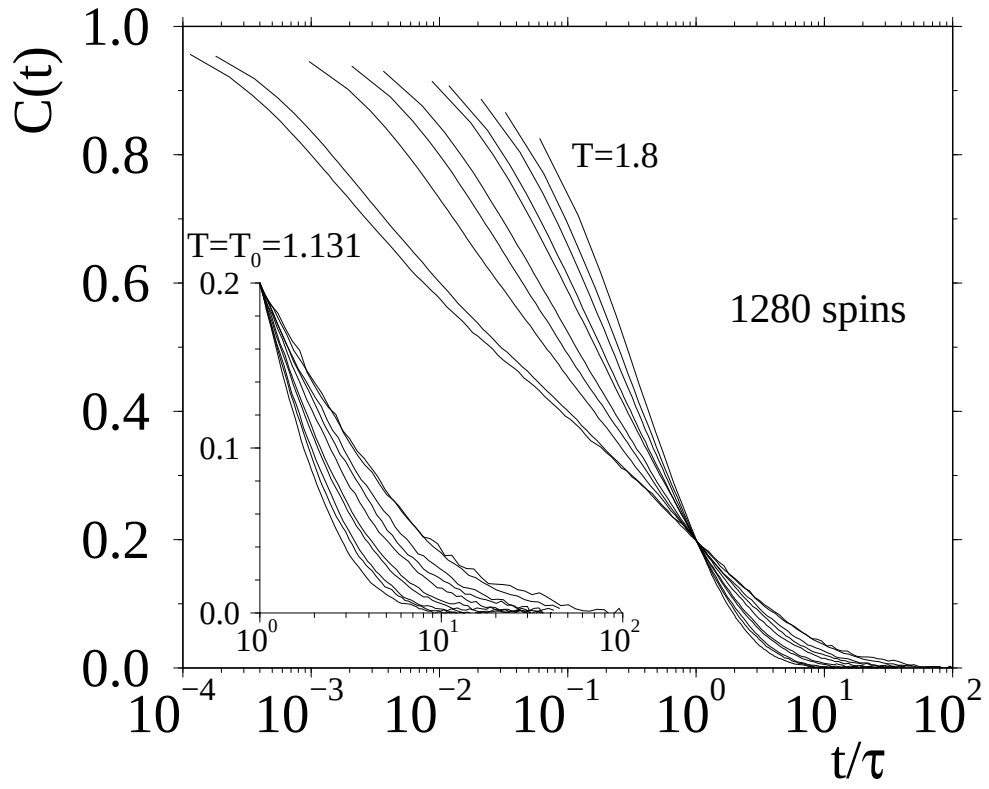


**Figure 4.16:** Plot of $C(t)$ vs. $t/\tau$ (where $\tau$ is defined via $C(t=\tau) = 0.2$, cf. eq. (4.26)), for $N = 1280$. Temperatures from right to left:$T = 1.8$, 1.6, 1.5, 1.4, 1.360, 1.280, 1.240, 1.2, 1.142, and 1.131. The inset shows a magnification of the part of the curves for $t/\tau > 1$.

The validity of eq. (4.29) can be checked if one plots $C(t,T)$ versus $x = t/\tau(T)$. If the superposition principle is valid the curves for the different temperatures should fall onto a master curve for large $x$. For very small values of $x$, i.e. in the early $\beta$-regime, no master curve is expected, since eq. (4.29) is supposed to hold only in the $\alpha$-regime. Fig. 4.16 shows this kind of scaling plot and we see that even for a rather large system, $N = 1280$, there is no indication for such a time-temperature position principle. Of course, it is possible that this failure to verify eq. (4.29) is simply due to finite-size effects. Thus, it would be desirable to check eq. (4.29) for much larger

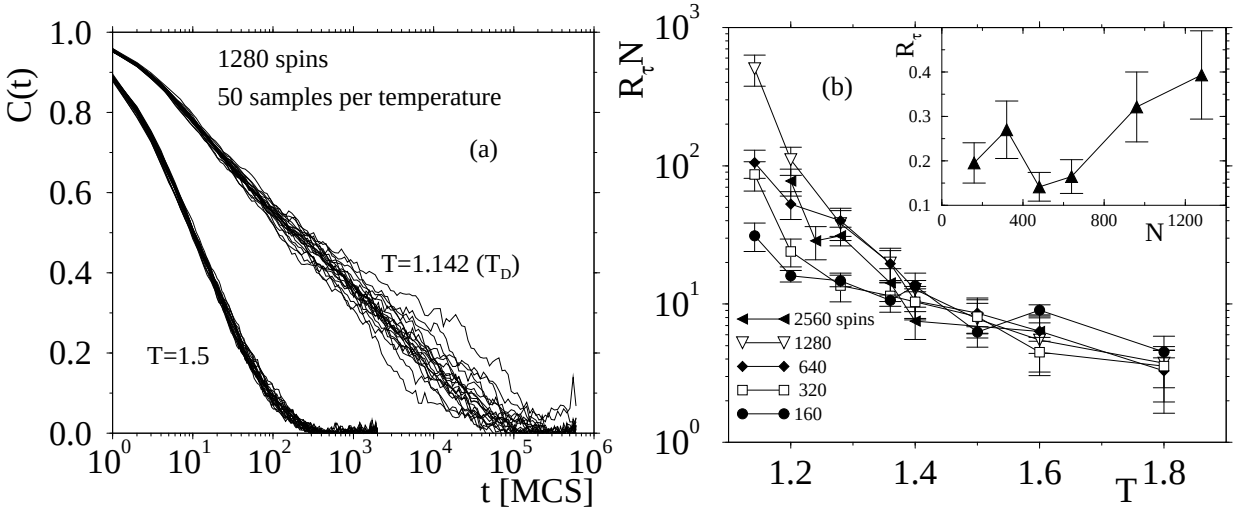


**Figure 4.17:** (a) Correlation functions for $50$ different realization of disorder. System with 1280 spins, temperature $T = 1.5$ and $T = 1.142 = T_D$. (b) Plot for the scaled quantity $R_\tau \cdot N$ as a function of temperature. The inset shows $R_\tau$ as a function of the system size at $T = 1.142 = T_D$.

systems. However, in view of the strong size dependence on the relaxation time $\tau$ near and below $T_D$, see Fig. 4.23 below, this is impossible for us with the present computer resources.

To conclude the presentation of the results for the dynamics at high temperature, we will concentrate on the self-averaging properties of $C(t)$. In ordinary statistical mechanics it is known that thermal fluctuations of important quantities such as the energy decreases with the system size as $N^{-1/2}$; since with disordered systems we have also to deal with the average over the disorder, one could also argue, using phenomenological arguments (Brout, 1959), that the sample-to-sample fluctuations go to zero in the limit of a large systems. A quantity with this property is called *self averaging* (Binder and Young, 1986; Fischer and Hertz, 1991). Although the argument of Brout assumed in principle short-range interactions, it is known (Mézard et al., 1987) that also with infinite range interactions the free energy, the energy, the magnetization are self averaging.

However other quantities, such as the spin glass order parameter, lack this property: responsible for that is the existence of many degenerate states which contribute to the Gibbs average (Mézard et al., 1984). A general criterion (Wiseman and Domany, 1998), especially suited for numerical studies, is the following: a measurement of a certain quantity $X$ (for instance the energy per spin, the magnetization, the susceptibility, or the relaxation times, as we will consider in the following) yields a different value for the thermal average $X_i$ of every sample $i$: this average value will be distributed according to the size $N$ of the system, and we will have a probability distribution $P_N(X)$. We can characterize this distribution by means of its average $[X]$ and relative variance $R_X(N)$

$$R_X(N) = \frac{[X^2] - [X]^2}{[X]^2}. \tag{4.30}$$

Here $[\cdot]$ stands again for the average over the disorder, i.e. $P_N$. According to the behavior as a function of $N \gg 1$, three regimes can be identified:

$$\begin{array}{ll} R_X \propto 1/N & \textit{strongly self-averaging} \\ R_X \propto 1/N^{\alpha},\ \alpha < 1 & \textit{weakly self-averaging} \\ R_X = \text{const} & \textit{non self-averaging}. \end{array} \tag{4.31}$$

Knowing these properties will help to decide whether or not it is necessary to average the results of a simulation over many independent realizations of the disorder even in the case that the size of the system is very large. We concentrate here on the dynamics of the system. It has been found that $C(t)$ is self-averaging for Ising random systems (Parisi et al., 1999). For the model we are studying the situation is *a priori* not clear, since the autocorrelation function is strongly linked to the order parameter $q_{EA}$ (which is exactly the long-time limit of $C(t)$). $q_{EA}$ is known to be discontinuous at $T_D$, and it can be that sample to sample fluctuations will results in strong fluctuations in the way $C(t)$ decay to $q_{EA}$ and subsequently to zero for finite systems. It is thus useful to analyze such behavior in detail.

In Fig. 4.17a we show the spin autocorrelation function for the system size $N = 1280$ for a selection of $50$ representative samples, at two different temperatures. From the figure it becomes clear that, at high temperatures ($T = 1.5 \approx 1.3T_D$), the sample to sample fluctuations are quite small and that therefore the system is probably self-averaging. For a temperature close to $T_D$ this is, however, not the case since sample to sample fluctuations are now of the same order as the typical relaxation time.

To study this effect in a more quantitative way we use the relaxation time $\tau$ as the observable $X$ discussed above. Using thus eq. (4.30) to define the quantity $R_\tau$ we can investigate the $N$ dependence of $R_\tau$. In Fig. 4.17b we show the temperature dependence of $R_\tau N$ for all system sizes investigated. We see that for high temperatures we do indeed find that this quantity goes to a constant of order one, *independent of the system size* and slightly dependent on the temperature. Hence we conclude that $R_\tau$ is proportional to $1/N$ and that the system is strong self-averaging. At low temperatures this is, however, no longer the case since there we see that the product increases with increasing system size and becomes, for the largest systems, as large $O(10^3)$. Thus this is evidence that the system is no longer self-averaging. To investigate this point closer, we plot in the inset $R_\tau$ at $T_D$ as a function of $N$. (Note that at this temperature we do not have data for the largest system size since the relaxation time becomes too large). From this graph we see that the value of $R_\tau$ is basically constant within the noise of the data, or shows even a slight trend to increase. Thus this is evidence that at this temperature the system is not self-averaging. We also mention that we expect that for sufficiently large $N$ self-averaging will be recovered for all $T > T_D$, although our data are not conclusive on this issue for $T \leq 1.3$, due to the strong finite size effects. A simple physical interpretation of these results is that, close to $T_D$ and with increasing system size, the effects of the mean field singularity become stronger and stronger, but they will not be homogeneous for every sample, as starts to be clear from Fig. 4.17.

### 4.2.2 A dynamic finite size scaling Ansatz

We have seen that, approaching the dynamical transition from above, the relaxation time of the spin autocorrelation function diverges as a function of the temperature like a power law (eq. (4.28)).

Let us now open a brief parenthesis to note that the divergence of relaxation times is a well known phenomenon characterizing *second order phase transitions* (where there is a single critical temperature $T_c$) and goes under the name of *critical slowing down*. This is observed in all dimensions, and the divergence of the relaxation times is closely related to the occurrence of a divergence in the susceptibility (Ma, 1976).Furthermore it is known that, at $T = T_c$ (Hohenberg and Halperin, 1977; Binder, 1992; Cardy, 1996), the relaxation time $\tau$ and the correlation length $\xi$ are related through

$$\tau \propto \xi^z. \tag{4.32}$$

$z$ goes under the name of dynamical critical exponent. In finite systems with linear dimension $L$ this critical divergence exhibits a finite size rounding, controlled by the rule that the rounding sets in when $L$ is comparable to $\xi$ (Binder, 1992). A dynamic finite-size scaling law holds (Goldschmidt, 1987; Wansleben and Landau, 1991)

$$\begin{aligned} &\tau = L^z f\left\{(T/T_c - 1)\, L^{1/\nu}\right\} \\ &f(x) \propto x^{-z\nu} \qquad x \to \infty \end{aligned} \tag{4.33}$$

where $\nu$ is the exponent giving the divergence of the correlation length $\xi \propto (T - T_c)^{-\nu}$. Note that for $T \gtrsim T_c$ eq. (4.33) gives $\tau \propto (T - T_c)^{-z\nu}$ (to be compared with eq. (4.28)) and that for finite systems eq. (4.32) takes the form

$$\tau \propto L^z. \tag{4.34}$$

We can now try to understand if a similar phenomenology occurs also in the Potts glass, although we have to keep in mind the differences with respect to ordinary critical phenomena, that is

- there is no divergent susceptibility at the *dynamical* transition $T_D$, at which relaxation times diverge in the thermodynamic limit;
- even the *static* phase transition at $T_0 < T_D$ is not an ordinary critical point, but shows characteristics of both first and second order phase transitions (discontinuous order parameter, finite susceptibility coming from the paramagnetic phase, absence of latent heat of transition).

The first thing to check is the dependence of $\tau$ with respect to the system size at the dynamical transition temperature $T_D$, which we know in advance for this system (De Santis et al., 1995). The result is shown in the inset of Fig. 4.18. The behavior is compatible with a power law

$$\tau \propto N^{z^*} \tag{4.35}$$

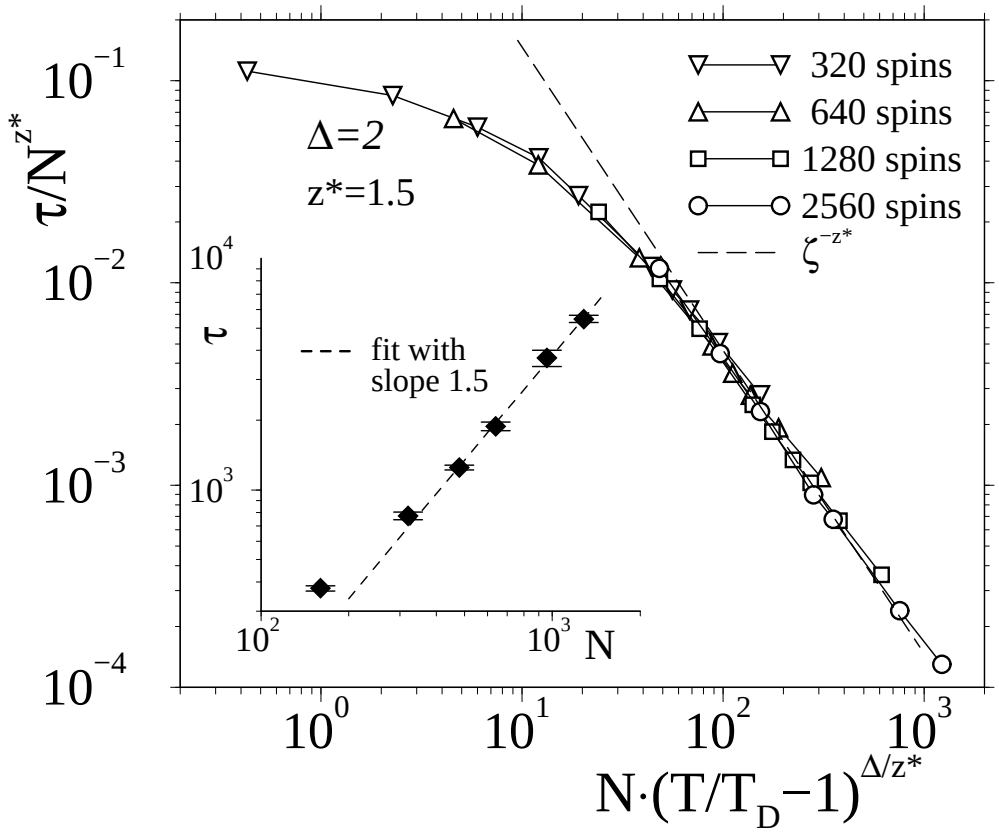


**Figure 4.18:** Log-log plot of the scaled relaxation time $\tau/N^{z*}$ vs the scaled distance $N(T/T_D-1)^{\Delta/z^*}$ from the dynamical transition temperature $T_D$, choosing $z^* = 1.5$ and $\Delta/z^* = 1.3$. The inset is a log-log plot of $\tau(T = T_D)$ vs $N$.

in analogy to the expression given in (4.34). The infinite range Potts glass has no intrinsic linear dimension, so the important quantity is the number of spins $N$ and $z^*$ plays the role of an effective exponent (in general $z^* = zd$ where $d$ is the dimension of the system. We will come back to this point later, when we will discuss what happens in the Sherrington -Kirkpatrick model). We see from the inset of Fig. 4.18 that for the $p = 10$ Potts glass $z^* \approx 1.5$. In order to provide a more systematic way of extrapolating the relaxation times to the thermodynamic limit, we assume that a dynamical finite size scaling hypothesis holds and make the Ansatz:

$$\tau = N^{z^*}\tilde{\tau}\left\{N(T/T_D-1)^{\Delta/z^*}\right\} \text{ for } N\to\infty \text{ and } (T/T_D-1)\to 0 \tag{4.36}$$

The scaling function $\tilde{\tau}(\zeta)$ must obey $\tilde{\tau}(\zeta\to\infty)\propto\zeta^{-z^*}$ to recover the proper thermodynamic limit; this finite size scaling form is inspired from eq. (4.33) and recovers as a limit the two results in eqs. (4.28) and (4.35). As can be seen from our data in Fig. 4.18 the Ansatz is well satisfied in the vicinity of the dynamical transition by the Potts glass. Our choice of $\Delta/z^* \approx 1.3$ implies $\Delta \approx 2$, consistent with the bound found when discussing Fig. 4.15. We see also that for large arguments the master curve does indeed show the expected power-law with an exponent $-z^*$ (dashed line). This gives good evidence for the validity of a dynamic finite size scaling law

close to the dynamical transition temperature $T_D$ (however, since in this model $T_0$ is very close to $T_D$, we cannot rule out a possible influence also of that transition on this result).

We stress again that eq. (4.36) has a well-based theoretical foundation for critical phenomena. For a spin glass transition, this is the case of the second order transition in the Sherrington-Kirkpatrick model (the infinite range Ising spin glass), where the temperatures $T_0$, $T_D$, and $T_s$ coincide at a unique critical temperature $T_c$. The dynamical exponent can be linked to static ones also for mean field models, but one has to be careful, since standard finite size scaling (and so also eq. (4.33)) are valid only for dimensions $d \leq d^*$ (Privman, 1990), with $d^*$ the upper critical dimension (that is, in the language of critical phenomena, the dimension above which the value of the exponents predicted from the mean field theory is correct). The connection is therefore done exactly at $d^*$ (Binder and Young, 1986) (the exponents valid there are considered correct in the mean field limit). In the Ising spin glass we have $d^* = 6$ (Binder and Young, 1986; Bhatt and Young, 1992), and the mean field result for the critical relaxation in spin glasses *with short range interaction* is $\tau \propto L^z$ with $z = 4$ (Zippelius, 1984). Since then at the upper critical dimension $\nu = \nu_{MF} = 1/2$ it turns out that $\Delta = z\nu_{MF} = 2$ and that $z^* = z/d^* = 2/3$; this results have also been found compatible with numerical simulations (Bhatt and Young, 1992). However, the value $z^* \approx 1.5$ found for the present model is clearly rather unusual and large, and we are not aware of any analytical estimates for this exponent.

### 4.2.3 Approach to broken ergodicity and dynamics in the low temperature phase

A further interesting question concerns the asymptotic decay of the correlation function $C(t)$ towards $q_{EA}$ as $t \to \infty$ at $T = T_D$. In the context of the structural glass transition the time regime during which the correlation functions are close to the plateau is called the "$\beta$-relaxation" whereas the decay below the plateau is called the "$\alpha$-relaxation" (Götze, 1989).

In the following we will discuss the shape of the correlation function $C(t)$ at $T_D$ in the time regime where it approaches the plateau. Detailed studies regarding the structure of mode-coupling equations (Götze, 1989) (which have the same structure of those obeyed by $C(t)$ in this model (Kirkpatrick and Wolynes, 1987)) have shown that in the thermodynamic limit $C(t) - q_{EA}$ decays like a power law

$$C(t) - q_{EA} \propto t^{-a} \text{ at } T = T_D. \tag{4.37}$$

A naive way to check for the presence of such a power law is to make a log-log plot of $C(t) - q_{EA}$ versus time. Fig. 4.19 shows such a plot for two relatively large systems (curves with open symbols) and we see immediately that there is no straight line, i.e. no power law dependence. However, one must recall that $C(t)$ shows a significant dependence on $N$ and that the prediction of eq. (4.37) seems to hold only for systems much larger than the ones studied here.

We know from the numerical solution of the replica-equations (De Santis et al., 1995) that $q_{EA}(T_D) = 0.328$. One thus can try to extrapolate the values of correlation functions for different $N$ at a given time. We have *a priori* no guide how to do it, since no theoretical argument exists. We used then, in the range $160 \leq N \leq 1280$ and $10 \leq t \leq 300$ two different extrapolation

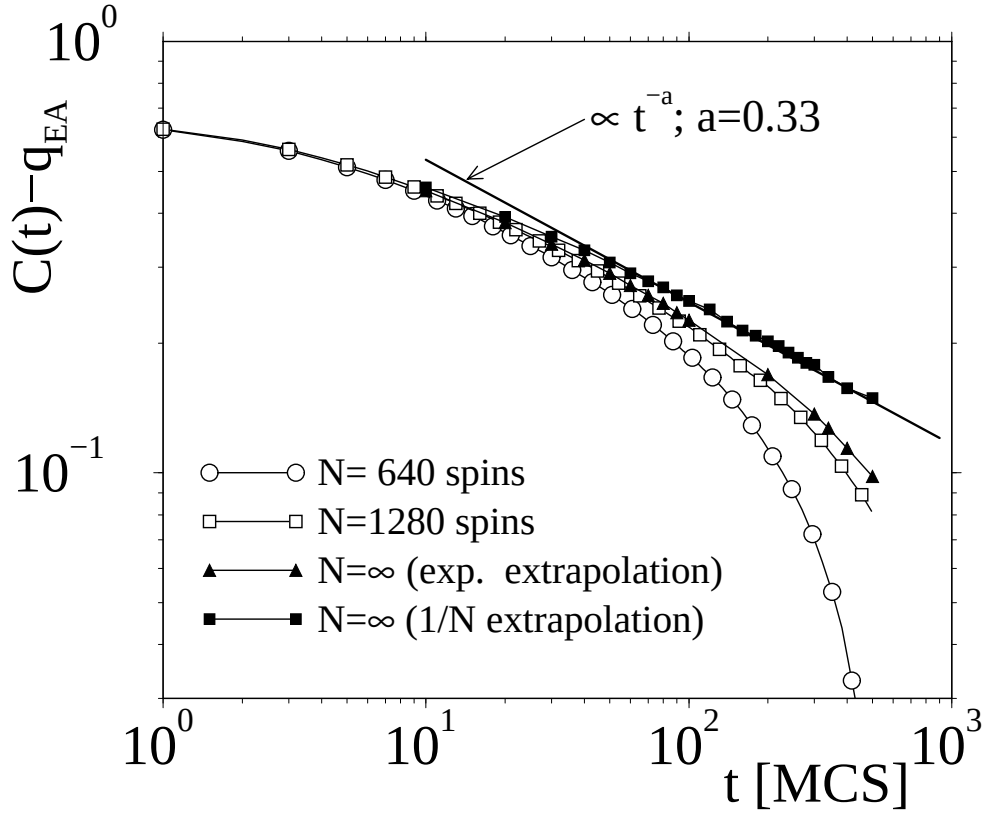


**Figure 4.19:** Log-log plot of the relaxation function $C(t) - q_{EA}$ versus time for $T = T_D$, using the theoretical value of $q_{EA}$. The curves with the open symbols are the data from the simulation for two system sizes ($N = 640,\ 1280$). The two curves with the filled symbols are the extrapolation of the simulation data to the case $N = \infty$ according to the extrapolations given in eqs. (4.38), (4.39) and shown in Fig. 4.20. The bold solid line is a fit with a power law.

methods, both giving good fits:

$$C(t, N) - q_{EA} \sim 1/N \tag{4.38}$$

$$C(t, N) - q_{EA} \sim \exp(-k \cdot N). \tag{4.39}$$

The quality of the two extrapolations is shown in Fig. 4.20. The first choice gives good results for $N \geq 480$; the second gives a better agreement with the data in all the time range and for all system sizes investigated, taking the constant $k = 1/400$. In Fig. 4.19 we have included the results of these two extrapolations also and we see that they do not give the same result. Since it is not clear which type of extrapolation is the correct one, it is difficult to tell what the shape of $C(t)$ in the thermodynamic limit really is. It is very interesting to note, however, that the extrapolation with the $1/N$ dependence gives a curve $C(t, N = \infty)$ which is very well compatible with a power law of the form given by eq. (4.37). Thus this gives some evidence that the extrapolation with $1/N$ is the correct one. The value for the exponent $a$ we read off is $0.33 \pm 0.04$.

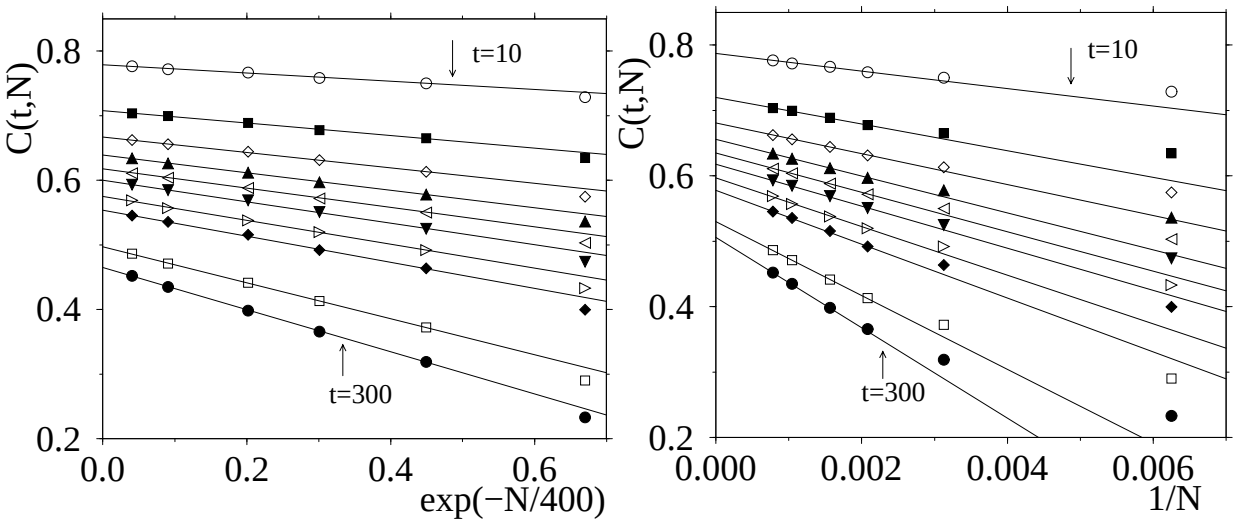


**Figure 4.20:** Results of the two extrapolation methods for $C(t, N)$, eqs. (4.38), (4.39). In both figures, the various points represent fixed-time extrapolations with, from top to bottom, $t = 10, 20, 30, 40, 50, 60, 80, 100, 200, 300$; the solid lines connecting them are results of best fits using linear regression.

It is also interesting to note that the theory predicts a correspondence between the value of $a$ and the exponent $\Delta$ from eq. (4.28) (Götze, 1989). For a given value of $a$ one can use (Götze, 1989; Kob, 1997)

$$\Delta = \frac{1}{2a} + \frac{1}{2b} \tag{4.40}$$

with the parameter $b$ linked to $a$ via

$$\frac{\Gamma^2(1+b)}{\Gamma(1+2b)} = \frac{\Gamma^2(1-a)}{\Gamma(1-2a)}. \tag{4.41}$$

Here $\Gamma(x)$ is the usual $\Gamma$-function $\Gamma(x) = \int_0^\infty e^{-t} t^{x-1} dt$ . If one uses the value $\Delta = 2.0$ and the above relations one finds $a = 0.36$, in very good agreement with the value determined from Fig. 4.19.

We now turn our attention to the low temperature regime $T < T_D$. At this temperature the free energy barriers in phase space do not diverge, since our system is *finite*, but tend to grow with the system size, since they have to approach the thermodynamic limit characterized by broken ergodicity. We can calculate and follow the decay of correlation functions only for $N = 160$ and $320$ because of the large relaxation times involved for larger systems. For $N = 640$, even using the parallel tempering algorithm to produce thermalized starting configurations for the dynamics, we can reach only $T = 1$. $C(t)$ at that temperature goes to zero after $3 \cdot 10^6$ MCS, which only for a single sample require $15$ hours of calculation.

The shape of $C(t)$ changes again with respect to the situation for $T \geq T_D$; in particular, now the presence of a plateau is clear, playing thus the role of the Edward-Anderson order parameter,

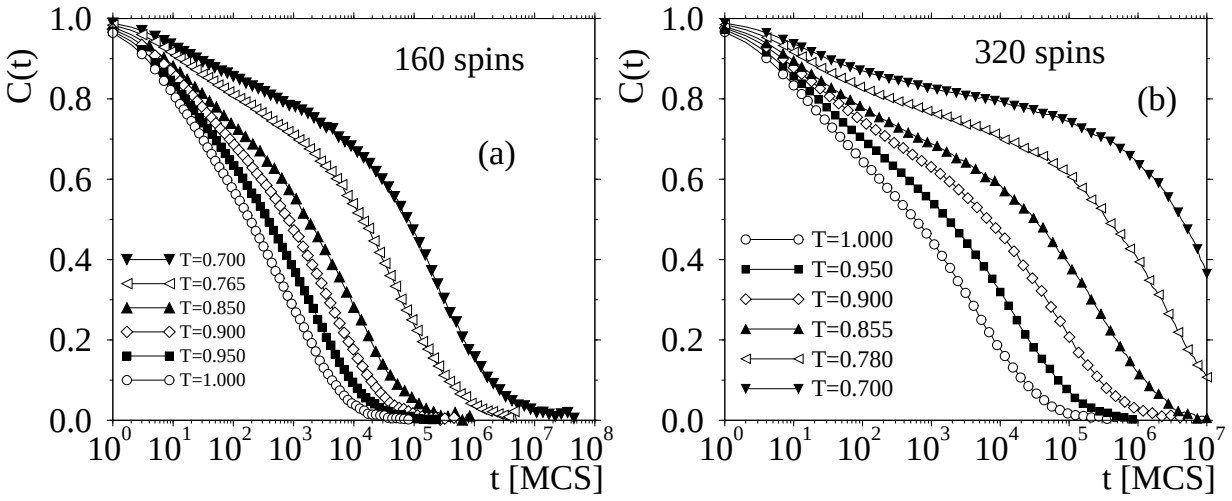


**Figure 4.21:** Time dependence of the correlation function $C(t)$ for various temperatures $T < T_D$; every curve is an average over $100$ different realizations of disorder. System sizes $160$ and $320$ spins respectively.

and connected also with the appearance of a second peak in the distribution function of the order parameter. The results are shown in Fig. 4.21 To produce this data we have used as initial configurations those *thermalized* with the parallel tempering method, and we let them evolve according to the usual Metropolis dynamics (single spin flip). We would also like to comment on the scaling property of $C(t)$ at low temperatures. We have already seen in the part devoted to the high temperature dynamics that the time-temperature superposition principle (TTSP) does not hold above $T_D$ (at least for the accessible system sizes). Also the typical feature of the plateau was not present. It is interesting now to see if TTSP is valid, since a plateau is clearly visible, Fig. 4.22. In particular for $N = 160$ we have been able to follow the complete decay of $C(t)$ to temperatures as low as $T = 0.7$ and in Fig. 4.22a we show the correlators as a function of the rescaled time $t/\tau$. If the curves for a wide range of temperatures ($0.7 \leq T \leq 1.2$) are considered one finds that an evidence for TTSP to hold is not that clear, since spreading is still present. However, if one uses only the curves for the lowest temperatures, see inset, one finds that they all collapse onto a nice master curve. Thus we conclude that at sufficiently low temperatures the time-temperature superposition principle does indeed hold. We mention also that the shape of this master curve is *not* an exponential, but that a stretched exponential with an exponent around 0.43 gives a satisfactory fit, as can be seen from the inset of Fig. 4.22a. Surprisingly such scaling holds also keeping fixed $T$ and considering different $N$, as Fig. 4.22b shows, although we cannot make any statement regarding the long time limit of the $C(t)$ for $320$ spins (since we were able to follow the dynamics only up to $C(t) = 0.4$).

One could argue that at low temperature the largest barrier dominates the dynamics and hence the relaxation depends on temperature only via a temperature dependent pre-factor (this is typical when the system relaxes to equilibrium "jumping" between different valleys in the configuration space, in the so-called *activated processes*). This temperature dependence would have to be

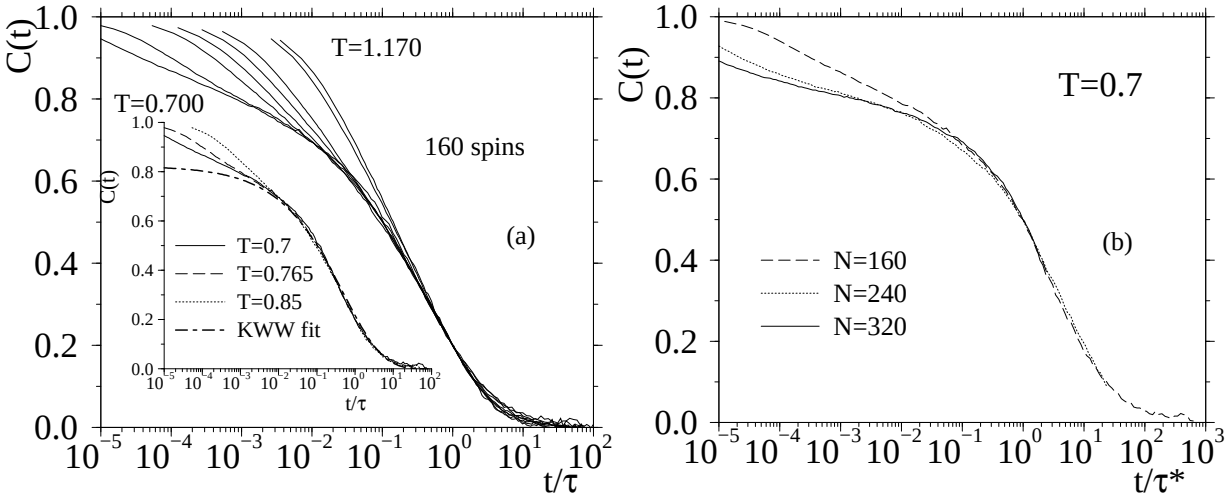


**Figure 4.22:** (a) Plot of $C(t)$ vs. $t/\tau$ for $N = 160$. The temperatures are $T = 0.7$, 0.765, 0.85, 0.9, 0.95, 1.0, 1.142, and 1.17 (left to right); the inset shows the same quantity only for the three lowest temperatures, together with the result of a KWW fit ($f \exp(-(t/\tau)^b)$) with $f \approx 0.81$ and exponent $b \approx 0.43$. Note that $f$ is also in good agreement with the $q_{EA}$ expected at that temperature, $0.82$ (see Fig. 4.5). (b) Scaling plot of the autocorrelation function at $T = 0.7$ for $N = 160, 240, 320$. The scaling time $\tau^*$ is modified with respect to the standard definition of $\tau$ such that $C(\tau^*) = 0.5$, since following the complete decay for $N = 320$ was computationally too expensive.

Arrhenius-like (that is $\tau \propto \exp(c/T)$) and in order to check this we show in Fig. 4.23 the $T$-dependence of $\tau$ for the different system sizes. One can easily identify three different regions: as we have already seen in Fig. 4.11 at high temperatures finite size effects are negligible and relaxation times do not depend on the system size. Approaching $T_D$ finite size effects start to be important and the system begin to feel the presence of the dynamical transition, and an approach to a divergence at $T = T_D$ starts to appear: the relaxation times can be scaled through the dynamic finite size scaling Ansatz (given above in eq. (4.36)). For $T < T_D$ the smaller system sizes ($160$ and $320$ spins) show indeed an Arrhenius behavior, with a size dependent activation energy (that is with different slopes in the Arrhenius plot). Also for $N = 640$ this behavior seems to hold, although the possible temperature range we can investigate does not extend to very low temperatures ($T = 1$ at best). We can obtain information on the size dependence of the barriers by looking at how relaxation times scale as a function of $N$. To do so, we fixed a temperature and consider the relaxation times as a function of $N$. We did this for two different temperatures, $T = 1$ (data up to $N = 640$) and $T = 0.7$ (data up to $N = 240$). In order to obtain useful information, we included also points coming from the simulation of smaller system sizes ($40$, $80$ and $480$ spins). The results are shown in Fig. 4.24, where we plot the logarithm of $\tau(T, N)$ vs. $N^{1/2}$.

The reason for this $N^{1/2}$ choice is that (i) it is very well compatible with our data and (ii) the Ising spin glass seems to have the same dependence (Mackenzie and Young, 1983). However, more

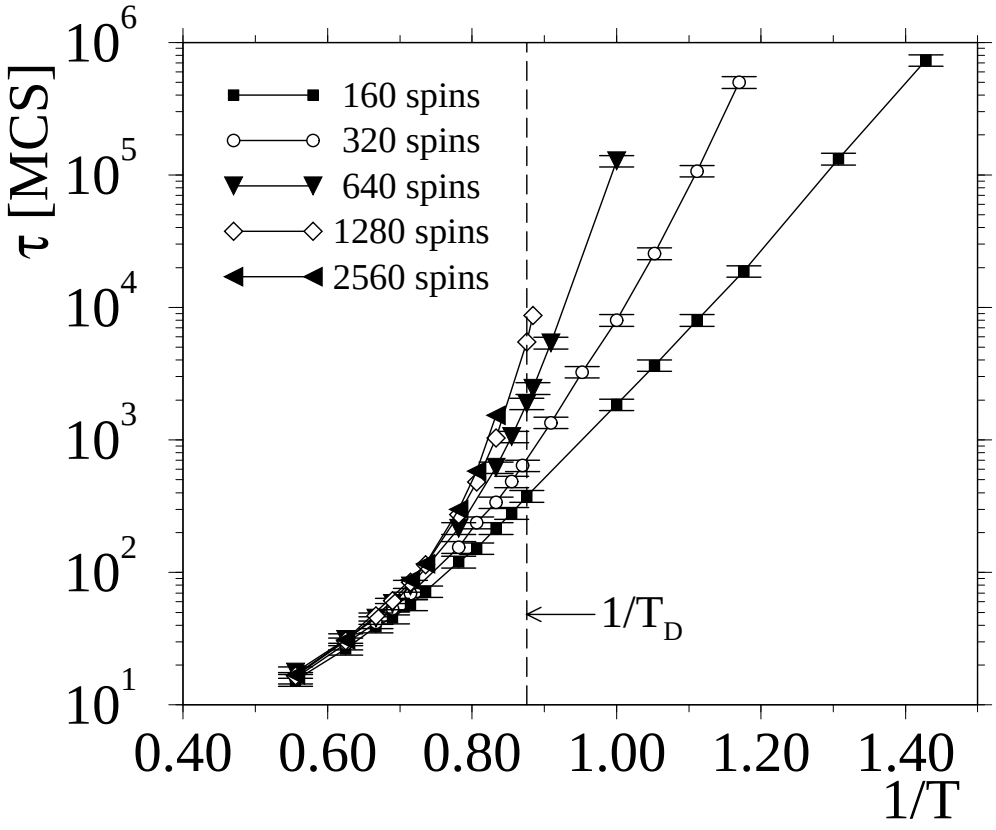


**Figure 4.23:** Relaxation time $\tau$ plotted vs. inverse temperature for different system sizes. The broken vertical line indicates the location of the dynamical transition for $N \to \infty$. Note the choice of a logarithmic scale for the ordinate. Error bars of $\tau$ are mostly due to the sample-to-sample fluctuation.

recent studies, supported also by analytical predictions (Billoire and Marinari, 2001), revised the value for the Ising case to $1/3$. We would like to note that for the present model the only analytical prediction concerns the barrier between the coexisting paramagnetic and spin glass phases at the static transition temperature $T_0$, which scales like $N^{1/2}$ (Gross et al., 1985). Whether this is true also for barriers between coexisting spin-glass states at lower temperatures is not yet clear, but our data seems to support a positive answer.

The difference between our results and those in the Ising case could also be due to a different structure of the replica-symmetry-breaking pattern in the two models, since $p = 2$ has a continuous replica-symmetry-breaking (Gross et al., 1985; Kirkpatrick and Wolynes, 1987; De Santis et al., 1995). In addition, for this model the exponent seems not to be related to spin reversal symmetry, since such a dependence is present also for the relaxation times of the correlation function of the rotational-invariant order parameter $C_{RI}(t)$. The results for the latter at $T = 1$ are shown in the inset of Fig. 4.24a. We have estimated as $\tau_{RI}$ the time it takes $C_{RI}(t)$ to reach the long-time constant value. The exponent $1/2$ is stable also if we consider points for the bigger system sizes

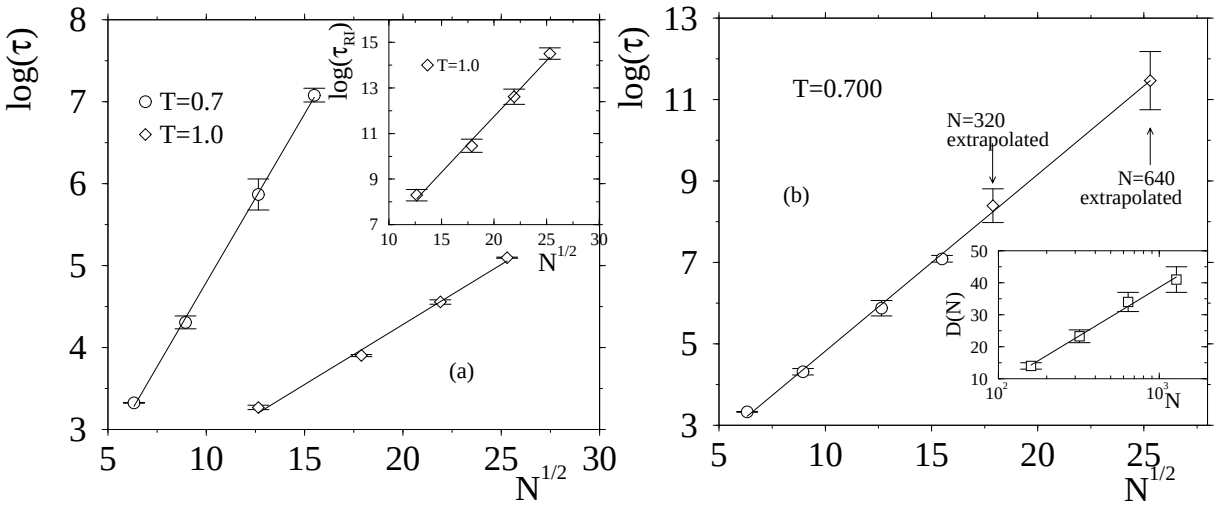


**Figure 4.24:** System size dependence of the logarithm of the relaxation time $\tau$ of $C(t)$; the two different sets correspond to $T = 1.0$ (up to $N = 640$) and $T = 0.7$ (up to $N = 240$). The inset shows the logarithm of the relaxation times for $C_{RI}(t)$ at $T = 1$ again as a function of $N^{1/2}$. (b) Logarithm of $\tau$ for $C(t)$ as in (a), but now with the two points obtained from the extrapolations of Fig. 4.23, see text for details. The inset shows the activation energies of the Arrhenius laws, always from Fig. 4.23, as a function of the size in a semilog plot.

($320$ and $640$) extrapolated according to the Arrhenius plot Fig. 4.23, (and marked with an arrow in Fig. 4.24b), although such an extrapolation has to be taken with care, since it involves times of the order of $10^6$ larger than what is possible to investigate in a reasonable amount of computer time. We note also that, if we determine the $N$-dependence of the activation energies $D(N)$ in the temperature regime where $\tau(T, N)$ shows an Arrhenius law ($\tau(T, N) \propto \exp(D(N)/T)$, from Fig. 4.23), we find that this energy increases only very slowly, i.e. like $\log(N)$, as shown in the inset of Fig. 4.24b. These points are also compatible with power law of $N$ with a small exponent ($\approx 0.1 = 1/p$). But also this extrapolation of the $D(N)$ is problematic, in view of the few points we have for $N = 640$ and $N = 1280$. (Note that the reason for the two different $N$-dependencies is related to the fact that the prefactor of the Arrhenius law depends on $N$ also.)

### 4.2.4 Single-spin relaxation and dynamical heterogeneities

In all the previous sections we have investigated the relaxation dynamics of the *whole* system and found that the time correlation functions show a non-exponential behavior. The purpose of this last part of the chapter is then to focus on the dynamics of the individual spins in order to obtain a better understanding for the occurrence of this non-exponentiality, present also in supercooled liquids.

In the latter case two very different *microscopic* scenarios have been proposed to explain this situation: in the first one, so-called "homogeneous", the particles relaxes practically identically following a non exponential statistical process. In a second scenario the non-exponential re-

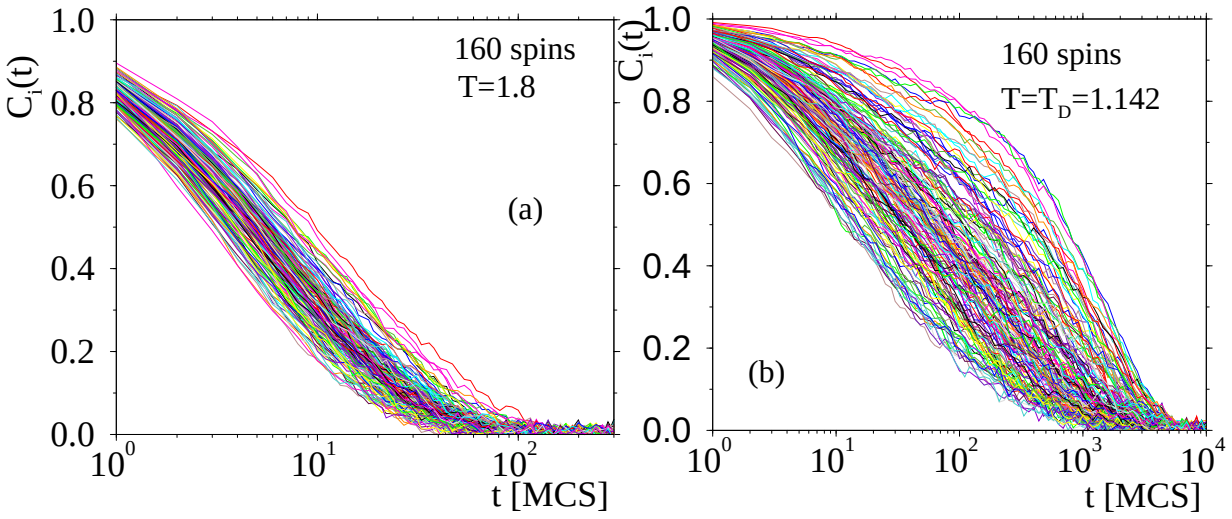


**Figure 4.25:** Time dependence of the single spin autocorrelation function $C_i(t)$ for $N = 160$ at $T = 1.8$ (a) and $T = T_D = 1.142$ (b). Each of the curves corresponds to a different spin.

laxation in supercooled liquids is due to the superposition of different processes (with respect, for instance, to the $\alpha$-relaxation times). According to this point of view, disordered systems at the microscopic level are characterized by "dynamical heterogeneities" (Sillescu, 1999; Ediger, 2000): each particle has a slightly different neighborhood affecting the dynamics of the particle. Note that these differences are present only on the time scale $\tau$ of the $\alpha$-relaxation, since afterward the particle has changed its neighborhood and hence its characteristic dynamics. If the dynamics is averaged over a time much larger than $\tau$, all the particles behave the same. However this is a scenario for supercooled liquids; for spin glasses the situation is different. The reason is that in supercooled liquids the disorder is self-induced during the dynamical and thermal history of the system. In spin glasses the disorder, given by the interactions $J_{ij}$, is quenched, that is in real systems the relaxation times of the couplings $J_{ij}$ are much larger than the typical relaxation time of the spins, so that the $J_{ij}$ can be considered, in a sense, frozen, quenched. That is way they are fixed in these models. The nature of the dynamics of the individual spins is thus an intrinsic property of each spin, depending on the way in which it is connected to the other ones by a set of different coupling constants. For a spin glass with short range interactions it is then expected that each individual spin has a different relaxation dynamics, and this is indeed what has been found in simulations of Ising spin glasses in two and three dimensions (Poole et al., 1997; Glotzer et al., 1998; Ricci-Tersenghi and Zecchina, 2000): dynamical heterogeneities, strongly dependent on the position of the spin in a lattice model. For spins systems with long range interactions the presence of such dynamical heterogeneities is however, *a priori*, not that clear: on one hand, since each spin interacts with many different ones, one might argue that on average the different spins show the same relaxation dynamics; on the other hand it is known (Binder and Young, 1986) that, also in systems with infinite range interactions, static quantities (such for instance energy per spin, local magnetizations) are not homogeneous. Numerical simulations offer in this respect a very useful tool.

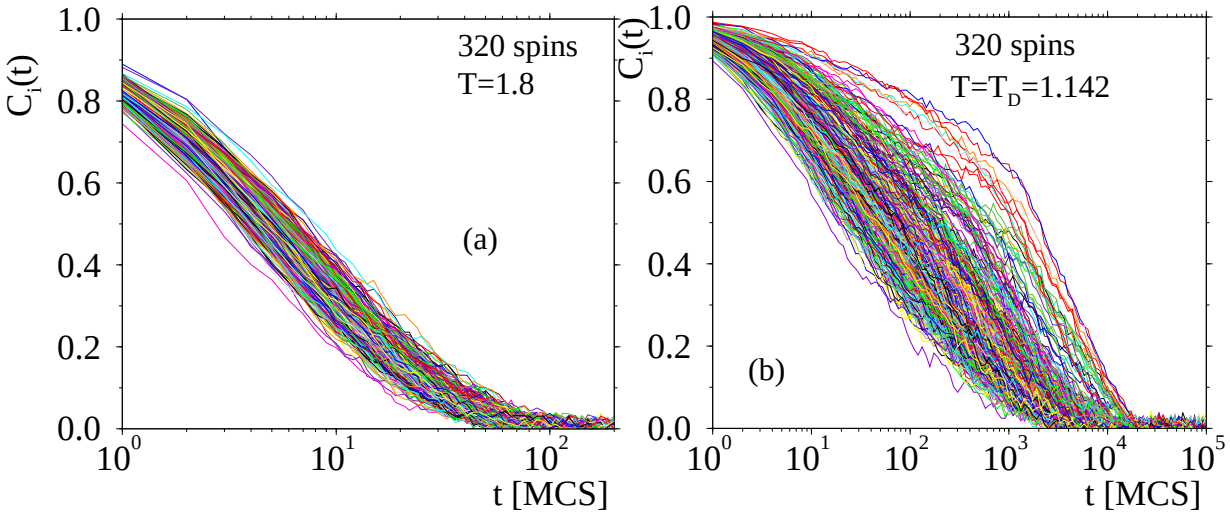


**Figure 4.26:** Time dependence of the single spin autocorrelation function $C_i(t)$ for $N = 320$ at $T = 1.8$ (a) and $T = T_D = 1.142$ (b). Each of the curves corresponds to a different spin.

In order to characterize the various individual dynamics we have calculated the autocorrelation functions $C_i(t)$ for every spin $i$:

$$C_i(t) = \frac{1}{p-1}\langle \vec{S}_i(t') \cdot \vec{S}_i(t'+t)\rangle. \tag{4.42}$$

Due to the single spin nature of the correlation function $C_i(t)$ it is necessary to make this average over a sufficiently long time in order to obtain a reasonable statistics. What happens is that for single spins a flip produces discrete jumps in the relaxation curve, and to have a good estimate we need to average over a large observation time. This is not necessary for the usual $C(t)$, since these effects are already averaged out over all spins. We found that an average over at least $1000$ $\alpha$-relaxation times is needed, and therefore the following results have been obtained only for relatively small system sizes and $10$ different samples for every temperature investigated. The procedure we adopted is the following: we performed a simulation run $100$ times longer than what takes to the normal correlation function $C(t)$ to decorrelate, and repeated this run $10$ times starting from different thermalized configurations. We paid attention to use, as starting point, configurations separated in normal dynamics by at least one $\tau$ ($\alpha$-correlation time), so that they can be considered decorrelated. This has been done for every different realization of disorder.

In Figs. 4.25 4.26 4.27 we show the time dependence of $C_i(t)$ for all the spins $i = 1, \ldots, N$ for three different system sizes $N = 160, 320$ and $640$ respectively. The temperatures are $1.8$ and $T_D$, i.e. the dynamical critical temperature at which the *average* relaxation dynamics, as measured by $C(t)$, is already strongly non-exponential for all system sizes investigated. From the figure we see that the relaxation dynamics for the different spins depends strongly on these spins in that, e.g., they relax to zero on time scales that span more than an order of magnitude. At a time where the correlation functions have reached $0.5$ of their initial value, the width of the range is even higher and increases rapidly with increasing system size. Furthermore we see from

the figures that the curves for the individual spins seem to occur in clusters, i.e. that they do not fill the interval between the slowest and the fastest relaxation in a homogeneous way, since the various $C_i(t)$, especially for medium and long times, occur in stripes. Below we will discuss the reason for this clustering in more detail.

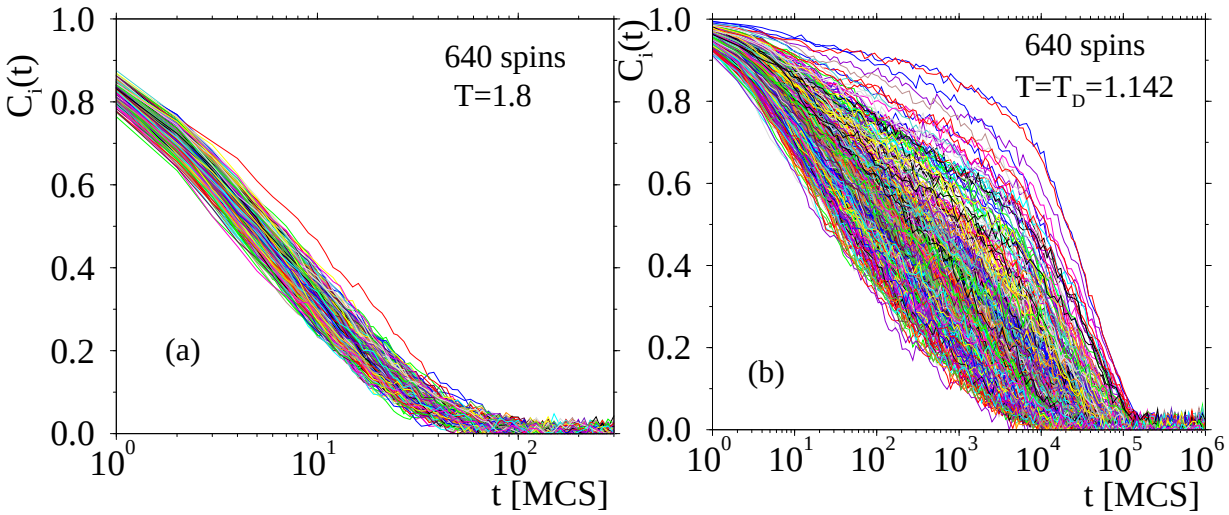


**Figure 4.27:** Time dependence of the single spin autocorrelation function $C_i(t)$ for $N = 640$ at $T = 1.8$ (a) and $T = T_D = 1.142$ (b). Each of the curves corresponds to a different spin.

In Fig. 4.28 we show the single spin autocorrelation function at a lower temperature for $160$ and $320$ spins. Comparing these curves with the ones in Figs. 4.25 and 4.26 we see that a decrease of $T$ has made the distribution of the relaxation dynamics even wider. Also the presence of the clustering of the curves is now much more pronounced. From Fig. 4.28 one also recognizes that the shape of the individual curves is not uniform at all since the ones which decay slowly tend to be, in the $\alpha$-regime, much steeper than the ones that decay more rapidly at early times. A more careful analysis shows that these slow spins show more or less a purely exponential relaxation whereas, as can already be seen from the figure, the fast ones show a strong deviation from a simple exponential and are better described by stretched exponentials. Thus we conclude that in this model the non-Debye behavior of $C(t)$ found at low $T$, see Fig. 4.22, is not due to a superposition of Debye laws with different relaxation times, but the sum of various different processes, some of which are Debye-like, some of which are not.

In order to understand the microscopic reason for the presence of these dynamical heterogeneities a bit better we have investigated to what extend the relaxation dynamics of an individual spin correlates with other quantities. For this it is necessary to characterize this dynamics in some way. As discussed above, the shape of the curves is not at all uniform, which makes such a characterization rather difficult. Therefore we decided to neglect all the variations of the shape completely and to characterize each curve just by the time it takes to a spin to decay to a given value. Therefore we defined two different relaxation times, $\tau_i^{(0.4)}$ and $\tau_i^{(0.7)}$, via

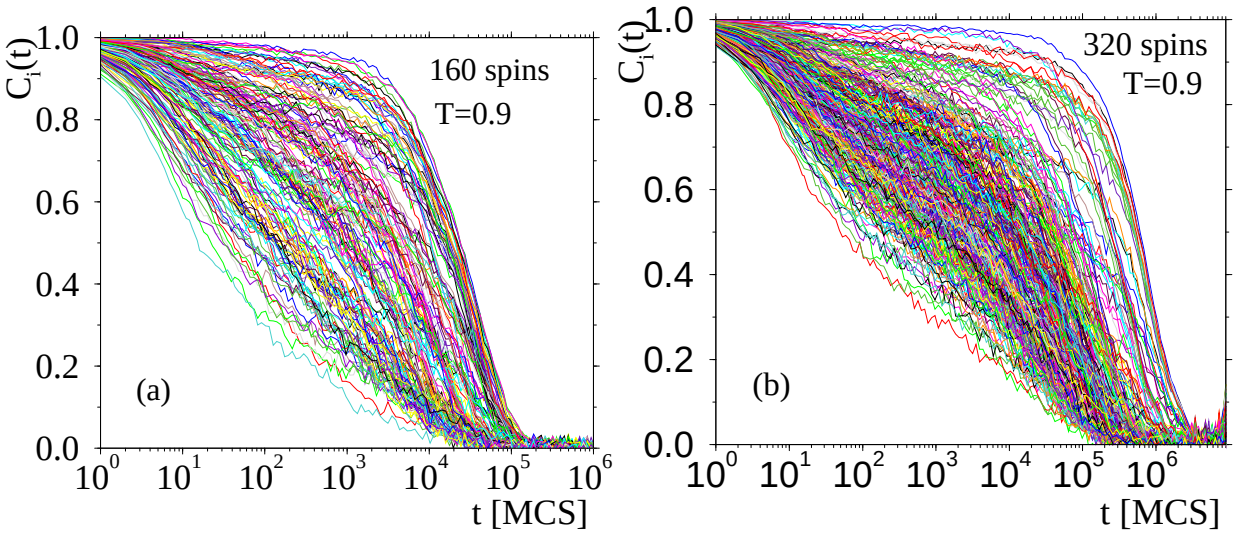


**Figure 4.28:** Time dependence of the single spin autocorrelation function $C_i(t)$ at $T = 0.9$ for $N = 160$ (a) and $N = 320$ (b). Each of the curves corresponds to a different spin.

$$C_i(t = \tau_i^{(0.4)}) = 0.4 \text{ and } C_i(t = \tau_i^{(0.7)}) = 0.7. \tag{4.43}$$

In Fig. 4.29 we show a scatter plot between $\langle e_i \rangle$, the average energy of spin $i$, and the relaxation time, for both definitions of $\tau_i$. We see that there is indeed a significant correlation between the energy and the relaxation time in that spins with high energy relax faster than the ones with low energy. This result is very reasonable since a spin that has a low energy will be reluctant to change its value and therefore to go (with high probability) to a state with a higher energy. From the figure we also recognize that the correlation is present for both definitions of $\tau_i$, from which we conclude that the details of this definition are not crucial. In order to investigate this point a bit closer we show in Fig. 4.30 a scatter plot of the relaxation time $\tau_i^{(0.7)}$ versus $\tau_i^{(0.4)}$ for the two temperatures. We see that although the correlation is not perfect, it is still very significant and therefore we conclude that the salient features of the correlation between the relaxation time and the mean energy shown in Fig. 4.29 will be observed even if a more careful characterization of the relaxation dynamics is made.

Of further interest is the question how the relaxation time of a given spin at a given temperature is related to the relaxation time of the same spin at a different temperature. This dependence is related to the question of "chaos in temperature" (Ritort, 1994), i.e. how the properties of a system change if temperature is changed. The term chaos in spin glasses addresses the possibility that a perturbation to the system can "reshuffle" the different weights of the equilibrium configurations. Besides changes in the magnetizations or in the coupling constants $J_{ij}$, also the variation of the temperature can be considered a perturbation. For mean field type systems subject to changes in temperature it is expected that these dependencies are rather weak (Kondor, 1989; Ritort, 1994). In agreement with this expectation we find that indeed the relaxation times

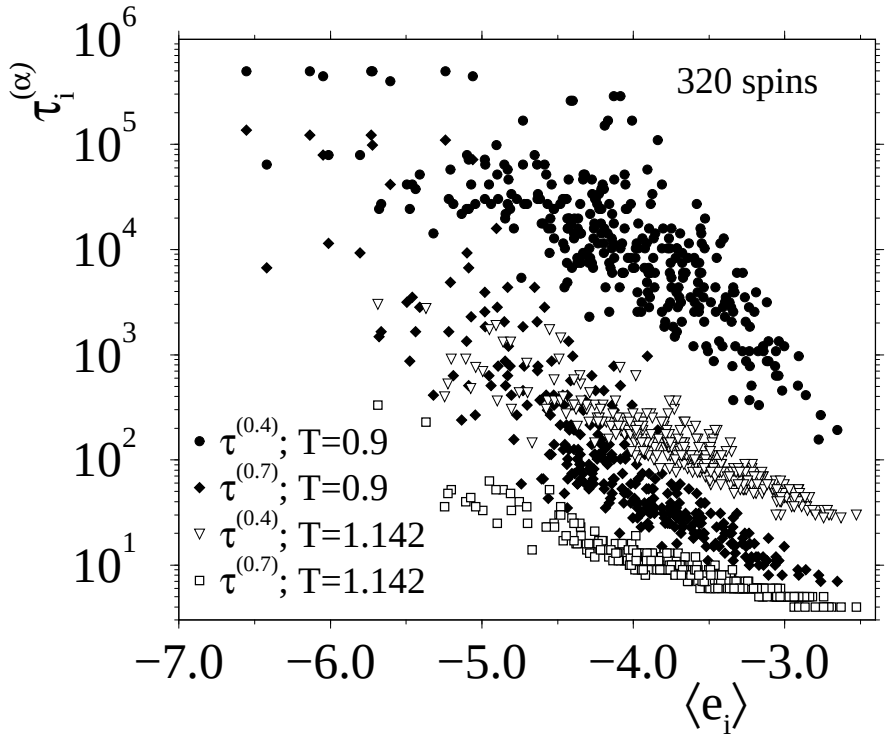


**Figure 4.29:** Scatter plot of $\tau_i$, the mean relaxation time of spin $i$ as defined in eq. (4.43), versus the mean energy $\langle e_i \rangle$. The open and closed symbols correspond to $T = 1.142$ and $T = 0.9$, respectively. The points are for a typical sample of 320 spins.

$\tau_i$ for $T = 0.9$ are strongly correlated with those at $T = 1.142$, see Fig. 4.30b, irrespective of the definition of $\tau_i$; this means that qualitative dynamical features for the single spins do not change, i. e. that spins that relax slowly (quickly) at a certain temperature maintain this characteristic also when $T$ is changed, even for rather large differences in temperature, where relaxation mechanisms are different (compare with Fig. 4.23). We see also that this property seems not to be strongly affected by finite size effects, see Fig. 4.30. Static quantities like the energy per spin $\langle e_i \rangle$ are even much stronger correlated, Fig. 4.31, between two different temperatures, than relaxation times, giving again further support to a weak influence of chaotic effects, at least due to temperature variations. Of course one has also to consider that the energy per spin is a much better defined quantity than the single relaxation times, and the fact that they behave consistently confirms the general picture.

Before we end we come back to the observation discussed above that some of the single spin autocorrelation functions occur in clusters (see Fig. 4.28). One potential reason that the relaxation dynamics of two spins is similar is that they are coupled together strongly, i.e. that their interaction constant $J_{ij}$ is large; in this way their tendency to flip would also be correlated, so we expect rather similar dynamics. In order to test this idea we identified for each realization of the disorder those spins that formed at $T = 0.9$ the clusters relaxing very slowly (this identification was done visually by means of plots like the one shown in Fig. 4.28b). Say that each of these

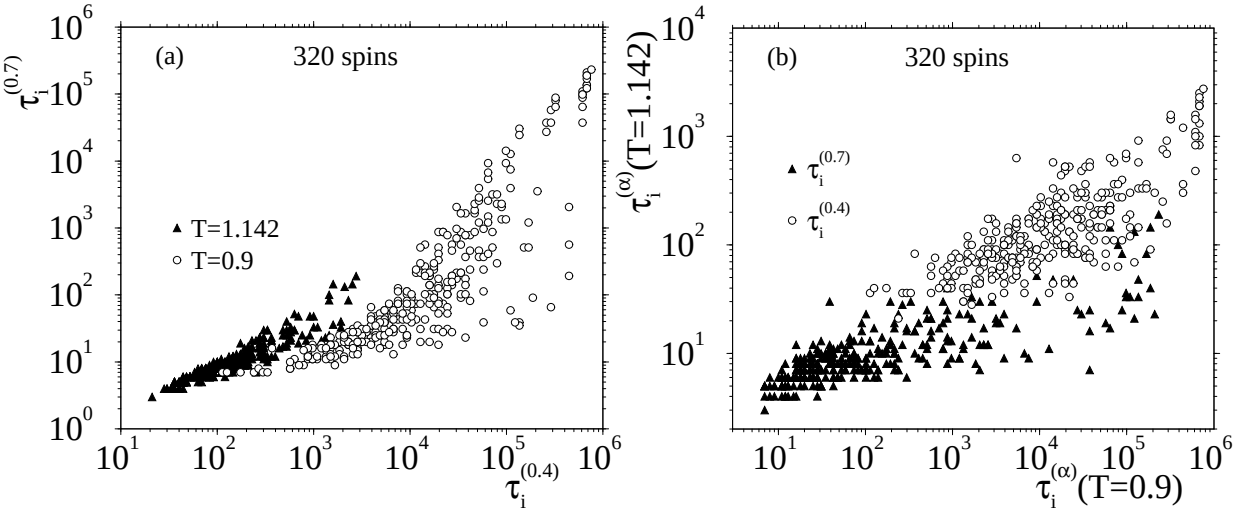


**Figure 4.30:** a) Plot of $\tau_i^{(0.7)}$ [defined by $C_i(t = \tau_i) = 0.7$] versus $\tau_i^{(0.4)}$ [defined by $C_i(t = \tau_i) = 0.4$], for $T = 0.9$ and $T = 1.142$ (open and filled symbols, respectively) showing that the two relaxation times are correlated. Each point correspond to a different spin. b) Plot of the relaxation times $\tau_i^{(0.4)}$ and $\tau_i^{(0.7)}$ at $T = 1.142$ versus these relaxation times at $T = 0.9$. Each point correspond to a different spin.

clusters involved $k$ curves. We then determined the $k(k-1)/2$ interaction constants between these $k$ spins. The values of these constants are shown in Fig. 4.32 for ten different realizations of the disorder (filled circles). Also included in the figure is the Gaussian distribution of the coupling constants. From this figure we see that most of the points corresponding to the couplings $J_{ij}$ are to the right of the mean of the distribution (vertical dashed line). Hence we conclude that the spins that form the slow cluster of relaxation curves are coupled together stronger than two arbitrary spins (since the Potts Hamiltonian favors bonding between spins linked by positive $J_{ij}$) and therefore form a "dynamical entity". We note, however, that the fact that two spins are strongly coupled does not necessarily make them slow: we have in fact evidence of strongly coupled spins whose relaxation time is fast, and also of strongly coupled spins with very different relaxation times. From this we can therefore conclude that such a strong coupling is only a necessary but not a sufficient condition for a slow dynamics. Another observation to make is that the size of the slowest clusters does not typically exceeds $6$ spins, and that the longest relaxation time is typically due to a simple-exponential relaxation. It might be that such clusters are linked to a recently proposed scenario for the glass transition based on metastability and nucleation (Crisanti and Ritort, 2001). The authors suggest that the "droplets" that nucleate are slowly relaxing structures composed by few particles/spins, giving rise to the typical slowing down and to Arrhenius behavior at low temperatures.

It is difficult to find a proper indicator linking static (the $J_{ij}$) and dynamical properties in this infinite range models, lacking by definition any geometry. Usually in finite dimensions clusters of spins can be visualized directly as spatial arrangements, so that it is clear the role of the local interactions in determining the dynamics, like in the case of two and three dimensional Ising

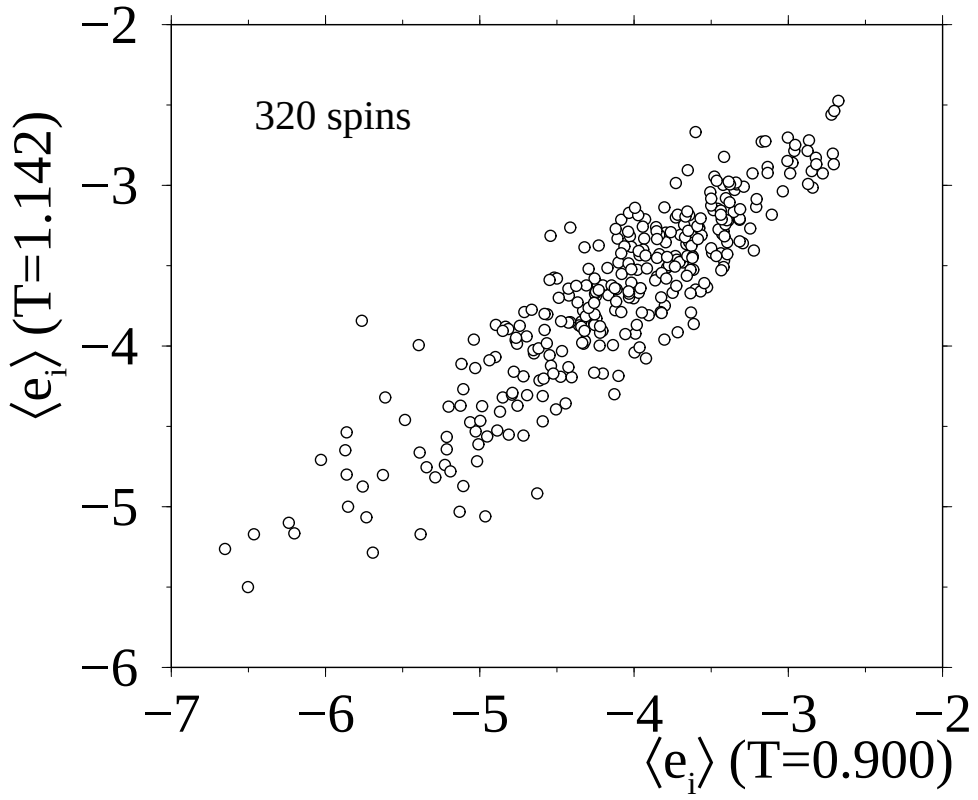


**Figure 4.31:** Plot of the energy per spin $\langle e_i \rangle$ energy at $T = 0.7$ vs. the same quantity at $T = 0.9$ for a system of 320 spin and a single realization of disorder. Every point correspond to a different spin.

systems (Poole et al., 1997; Glotzer et al., 1998; Ricci-Tersenghi and Zecchina, 2000). On the other hand it is also very interesting to note that such strongly heterogeneous behavior can be seen in "non real space" models. A tentative interpolation between the two cases has been recently done (Barrat and Zecchina, 1999) using systems with finite (i.e. $O(1)$) but random connectivity (random graphs).

Recently another observable has been introduced to study the onset of non-exponentiality and the loss of ergodicity in mean-field spin-glass models with a dynamical transition, and used to interpret the behavior of supercooled liquids (Franz and Parisi, 2000). The idea is that, as a static phase transition is associated with the divergence of a static susceptibility related to the fluctuation of the order parameter, the same can be extended to dynamical phase transitions introducing a dynamical susceptibility. This dynamical susceptibility is thus related to the fluctuations of the Edwards-Anderson order parameter. Therefore the following function is introduced:

$$\chi(t) = N \left[ \langle c(t)^2 \rangle - \langle c(t) \rangle^2 \right]_{av} \qquad c(t) = \frac{1}{N} \sum_i^N \frac{\vec{S}_i(t') \cdot \vec{S}_i(t'+t)}{p-1} \tag{4.44}$$

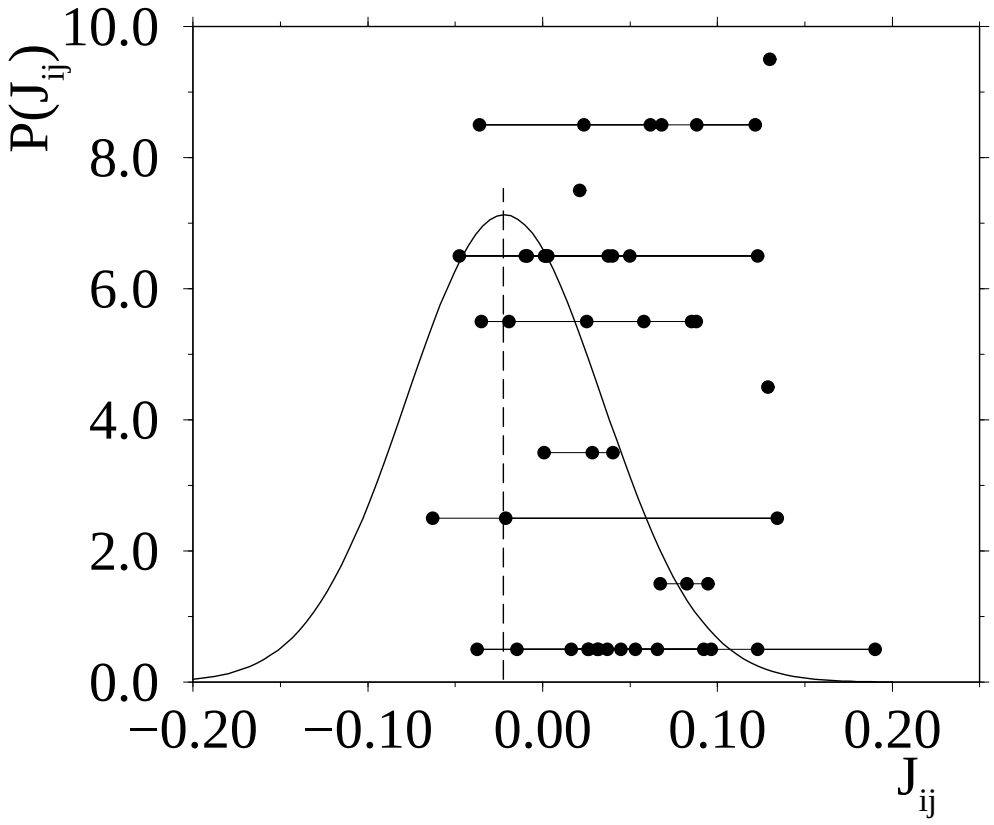


**Figure 4.32:** Values of the bonds between spins with very slow relaxation in 10 different disorder realizations for 320 spins at a temperature $T = 0.9$ (filled circles). For clarity the points have been displaced vertically by various amounts. The continuous curve shows the Gaussian distribution from which the $J_{ij}$ are extracted and the vertical dashed line shows its mean.

where $C(t) = [\langle c(t) \rangle]_{av}$ is the usual correlation function defined in eq. 4.23. Fluctuations of the standard $C(t)$ for every realization of disorder are due to the fact that the spins relaxes in different ways, heterogeneously.

A connection with the heterogeneous aspect of the dynamics, which we investigated up to now only through the difference among the various $C_i(t)$-eq. (4.42)-can be seen rewriting eq. (4.44). If we call, for simplicity of notation,

$$q_i(t) = \frac{\vec{S}_i(t') \cdot \vec{S}_i(t'+t)}{p-1}, \tag{4.45}$$

we have that

$$\chi(t) = \frac{1}{N^2} \left[ \left\langle \left( \sum_i q_i(t) - \sum_i \langle q_i(t) \rangle \right) \right\rangle^2 \right] \tag{4.46}$$

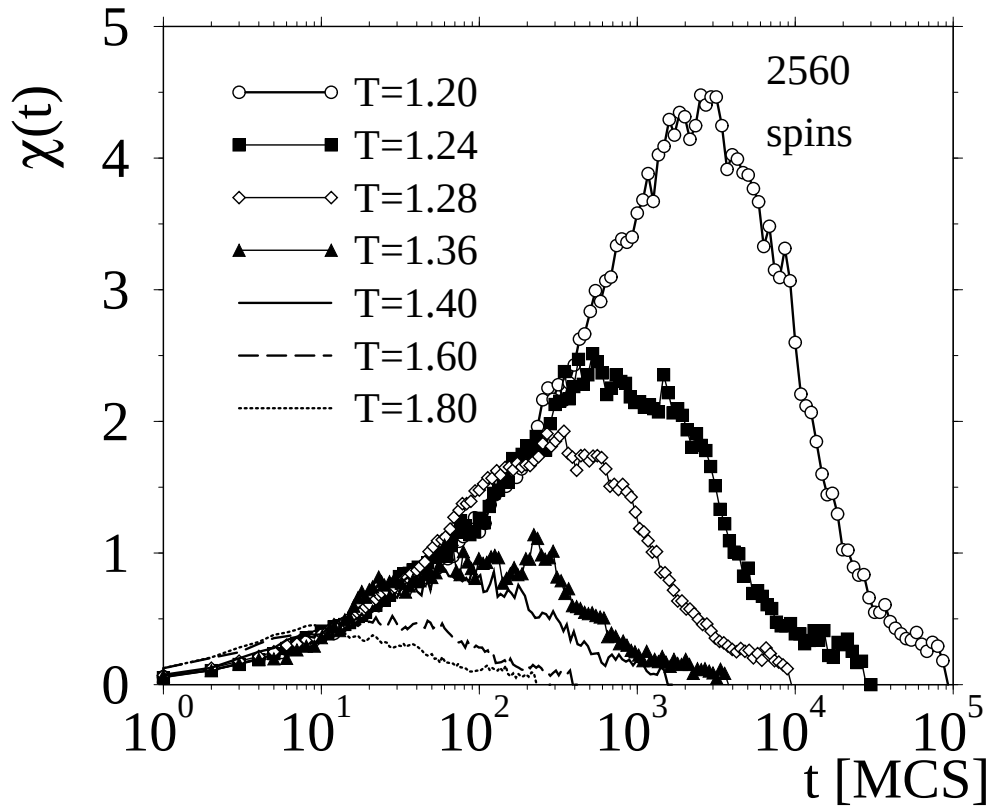


**Figure 4.33:** The non-linear dynamical susceptibility $\chi(t)$ defined in eq. (4.44) for the system size $2560$ spins, as a function of time for various temperatures.

Note that $\langle q_i(t)\rangle = C_i(t)$. Different from our investigation now is then the role of the fluctuation around this functions, and the final average over the disorder. However there are elements to interpret $\chi(t)$ as an indicator for the appearance of dynamical heterogeneities in the system (Franz and Parisi, 2000).
$\chi(t)$ has been studied analytically and numerically (Franz and Parisi, 2000) in the $p$-spin spherical model for spin glasses, whose physics is analogous to the one of the Potts glass with $p > 4$, and thus to the model we are studying. Both a dynamical and a static phase transition are present, and this model is particularly used for analytical investigations (Crisanti and Sommers, 1992; Crisanti et al., 1993). It has been found that $\chi(t)$ presents a maximum at a time $t^*$, which becomes larger and larger as the dynamical transition is approached from above. Also the height of this maximum $\chi^* = \chi(t^*)$ grows with the temperature. Actually a power law divergence is found for both of them

$$t^* \propto (T - T_D)^{-\gamma} \qquad \chi^* \propto (T - T_D)^{-\alpha}. \tag{4.47}$$

For the $p$-spin spherical model with $p = 3$, $\chi(t)$ has been calculated throughout numerical integration of the equations of motion, and a subsequent fit gave the values $\alpha = 1.1$ and $\gamma = 0.52$

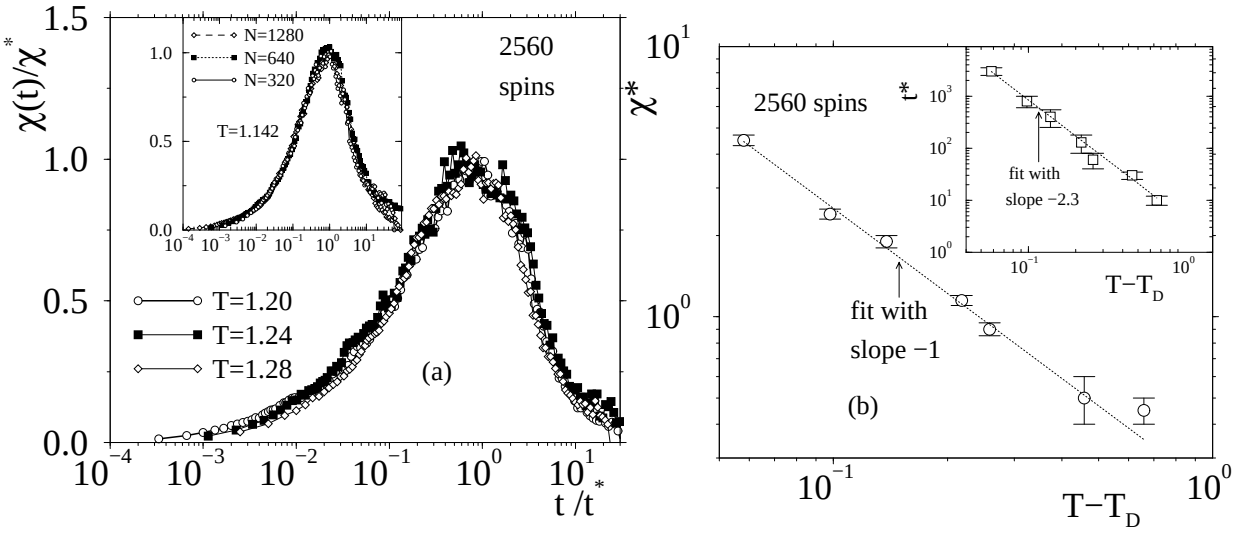


**Figure 4.34:** (a) The dynamic susceptibility rescaled. The plot shows $\chi(t)/\chi^*$ versus $t/t^*$ (see text for the definition of the quantities). In the main plot the curves are for $2560$ spins and $T = 1.20, 1.24, 1.28$. The inset shows the same rescaling but at fixed temperature $T = T_D = 1.142$ and three system sizes $N = 320, 640, 1280$. (b) Log-log plot of the temperature dependence of the maximum of $\chi(t)$ for $2560$ spins: the dotted line is a fit with exponent $-1.0 \pm 0.2$. In the inset the same for the position of the maximum. The dotted line is a fit with an exponent $-2.3 \pm 0.3$.

(Franz and Parisi, 2000).

We can calculate $\chi(t)$ directly from our simulation data, and this offers a useful complement to the investigation of the dynamical heterogeneities, since we can investigate what happens for large systems ($1280$ and $2560$ spins) approaching $T_D$ from above. For these system sizes, close to the dynamical transition, a detailed study of the single spin correlation function is not feasible, since it involves, as we have seen, an effort of at least $2$ orders of magnitude more than that required to follow the total relaxation of the system. $\chi(t)$ as a function of time for various temperatures and $N = 2560$ is presented in Fig. 4.33. Qualitatively the results resemble those already found for the $p$-spin spherical model. A maximum is present. It is very broad for high temperatures ($1.8 \leq T \leq 1.5$) but sharpening as $T_D$ is approached. Also clear is the progressive growing of the height of the maximum. We also notice that the curves can be superimposed onto each other to give a master curve when we plot $\chi(t)/\chi^*$ versus $t/t^*$, see Fig. 4.34a. We are not aware of an analytical prediction of this result, but it might be that it can result from the structure of the equation of motion describing the system. This scaling works close to $T_D$, since it is there that a maximum is well defined. The same kind of scaling works also using different system sizes and fixed temperature, as the inset of Fig. 4.34a shows, for $T = T_D = 1.142$ and $N = 320, 640, 1280$.

The temperature dependences of the position $t^*$ of the maximum and of its height are compatible with power law divergencies like in eq. (4.47), see Fig. 4.34b, where they are plotted for the

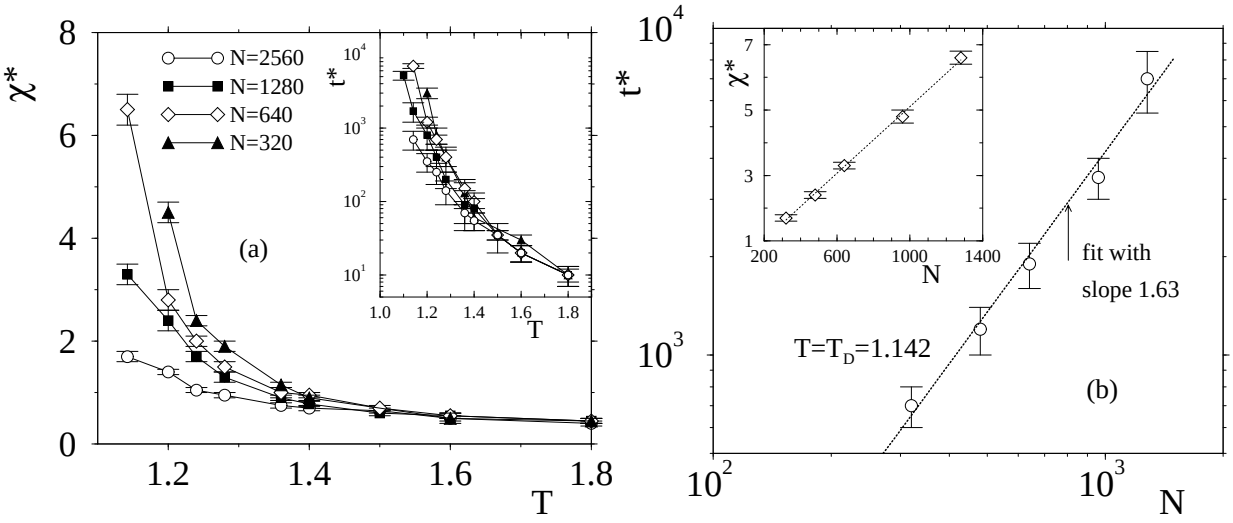


**Figure 4.35:** (a) Height of the maximum $\chi^*$ of $\chi(t)$ as a function of the temperature for different system sizes. In the inset log-log plot of the position of the maximum $t^*$ of $\chi(t)$ as a function of temperature for different system sizes. (b) System size dependence at $T = T_D = 1.142$ of the position of the maximum of $\chi(t)$ in a log-log plot. The dashed line is a fit to a power law with exponent $1.63 \pm 0.15$. In the inset the same for the height of the maximum. A linear dependence on $N$is given by the dotted line.

largest system size $N = 2560$. In our case $\gamma = 2.3 \pm 0.3$, compatible with the divergence of the relaxation time $\tau$, and $\alpha = 1.0 \pm 0.2$. The values of these exponents are calculated by means of a power-law fit, also included in the figure.

The system size dependence of $t^*$ and $\chi^*$ are shown in Figs. 4.35. Both increase monotonically with the system size, as appears from the figures. It is interesting to note that the position of the maximum, at $T = T_D$, diverges as a power law with the system size $t^* \propto N^c$, with $c = 1.63 \pm 0.15$ compatible with the value found for $z^* \approx 1.5$ that determines the divergence of the relaxation time $\tau$ at the dynamical critical temperature. This contributes further to the idea that these two timescales $\tau$ and $t^*$ are related to the same physical phenomenon of the breaking of the ergodicity. We find also that at $T_D$ the height of the maximum diverges linearly with $N$. Everything is then compatible with the appearance of divergencies in $\chi(t)$, at the temperature $T_D$ were the static spin glass susceptibility is still finite.

It is clear that the observations presented in this section are only modest first steps addressing the dynamics of the individual spins in the low temperature phase. It certainly would be interesting and useful to understand better how the distribution of the relaxation times of the spins depends on the system size and on temperature in order to obtain a better comprehension how the mean relaxation dynamics of the system is related to the one of the single spins. However, due to the high computational demand for this kind of investigations such studies have to be left to the future.

# Chapter 5

# The Potts glass in three dimensions

## 5.1 Statics

In the infinite-range case, the computation time per Monte Carlo sweep is of the order $N^2$, since the system is fully connected, and the choice of the distribution of the interactions was not influent (in the Ising case, for instance, it can also be shown that the leading terms in finite size scaling coincide (Parisi et al., 1993a)). In the short range case the computation time is proportional to $N$. We make use of the Heat-Bath method, which works better with a bimodal distribution of bonds, as we explained in chapter 3, devoted to the numerical methods. We just remind that, in the single-spin-flip process, to every possible state $l \in \{1, \ldots, p\}$ a probability

$$p_l = \frac{e^{-\beta E_l}}{\sum_{m=1}^{p} e^{-\beta E_m}} \tag{5.1}$$

is assigned, where $E_l$ is the total energy of the system if the spin to flip is in the state $l$ (Newman and Barkema, 1999). The calculation of the exponentials is usually computationally expensive, and can be avoided in the case of a $\pm J$ distribution, since all the possible values can be tabulated in advance. Note that the calculation of $p_l$ involves only a sum over the nearest neighbors, since the Hamiltonian can be decomposed into the terms involving the chosen spin and those which don't. This latter part is the same for all possible value of $l$ and so cancels in the expression (5.1). Given the advantages of this algorithm in the short range model, in this case the choice of $P(J_{ij})$ starts to be important. We recall that the Hamiltonian is given by

$$\mathcal{H} = -\frac{1}{2} \sum_{i,j} J_{ij}(p\delta_{\sigma_i \sigma_j} - 1). \tag{5.2}$$

where the sum is over nearest neighbors (6 for every spin in three dimensions). We always use in this chapter $p = 10$, and we work in units of $k_B = 1$. The form of the bimodal distribution is

$$P(J_{ij}) = x\delta(J_{ij} - J) + (1 - x)\delta(J_{ij} + J). \tag{5.3}$$

We use the following notation for the moments

$$\begin{aligned} J_0 &= [J_{ij}]_{av} \\ (\Delta J)^2 &= [J_{ij}^2]_{av} - [J_{ij}]_{av}^2. \end{aligned} \tag{5.4}$$

The relation with $x$ and $J$ defined in eq. (5.3) is given by

$$x = \frac{1}{2}\left(1 + \frac{J_0}{J}\right) \qquad J = \sqrt{J_0^2 + (\Delta J)^2}. \tag{5.5}$$

In mean-field theory the second moment controls the transition temperature (Cwilich and Kirkpatrick, 1989), which in these units is given by $T_c = \sqrt{z}\Delta J$, where $z$ is the coordination number ($z = 2d$ for short range models in spatial dimension $d$). We use here the generic notation $T_c$, since *a priori* we do not know how much of the mean-field picture will survive in finite dimension. This $T_c$ is best identified with what we labeled as $T_s$ in chapter 2. It is the true transition temperature for $p = 2, 3, 4$ and the "spinodal-like" temperature for $p > 4$ (the temperature at which the extrapolated high temperature susceptibility would diverge).

Note that, in case of distributions centered around zero (that is, $J_0 = 0$), the value of $J$ and of the second moment $\Delta J$ coincide, that is why $J$ is usually taken to normalize the temperature scale. For a generic $J_0 \neq 0$ this is no longer true. In all the study of the Potts model in finite dimensions we always used $\Delta J = 1$ and varied $J_0$, and fixed the other units according to eq. (5.5). As we have seen when discussing the infinite-range model, ferromagnetic ordering is expected to be predominant if $J_0 = 0$ and $p > 4$, and one needs to add antiferromagnetic couplings to avoid it, and enter the glass phase at a temperature higher than the one at which ferromagnetic order would set in (this part has been discussed in chapter 2; for a reference see (Elderfield and Sherrington, 1983a)). We checked that it is indeed the case also for the three dimensional model, taking $x = 0.5$ and $J_0 = 0$. The equal concentration of bonds has the same first two moments of a Gaussian centered around zero. We just remind that the nature of ferromagnetic order in regular ($J_{ij} = 1$) Potts model is characterized by first order phase transitions, that have large jumps in the order parameter (the magnetization) the bigger the number of states $p$. In the mean-field limit the regular ferromagnetic Potts model undergoes a first-order phase transition for every $p > 2$. In two dimensions, it is known that the transition is second order for $p = 2, 3, 4$ and first order for $p > 4$. In general, the mean-field behavior prevails in all dimensions bigger than one for $p > 4$ (as well as for $d > 4$ dimensions for all values of $p$). These features are reviewed in (Wu, 1982). So, always in the regular case, for $p = 10$ one has a rather strong first order phase transition. This case has been largely studied in two dimensions, where indeed a strong first order phase transition is present, with a jump of the magnetization at the transition from zero to 0.857 (Baxter, 1982). In three dimensions one expects an even stronger transition, because the tendency towards mean-field behavior is increased.

Coming back to the disordered case with equal concentration of ferro- and antiferromagnetic bonds, we see from Fig. 5.1a indeed that one has a fast growing ferromagnetic susceptibility $\chi_{FM} = N[\langle m^2 \rangle]_{av}$, indicative of the tendency to ferromagnetic ordering, and there are no signs of discontinuity in the temperature regime we look at. Note that in the Ising case this tendency to ferromagnetism is absent for such values of the concentration. It is not the purpose of this work to investigate further the nature of this ferromagnetic-like transition. In mean-field theory it is first-order (Elderfield and Sherrington, 1983b). In general the effect of disorder on first order transition in finite dimensions is not clear, it can make the transition weaker or even turn it into a second order one. Analytical results are present only for two dimensional systems. In

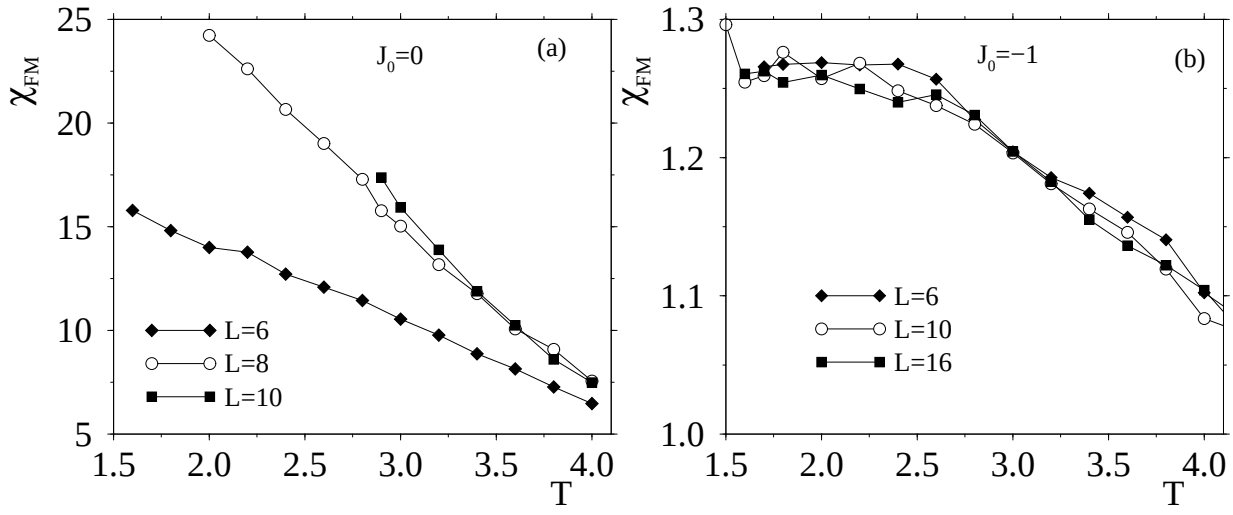


**Figure 5.1:** (a)Ferromagnetic susceptibility $\chi_{FM} = N[\langle m^2 \rangle]_{av}$ in the Potts disordered model (from now on is always $d = 3$) with a symmetric bimodal distribution of bonds ($J_0 = 0$) (see text for details). We show results for three different system sizes, $L = 6, 8, 10$. (b) Same quantity, but for a value $J_0 = -1$, where we expect a spin glass phase from the mean-field approximation.

two dimensions in presence of disorder all (eventually present) discontinuities in the thermodynamical quantities are eliminated, so only second order transitions can take place (Aizenmann and Wehr, 1989). For a recent numerical investigation in the Potts case (in two dimensions), see (Olson and Young, 1999). From the data we have at the moment then we cannot make strong statements about the nature of the transition and the problem remains open. It might be that at lower temperatures one finds also competition between ferromagnetic and spin glass phase.

The large part of our investigation has been devoted to the case $J_0 = -1$ and $\Delta J = 1$. In this way we are far enough from the effect of ferromagnetic ordering, but we have still a reasonable concentration of ferromagnetic bonds. From the mean-field guide this would correspond to a region with spin glass ordering occurring. The concentration of ferromagnetic bonds is given, from (5.5), by $x = (1 - 1/\sqrt{2})/2 \approx 0.15$ with a strength $J = \sqrt{2}$. In this case the ferromagnetic quantities remain small through the temperature range investigated,see the susceptibility in Fig. 5.1b.

The energy per spin does not present particular features, and tend to slowly approach a constant value below $T = 2.0$. The average is done on $100$ different realizations of disorder. What is remarkable, after the experience with the infinite range case, is the practical absence of finite size effects for the sizes investigated, $L = 6, 10, 16$. The energy decreases almost linearly in temperature and approaches a value $\approx -8.8$ at low temperatures. This value of the low temperature energy is not far from the one we would obtain considering a ground state in which only the energetically favored ferromagnetic bonds are satisfied. In fact, in such a case we would have

$$e = 3[-pJx + xJ - (1 - x)J] = -3J[(p - 2)x + 1] \approx -9.3 \, , \tag{5.6}$$

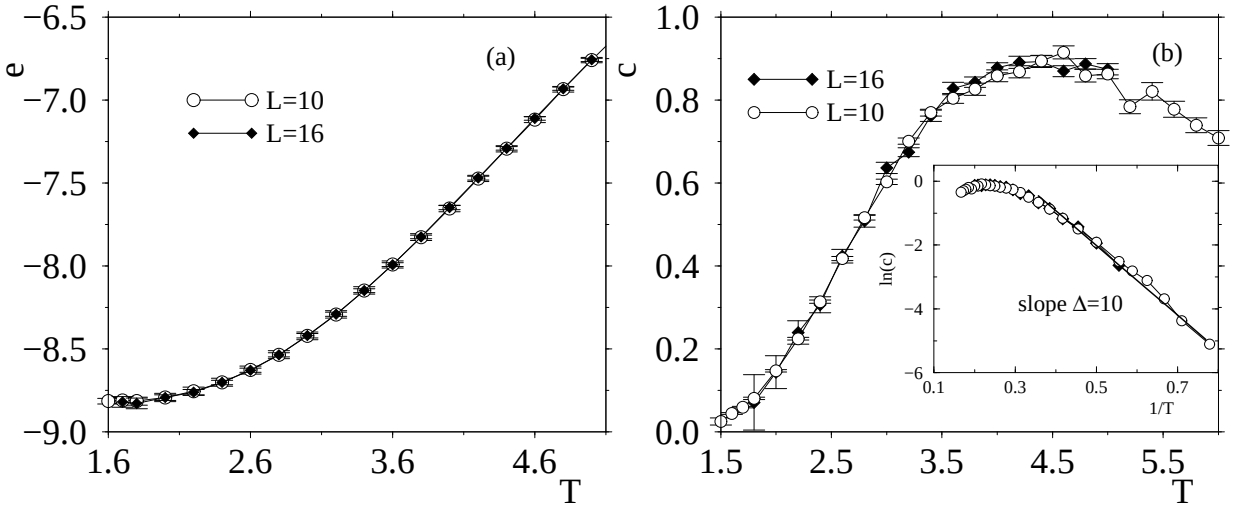


**Figure 5.2:** (a) Energy per spin in the case of asymmetric bond distribution, $J_0 = -1$. $L = 6$ is not included since it also superimposes on the two curves, as in the case of the specific heat. (b) Specific heat for the Potts glass. The inset shows the logarithm of $c$ plotted versus inverse temperature, so indicate at low temperatures a dependence of the kind $c \propto \exp(-\Delta/T)$, with $\Delta \approx 10$. See text for details.

about $5\%$ different from the value we read from Fig. 5.2. Also the specific heat, calculated through the fluctuation of the energy, $c = N[\langle e^2\rangle - \langle e\rangle^2]_{av}/T^2$ does not show the presence of finite size effects. It is characterized by a rather broad region at about $T = 4.5$, and then decays to zero for $T \to \infty$ (the non-interacting case) and for $T \to 0$. Note that the presence of a broad maximum is common in spin glasses (also in the experimental realizations (Fischer and Hertz, 1991)) and is not indicative of a phase transition. For instance, it is present in the two dimensional Ising case (Morgenstern and Binder, 1980), where there is no spin glass transition at finite temperature. At low temperatures in our case the specific heat seems to decay to zero exponentially like $\exp(-\Delta/T)$, with $\Delta \approx 10$. This is typical if there is a gap of order $\Delta$ between the energy of the ground state and of the first excitations (Morgenstern and Binder, 1980). A maybe too naive interpretation in terms of two-level system obeying classical statistical mechanics give also this exponential behavior, and a maximum located in the region of $\Delta/2$.

In order to understand better the behavior of the model, we need to have a look at the moments of the order parameter, calculated as usual with the help of two independent replicas, see the definition we give in eq. (3.14). Very important is then the behavior of the spin-glass susceptibility $\chi_{SG} = N(p-1)^{-1}[\langle q^2\rangle]_{av}$, and of the cumulants of the order parameter. We gave an extensive introduction to the importance of these quantities in section 4.1.2, discussing the results of the fully connected model. $\chi_{SG}$ is shown in Fig. 5.3a. In analogy with the previous quantities, it does not show finite size effects at all. We recall that $\chi_{SG}$ is defined in such a way as to diverge (in the limit $N \to \infty$) when a spin-glass phase is entered. Therefore this absence of $N$ dependence, and the fact that this function remains of order $1$, does not speak in favor of a finite temperature phase transition, in the regime we are able to access. We remark also that the lowest

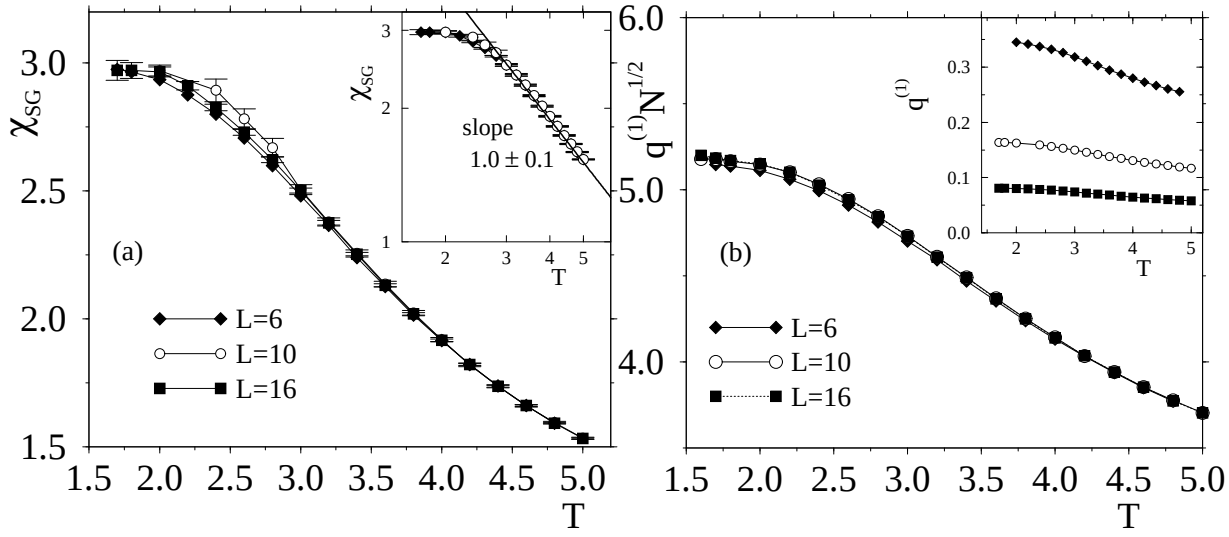


**Figure 5.3:** (a) Spin glass susceptibility as a function of the temperature. In the inset we show a log-log plot of the same quantity. (b) Scaled first moment of the order parameter as a function of the temperature. The insets shows the first moment, decreasing as a function of the system size.

temperature we simulated, $T = 1.4$, is already rather small, since the dynamics, discussed in the next section, gives relaxation times on the order of $10^8$ MCS, representing a practical limit to the investigation of lower temperatures. The fact that the susceptibility shows no finite size effects is indicative that the second moment of the order parameter scale like $N^{-1}$, the value expected at high temperatures where there is no spin glass order. This result comes from the first term in a high temperature expansion, see the discussion in (Peters et al., 1996). In the inset of the picture we show also a double log plot of the susceptibility. It is compatible with a power-law, and the exponent is $-1$, that is $\chi_{SG} \propto T^{-1}$. This behavior indicates that, according to the classical theory of critical phenomena, the system is below the lower critical dimension $d_l$. The lower critical dimension represents the spatial dimension above which one starts to have a phase transition at finite temperature. The expected scaling behavior for the susceptibility is in fact the following

$$\chi_{SG} \propto \begin{cases} T^{-\gamma} & \text{for } d < d_l \\ \exp(C/T^{\sigma}) & \text{for } d = d_l \\ |T - T_c|^{-\gamma} & \text{for } d > d_l \end{cases} \tag{5.7}$$

(see, e.g., (Binder and Reger, 1992)). We however remark the fact that the susceptibility remains rather small, and increases of about a factor $3$ only, so also this power law has to be considered with care.

The scenario is further confirmed by the analysis of the first moment of the order parameter. As we can see from Fig. 5.3b, there is a strong decrease of this quantity as a function of the system size. A scaling plot of $N^{1/2} q^{(1)}$ versus $T$ show the behavior better, and is clear evidence of the absence of spin-glass order in the temperature regime we investigate. We can then conclude that the first moment of the spin glass order parameter goes to zero in the thermodynamic limit.

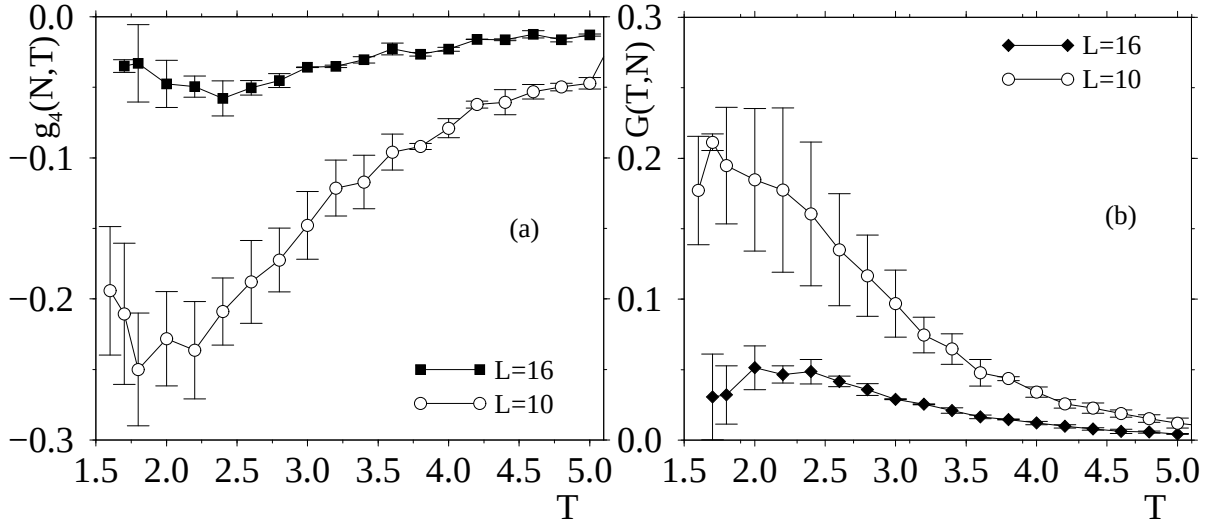


**Figure 5.4:** (a) $g_4(N,T)$ cumulant as a function of temperature for various system sizes. (b) Guerra parameter again for different system sizes. No indication for a spin glass transition can be inferred. We plot no data for $L = 6$ since they are rather noisy and would require a large statistics, but they do confirm the tendency of the behavior.

The order parameter distribution does consequently not show any development of structures, but remains localized around the mean value, and does not broadens or show peaks in addition to the one moving towards zero with the system size. This scenario seems then to exclude spin glass ordering at finite temperature in the $p = 10$ Potts glass in three dimension. As last confirmation of it, we show the cumulants used in the study of spin glasses, namely the fourth order cumulant $g_4(T,N)$ and the Guerra parameter, defined in eqs. (4.17) and (4.18). We just remind that they are expected to show features like crossing of the various curves for different system sizes or development of a minimum in case or phase transitions. In particular the Guerra parameter signals the appearing of lack of self-averaging (we discussed the behavior in the chapter devoted to the infinite range model; for a detailed account, see section 4.1.2). Common characteristics in this three dimensional model are the absence of crossing points and the clear tendency to reach the value zero as the system size is increased. This is in agreement with the renormalization-group calculations of (Benyoussef and Loulidi, 1996). They found that, in finite dimension and with respect to spin glass ordering, for every number of Potts states $p > 3$ the lower critical dimension equal to $4$ (that is there is no finite temperature spin glass transition also in smaller dimension).

## 5.2 Dynamics

In the study of the dynamics we concentrate on the spin autocorrelation function $C(t)$.

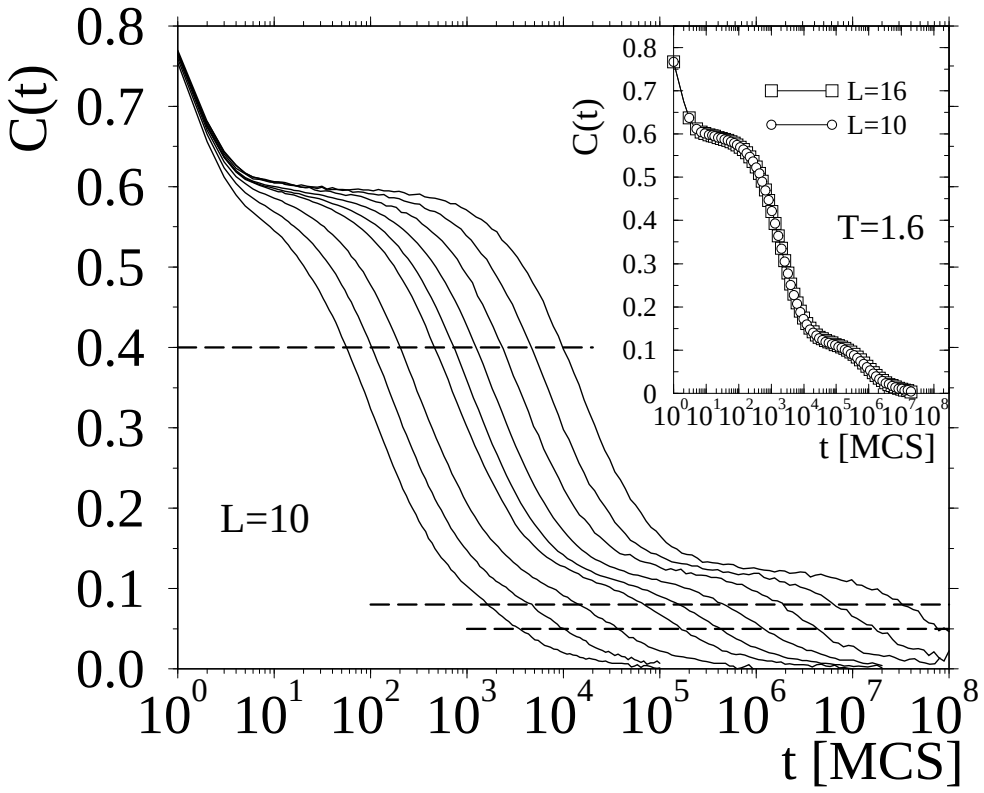


**Figure 5.5:** Spin autocorrelation function for the Potts glass, $L = 10$, for various temperature. Starting to the left, $T = 2.4, 2.2, 2.0, 1.8, 1.7, 1.6, 1.5, 1.4, 1.3$. The inset shows $C(t)$ for both L=10 and L=16 at $T = 1.6$. They cannot be distinguished.

It is defined as in the infinite range case

$$C(t) = \frac{1}{N(p-1)} \sum_i \left[ \left\langle \vec{S}_i(t') \cdot \vec{S}_i(t'+t) \right\rangle \right]_{av} . \tag{5.8}$$

The results for $L = 10$ are shown in Fig. 5.5. Before commenting them in detail, we note again, as in the statics, the absence of finite size effects, in the range we were able to investigate. We can see it in the inset of Fig 5.5, the correlation functions at $T = 1.6$ for both $L = 10$ and $L = 16$ (that is $1000$ and $4096$ spins respectively): the curves superimpose. We therefore will describe the system with $L = 10$, because it permits to reach lower temperatures, and we think we do not lose generality in the description of the physics.

The dynamics at high temperatures, when the relaxation times for a complete decorrelation are of the order of $10^5$ MCS, shows two different relaxation processes, one very fast, on the order of $10$ MCS, which is not much temperature dependent, and another one, responsible for the progressive slowing of the dynamics as the temperature is lowered. This separation of timescales gives rise to a well defined plateau, with a height of about $0.6$, whose lifetime increases lowering the temperature. For temperatures $T \leq 2$ another relaxation (or timescale) comes into play,

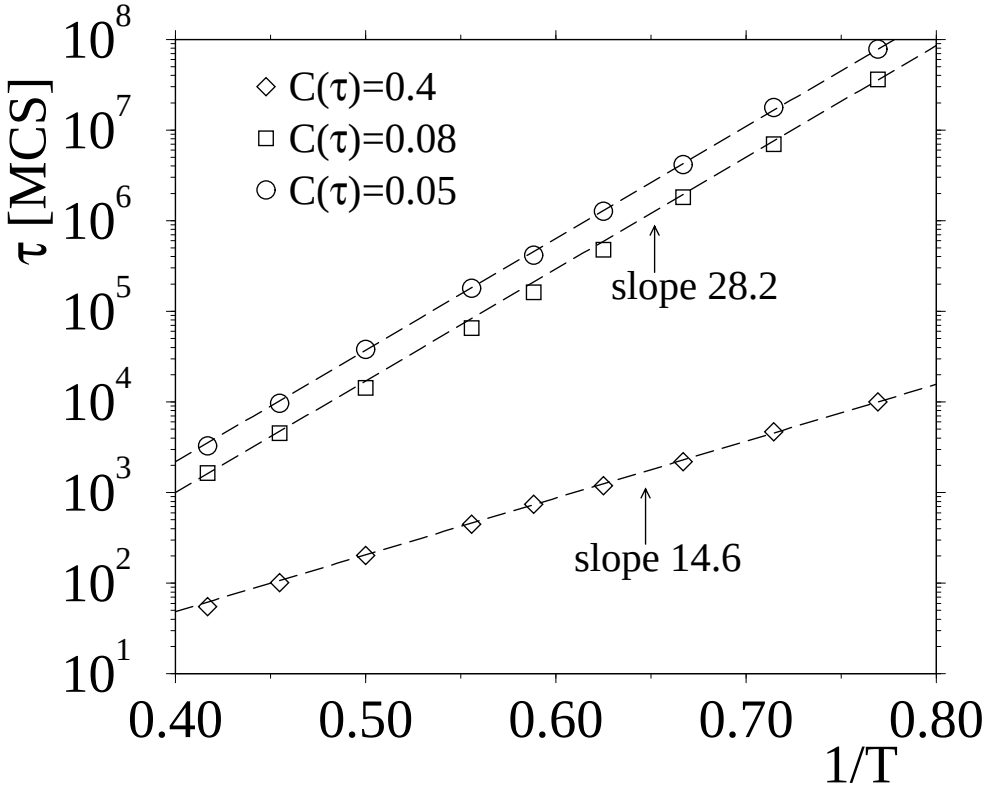


**Figure 5.6:** Relaxation times as a function of the inverse temperature in an Arrhenius plot. The dotted lines are result of fit, and the value of the barriers obtained is also shown

giving rise to a second plateau, at a height of about $0.12$, and independent of the temperature. We have then three different timescales, two of which vary strongly as a function of the temperature. It is not easy and unique to define relaxation times in these cases. The reason is that it is not possible to obtain time-temperature superposition between the different correlators. Time-temperature superposition means the possibility of getting a master curve from all correlators plotting them as a function of the rescaled variable $t/\tau$. This is in fact always true for curves like exponential $\exp(-t/\tau)$ or stretched exponentials $\exp(-(t/\tau)^b)$. We consider three values of the correlator, $0.4$ below the first plateau, and $0.08$ and $0.05$ below the second one, as shown in Fig. 5.5.

From Fig. 5.7 it appears that the time-temperature superposition is satisfied partially for these definitions. It holds in the region of the relaxation time, and fails as soon as another relaxation comes into play, see Fig. 5.7. We define then as relaxation times $\tau^{(1,2,3)}$ the time it takes the autocorrelation function to reach the above values, respectively. The results are shown in Fig. 5.6, in an Arrhenius plot, $\tau$ versus $1/T$ in a semilog plot. There is no doubt that all the three curves give straight lines, indicative then of temperature dependences of the kind $\tau \propto \exp(B/T)$. There are two different slopes. The curves for $\tau^{(2)}$ and $\tau^{(3)}$ in fact are parallel, giving evidence that they describe the same relaxation processes and there is therefore no other timescale involved, which

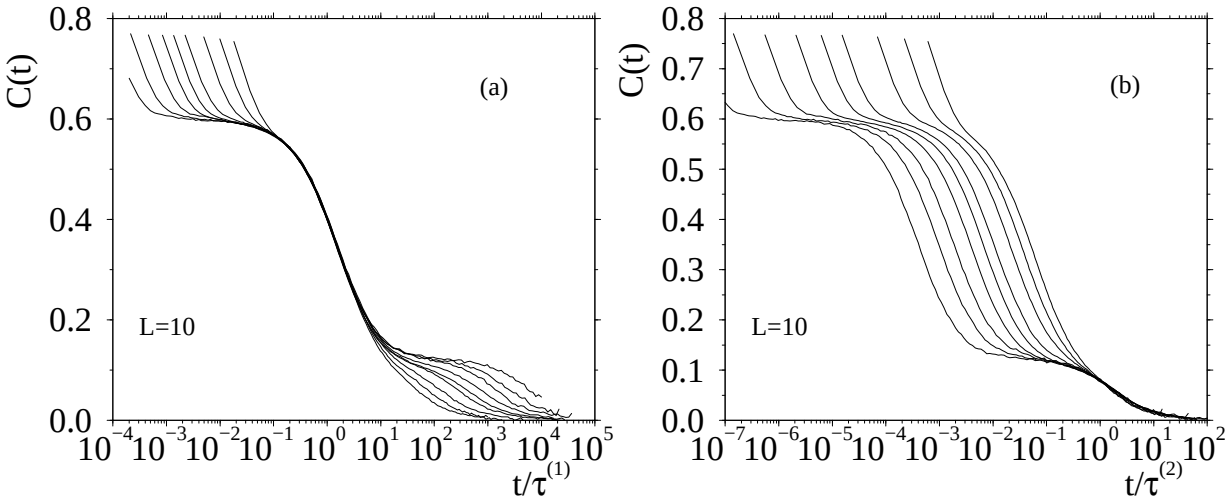


**Figure 5.7:** (a) Time-temperature superposition principle (TTSP) at work with a definition of $\tau^{(1)}$ such that $C(\tau^{(1)}) = 0.4$. (b) TTSP for a definition of $\tau^{(2)}$ such that $C(\tau^{(2)}) = 0.08$. This second case is analogous to $\tau^{(3)}$ such that $C(\tau^{(3)}) = 0.05$.

is not visible solely from the inspection of the correlation functions. The slopes of the curves, that is the $B$ in the Arrhenius formula defined above, are $B_1 \approx 14.6 \pm 0.1$ and $B_{2,3} \approx 28.2 \pm 0.2$. There is practically a factor two between them, and, if we consider that in this simulation we have $J = \sqrt{2}$, they are very close to $B^{(1)} \approx pJ$ and $B^{(2,3)} \approx 2pJ$, corresponding respectively to the energies of one and two (ferromagnetic) bonds. To understand this behavior, we investigate also the single spin dynamics, as we have done in the infinite range case. Details are like in the infinite range case, section 4.2.4, we collect statistics for a time of about $10^3$ times the longest relaxation of $C(t)$. Although this kind of study is done within a single sample, we performed the same analysis on two further realization of disorder and saw that there is no difference between the results. We did it mainly for three temperatures, $T = 1.6, 2.0, 2.4$. Lower temperatures do not permit to get a sufficiently good statistics, but we will see that the picture emerging is nevertheless rather clear. Result are shown in Figs 5.8. A large part of the curves relaxes very fast. They correspond to about $40\%$ of the total number of spins. The remaining curves instead have longer relaxation times, that do not vary continuously but present a gap with respect to the very fast spins. This gives rise then to the first plateau. Its height is also explained, since with this microscopic results is given by $1 - 0.4 = 0.6$. It is the percentage of curves relaxing with times larger than $5$ MCS. This result comes from summing all the $C_i(t)$. The remaining spins can be classified into three parts. Looking at the temperature $1.6$, one group relaxes at intermediate times (that is about $t \approx 10^4$ MCS in the picture referring to temperature $T = 1.6$). Their have all very similar shape, that turns out to be a simple exponential. Another group is also very similar to this one, although formed by a smaller number of spins. They relax with times centered around $t \approx 10^7$ and are again simple exponential functions. The remaining $3 - 4\%$ cannot be included in these two groups, and have rather heterogeneous relaxations. Since we are dealing mostly with exponential functions, we define a relaxation time per spin as the time it takes the single

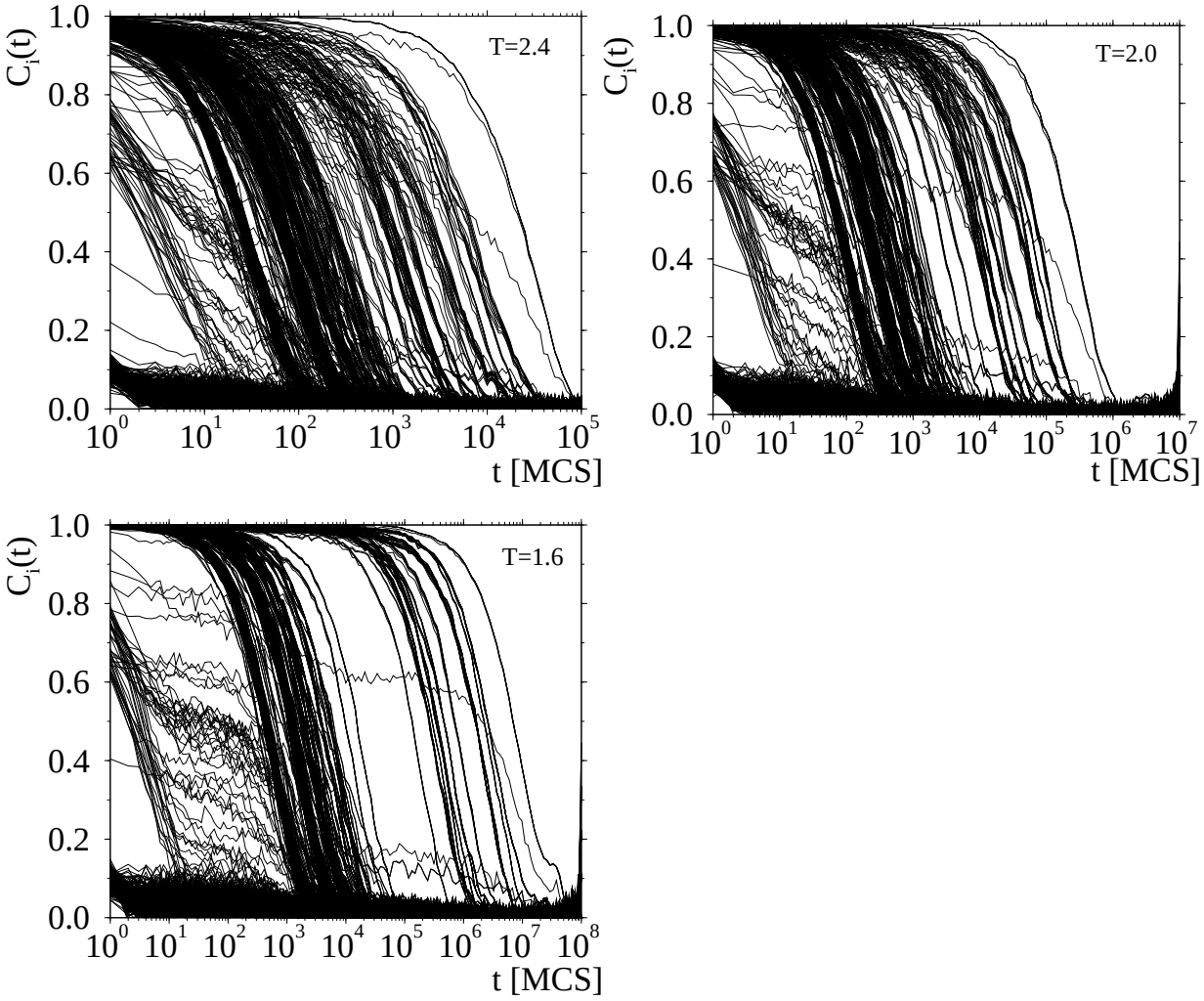


**Figure 5.8:** Single spin relaxation functions for $L = 10$ at three different temperatures, $T = 2.4, 2.0, 1.6$

correlation functions to decay to $1/e$. Then, for every spin, we make the following Arrhenius *Ansatz*

$$\tau_i = a_i \exp(b_i/T), \qquad i \in \{1, \ldots, N\}. \tag{5.9}$$

In this way we can have a look at barriers for every spin. Since, for every spin, we have two unknowns, we need also two different relaxation times to calculate them. We use two set of couples, namely $[\tau_i(T = 2.4);\ \tau_i(T = 2.0)]$ and $[\tau_i(T = 2.0);\ \tau_i(T = 1.6)]$. Given two temperatures $T_1$ and $T_2$, $b_i$ is given through the formula

$$b_i(1/T_1 - 1/T_2) = \log(\tau(T_1)) - \log(\tau(T_2)) \tag{5.10}$$

and then it is easy to obtain the $a_i$'s, substituting inside relation (5.9).

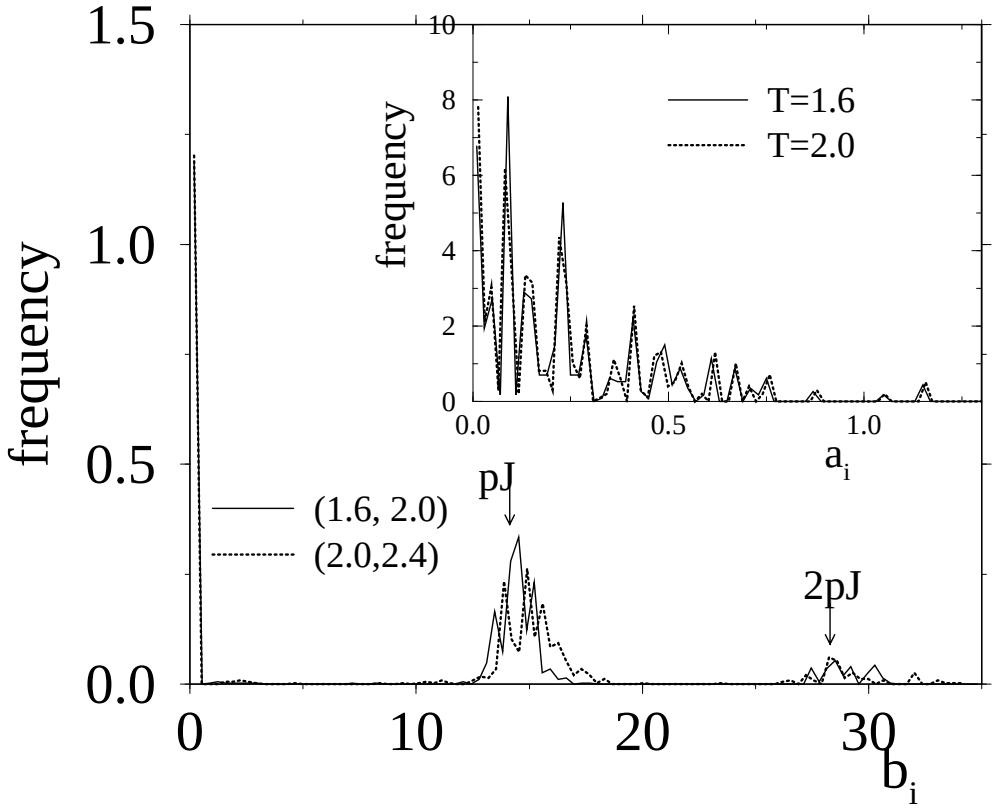


**Figure 5.9:** Normalized distribution of the barriers $b_i$. Two curves are shown, corresponding to data obtained with the couples of temperatures (1.6,2.0) and (2.0,2.4). In the inset we show the normalized distribution of the coefficients $a_i$ obtained substituting the value of the barriers for temperatures $1.6$ and $2.0$. See text for details.

We show the plot of the distribution of $a_i$ and $b_i$ in Fig. 5.9. We can note that there is also no significant difference between the choice of the temperatures, they give the same result. In particular, the barriers $b_i$ assume values that are peaked around zero, $pJ$, and $2pJ$, thus explaining the origin of the slopes of the total relaxation times $\tau^{(1,2,3)}$. The sum of these exponential curves, with well separated timescales when $T$ is of the same order of magnitude as $J$ (remember that we set $k_B = 1$) produces then the structure we have observed for the total $C(t)$.

The presence of such well defined elementary processes indicates that it might be possible to obtain a simple explanation for these features. The one we propose is based on combinatorial and energetic considerations. First of all, since the system has only a small amount (about $15\%$) of ferromagnetic bonds with respect to antiferromagnetic one, there will be spins interacting with their nearest neighbors solely through antiferromagnetic interactions. These spins can relax very fast, since they have $6$ neighbors and $p = 10$ states at disposal, so they can satisfy easily all the bonds (which encourage the interacting spins to be in different states) and flip easily. The probability of having spins with such neighbors configuration is given by $(1-x)^6$ (or to the power of $2d$ in dimension $d$). For our choice of $x = (1 - 1/\sqrt{2})/2 \approx 0.15$ we have that the probability

of having such spins is about $0.39$, which accounts then for the previously estimated $40\%$ of fast relaxing spins. In general, to extend the idea, the probability of having $k$ ferromagnetic bonds out of $n$ is given by

$$P(k,n) = \frac{n!}{k!(n-k)!}\, x^k\, (1-x)^{n-k}. \tag{5.11}$$

So, a first approach is to say that a spin with $k$ ferromagnetic bonds would relax with a barrier given by $kpJ$. Just to compare with numbers, we have $P(1,6) \approx 0.40$, $P(2,6) \approx 0.17$, $P(3,6) = 4 \cdot 10^{-2}$ and so on, with $P(k \geq 4, 6) \leq 5 \cdot 10^{-3}$. This approach has two problems. It produces a second plateau at a height $0.21$ (resulting from the sum of probabilities with $k \geq 2$) and gives still a rather high probability to have also a third plateau at a height of about $0.046$, which we do not observe. It is then necessary to refine the idea. Spins with a single ferromagnetic bond need to overcome a barrier of $pJ$. The spins with two ferromagnetic bonds need not necessarily overcome a barrier of $2pJ$. In fact, if at least one of the two others neighbor spins has only one ferromagnetic bond, then it will relax with a barrier $pJ$, and can permit in this way to the spin with two ferromagnetic bonds to relax overcoming a barrier of $pJ$. The probability of such shells of spins is given by $P(2,6)$, that is the probability for the spin to have only $2$ ferromagnetic bonds with its neighbors, times the probability that one of these two spins have no further ferromagnetic bond with its remaining $5$ neighbors, given by $P(0,5)$. We have then $P(2,6) \cdot P(0,5) \approx 0.077$, so that the total percentage of spins relaxing with barriers bigger than $pJ$ is lowered to $0.13$, very close to the value we find for the second plateau, which is around $0.12$. Extending the reasoning also to spins relaxing with $3pJ$ barriers, we find that the height of a third plateau would be around $0.006$. This value is small but not zero. We do not observe a third plateau, nor do we have evidence of spins relaxing with barrier bigger than $2pJ$. The picture we suggested is valid when all the bonds are satisfied. As we have seen this is not perfectly correct, since the low temperature value of the energy is about $5\%$ bigger. It might then be that the disorder creates some spin configurations in which not all the bonds are satisfied and spins which share these bonds tend to have a high flipping rate, relaxing faster, in addition to the processes we have described, and we do not observe more plateaus. We cannot also completely exclude that the absence of further plateaus is a finite-size effect. Since probabilities into play are, as we have seen, on the order of $0.6\%$, it might be that a number of spin of order $1000$ is not yet sufficient to observe them.

The processes we described up to now are local, and depend strongly on the choice of the probability distribution of the interaction, a bimodal one, where the only possibility are $\pm J$ with different weights. Different distributions can then give rise to a different dynamical behavior. This is indeed the case for a Gaussian distribution of bonds

$$P(J_{ij}) = \frac{1}{\sqrt{2\pi}(\Delta J)} \exp\left[-\frac{(J_{ij}-J_0)^2}{2(\Delta J)^2}\right] \tag{5.12}$$

with $J_0$ and $\Delta J$ defined as in eq. (5.4) and with the same value $J_0 = -1,\ \Delta J = 1$ as in the simulations with the bimodal distribution. Here the ferromagnetic bonds have a continuous spectrum of values, therefore we do not expect a separation of timescales as in the previous case.

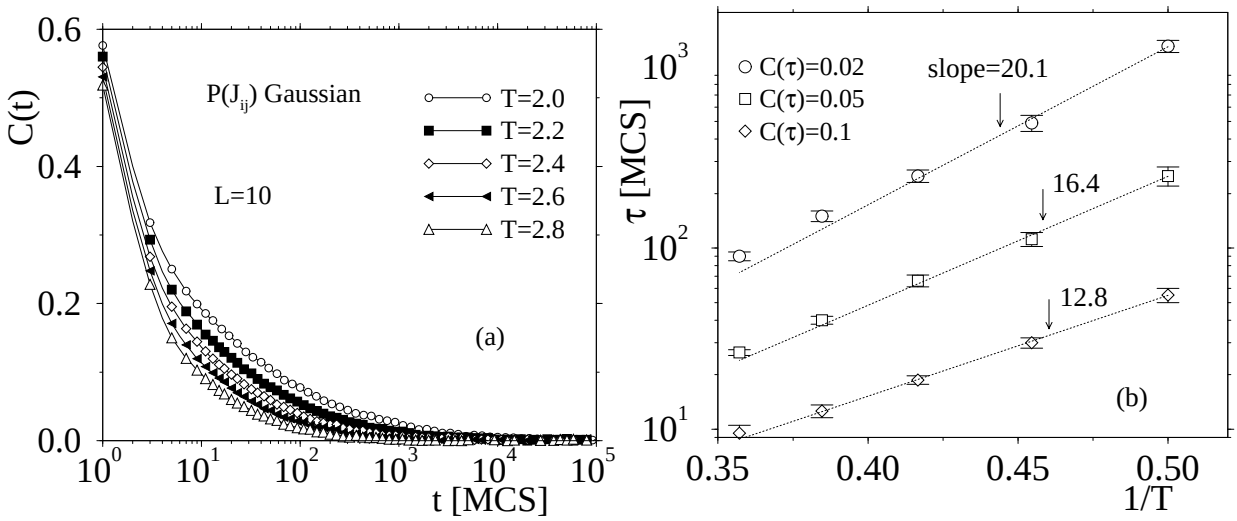


**Figure 5.10:** (a) Autocorrelation functions in the case of Gaussian distribution of the $J_{ij}$. (b) Arrhenius plot of the relaxation times in the Gaussian case. The values of the barriers are also shown.

This is indeed what happens, as we can see from Fig. 5.10a. The plateau structure disappears, there is a rather fast relaxation at the beginning and then the curves slow down as the temperature is lowered. Again it is not that clear how to define a relaxation time, since also with this choice of interactions there are problems with the time-temperature superposition principle and we took three reference points for the correlation function, namely $0.1,\ 0.05$ and $0.002$. Their behavior with respect to temperature is again Arrhenius-like, as Fig. 5.10b shows. But the slope of the curves tend to vary smoothly as a function of the point with respect to which the relaxation time is measured. A smaller value of the latter correspond to an increasing value of the slope. This is however a further indication of the fact that local processes determine the physics of the system, since now the strength of the bonds varies continuously, and so do the barriers that the various spin have to overcome in order to complete a relaxation process. The three dimensional ten state Potts glass does not show a spin-glass phase transition at finite temperature, as instead the infinite range version of the model does, nor seems to indicate the features of a dynamical transition at finite temperature, with relaxation times diverging like $(T - T_D)^{-\Delta}$.

# Chapter 6

# Conclusions

In this thesis we have presented the first detailed Monte Carlo investigation of the ten state Potts glass model, both in the infinite range (that is fully connected) version as well as in three dimensions. This spin model is very interesting since it is known that, in the thermodynamic limit, it exhibits both a dynamical transition at $T_D$ where the system loses ergodicity, and a static transition at $T_0 < T_D$ where a spin glass order parameter appears discontinuously. This behavior includes all qualitative features present in the phenomenological theories for the structural glass transition in supercooled liquids. In particular, the equations of motion for the spin autocorrelation function have the same structure as those describing structural arrest in the idealized mode coupling theory, and the static phase transition has been related to the hypothetical presence of a phase transition to a thermodynamic stable structural glass state.

Several aims motivated our work. We want to verify if these predictions can be observed by means of Monte Carlo simulations, and to understand how the various transitions are modified (essentially rounded off) by the finite size of the system, that always prevents the system from losing ergodicity. Important is also to see how much simulations can contribute to determine the properties of the model, and to investigate if the transitions survive also in a three dimensional version of the system. Answers to these questions are not only of interest for a better understanding of the statistical mechanics of the present model system, they may also be useful to help with the interpretation of simulations of models for the structural glass transition.

We summarize at this point the main results of our work. The main part of the investigation has been devoted to the fully connected version of the model.

- Already at the level of the energy per spin, the system shows strong finite size effects in the proximity of the phase transitions region. At high temperature the behavior is understood and the difference between the energy of the finite system and the one in the thermodynamic limit goes like $N^{-1}$, while close to the static phase transition the data seem better described by a $N^{-2/3}$ scaling. This result is similar to what happens in second-order phase transitions in mean field spin glass models (like in the Ising case), although in the Potts model with a number of states $p > 4$ the transition is first order without latent heat.

- A simple extrapolation of the total entropy from the high temperature phase to zero, in the spirit of Gibbs and DiMarzio does not locate the static phase transition properly. The right

quantity going to zero at the transition is the complexity, that is the logarithm of basins in the *free* energy landscape. This quantity starts to be extensive, coming from the high temperature phase, at the dynamical transition temperature, and vanishes approaching the static transition temperature. How to calculate it from a simulation in spin systems is still an open problem. Moreover, the vicinity of $T_D$ and $T_0$ in the system we studied and the presence of strong finite size effects and consequent rounding of the transitions are further sources of difficulty.

- The spin glass susceptibility measures the tendency to spin glass ordering, and diverges when the spin glass phase is entered. For this model an extrapolation of the high temperature result would locate a divergence at a temperature $T_s < T_0$. This is analogous to a "spinodal" temperature of a standard first order phase transition, but in our case it has no physical meaning, since due to the instability of the paramagnetic (replica symmetric) phase into the spin glass one for every temperature $T < T_0$, one cannot follow the disordered branch of the free energy up to $T = T_s$ (in the thermodynamic limit). So, coming from the high temperature phase, the spin glass susceptibility remains finite at the dynamical transition temperature and also upon approaching the static transition.

- The analysis of the order parameter distribution at low temperatures seems to support the scenario predicted by the one step replica symmetry breaking solution, with the presence of two peaks. Their position is also in quantitative agreement with the theory. The study in this low temperature regime has been possible thank to the use of the parallel tempering, an optimized Monte Carlo implementation particularly effective in the study of glassy systems. Also the scaling behavior of the $k$-th moments of this distribution goes like $N^{-k/2}$ at high temperatures and like $N^{-k/3}$ close to the transitions region.

- In order to quantitatively locate the static phase transition we use the method of the order parameter cumulants, usually very effective with standard first and second order phase transitions. Here, however, apparent crossing points are present but do not locate the phase transition at the same temperature as predicted by the theory and moreover, using two different cumulants, the results do not agree between them. So strong corrections to scaling are probably present, and it might be that the crossing points are spurious. Finite size corrections to the main thermodynamic quantities are still unknown in the mean-field (replica symmetry breaking) approach to this problem. Their knowledge would be valuable in the interpretation of these results.

- The dynamics at high temperatures $T \geq T_D$ shows unexpected strong finite size effects. Two relaxation behaviors are hardly seen even for the largest system size investigated. There is also, in this temperature regime, no indication of the development of a plateau in the spin autocorrelation function, contrary to the expectation from the mean-field theory. There is furthermore no evidence that the time-temperature superposition principle, that describes the scaling of the autocorrelation functions when plotted as a function of $t/\tau$, with $\tau$ the relaxation time, holds.

- The dynamics progressively slows down upon approaching $T_D$, and there is the development of an apparent singularity of the kind $(T - T_D)^{-\Delta}$, ($\Delta \approx 2$) which is avoided then at lower temperatures because finite size systems are always ergodic, and Arrhenius relaxation appears. The relaxation time at $T_D$ diverges as a function of the system size like $N^{1.5}$, an exponent much larger than the $2/3$ found for the infinite range Ising spin glass. We are able to describe the apparent singularity and the latter power law with a phenomenological *dynamic finite size scaling* Ansatz, which holds close to the dynamical transition temperature.

- The dynamics at $T_D$ shows non-self-averaging effects, which means that it depends still on the microscopic realization of the bond configurations also in the thermodynamic limit.

- At low temperatures $T < T_0$ a plateau at intermediate times appears in the spin autocorrelation function, and it is related to the second peak in the order parameter distribution (Edwards-Anderson order parameter - $q_{EA}$). In this regime, the time-temperature superposition principle is satisfied, and the master curve can be fitted very well at long times with a stretched exponential. The barriers in the Arrhenius relaxation seem to diverge with the size like $N^{1/2}$.

- We analyzed the single spin dynamics up to temperatures much lower than the dynamical transition one. We found strong dynamical heterogeneities, which explain the non-exponentiality of the spin autocorrelation function. We found also strong correlations between static and dynamical properties (such as for instance the energy per spin and the single spin relaxation times). We found also that at low temperatures the spins seem to relax according to dynamical clusters, probably because of the strong bonds between them.

- We investigated also the recently proposed dynamic susceptibility, a four point correlation function measuring also the degree of heterogeneity in the system. We found that it exhibits a maximum as a function of time, and confirm the presence of power law divergences as a function of the distance from the dynamical transition temperature for both the position and the height of the maximum. The exponents seem not to be universal, since they are different from those found for a $p$-spin spherical model. We investigated also the size dependence of the interesting quantities, and this analysis seems to connect the times at which a maximum occurs to the relaxation times of the standard spin autocorrelation function.

The simulations of the three dimensional version of the model are particularly interesting to see if this complex scenario, found for the mean field theory and qualitatively confirmed also in the finite size fully connected version, survives. We used mainly a bimodal distribution of bonds, of strength $\pm pJ = \pm 10J$.

- The model tends to acquire ferromagnetic order if we use an equal concentration of ferro- and antiferromagnetic bonds. This is reminiscent of what has been found also in the mean-field version. This ferromagnetic transition is however not as strong as expected in the pure ferromagnetic version of the model, which exhibits a first order transition. The nature

of this "disordered" Potts ferromagnet is an open problem, we did not investigate further whether a second order transition occurs or a weak first order one. To avoid this spontaneous magnetization, we have to add more antiferromagnetic bonds.

- Finite size effects are practically absent in the size and temperature region investigated, quite contrary to the fully connected case. Coming from the high temperature phase, the energy decreases smoothly and almost linearly in temperature to reach an almost constant value at low temperature. The specific heat shows a broad peak at intermediate temperatures, which is probably indicative of developing of short range order in the model, and it is difficult to connect it to a phase transition.

- The spin glass susceptibility does not show any tendency to diverge at a finite temperature. Also for this quantity finite size effects are negligible, and the behavior is the one expected in the absence of transition at finite $T$. Its behavior is compatible with a power law behavior $\chi_{SG} \propto T^{-1}$, indicative of a system below the lower critical dimension. The spin glass order parameter scales very well like $N^{-1/2}$, so we argue that it vanishes in the thermodynamic limit in the temperature region accessible to our simulations.

- The analysis of the order parameter cumulants does not show any behavior indicating any spin glass phase transition, not even qualitatively (remember that the method failed in locating exactly the transition temperature in the infinite range case, but was qualitatively compatible with the presence of a transition). The cumulants tend to go to zero when the system size increases.

- As far as dynamics is concerned, there is a clear presence of two timescales, also for high temperature (i.e. relaxation times less than $10^4$ MCS), while there are three distinct timescales when the temperature is decreased further. These timescales are well separated, and produce two distinct plateaus in the spin autocorrelation function. The relaxation times associated to the two longest timescale have an Arrhenius behavior, with barriers of the order of $10J$ and $20J$.

- The analysis of the single spin dynamics, given mostly by simple exponential functions, confirm the presence of three kinds of barrier, $0,\ 10J,\ 20J$. We related it to the number of ferromagnetic bonds of each spin with its nearest neighbors, and this permits to understand also quantitatively the height of the two plateaus.

- The use of a Gaussian distribution of bonds instead of a bimodal eliminates the strong separation of timescales, giving further evidence to the role of the local bonds in determining the behavior of the model.

This system, in its fully connected version, is a prototype model for the study of the glass transition. Its extension to short-range forces in three dimensions does not show a finite temperature phase transition. To mimic what happens in real orientational glasses it might be interesting to include power law interactions among the spins, since in real materials long-range effective interactions (mediated by phonons) play an important role. Such "crossover" studies are however

at present rather difficult, due to the long relaxation times and the lack of algorithms permitting exhaustive studies. Also the study of this model in magnetic field can be very interesting in elucidating the competition between ferromagnetic and (spin) glass ordering.

# Appendix A

# Programs

In this appendix we give three codes, representative of those used in this work.

- The first is the one used to simulate the infinite range model with a Gaussian distribution of bonds, by means of the single spin-flip Metropolis algorithm.
- The second code implements the parallel tempering algorithm, again for the infinite range model with Gaussian bonds. It makes use of specific MPI (Message Passing Interface) to implement global parallel features.
- The third code simulates a short range Potts glass with bimodal interactions. The algorithm implemented is the Heat-Bath.

We give also an example of a input file for the first code. This input file is rather general and also the other codes use similar ones.

```
ccccccccccccccccccccccccccccccccccccccccccccccccccccccccccccccccccccc
c Single spin flip Metropolis simulation of the infinite range
c Potts glass
ccccccccccccccccccccccccccccccccccccccccccccccccccccccccccccccccccccc


c-----this program is intended to simulate random bond potts model
c-----with infinite range interactions among the spins, that is in
c-----the mean field approximation

c-----Improved version: the status of the random number generator is
c-----saved. And the data saved in a buffer before being written.

      PROGRAM potts

      IMPLICIT NONE
      INTEGER*4 ns,ntotstep,nmax,pstates,ncorrel
      INTEGER*4 ncorrelnew,ndiv,ncorr,npartial
      PARAMETER (ns=320,nmax=ns*3,pstates=10,ncorrel=150,ndiv=4)
      PARAMETER (npartial=ncorrel)
      REAL*8 bond(ns,ns),jij,totbond
      INTEGER*4 state_all(ns),irn(nmax),cortim(ncorrel*ndiv)
      INTEGER*4 partial(ns,npartial)
      INTEGER*4 temp_s,kran,state,iseed
      REAL*8 energy(ns),entot,temp_en,delta,ener,en1
      REAL*8 gain,loose
      REAL*8 boltz,temper
      REAL*8 comp,ensim,conv,count,convb
      INTEGER*4 t,i,j,jj,ks,jran,p,k,ncrit
      INTEGER*4 qlines,rlines,setequil,matseed,runseed,waste
      CHARACTER*50 filout,filin,outfile,final,logfile,outlog,status
      CHARACTER*50 meanofp,varofp
      INTEGER*4 nstart,tstop,nstop,setrand,nspin,logbump
      REAL*8 convran,hhh
      INTEGER*4 time_v(npartial),pcount
      REAL*8 simen_v(npartial)
c-----info variables
      INTEGER*4 infoncorrel,infondiv
      REAL*8 quenchtemp
c-----for the gaussian distribution
      REAL*8 j0,dj,gau(ns)

c-----in common with the random number generator
      INTEGER len1,len2,ifd1,ifd2,ipnt1,ipnt2,ipnf1,ipnf2
      PARAMETER (len1=9689,ifd1=471)
      PARAMETER (len2=127,ifd2=30)
      INTEGER*2 inxt1(len1)
      INTEGER*2 inxt2(len2)
      INTEGER*4 ir1(len1)
      INTEGER*4 ir2(len2)

      COMMON /nran/irn
      COMMON /rantool/ipnt1,ipnf1,ipnt2,ipnf2,inxt1,inxt2,ir1,ir2
      COMMON /bonds/gau

c-----THE PROGRAM STARTS

c      nspin=50                          !spin written in a single line
      nstop=0
      convran=2.**(-32)*(1.d0-1.d-15)
      j0=(3.-pstates)/(ns-1.)
      dj=1./sqrt(ns-1.)
      conv=1.*pstates

      DO i=1,ns
       DO j=1,ns
        bond(j,i)=0.
       ENDDO
      ENDDO
      DO i=1,ns
       gau(i)=0.
      ENDDO

      DO i=1,npartial
       time_v(i)=0
       simen_v(i)=0.
       DO j=1,ns
        partial(j,i)=0
       ENDDO
      ENDDO


c-----reading from the input file and construction of the bond matrix
      print*,'I need the input file'
      READ(5,FMT='(a)') filin
      OPEN(061,file=filin)
       READ(061,*) matseed
       READ(061,*) runseed
       READ(061,*) nstart
       READ(061,*) ntotstep
       READ(061,*) temper
       READ(061,*) infoncorrel
       READ(061,*) infondiv
       READ(061,*) nspin
       READ(061,*) quenchtemp
       READ(061,FMT='(a)') meanofp
       READ(061,FMT='(a)') varofp
       READ(061,*) setequil
       READ(061,*) setrand
       READ(061,FMT='(a)') logfile
       READ(061,FMT='(a)') filout
       READ(061,FMT='(a)') status
       READ(061,FMT='(a)') final

c~~~~~~~~~~~~~~~~~~~~~~~~~~~~~~~~~~~~~~~~~~~~~~~~~~~~~~~~~~~~~~~~~~~~~~~
c-----initialization of the bond matrix: double delta distribution
```

```
c-----some useful constants
      qlines=int(ns/nspin)
      rlines=mod(ns,nspin)

      CALL firstran(matseed)
      DO k=1,1000
       CALL ransi(nmax)
       DO i=1,3*ns
        waste=irn(i)
       ENDDO
      ENDDO

      DO j=1,ns-1
       CALL gauss(j0,dj)
       DO i=j+1,ns
         jij=gau(i)
         IF (i.eq.j) jij=0.
         bond(j,i)=jij
         bond(i,j)=jij
       ENDDO
      ENDDO

      totbond=0.
      DO j=1,ns
       DO i=1,ns
        totbond=totbond+bond(i,j)
       ENDDO
      ENDDO
      totbond=totbond/2.
c~~~~~~~~~~~~~~~~~~~~~~~~~~~~~~~~~~~~~~~~~~~~~~~~~~~~~~~~~~~~~~~~~~~~~~~~~~~~~~~~
       IF (setequil.eq.0) THEN
        READ(061,FMT='(a)') outlog
        READ(061,FMT='(a)') outfile
       ENDIF
       IF (setequil.ne.0.or.setrand.eq.1.or.quenchtemp.lt.100.) THEN
        IF (qlines.ne.0) THEN
         READ(061,139) ((state_all(i),i=(k-1)*nspin+1,k*nspin),
     &     k=1,qlines)
        ENDIF
        READ(061,139) (state_all(i), i=qlines*nspin+1,ns)
       ENDIF
       IF (setrand.eq.1) THEN
        READ(061,*) ipnt1,ipnf1,ipnt2,ipnf2
        DO i=1,9689
         READ(061,*) ir1(i)
        ENDDO
        DO i=1,127
         READ(061,*) ir2(i)
        ENDDO
       ENDIF
      CLOSE(061)
```

```
c-----opening the output files
      IF (setequil.eq.1) THEN
      OPEN(072,file=filout,access='append')
       IF (setrand.eq.0) THEN
       WRITE(072,109) ns,'number of spins'
       WRITE(072,109) pstates,'number of states'
       WRITE(072,109) matseed,'matrix seed'
       WRITE(072,109) runseed,'run seed'
       WRITE(072,109) nstart,'time to start with'
       WRITE(072,109) ntotstep,'number of timesteps'
       WRITE(072,119) temper,'temperature'
       WRITE(072,109) ncorrel,'points for the log scale'
       WRITE(072,109) ndiv,'number of bumps'
       WRITE(072,109) nspin,'spins per line'
       WRITE(072,119) quenchtemp,'temperature of the quench'
       WRITE(072,129) ' mean: j0=(3.-pstates)/(ns-1.)'
       WRITE(072,129) 'variance: dj=1./sqrt(ns-1.)'
       WRITE(072,109) setequil,'equilibrium flag'
       WRITE(072,109) setrand,'rng flag'
       WRITE(072,FMT='(a)') logfile
       WRITE(072,FMT='(a)') filout
       WRITE(072,FMT='(a)') final
       ENDIF
      ENDIF

      OPEN(071,file=logfile,access='append')
       WRITE(071,109) ns,'number of spins'
       WRITE(071,109) pstates,'number of states'
       WRITE(071,109) matseed,'matrix seed'
       WRITE(071,109) runseed,'run seed'
       WRITE(071,109) nstart,'time to start with'
       WRITE(071,109) ntotstep,'number of timesteps'
       WRITE(071,119) temper,'temperature'
       WRITE(071,109) ncorrel,'points for the log scale'
       WRITE(071,109) ndiv,'number of bumps'
       WRITE(071,109) nspin,'spins per line'
       WRITE(071,119) quenchtemp,'temperature of the quench'
       WRITE(071,129) ' mean: j0=(3.-pstates)/(ns-1.)'
       WRITE(071,129) 'variance: dj=1./sqrt(ns-1.)'
       WRITE(071,109) setequil,'equilibrium flag'
       WRITE(071,109) setrand,'rng flag'
       WRITE(071,FMT='(a)') logfile
       WRITE(071,FMT='(a)') filout
       WRITE(071,FMT='(a)') final



c-----warming for the random number generator
      IF (setrand.ne.1) THEN
      CALL firstran(runseed)
      DO k=1,1000
       CALL ransi(nmax)
```

```
       DO i=1,3*ns
        waste=irn(i)
       ENDDO
      ENDDO
      ENDIF

c-----needed only for the equilibration run, NOT for the equilibrium
c      run!
      IF (setequil.eq.0.and.setrand.ne.1.and.quenchtemp.gt.100.) THEN
       DO i=1,ns
        state_all(i)=0
       ENDDO
       CALL ransi(nmax)
       DO i=1,ns
        state_all(i)=(irn(i)*convran+.5)*pstates
       ENDDO
      ENDIF

c---- compute the times at which the correlation functions are evaluated
c
      p=ncorrel
      p=p-1
      DO k=1,p
       cortim(k)=nint(dfloat(ntotstep)**(k/dfloat(p+1)))
      ENDDO
      cortim(1)=0
      k=2
      j=2
   20 IF( j .gt. p) goto 30
      IF( cortim(j) .ne. cortim(k) ) THEN
        k=k+1
        cortim(k)=cortim(j)
        j=j+1
      else
        j=j+1
      ENDIF
      goto 20

   30 IF( ncorrel .eq. 0 ) THEN
        ncorrelnew=0
      else
        cortim(k+1)=ntotstep
        ncorrelnew=k+1
      ENDIF

      ncorr=ncorrelnew
      DO j=1,ndiv-1
       DO k=1,ncorrelnew
       IF (cortim(k)+j*ntotstep/ndiv.gt.ntotstep) goto 50
       ncorr=ncorr+1
       cortim(ncorr)=cortim(k)+j*ntotstep/ndiv
       ENDDO
 50    continue
       ENDDO


       DO k=1,ncorr
         WRITE(071,*) cortim(k)
       ENDDO


c------calculation of the total energy and of the energy arrays
       entot=0.
       DO i=1,ns
        state=state_all(i)
        ener=0.
        DO j=1,ns
         gain=0.
         IF (state.eq.state_all(j)) ener=ener+bond(i,j)
        ENDDO
        energy(i)=-ener
       entot=entot+energy(i)
       ENDDO
       en1=entot

 c-----writing down the step number 0!
       t=nstart
       ensim=(conv*entot/2.+totbond)/ns
       IF (nstart.eq.0) THEN
        WRITE(071,*) t,ensim,state_all(1),state_all(2)
        IF (setequil.eq.1) THEN
         WRITE(072,*)t,ensim
         IF (qlines.ne.0) THEN
         WRITE(072,139) ((state_all(i),i=(k-1)*nspin+1,k*nspin),
     &     k=1,qlines)
         ENDIF
         WRITE(072,139) (state_all(i), i=qlines*nspin+1,ns)
        ENDIF
       ENDIF



 c-----THE CORE OF THE PROGRAM
 c-----Monte Carlo Calculation

       count=0
       ensim=0.
       pcount=0
       ncrit=0
       tstop=ntotstep/4
       logbump=ntotstep/200
       convb=(1.*pstates)/temper

       DO t=nstart+1,ntotstep
 c-----single monte carlo sweep: ns spin updated
        CALL ransi(nmax)
```

```
       DO ks=1,3*ns,3
c-----single ranDOm spin flip
        temp_s=0
        jran=(irn(ks)*convran+.5)*ns+1
        kran=(irn(ks+1)*convran+.5)*pstates+1
        comp=(irn(ks+2)*convran+.5)
        temp_s=mod(kran,pstates)

c-----comparison and importance sampling
 26     temp_en=0.
        DO j=1,ns
         gain=0.
         IF (temp_s.eq.state_all(j)) temp_en=temp_en-bond(j,jran)
        ENDDO

        delta=temp_en-energy(jran)

        IF (delta.le.0.) THEN
         goto 23
        else IF (delta.gt.0.) THEN
         boltz=exp(-delta*convb)
         IF (boltz.gt.comp) goto 23
         IF (boltz.le.comp) goto 24
        ENDIF

 23     continue

        energy(jran)=temp_en
        entot=energy(jran)
        DO i=1,jran-1
         IF (state_all(jran).eq.state_all(i))
     &       energy(i)=energy(i)+bond(i,jran)
         IF (temp_s.eq.state_all(i))
     &       energy(i)=energy(i)-bond(i,jran)
         entot=entot+energy(i)
        ENDDO
        DO i=jran+1,ns
         IF (state_all(jran).eq.state_all(i))
     &       energy(i)=energy(i)+bond(i,jran)
         IF (temp_s.eq.state_all(i))
     &       energy(i)=energy(i)-bond(i,jran)
         entot=entot+energy(i)
        ENDDO
        state_all(jran)=temp_s

 24     continue
        ensim=(conv*entot/2.+totbond)/ns
       ENDDO


      ensim=(conv*entot/2.+totbond)/ns
```

```
       IF (mod(t,logbump).eq.0) THEN
        WRITE(071,*) t,ensim,state_all(1),state_all(2)
        CALL FLUSH(071)
       ENDIF

c------writing down something
       IF (setequil.eq.1) THEN
        DO j=1,ncorr
         IF (t.eq.cortim(j)) THEN
          pcount=pcount+1
          time_v(pcount)=t
          simen_v(pcount)=ensim
          DO k=1,ns
           partial(k,pcount)=state_all(k)
          ENDDO
         ENDIF
        ENDDO

        IF (pcount.ge.(npartial-ndiv).and.pcount.le.npartial) ncrit=1

        IF (ncrit.eq.1.or.t.eq.ntotstep.or.
     &      mod(t,tstop).eq.0) THEN
         DO jj=1,pcount
          WRITE(072,*) time_v(jj), simen_v(jj)
          IF (qlines.ne.0) THEN
           WRITE(072,139) ((partial(i,jj),i=(k-1)*nspin+1,k*nspin),
     &     k=1,qlines)
          ENDIF
          WRITE(072,139) (partial(i,jj), i=qlines*nspin+1,ns)
          CALL flush(072)
         ENDDO
         DO i=1,npartial
          time_v(i)=0
          simen_v(i)=0.
          DO j=1,ns
           partial(j,i)=0
          ENDDO
         ENDDO
         pcount=0
         ncrit=0
        ENDIF
       ENDIF


c-----status of the random number generator
       IF (mod(t,tstop).eq.0) THEN
        nstop=nstop+1
        OPEN(073,file=status)
         WRITE(073,109) matseed,'matrix seed'
         WRITE(073,109) runseed,'run seed'
         WRITE(073,109) nstop*tstop,'time to start with'
         WRITE(073,109) ntotstep,'number of timesteps'
         WRITE(073,119) temper,'temperature'
```

```
          WRITE(073,109) ncorrel,'points for the log scale'
          WRITE(073,109) ndiv,'number of bumps'
          WRITE(073,109) nspin,'spins per line'
          WRITE(073,119) quenchtemp,'temperature of the quench'
          WRITE(073,129) ' mean: j0=(3.-pstates)/(ns-1.)'
          WRITE(073,129) 'variance: dj=1./sqrt(ns-1.)'
          WRITE(073,109) setequil,'equilibrium flag'
          WRITE(073,109) 1,'rng flag'
          WRITE(073,FMT='(a)') logfile
          WRITE(073,FMT='(a)') filout
          WRITE(073,FMT='(a)') status
          WRITE(073,FMT='(a)') final
          IF (setequil.eq.0) THEN
           WRITE(073,FMT='(a)') outlog
           WRITE(073,FMT='(a)') outfile
          ENDIF
          IF (qlines.ne.0) THEN
          WRITE(073,139) ((state_all(i),i=(k-1)*nspin+1,k*nspin),
     &    k=1,qlines)
          ENDIF
          WRITE(073,139) (state_all(i), i=qlines*nspin+1,ns)
          WRITE(073,*) ipnt1,ipnf1,ipnt2,ipnf2
          DO i=1,9689
           WRITE(073,*) ir1(i)
          ENDDO
          DO i=1,127
           WRITE(073,*) ir2(i)
          ENDDO
          CALL flush(073)
         CLOSE(073)
        ENDIF

       ENDDO
c----end of the Monte Carlo calculation
c----END OF THE CORE PART

c
c-----IF this is an equilibration run, there is the need to supply a new
c     (restart) file. in order to start the simulation at equilibrium

       IF (setequil.eq.0) THEN
        OPEN(074,file=final)
         WRITE(074,109) matseed, 'matrix seed'
         WRITE(074,109) runseed+3000, 'run seed'
         WRITE(074,109) 0,'time to start with'
         WRITE(074,109) ntotstep, 'number of timesteps'
         WRITE(074,119) temper, 'temperature'
         WRITE(074,109) ncorrel,'points for the log scale'
         WRITE(074,109) ndiv,'number of bumps'
         WRITE(074,109) nspin,'spins per line'
         WRITE(074,119) quenchtemp,'temperature of the quench'
         WRITE(074,129) ' mean: j0=(3.-pstates)/(ns-1.)'
         WRITE(074,129) 'variance: dj=1./sqrt(ns-1.)'
         WRITE(074,109) setequil+1, 'equilibrium flag'
         WRITE(074,109) 0,'rng flag'
         WRITE(074,129) outlog
         WRITE(074,129) outfile
         WRITE(074,129) status
         WRITE(074,*) 'no need for a final file'

         IF (qlines.ne.0) THEN
         WRITE(074,139) ((state_all(i),i=(k-1)*nspin+1,k*nspin),
     &    k=1,qlines)
         ENDIF
         WRITE(074,139) (state_all(i), i=qlines*nspin+1,ns)
         CALL flush(074)
        CLOSE(074)
       ENDIF

       IF (setequil.eq.1) THEN
        CLOSE(072)
       ENDIF

109    FORMAT(I8,1x,A30)
119    FORMAT(f10.6,1x,A30)
129    FORMAT(A40)
139    FORMAT(100I1)
       END



       SUBROUTINE gauss(j0,dj)
c-----Gaussian distributed random number generator
       IMPLICIT NONE
       INTEGER*4 ns,nmax,k,i,ngauss
       REAL*8 x1,v1,v2,y1,y2,fx1,aux,j0,dj,convran
       PARAMETER (ns=320,nmax=3*ns)
       INTEGER*4 irn(nmax)
       REAL*8 gau(ns)
       INTEGER len1,len2,ifd1,ifd2,ipnt1,ipnt2,ipnf1,ipnf2
       PARAMETER (len1=9689,ifd1=471)
       PARAMETER (len2=127,ifd2=30)
       INTEGER*2 inxt1(len1)
       INTEGER*2 inxt2(len2)
       INTEGER*4 ir1(len1)
       INTEGER*4 ir2(len2)
       COMMON /nran/irn
       COMMON /rantool/ipnt1,ipnf1,ipnt2,ipnf2,inxt1,inxt2,ir1,ir2
       COMMON /bonds/gau


       convran=2.**(-32)*(1.d0-1.d-15)

       ngauss=1

       DO i=1,ns
```

```
       gau(i)=0.
      ENDDO

 41   CALL ransi(nmax)
      DO i=1,nmax,2
       v1=irn(i)*convran*2.
       v2=irn(i+1)*convran*2.
       x1=v1**2+v2**2
       IF (x1.gt.1..or.x1.eq.0.) THEN
        goto 40
       ENDIF
       IF (ngauss.gt.ns) goto 42
       fx1=1./x1
       aux=sqrt(-2.*fx1*log(x1))
       y1=aux*v2
       y2=aux*v1
       gau(ngauss)=y1
       gau(ngauss+1)=y2
       ngauss=ngauss+2
 40    continue
      ENDDO

      IF (ngauss.lt.ns) goto 41

 42   continue

      DO i=1,ns
       gau(i)=gau(i)*dj+j0
c       print*, gau(i)
c       read*,hhh
      ENDDO
      return

      END


      SUBROUTINE firstran(iseed)
c-----setup for the random number generator
c     sequential version
c     shift register random generator with very long period
      implicit REAL*8 (a-h,o-z)

      save
      PARAMETER (mult=32781)
      PARAMETER (mod2=2796203,mul2=125)
c     PARAMETER (two=2d0,tm32=two**(-32))
      PARAMETER (len1=9689,ifd1=471)
      PARAMETER (len2=127,ifd2=30)
      INTEGER*2 inxt1(len1)
      INTEGER*2 inxt2(len2)
      INTEGER*4 ir1(len1)
      INTEGER*4 ir2(len2)
      INTEGER*4 ns,nmax
      PARAMETER (ns=320,nmax=3*ns)
      INTEGER*4 irn(nmax)
c      PARAMETER (mxnx=500,mxny=500)
c      PARAMETER (mxsp=mxnx*mxny)
c      PARAMETER (mxrn=16*mxsp+1024)
      COMMON /nran/irn
      COMMON /rantool/ipnt1,ipnf1,ipnt2,ipnf2,inxt1,inxt2,ir1,ir2

      k=3**18+2*iseed
      k1=1313131*iseed
      k1=k1-(k1/mod2)*mod2
      DO i=1,len1
         k=k*mult
         k1=k1*mul2
         k1=k1-(k1/mod2)*mod2
         ir1(i)=k+k1*8193
c        write(6,*)i,k,k1,ir1(i)
      ENDDO
      DO i=1,len2
         k=k*mult
         k1=k1*mul2
         k1=k1-(k1/mod2)*mod2
         ir2(i)=k+k1*4099
c        write(6,*)i,k,k1,ir1(i)
      ENDDO
      DO i=1,len1
         inxt1(i)=i+1
      ENDDO
      inxt1(len1)=1
      ipnt1=1
      ipnf1=ifd1+1
      DO i=1,len2
         inxt2(i)=i+1
      ENDDO
      inxt2(len2)=1
      ipnt2=1
      ipnf2=ifd2+1
      return
      END


      SUBROUTINE ransi(n)
c-----random number generator
c     sequential version
c     shift register random generator with very long period
      implicit REAL*8 (a-h,o-z)
      save
      PARAMETER (mult=32781)
      PARAMETER (mod2=2796203,mul2=125)
c     PARAMETER (two=2d0,tm32=two**(-32))
      PARAMETER (len1=9689,ifd1=471)
      PARAMETER (len2=127,ifd2=30)
      INTEGER*2 inxt1(len1)
```

```
      INTEGER*2 inxt2(len2)
      INTEGER*4 ir1(len1)
      INTEGER*4 ir2(len2)
      INTEGER*4 ns,nmax,n
      PARAMETER (ns=320,nmax=3*ns)
      INTEGER*4 irn(nmax)

c      PARAMETER (mxnx=500,mxny=500)
c      PARAMETER (mxsp=mxnx*mxny)
c      PARAMETER (mxrn=16*mxsp+1024)
      COMMON /nran/irn
      COMMON /rantool/ipnt1,ipnf1,ipnt2,ipnf2,inxt1,inxt2,ir1,ir2

c     calculate n random numbers
      DO i=1,n
         l=ieor(ir1(ipnt1),ir1(ipnf1))
         k=ieor(ir2(ipnt2),ir2(ipnf2))
c        write(6,*) i,ipnt1,ipnt2,l,k,ieor(k,l)
         irn(i)=ieor(k,l)
         ir1(ipnt1)=l
         ipnt1=inxt1(ipnt1)
         ipnf1=inxt1(ipnf1)
         ir2(ipnt2)=k
         ipnt2=inxt2(ipnt2)
         ipnf2=inxt2(ipnf2)
      ENDDO
      return

      END
```

This is an example of an input file for the previous code (single flip Metropolis simulation of the infinite range Potts glass). Withouth comment are the names of the files used by the program.

```
56747          seed for the interactions
7206           seed for the run
0              starting time
1000           number of timesteps
1.8            temperature
150            points for the time scale
10             number of time origins
50             spins per line
999.           temperature of the quench
(3-p)/(N-1)
1/N-1
0              equilibrium/production run variable
0              restart variable
run0001.log
run0001.dat
status_rng_0001
restart0001
eq_run0001.log
eq_run0001.dat
```

```
ccccccccccccccccccccccccccccccccccccccccccccccccccccccccccccccccccccccc
c Parallel tempering simulation of the infinite range Potts Glass
c
ccccccccccccccccccccccccccccccccccccccccccccccccccccccccccccccccccccccc
c
c  This program is intended to simulate random bond potts model
c  with infinite range interactions among the spins, that is in
c  the mean field approximation
c
c  parallel tempering algorithm
c
c  structure of the random walk file: step, temperature of the i-proc
c  this program uses LINEAR time scales
c  the program can be restarted thanks to the status_rng_* files
c
c  important variables/parameters:
c  - locstep= number of steps in each local updating;
c  - npoints: how many configurations to write down
c  - setstop: how many times to save the status of the program:
c    REMEMBER: npoints/setstop MUST be an integer number

c  - temptoproc(:): array that, given a temperature, tells which
c                   processor has that temperature;
c  - proctotemp(:): array that, given a processor, tells its
c                   temperature;
c   both this variables are meaningful only for the master PE

c   the logfile is intended to be teperature-ordered (that is the
c   eq_run0001.log is the logfile corresponding to temperature 01);
c   it is updated at every stop, that is at every writing of the
c   status files, and has a list of the energy as a function of time.
c   There is also a end-file, that signals when the program ends:
c   this is useful when we want to restart the program, making a
c   chain of submissions in the queuing system


      PROGRAM potts

      IMPLICIT NONE
      INCLUDE 'mpif.h'
      INTEGER*4 ns,ntotstep,nmax,pstates
      INTEGER*4 ndiv,ncorr
      PARAMETER (ns=640,nmax=ns*3,pstates=10)
      REAL*8 bond(ns,ns),jij,totbond
      INTEGER*4 state_all(ns),irn(nmax)
      INTEGER*4 temp_s,kran,state,iseed
      REAL*8 energy(ns),entot,temp_en,delta,ener,en1
      REAL*8 gain,loose
      REAL*8 boltz,temper
      REAL*8 comp,ensim,conv,count,convb
      INTEGER*4 i,j,jj,ks,jran,p,k,t,init
      INTEGER*4 qlines,rlines,setequil,matseed,runseed,waste
      CHARACTER*50 filout,filin,outfile,final,logfile,outlog
      CHARACTER*50 status_rng
      INTEGER*4 nstart,tstop,nstop,setrand,nspin
      REAL*8 convran
 c-----info variables
      REAL*8 quenchtemp
      CHARACTER*50 meanofp,varofp
 c-----PARALLEL VARIABLES
      INTEGER myid, numprocs,ierr,kmax,involved
      INTEGER dest,source,kappa,kappacrit
      INTEGER*4 locstart,locend,locstep,maxtemp
      INTEGER*4 shift,couple,ncouples,seedcouple
      PARAMETER (maxtemp=64)
      INTEGER setstop, npoints
      INTEGER rest1,rest2,cfr1,cfr2,hundr,myfile,dec
      INTEGER adam,eve,othertemp,indexch
      INTEGER istatus(MPI_STATUS_SIZE),success
      INTEGER temptoproc(0:maxtemp-1),inttemper,me
      INTEGER proctotemp(0:maxtemp-1)
      REAL*8 encfr(0:maxtemp-1),rdelta,rboltz,rtemper(0:maxtemp-1)
      REAL*8 hhh,rcomp,t_adam,t_eve
      CHARACTER*50 alltemper,filpara
      CHARACTER*50 out(0:maxtemp-1),rest(0:maxtemp-1)
      CHARACTER*50 logf(0:maxtemp-1),stat(0:maxtemp-1)
      INTEGER idum,l,countbump,punit,nbump
      INTEGER*4 foridum
      REAL*8 RAN1,auxcomp,garb
      REAL*8 time_0,time_1,ptime_0,ptime_1,comm_time
      INTEGER, ALLOCATABLE :: bumpconf(:,:),wconf(:,:)
      REAL, ALLOCATABLE :: bumpener(:),wener(:)
      INTEGER, ALLOCATABLE :: bumptemp(:),wtemp(:)
      INTEGER smatrix,svector,stag,dtag,nrand
      INTEGER, ALLOCATABLE :: randomw(:,:)
      REAL*8,  ALLOCATABLE :: enewalk(:,:)

 c-----for the gaussian distribution
      REAL*8 j0,dj,gau(ns)

 c-----in common with the random number generator
      INTEGER*4 len1,len2,ifd1,ifd2,ipnt1,ipnt2,ipnf1,ipnf2
      PARAMETER (len1=9689,ifd1=471)
      PARAMETER (len2=127,ifd2=30)
      INTEGER*4 inxt1(len1)
```

```
      INTEGER*4 inxt2(len2)
      INTEGER*4 ir1(len1)
      INTEGER*4 ir2(len2)

      COMMON /nran/irn
      COMMON /rantool/ipnt1,ipnf1,ipnt2,ipnf2,inxt1,inxt2,ir1,ir2
      COMMON /bonds/gau


c
c-----THE PROGRAM STARTS
c


c
c-----initializing the parallel part
c
      CALL MPI_INIT(ierr)
      CALL MPI_COMM_RANK( MPI_COMM_WORLD, myid, ierr )
      CALL MPI_COMM_SIZE( MPI_COMM_WORLD, numprocs, ierr )

      comm_time=0.
      time_0=0.
      time_1=0.
      ptime_0=0.
      ptime_1=0.

      ncouples=numprocs-1
      myfile=myid+1
      cfr1=100
      cfr2=10
      hundr=INT(myfile/100)
      rest1=MOD(myfile,cfr1)
      dec=INT(rest1/10)
      rest2=MOD(myfile,cfr2)

       filin='input_0'//char(48+hundr)//char(48+dec)//char(48+rest2)
c      filin='restart0'//char(48+hundr)//char(48+dec)//char(48+rest2)
c      filin='status_rng_0'//char(48+hundr)//char(48+dec)//char(48+rest2)
      alltemper='temper.dat'

      CALL MPI_BARRIER(MPI_COMM_WORLD,IERR)

       DO i=0,numprocs-1
        myfile=i+1
        cfr1=100
        cfr2=10
        hundr=INT(myfile/100)
        rest1=MOD(myfile,cfr1)
        dec=INT(rest1/10)
        rest2=MOD(myfile,cfr2)
        out(i)='eq_run0'//char(48+hundr)//char(48+dec)//
     &       char(48+rest2)//'.dat'
        rest(i)='restart0'//char(48+hundr)//char(48+dec)//
     &       char(48+rest2)
        logf(i)='eq_run0'//char(48+hundr)//char(48+dec)//
     &       char(48+rest2)//'.log'
        stat(i)='status_rng_0'//char(48+hundr)//char(48+dec)//
     &       char(48+rest2)
c        print*, rest(i),stat(i)
       ENDDO


      DO i=0,maxtemp-1
       rtemper(i)=0.
       encfr(i)=0.
       temptoproc(i)=0
       proctotemp(i)=0
      ENDDO

      OPEN(062,file=alltemper)
       DO i=0,numprocs-1
        READ(062,*) rtemper(i)
       ENDDO
      CLOSE(062)

      DO i=0,numprocs-1
       temptoproc(i)=i
       proctotemp(i)=i
      ENDDO

      indexch=0

c-----some constants
      nspin=50          !spin written in a single line
      quenchtemp=999.   !pt always start from T=infin.
      lines=int(ns/nspin)
      rlines=mod(ns,nspin)
      nstop=0
      convran=2.**(-32)*(1.d0-1.d-15)
      j0=(3.-pstates)/(ns-1.)
      dj=1./sqrt(ns-1.)
      conv=1.*pstates

      DO i=1,ns
       DO j=1,ns
        bond(j,i)=0.
       ENDDO
```

```
      ENDDO
      DO i=1,ns
       gau(i)=0.
      ENDDO

c
c-----READING from the INPUT file and construction of the bond matrix
c
c      print*,'I need the input file'
c      READ(5,FMT='(a)') filin
      OPEN(061,file=filin)
       READ(061,*) matseed
       READ(061,*) runseed
       READ(061,*) nstart
       READ(061,*) ntotstep
       READ(061,*) inttemper
       READ(061,*) locstep
       READ(061,*) npoints
       READ(061,*) nspin
       READ(061,*) setstop
       READ(061,FMT='(a)') meanofp
       READ(061,FMT='(a)') varofp
       READ(061,*) setequil
       READ(061,*) setrand
       READ(061,FMT='(a)') logfile
       READ(061,FMT='(a)') filout
       READ(061,FMT='(a)') status_rng
       READ(061,FMT='(a)') final
c
c-----initialization of the bond matrix: gaussian distribution
c
      CALL firstran(matseed)
      DO k=1,1000
       CALL ransi(nmax)
       DO i=1,3*ns
        waste=irn(i)
       ENDDO
      ENDDO

      DO j=1,ns-1
       CALL gauss(j0,dj)
       DO i=j+1,ns
         jij=gau(i)
         IF (i.eq.j) jij=0.
         bond(j,i)=jij
         bond(i,j)=jij
       ENDDO
      ENDDO

      totbond=0.
      DO j=1,ns
       DO i=1,ns
        totbond=totbond+bond(i,j)
       ENDDO
      ENDDO
      totbond=totbond/2.
c
      IF (setequil.eq.0) THEN
       READ(061,FMT='(a)') outlog
       READ(061,FMT='(a)') outfile
      ENDIF
      IF (setequil.ne.0.or.setrand.eq.1.or.quenchtemp.lt.100.) THEN
       IF (qlines.ne.0) THEN
        READ(061,139) ((state_all(i),i=(k-1)*nspin+1,k*nspin),
     &    k=1,qlines)
       ENDIF
         READ(061,139) (state_all(i), i=qlines*nspin+1,ns)
      ENDIF
c-----the inclusion of the variable shift is very important, and was not
c     present in the serial version of the code: takes memory of the
c     status of the parallel calculation
      shift=0
      IF (setrand.eq.1) THEN
       READ(061,*) shift
       READ(061,*) ipnt1,ipnf1,ipnt2,ipnf2
       DO i=1,9689
        READ(061,*) ir1(i)
       ENDDO
       DO i=1,127
        READ(061,*) ir2(i)
       ENDDO
      ENDIF
      CLOSE(061)
c-----another instruction different from the serial version: also the
c     positions  of all the temperatures have to be saved
      IF (myid.eq.0.and.setrand.eq.1) THEN
       OPEN(065,file='status_rng_glob')
        READ(065,149) (temptoproc(i), i=0,numprocs-1)
        READ(065,149) (proctotemp(i), i=0,numprocs-1)
       CLOSE(065)
      ENDIF

c
c----the random walk
c
      IF (setequil.eq.0) filpara='para_run.dat'
```

```
      IF (setequil.eq.1) filpara='para_equ.dat'

c
c-----opening the output files
c
      IF (setequil.eq.1) THEN
       OPEN(072,file=filout,position='append')
       IF (setrand.eq.0) THEN
        WRITE(072,109) ns,'number of spins'
        WRITE(072,109) pstates,'number of states'
        WRITE(072,109) matseed,'matrix seed'
        WRITE(072,109) runseed,'run seed'
        WRITE(072,109) nstart,'time to start with'
        WRITE(072,109) ntotstep,'number of timesteps'
        WRITE(072,119) rtemper(inttemper),'temperature'
        WRITE(072,109) locstep,'how often the PT occurs'
        WRITE(072,109) npoints,'number of bumps'
        WRITE(072,109) nspin,'spins per line'
        WRITE(072,109) setstop,'how many times the status'
        WRITE(072,129) ' mean: j0=(3.-pstates)/(ns-1.)'
        WRITE(072,129) 'variance: dj=1./sqrt(ns-1.)'
        WRITE(072,109) setequil,'equilibrium flag'
        WRITE(072,109) setrand,'rng flag'
        WRITE(072,FMT='(a)') logfile
        WRITE(072,FMT='(a)') filout
        WRITE(072,FMT='(a)') final
       ENDIF
       CLOSE(072)
      ENDIF

      IF (myid.eq.0) THEN
       IF (setrand.eq.0) THEN
        OPEN(071,file=logfile,position='append')
        WRITE(071,109) ns,'number of spins'
        WRITE(071,109) pstates,'number of states'
        WRITE(071,109) matseed,'matrix seed'
        WRITE(071,109) runseed,'run seed'
        WRITE(071,109) nstart,'time to start with'
        WRITE(071,109) ntotstep,'number of timesteps'
        WRITE(071,119) rtemper(inttemper),'temperature'
        WRITE(071,109) locstep,'how often the PT exchange occurs'
        WRITE(071,109) npoints,'number of bumps'
        WRITE(071,109) nspin,'spins per line'
        WRITE(071,109) setstop,'how many times the status'
        WRITE(071,129) ' mean: j0=(3.-pstates)/(ns-1.)'
        WRITE(071,129) 'variance: dj=1./sqrt(ns-1.)'
        WRITE(071,109) setequil,'equilibrium flag'
        WRITE(071,109) setrand,'rng flag'
        WRITE(071,FMT='(a)') logfile
        WRITE(071,FMT='(a)') filout
        WRITE(071,FMT='(a)') final
        CLOSE(071)
       ENDIF
      ENDIF


c
c-----first temperature
c
      temper=rtemper(inttemper)
c
c-----dynamical memory allocation
c
      kappacrit=ntotstep/(npoints*locstep)
      nbump=npoints/setstop
      tstop=ntotstep/setstop
      nrand=ntotstep/locstep/setstop

      IF (nstop.eq.0) THEN
       ALLOCATE(bumpconf(ns,0:nbump))
       ALLOCATE(bumptemp(0:nbump),bumpener(0:nbump))
       ALLOCATE(randomw(0:numprocs-1,0:nbump))
       ALLOCATE(enewalk(0:numprocs-1,1:nbump))
       IF (myid.eq.0) THEN
        DO i=0,numprocs-1
         randomw(i,indexch)=proctotemp(i)
        ENDDO
       ENDIF
       bumpconf=0.
       bumptemp=0
       bumpener=0.
      ENDIF


c
c-----warming for the random number generator
c
      IF (setrand.ne.1) THEN
      CALL firstran(runseed)
      DO k=1,1000
       CALL ransi(nmax)
       DO i=1,3*ns
        waste=irn(i)
       ENDDO
      ENDDO
      ENDIF
c
```

```
c-----needed only for the equilibration run, NOT for the equilibrium
c     run; and only when quenching from infinity
c
      IF (setequil.eq.0.and.setrand.ne.1.and.quenchtemp.lt.100.) THEN
       DO i=1,ns
        state_all(i)=0
       ENDDO
       CALL ransi(nmax)
       DO i=1,ns
        state_all(i)=(irn(i)*convran+.5)*pstates
       ENDDO
      ENDIF
c
c-----calculation of the total energy and of the energy arrays
c
      entot=0.
      DO i=1,ns
       state=state_all(i)
       ener=0.
       DO j=1,ns
        gain=0.
        IF (state.eq.state_all(j)) ener=ener+bond(i,j)
       ENDDO
       energy(i)=-ener
       entot=entot+energy(i)
      ENDDO
      en1=entot

c
c-----writing down the step number 0!
c
      t=nstart
      countbump=0
      ensim=(conv*entot/2.+totbond)/ns

      IF (nstart.eq.0) THEN
c       OPEN(071,file=logfile,position='append')
c       WRITE(071,159) t,ensim
c       WRITE(071,*) t,ensim,state_all(1),state_all(2)
       IF (setequil.eq.1) THEN
        DO i=1,ns
         bumpconf(i,countbump)=state_all(i)
        ENDDO
        bumpener(countbump)=ensim
        bumptemp(countbump)=inttemper
        countbump=countbump+1
       ENDIF
c       CLOSE(071)
    ENDIF

 c
 c-----time evaluation
 c
       time_0=MPI_Wtime()

 c
 c-----THE CORE OF THE PROGRAM
 c-----Monte Carlo Calculation
 c
       count=0
       ensim=0.
       convb=(1.*pstates)/temper
       locstart=nstart
       kappa=0
       indexch=1
       countbump=1
  100  locend=locstart+locstep

       DO t=locstart+1,locend
 c      if (myid.eq.0) print*,t
 c-----single monte carlo sweep: ns spin updated
        CALL ransi(nmax)
        DO ks=1,3*ns,3
 c-----single random spin flip
         temp_s=0
         jran=(irn(ks)*convran+.5)*ns+1
         kran=(irn(ks+1)*convran+.5)*pstates+1
         comp=(irn(ks+2)*convran+.5)
         temp_s=mod(kran,pstates)

 c-----comparison and importance sampling
         temp_en=0.
         DO j=1,ns
          gain=0.
          IF (temp_s.eq.state_all(j)) temp_en=temp_en-bond(j,jran)
         ENDDO

         delta=temp_en-energy(jran)

         IF (delta.le.0.) THEN
          goto 60
         else IF (delta.gt.0.) THEN
          boltz=exp(-delta*convb)
          IF (boltz.gt.comp) goto 60
          IF (boltz.le.comp) goto 70
         ENDIF
```

```
 60     continue

        energy(jran)=temp_en
        entot=energy(jran)
        DO i=1,jran-1
         IF (state_all(jran).eq.state_all(i))
     &       energy(i)=energy(i)+bond(i,jran)
         IF (temp_s.eq.state_all(i))
     &       energy(i)=energy(i)-bond(i,jran)
         entot=entot+energy(i)
        ENDDO
        DO i=jran+1,ns
         IF (state_all(jran).eq.state_all(i))
     &       energy(i)=energy(i)+bond(i,jran)
         IF (temp_s.eq.state_all(i))
     &       energy(i)=energy(i)-bond(i,jran)
         entot=entot+energy(i)
        ENDDO
        state_all(jran)=temp_s

 70     continue
        ensim=(conv*entot/2.+totbond)/ns
       ENDDO

      ENDDO
c----end of the Monte Carlo calculation


c
c----beginning of the parallel tempering part
c
      encfr(myid)=ensim*ns

      CALL MPI_BARRIER(MPI_COMM_WORLD,ierr)

      CALL MPI_GATHER(encfr(myid),1,MPI_REAL8,encfr,1,
     &               MPI_REAL8,0,MPI_COMM_WORLD,ierr)

      kappa=kappa+1
      IF (myid.eq.0) THEN
       IF (shift.eq.0.and.numprocs.gt.2) THEN
        shift=1
       ELSE
        shift=0
       ENDIF

       CALL ransi(nmax)

       DO couple=0,ncouples-1,2
        involved=couple+1*shift

        IF (involved.eq.numprocs-1) GOTO 210
        adam=temptoproc(involved)
        eve=temptoproc(involved+1)

        rcomp=(irn(couple+1)*convran+.5)
        t_adam=rtemper(proctotemp(adam))
        t_eve=rtemper(proctotemp(eve))
        rdelta=(encfr(adam)-encfr(eve))*(1./t_eve
     &   -1./t_adam)
        success=0

        IF (rdelta.le.0.) THEN
         success=1
         GOTO 80
        ELSE IF (rdelta.gt.0.) THEN
         rboltz=exp(-rdelta)
         IF (rboltz.gt.rcomp) THEN
          success=1
          goto 80
         ELSE IF (rboltz.le.rcomp) THEN
          goto 90
         ENDIF
        ENDIF

 80     CONTINUE

        temptoproc(involved)=eve
        temptoproc(involved+1)=adam
        proctotemp(adam)=involved+1
        proctotemp(eve)=involved

 90     CONTINUE
       ENDDO              ! the one on adam and eve
 210   CONTINUE



      ENDIF    ! the one on the master processor

      CALL MPI_SCATTER(proctotemp,1,MPI_INTEGER,inttemper,
     &                1,MPI_INTEGER,0,MPI_COMM_WORLD,ierr)

      temper=rtemper(inttemper)
      convb=(1.*pstates)/temper
```

```
      CALL MPI_BARRIER(MPI_COMM_WORLD,ierr)


c-----and now writing down the results
      IF (mod(kappa,kappacrit).eq.0) THEN
       IF (setequil.eq.1) THEN
        DO i=1,ns
         bumpconf(i,countbump)=state_all(i)
        ENDDO
        bumpener(countbump)=ensim
        bumptemp(countbump)=inttemper
        countbump=countbump+1
       ENDIF
       IF (myid.eq.0) THEN
        DO i=0,numprocs-1
     randomw(i,indexch)=proctotemp(i)
         enewalk(i,indexch)=encfr(temptoproc(i))
        ENDDO
        indexch=indexch+1
       ENDIF
      ENDIF

      locstart=locend

c
c-----status of the random number generator and output
c
      IF (mod(locend,tstop).eq.0) THEN
       nstop=nstop+1
       status_rng=stat(myid)
       OPEN(073,file=status_rng)
       WRITE(073,109) matseed,'matrix seed'
       WRITE(073,109) runseed,'run seed'
       WRITE(073,109) nstart+nstop*tstop,'time to start with'
       WRITE(073,109) ntotstep,'number of timesteps'
       WRITE(073,109) inttemper,'temperature'
       WRITE(073,109) locstep,'how often the PT occurs'
       WRITE(073,109) npoints,'number of bumps'
       WRITE(073,109) nspin,'spins per line'
       WRITE(073,109) setstop,'how many times the status'
       WRITE(073,129) ' mean: j0=(3.-pstates)/(ns-1.)'
       WRITE(073,129) 'variance: dj=1./sqrt(ns-1.)'
       WRITE(073,109) setequil,'equilibrium flag'
       WRITE(073,109) 1,'rng flag'
       WRITE(073,FMT='(a)') logfile
       WRITE(073,FMT='(a)') filout
       WRITE(073,FMT='(a)') status_rng
       WRITE(073,FMT='(a)') final
       IF (setequil.eq.0) THEN
        WRITE(073,FMT='(a)') outlog
        WRITE(073,FMT='(a)') outfile
       ENDIF
       IF (qlines.ne.0) THEN
        WRITE(073,139) ((state_all(i),i=(k-1)*nspin+1,k*nspin),
     &    k=1,qlines)
       ENDIF
       WRITE(073,139) (state_all(i), i=qlines*nspin+1,ns)
       WRITE(073,109) shift,'shift for the PT'
       WRITE(073,*) ipnt1,ipnf1,ipnt2,ipnf2
       DO i=1,9689
        WRITE(073,*) ir1(i)
       ENDDO
       DO i=1,127
        WRITE(073,*) ir2(i)
       ENDDO
       CALL flush(073)
       CLOSE(073)
       IF (myid.eq.0) THEN
        OPEN(076,file='status_rng_glob')
        WRITE(076,149) (temptoproc(i), i=0,numprocs-1)
        WRITE(076,149) (proctotemp(i), i=0,numprocs-1)
        CLOSE(076)
       ENDIF
c
c-----the output
c
       IF (setequil.eq.1) THEN
        ALLOCATE(wconf(ns,0:nbump),wener(0:nbump),wtemp(0:nbump))
        CALL MPI_BARRIER(MPI_COMM_WORLD,ierr)

        IF (myid.eq.0) THEN
         DO i=0,numprocs-1
          punit=111+i
          OPEN(punit,file=out(i),position='append')
         ENDDO
         wconf=bumpconf
         wener=bumpener
         wtemp=bumptemp
         init=0
         IF (setrand.eq.1.or.nstop.gt.1) init=1
         DO j=init,nbump
          punit=111+wtemp(j)
          WRITE(punit,159) j*(locstep*kappacrit)+nstart+(nstop-1)*tstop,
     &         wener(j),myid
          IF (qlines.ne.0) THEN
```

```
         WRITE(punit,139) ((wconf(l,j),l=(k-1)*nspin+1,k*nspin),
     &     k=1,qlines)
         ENDIF
         WRITE(punit,139) (wconf(l,j), l=qlines*nspin+1,ns)
         CALL flush(punit)
        ENDDO
       ENDIF
       CALL MPI_BARRIER(MPI_COMM_WORLD,ierr)
       i=1
222  CONTINUE

       source=i
       dest=0
       stag=1
       dtag=1
       smatrix=ns*(nbump+1)
       svector=nbump+1
       IF (myid.eq.source) THEN
        CALL MPI_SEND(bumpconf,smatrix,MPI_INTEGER,dest,1,
     &                MPI_COMM_WORLD,ierr)
        CALL MPI_SEND(bumptemp,svector,MPI_INTEGER,dest,2,
     &                MPI_COMM_WORLD,ierr)
        CALL MPI_SEND(bumpener,svector,MPI_REAL,dest,3,
     &               MPI_COMM_WORLD,ierr)
       ENDIF
       IF (myid.eq.dest) THEN
        CALL MPI_RECV(wconf,smatrix,MPI_INTEGER,source,1,
     &               MPI_COMM_WORLD,istatus,ierr)
        CALL MPI_RECV(wtemp,svector,MPI_INTEGER,source,2,
     &               MPI_COMM_WORLD,istatus,ierr)
        CALL MPI_RECV(wener,svector,MPI_REAL,source,3,
     &               MPI_COMM_WORLD,istatus,ierr)
       ENDIF

       IF (myid.eq.0) THEN
        DO j=init,nbump
         punit=111+wtemp(j)
         WRITE(punit,159) j*(locstep*kappacrit)+nstart+(nstop-1)*tstop, countbump=1
     &     wener(j),i
         IF (qlines.ne.0) THEN
         WRITE(punit,139) ((wconf(l,j),l=(k-1)*nspin+1,k*nspin),
     &     k=1,qlines)
         ENDIF
         WRITE(punit,139) (wconf(l,j), l=qlines*nspin+1,ns)
         CALL flush(punit)
        ENDDO
       ENDIF
       CALL MPI_BARRIER(MPI_COMM_WORLD,ierr)
```

```
       i=i+1
       IF (i.gt.numprocs-1) GOTO 444
       GOTO 222

 444  CONTINUE

       IF (myid.eq.0) THEN
        DO i=0,numprocs-1
         punit=111+i
         CLOSE(punit)
        ENDDO
       ENDIF

       DEALLOCATE(wconf,wener,wtemp)

      ENDIF   ! the one on setequil.
c
c--------writing random walk and logfile with the energies
c
       IF (myid.eq.0) THEN
        init=0
        IF (setrand.eq.1.or.nstop.gt.1) init=1
        OPEN(075,FILE=filpara,POSITION='append')
        OPEN(071,FILE=logfile,POSITION='append')
        DO j=init,nbump
         WRITE(075,149) j*(locstep*kappacrit)+nstart+(nstop-1)*tstop,
     &               (randomw(i,j), i=0,numprocs-1)
        ENDDO
        DO j=1,nbump
         WRITE(071,179) j*(locstep*kappacrit)+nstart+(nstop-1)*tstop,
     &               (enewalk(i,j)/ns, i=0,15) ! we write only
                                               ! up to the
                ! 15th temperature
        ENDDO
        CLOSE(075)
        CLOSE(071)
       ENDIF

c-----here is the part to un-comment in order to stop the program------
c      IF ((nstart+nstop*tstop).eq.ntotstep) GOTO 278
c      stop !*************************************************
c-------------------------------------------------------------------
278   CONTINUE

c
c-----there is the need of a new dynamical allocation
c
```

```
       IF (nstop.ne.0) THEN
        DEALLOCATE(bumpconf,bumptemp,bumpener,randomw,enewalk)
        ALLOCATE(bumpconf(ns,0:nbump))
        ALLOCATE(bumptemp(0:nbump),bumpener(0:nbump))
        ALLOCATE(randomw(0:numprocs-1,0:nbump))
        ALLOCATE(enewalk(0:numprocs-1,1:nbump))
        IF (myid.eq.0) THEN
         indexch=1
        ENDIF
        bumpconf=0.
        bumptemp=0
        bumpener=0.
       ENDIF

      ENDIF  ! the one on tstop

      IF (locend.lt.ntotstep) GOTO 100      ! back to the beginning of
                                            ! local MC
 110  CONTINUE

      time_1=MPI_Wtime()
      IF (myid.eq.0) THEN
       print*,'total time',time_1-time_0
      ENDIF



      CALL MPI_FINALIZE(ierr)

c
c-----end of the parallel part
c
c----END OF THE CORE PART
c

c
c-----IF this is an equilibration run, there is the need to supply a new
c     (restart) file. in order to start the simulation at equilibrium

      final=rest(inttemper)
      IF (setequil.eq.0) THEN
       OPEN(074,file=final)
       WRITE(074,109) matseed, 'matrix seed'
       WRITE(074,109) runseed+300, 'run seed'
       WRITE(074,109) 0,'time to start with'
       WRITE(074,109) ntotstep, 'number of timesteps'
       WRITE(074,109) inttemper, 'temperature'
       WRITE(074,109) locstep,'how often the PT occurs'
       WRITE(074,109) npoints,'number of bumps'
       WRITE(074,109) nspin,'spins per line'
       WRITE(074,109) setstop,'how many times the status'
       WRITE(074,129) ' mean: j0=(3.-pstates)/(ns-1.)'
       WRITE(074,129) 'variance: dj=1./sqrt(ns-1.)'
       WRITE(074,109) setequil+1, 'equilibrium flag'
       WRITE(074,109) 0,'rng flag'
       WRITE(074,129) logf(inttemper)
       WRITE(074,129) out(inttemper)
       WRITE(074,129) stat(inttemper)
       WRITE(074,*) 'no need for a final file'

       IF (qlines.ne.0) THEN
       WRITE(074,139) ((state_all(i),i=(k-1)*nspin+1,k*nspin),
     &  k=1,qlines)
       ENDIF
       WRITE(074,139) (state_all(i), i=qlines*nspin+1,ns)
       CALL flush(074)
       CLOSE(074)
      ENDIF

c
c-----now an info-file, just to know if the program ended
c
      IF (setequil.eq.1) THEN
       IF (myid.eq.0) THEN
        OPEN(077,file='end_file')
        WRITE(077,*) 'this is only an info-file'
        CLOSE(077)
       ENDIF
      ENDIF



 109   FORMAT(I8,1x,A30)
 119   FORMAT(f20.6,1x,A30)
 129   FORMAT(A30)
 139   FORMAT(100I1)
 149   FORMAT(1x,I7,30(1x,I3))
 179   FORMAT(1x,I7,20(1x,f7.4))
 159   FORMAT(I8,1x,f20.6,1x,I3)

       END




      SUBROUTINE gauss(j0,dj)
c-----Gaussian distributed random number generator
```

```
      IMPLICIT NONE
      INTEGER*4 ns,nmax,k,i,ngauss
      REAL*8 x1,v1,v2,y1,y2,fx1,aux,j0,dj,convran
      PARAMETER (ns=640,nmax=3*ns)
      INTEGER*4 irn(nmax)
      REAL*8 gau(ns)
      INTEGER*4 len1,len2,ifd1,ifd2,ipnt1,ipnt2,ipnf1,ipnf2
      PARAMETER (len1=9689,ifd1=471)
      PARAMETER (len2=127,ifd2=30)
      INTEGER*4 inxt1(len1)
      INTEGER*4 inxt2(len2)
      INTEGER*4 ir1(len1)
      INTEGER*4 ir2(len2)
      COMMON /nran/irn
      COMMON /rantool/ipnt1,ipnf1,ipnt2,ipnf2,inxt1,inxt2,ir1,ir2
      COMMON /bonds/gau


      convran=2.**(-32)*(1.d0-1.d-15)
      ngauss=1

      DO i=1,ns
       gau(i)=0.
      ENDDO

41    CALL ransi(nmax)
      DO i=1,nmax,2
       v1=irn(i)*convran*2.
       v2=irn(i+1)*convran*2.
       x1=v1**2+v2**2
       IF (x1.gt.1..or.x1.eq.0.) THEN
        goto 40
       ENDIF
       IF (ngauss.gt.ns) goto 42
       fx1=1./x1
       aux=sqrt(-2.*fx1*log(x1))
       y1=aux*v2
       y2=aux*v1
       gau(ngauss)=y1
       gau(ngauss+1)=y2
       ngauss=ngauss+2
40     continue
      ENDDO

      IF (ngauss.lt.ns) goto 41
42    continue

      DO i=1,ns
       gau(i)=gau(i)*dj+j0
      ENDDO
      return
      END


c
c     random number generator for the spin flip
c     shift register random generator with very long period
c     ref:

      SUBROUTINE firstran(iseed)
c-----setup for the random number generator
c     sequential version
c      implicit REAL*8 (a-h,o-z)

      IMPLICIT NONE
      save
      INTEGER*4 mult,mod2,mul2,len1,ifd1,len2,ifd2
      INTEGER*4 k,k1,iseed,i,ipnt1,ipnt2,ipnf1,ipnf2
      PARAMETER (mult=32781)
      PARAMETER (mod2=2796203,mul2=125)
c     PARAMETER (two=2d0,tm32=two**(-32))
      PARAMETER (len1=9689,ifd1=471)
      PARAMETER (len2=127,ifd2=30)
      INTEGER*4 inxt1(len1)
      INTEGER*4 inxt2(len2)
      INTEGER*4 ir1(len1)
      INTEGER*4 ir2(len2)
      INTEGER*4 ns,nmax
      PARAMETER (ns=640,nmax=3*ns)
      INTEGER*4 irn(nmax)
c      PARAMETER (mxnx=500,mxny=500)
c      PARAMETER (mxsp=mxnx*mxny)
c      PARAMETER (mxrn=16*mxsp+1024)
      COMMON /nran/irn
      COMMON /rantool/ipnt1,ipnf1,ipnt2,ipnf2,inxt1,inxt2,ir1,ir2

      k=3**18+2*iseed
      k1=1313131*iseed
      k1=k1-(k1/mod2)*mod2
      DO i=1,len1
         k=k*mult
         k1=k1*mul2
         k1=k1-(k1/mod2)*mod2
         ir1(i)=k+k1*8193
c        write(6,*)i,k,k1,ir1(i)
      ENDDO
      DO i=1,len2
```

```
         k=k*mult
         k1=k1*mul2
         k1=k1-(k1/mod2)*mod2
         ir2(i)=k+k1*4099
c        write(6,*)i,k,k1,ir1(i)
      ENDDO
      DO i=1,len1
         inxt1(i)=i+1
      ENDDO
      inxt1(len1)=1
      ipnt1=1
      ipnf1=ifd1+1
      DO i=1,len2
         inxt2(i)=i+1
      ENDDO
      inxt2(len2)=1
      ipnt2=1
      ipnf2=ifd2+1
      return
      END

      SUBROUTINE ransi(n)
c-----random number generator
c     sequential version
c     shift register random generator with very long period
c      implicit REAL*8 (a-h,o-z)

      IMPLICIT NONE
      save
      INTEGER*4 mult,mod2,mul2,len1,ifd1,len2,ifd2
      INTEGER*4 k,k1,iseed,i,ipnt1,ipnt2,ipnf1,ipnf2,l
      PARAMETER (mult=32781)
      PARAMETER (mod2=2796203,mul2=125)
c     PARAMETER (two=2d0,tm32=two**(-32))
      PARAMETER (len1=9689,ifd1=471)
      PARAMETER (len2=127,ifd2=30)
      INTEGER*4 inxt1(len1)
      INTEGER*4 inxt2(len2)
      INTEGER*4 ir1(len1)
      INTEGER*4 ir2(len2)
      INTEGER*4 ns,nmax,n
      PARAMETER (ns=640,nmax=3*ns)
      INTEGER*4 irn(nmax)

c      PARAMETER (mxnx=500,mxny=500)
c      PARAMETER (mxsp=mxnx*mxny)
c      PARAMETER (mxrn=16*mxsp+1024)
      COMMON /nran/irn
      COMMON /rantool/ipnt1,ipnf1,ipnt2,ipnf2,inxt1,inxt2,ir1,ir2

c     calculate n random numbers
      DO i=1,n
         l=ieor(ir1(ipnt1),ir1(ipnf1))
         k=ieor(ir2(ipnt2),ir2(ipnf2))
c        write(6,*) i,ipnt1,ipnt2,l,k,ieor(k,l)
         irn(i)=ieor(k,l)
         ir1(ipnt1)=l
         ipnt1=inxt1(ipnt1)
         ipnf1=inxt1(ipnf1)
         ir2(ipnt2)=k
         ipnt2=inxt2(ipnt2)
         ipnf2=inxt2(ipnf2)
      ENDDO
      return
      END
```

```
ccccccccccccccccccccccccccccccccccccccccccccccccccccccccc
c Heat Bath simulation of the short range Potts glass
c
ccccccccccccccccccccccccccccccccccccccccccccccccccccccccc

      PROGRAM potts3D
c     --------------
c Monte Carlo code for short range Potts models
c A bimodal distribution of bonds is used


      IMPLICIT NONE
      INTEGER*4 boxlenght,ns,dim          ! lattice's dimensions
      INTEGER*4 nnnumber,pstates,nmax
      INTEGER*4 ndiv,ncorrel,npartial,p
      INTEGER*4 ncorrelnew,ncorr,ncrit
      INTEGER*4 logbump,tstop,pbump,pstop
      PARAMETER (pstop=1)                 ! how many times the status
      PARAMETER (pbump=100)               ! how many log-points
      PARAMETER (dim=3,nnnumber=2*dim)    ! NB: ntotstep must be a
      PARAMETER (boxlenght=16)            !     multiple of both tstop
      PARAMETER (ns=boxlenght**3)         !     and logbump
      PARAMETER (pstates=10,nmax=2*ns)
      PARAMETER (ndiv=4,ncorrel=150)
      PARAMETER (npartial=ncorrel)
      INTEGER*4 neigh(nnnumber,ns)        ! neighbors
      INTEGER*4 coupling(nnnumber,ns)     ! interactions
      INTEGER*4 stateall(ns)              ! configuration
      INTEGER*4 engtot,totbond
      INTEGER*4 i,j,jran,ks,k,waste,jj
      INTEGER*4 sold,snew                 ! new and old spin
      INTEGER*4 delta,shift               ! integer for J=+/-1
      INTEGER*4 nstart,ntotstep,t
      INTEGER*4 irn(nmax),runseed,matseed ! random numbers
      INTEGER*4 infoncorrel
      INTEGER*4 infondiv,nspin,setequil
      INTEGER*4 setrand,qlines,rlines
      INTEGER*4 cortim(ncorrel*ndiv)
      INTEGER*4 partial(ns,npartial)
      INTEGER*4 time_v(npartial),pcount
      INTEGER*4 check(2*dim),ehb(pstates)
      REAL*8 probhb(pstates),normprob,cumul,touse(nmax)

      REAL*8 temper,boltzfct(4*dim+1)
      REAL*8 btemper,rescal,j0,dj
      REAL*8 conv,ensim,comp,convran,hhh
c      PARAMETER (conv=1.)                ! NB: this is the prefactor
      REAL*8 quenchtemp                   ! --- in the Hamiltonian
      REAL*8 simen_v(npartial)

      CHARACTER*50 filout,filin
      CHARACTER*50 meanofp,varofp
      CHARACTER*50 logfile,status,final
      CHARACTER*50 outlog,outfile

      INTEGER len1,len2,ifd1,ifd2         ! this part is in
      INTEGER ipnt1,ipnt2,ipnf1,ipnf2     ! common with the
      PARAMETER (len1=9689,ifd1=471)      ! random number
      PARAMETER (len2=127,ifd2=30)        ! generator
      INTEGER*2 inxt1(len1)               !
      INTEGER*2 inxt2(len2)               !
      INTEGER*4 ir1(len1)                 !
      INTEGER*4 ir2(len2)                 !

      COMMON /nran/irn
      COMMON /rantool/ipnt1,ipnf1,ipnt2,ipnf2,inxt1,inxt2,ir1,ir2


c READING THE INPUT FILE
c ----------------------

      print*,'I need the input file'
      READ(5,FMT='(a)') filin

      OPEN(061,file=filin)

        READ(061,*) matseed
        READ(061,*) runseed
        READ(061,*) nstart
        READ(061,*) ntotstep
        READ(061,*) temper
        READ(061,*) infoncorrel
        READ(061,*) infondiv
        READ(061,*) nspin
        READ(061,*) quenchtemp
        READ(061,FMT='(a)') meanofp
        READ(061,FMT='(a)') varofp
        READ(061,*) setequil
        READ(061,*) setrand
        READ(061,FMT='(a)') logfile
        READ(061,FMT='(a)') filout
        READ(061,FMT='(a)') status
        READ(061,FMT='(a)') final

        qlines=int(ns/nspin)
```

```
      rlines=mod(ns,nspin)

      IF (setequil.eq.0) THEN
        READ(061,FMT='(a)') outlog
        READ(061,FMT='(a)') outfile
      ENDIF

      IF (setequil.ne.0.or.setrand.eq.1.or.quenchtemp.lt.100.) THEN
        IF (qlines.ne.0) THEN
          READ(061,139) ((stateall(i),i=(k-1)*nspin+1,k*nspin),
     &                    k=1,qlines)
        ENDIF
        IF (rlines.NE.0) THEN
          READ(061,139) (stateall(i), i=qlines*nspin+1,ns)
        ENDIF
      ENDIF

c At this point we have to initialize the lattice and the interactions
c we do it now because, in case of restart, there can be problems with
c the two sequences of pseudo-random numbers, namely matseed (for the
c interactions) and runseed (for the dynamics)
c Lattice and interactions:
c j0 and dj are those for a gaussian distribution; they are converted
c for the +-J thanks to the variable "rescal" that fixes J, that is
c the coupling constant, and to "concentr" (in the coupl3D routine)
c that set the concentration x of positive bonds; the +- distribution
c is given by P(J_ij)=x*d(J_ij-J)+(1-x)*d(J_ij+J)
c cfr Dillmann et al, J. Stat. Phys. 92, 57 (1998)

      j0=-1.
      dj=1.

      CALL lat3d(neigh)
      CALL coupl3d(neigh,coupling,matseed,j0,dj)

c now, if we have to read from a "status" file, we need to know all the
c information about the random number generator of the dynamics

      IF (setrand.eq.1) THEN
        READ(061,*) ipnt1,ipnf1,ipnt2,ipnf2
        DO i=1,9689
          READ(061,*) ir1(i)
        ENDDO
        DO i=1,127
          READ(061,*) ir2(i)
        ENDDO
      ENDIF

      CLOSE(061)


c OPENING THE OUTPUT FILES
c ------------------------

      OPEN(071,file=logfile,access='append')

      IF (setequil.eq.1) THEN
        OPEN(072,file=filout,access='append')
      ENDIF

      IF (setequil.eq.1.and.setrand.eq.0) THEN
        WRITE(072,109) ns,'number of spins'
        WRITE(072,109) pstates,'number of states'
        WRITE(072,109) matseed,'matrix seed'
        WRITE(072,109) runseed,'run seed'
        WRITE(072,109) nstart,'time to start with'
        WRITE(072,109) ntotstep,'number of timesteps'
        WRITE(072,119) temper,'temperature'
        WRITE(072,109) ncorrel,'points for the log scale'
        WRITE(072,109) ndiv,'number of bumps'
        WRITE(072,109) nspin,'spins per line'
        WRITE(072,119) quenchtemp,'temperature of the quench'
        WRITE(072,129) 'mean: j0=-1'
        WRITE(072,129) 'variance: dj=1'
        WRITE(072,109) setequil,'equilibrium flag'
        WRITE(072,109) setrand,'rng flag'
        WRITE(072,FMT='(a)') logfile
        WRITE(072,FMT='(a)') filout
        WRITE(072,FMT='(a)') final
      ENDIF

      WRITE(071,109) ns,'number of spins'
      WRITE(071,109) pstates,'number of states'
      WRITE(071,109) matseed,'matrix seed'
      WRITE(071,109) runseed,'run seed'
      WRITE(071,109) nstart,'time to start with'
      WRITE(071,109) ntotstep,'number of timesteps'
      WRITE(071,119) temper,'temperature'
      WRITE(071,109) ncorrel,'points for the log scale'
      WRITE(071,109) ndiv,'number of bumps'
      WRITE(071,109) nspin,'spins per line'
      WRITE(071,119) quenchtemp,'temperature of the quench'
      WRITE(071,129) ' mean: j0=-1.'
      WRITE(071,129) 'variance: dj=1'
      WRITE(071,109) setequil,'equilibrium flag'
      WRITE(071,109) setrand,'rng flag'
```

```
      WRITE(071,FMT='(a)') logfile
      WRITE(071,FMT='(a)') filout
      WRITE(071,FMT='(a)') final


C TIME-SCALE
c ----------

c compute the times at which the correlation functions are evaluated

      p=ncorrel
      p=p-1
      DO k=1,p
       cortim(k)=nint(dfloat(ntotstep)**(k/dfloat(p+1)))
      ENDDO
      cortim(1)=0
      k=2
      j=2
   20 IF( j .gt. p) goto 30
      IF( cortim(j) .ne. cortim(k) ) THEN
        k=k+1
        cortim(k)=cortim(j)
        j=j+1
      else
        j=j+1
      ENDIF
      goto 20

   30 IF( ncorrel .eq. 0 ) THEN
        ncorrelnew=0
      ELSE
        cortim(k+1)=ntotstep
        ncorrelnew=k+1
      ENDIF

      ncorr=ncorrelnew
      DO j=1,ndiv-1
       DO k=1,ncorrelnew
       IF (cortim(k)+j*ntotstep/ndiv.gt.ntotstep) goto 50
       ncorr=ncorr+1
       cortim(ncorr)=cortim(k)+j*ntotstep/ndiv
       ENDDO
 50    continue
      ENDDO

      DO k=1,ncorr
        WRITE(071,*) cortim(k)
      ENDDO


c INITIALIZATION
c --------------

c definition of: lattice; interactions; energy; temperature;
c
c N.B. : concerning the energy, engtot is ONLY the contribution due to
c---     the interactions among spins: then every other rescaling has
c        to be PROPERLY taken into account, both in the ENERGY and in
c        the TEMPERATURE.


c Some parameters

      convran=2.**(-32)*(1.d0-1.d-15)
      tstop=ntotstep/pstop
      logbump=ntotstep/pbump
      rescal=SQRT(j0**2+dj**2)
      conv=1.*pstates*rescal
      btemper=temper/conv            ! the rescaled temperature for
                                     ! the boltzmann weight

      CALL boltzw(btemper,boltzfct)


c Warming for the random number generator

      IF (setrand.ne.1) THEN
        CALL firstran(runseed)
        DO k=1,1000
          CALL ransi(nmax)
          DO i=1,2*ns
            waste=irn(i)
          ENDDO
        ENDDO
      ENDIF

c Initialization of the buffers for the output

      DO i=1,npartial
       time_v(i)=0
       simen_v(i)=0.
       DO j=1,ns
        partial(j,i)=0
       ENDDO
      ENDDO
```

```
c Initialization of the lattice
c Needed only for the equilibration run, NOT for the equilibrium
c run!

      IF (setequil.EQ.0.and.setrand.NE.1.and.quenchtemp.GT.100.) THEN
        DO i=1,ns
          stateall(i)=0
        ENDDO
        CALL ransi(nmax)
        DO i=1,ns
          stateall(i)=(irn(i)*convran+.5)*pstates
        ENDDO
      ENDIF

c energy of the first configuration

      CALL totaleng(stateall,neigh,coupling,engtot,totbond)
      print*,totbond


c STEP NUMBER ZERO
c ----------------

c writing down the step number 0!

      t=nstart
c      ensim=conv*(engtot)/ns   !  <----------------------definition of
      ensim=(conv*(engtot)+rescal*totbond)/ns
                               !                        the hamiltonian
      IF (nstart.eq.0) THEN
        WRITE(071,*) t,ensim,stateall(1),stateall(2)
        IF (setequil.eq.1) THEN
          WRITE(072,*) t,ensim
          IF (qlines.ne.0) THEN
            WRITE(072,139) ((stateall(i),i=(k-1)*nspin+1,k*nspin),8888
     &                     k=1,qlines)
          ENDIF
          IF (rlines.NE.0) THEN
            WRITE(072,139) (stateall(i), i=qlines*nspin+1,ns)
          ENDIF
        ENDIF
      ENDIF


c The CORE of the program: HEAT ALGORITHM
c -----------------------------------------

      ensim=0.

      DO t=nstart+1,ntotstep        ! single monte carlo sweep:
                                    ! ns spin updated
        CALL ransi(nmax)
        DO i=1,2*ns,2
          touse(i)=irn(i)*convran+0.5
          touse(i+1)=(irn(i+1)*convran+.5)*ns+1
        ENDDO

        DO ks=1,2*ns,2                    ! single random spin flip
          comp=touse(ks)
          jran=touse(ks+1)
          sold=stateall(jran)
          DO j=1,pstates
            ehb(j)=7
          ENDDO
          DO i=1,6
            snew=stateall(neigh(i,jran))
            ehb(snew+1)=ehb(snew+1)-coupling(i,jran)
          ENDDO
          normprob=0.
          DO i=1,pstates
            probhb(i)=boltzfct(ehb(i))
            normprob=normprob+probhb(i)
          ENDDO
          normprob=1./normprob
          cumul=0.
          DO i=1,pstates
            cumul=cumul+probhb(i)*normprob
            IF (comp.LE.cumul) THEN
              stateall(jran)=i-1
              GOTO 8888
            ENDIF
          ENDDO
          CONTINUE
          engtot=engtot-ehb(sold+1)+ehb(stateall(jran)+1)
        ENDDO

c pay attention to the definition of the hamiltonian; in
c particular the role of the multiplicative constants
        ensim=(conv*(engtot)+rescal*totbond)/ns

c writing down something:

c a): the configurations buffered

        IF (mod(t,logbump).EQ.0) THEN
          WRITE(071,*) t,ensim,stateall(1),stateall(2)
```

```
          CALL FLUSH(071)
        ENDIF

        IF (setequil.EQ.1) THEN
          DO j=1,ncorr
            IF (t.EQ.cortim(j)) THEN
              pcount=pcount+1
              time_v(pcount)=t
              simen_v(pcount)=ensim
              DO k=1,ns
                partial(k,pcount)=stateall(k)
              ENDDO
            ENDIF
          ENDDO
          IF (pcount.GE.(npartial-ndiv).AND.pcount.LE.npartial) THEN
            ncrit=1
          ENDIF
          IF (ncrit.EQ.1.OR.t.EQ.ntotstep.OR.MOD(t,tstop).EQ.0) THEN
            DO jj=1,pcount
              WRITE(072,*) time_v(jj),simen_v(jj)
              IF (qlines.ne.0) THEN
                WRITE(072,139) ((partial(i,jj),
     &             i=(k-1)*nspin+1,k*nspin), k=1,qlines)
              ENDIF
              IF (rlines.NE.0) THEN
                WRITE(072,139) (partial(i,jj), i=qlines*nspin+1,ns)
              ENDIF
              CALL flush(072)
            ENDDO
            DO i=1,npartial
              time_v(i)=0
              simen_v(i)=0.
              DO j=1,ns
                partial(j,i)=0
              ENDDO
            ENDDO
            pcount=0
            ncrit=0
          ENDIF
        ENDIF

      ENDDO                         ! end of the MC sweep

c
c RESTART FILE
c ------------
c if this is an equilibration run, there is the need to supply a new
c  (restart) file, in order to start the simulation at equilibrium

        IF (setequil.eq.0) THEN
          OPEN(074,file=final)
            WRITE(074,109) matseed, 'matrix seed'
            WRITE(074,109) runseed+3000, 'run seed'
            WRITE(074,109) 0,'time to start with'
            WRITE(074,109) ntotstep, 'number of timesteps'
            WRITE(074,119) temper, 'temperature'
            WRITE(074,109) ncorrel,'points for the log scale'
            WRITE(074,109) ndiv,'number of bumps'
            WRITE(074,109) nspin,'spins per line'
            WRITE(074,119) quenchtemp,'temperature of the quench'
            WRITE(074,129) ' mean: j0=-1'
            WRITE(074,129) 'variance: dj=1./sqrt(ns-1.)'
            WRITE(074,109) setequil+1, 'equilibrium flag'
            WRITE(074,109) 0,'rng flag'
            WRITE(074,129) outlog
            WRITE(074,129) outfile
            WRITE(074,129) status
            WRITE(074,*) 'no need for a final file'

            IF (qlines.ne.0) THEN
              WRITE(074,139) ((stateall(i),i=(k-1)*nspin+1,k*nspin),
     &         k=1,qlines)
            ENDIF
            IF (rlines.NE.0) THEN
              WRITE(074,139) (stateall(i), i=qlines*nspin+1,ns)
            ENDIF
            CALL flush(074)
          CLOSE(074)
        ENDIF

        IF (setequil.eq.1) THEN
          CLOSE(072)
        ENDIF
        CLOSE(071)



c The various formats
c -------------------

109   FORMAT(I8,1x,A30)
119   FORMAT(f10.6,1x,A30)
129   FORMAT(A40)
139   FORMAT(100I1)

      END
```

```
c Creation of a 3D simple cubic lattice with periodic boundaries
      SUBROUTINE lat3d(neigh)
c     ----------------------
c Description: the subroutine defines the topology of the lattice;
c              the current implementation gives a 3D simple cubic
c              lattice with periodic boundary conditions.
c Output: a two-dimensional array; the column number corresponds to
c         the lattice point, and the various elements of each column
c         (that is the various lines) define the neighbours of that
c         point.
c
c History:
c Version   Date       Comment
c -------   ----       -------
c 1.0       25-10-00   Original code  C.B.
c
c Declarations
      IMPLICIT NONE
      INTEGER*4 boxlenght,ns,dim        ! lattice's dimensions
      PARAMETER (dim=3)
      PARAMETER (boxlenght=16)
      PARAMETER (ns=boxlenght**3)
      INTEGER*4 neigh(2*dim,ns)         ! neighbours' list
      INTEGER*4 nx,ny,nz,px,py,pz
      INTEGER*4 spinposit,i,j

c variables initialization
      DO i=1,ns
        DO j=1,2*dim
          neigh(j,i)=0
        ENDDO
      ENDDO

c construction of the lattice: list of nearest neighbours

      DO nz=1,boxlenght
        pz=nz-1
        DO ny=1,boxlenght
          py=ny-1
          DO nx=1,boxlenght
            px=nx
            spinposit=px+py*boxlenght+pz*boxlenght**2
            IF (nx.ne.1) THEN
              neigh(1,spinposit)
     &        =px-1+py*boxlenght+pz*boxlenght**2
            ELSE
              neigh(1,spinposit)
     &        =boxlenght+py*boxlenght+pz*boxlenght**2
            ENDIF
            IF (nx.ne.boxlenght) THEN
              neigh(2,spinposit)
     &        =px+1+py*boxlenght+pz*boxlenght**2
            ELSE
              neigh(2,spinposit)
     &        =1+py*boxlenght+pz*boxlenght**2
            ENDIF
            IF (ny.ne.1) THEN
              neigh(3,spinposit)
     &        =px+(py-1)*boxlenght+pz*boxlenght**2
            ELSE
               neigh(3,spinposit)
     &        =px+(boxlenght-1)*boxlenght+pz*boxlenght**2
            ENDIF
            IF (ny.ne.boxlenght) THEN
              neigh(4,spinposit)
     &        =px+(py+1)*boxlenght+pz*boxlenght**2
            ELSE
               neigh(4,spinposit)
     &        =px+0*boxlenght+pz*boxlenght**2
            ENDIF
            IF (nz.ne.1) THEN
              neigh(5,spinposit)
     &        =px+py*boxlenght+(pz-1)*boxlenght**2
            ELSE
               neigh(5,spinposit)
     &        =px+py*boxlenght+(boxlenght-1)*boxlenght**2
            ENDIF
            IF (nz.ne.boxlenght) THEN
              neigh(6,spinposit)
     &        =px+py*boxlenght+(pz+1)*boxlenght**2
            ELSE
               neigh(6,spinposit)
     &        =px+py*boxlenght+0*boxlenght**2
            ENDIF
          ENDDO
        ENDDO
      ENDDO

      RETURN
      END


c Definition of the interactions among nearest neighbors
```

```
      SUBROUTINE coupl3d(neigh,coupling,matseed,j0,dj)
c     ----------------------------------------
c Description: the subroutine defines the interactions among nearest
c              neighbors; this interactions are symmetric.
c              for the present model, the interactions are taken from
c              a bimodal distributions
c
c Input : a two dimensional array containing the list of nearest
c         neighbours;
c Output: the array containing information about the interactions.
c
c History:
c Version   Date       Comment
c -------   ----       -------
c 0.1       02-10-00   starting code  C.B.
c
c Declarations
      IMPLICIT NONE
      INTEGER*4 boxlenght,ns,dim,nmax   ! lattice's dimensions
      PARAMETER (dim=3)
      PARAMETER (boxlenght=16)
      PARAMETER (ns=boxlenght**3)
      PARAMETER (nmax=2*ns)
      INTEGER*4 neigh(2*dim,ns)         ! neighbors
      INTEGER*4 coupling(2*dim,ns)      ! interactions
      INTEGER*4 i,j,k,symm,check
      INTEGER*4 count,jint
      REAL*8 jrea,concentr,waste,convran
      REAL*8 j0,dj,rescal

      INTEGER*4 irn(nmax),matseed ! random numbers

      INTEGER len1,len2,ifd1,ifd2         ! this part is in
      INTEGER ipnt1,ipnt2,ipnf1,ipnf2     ! common with the
      PARAMETER (len1=9689,ifd1=471)      ! random number
      PARAMETER (len2=127,ifd2=30)        ! generator
      INTEGER*2 inxt1(len1)               !
      INTEGER*2 inxt2(len2)               !
      INTEGER*4 ir1(len1)                 !
      INTEGER*4 ir2(len2)                 !

      COMMON /nran/irn
      COMMON /rantool/ipnt1,ipnf1,ipnt2,ipnf2,inxt1,inxt2,ir1,ir2

c concentration now equal 1/2

      rescal=SQRT(j0**2+dj**2)
      concentr=(1.+j0/rescal)*0.5

 c a first dumb initialization, to have a better control later
       DO i=1,ns
         DO j=1,2*dim
           coupling(j,i)=1111
         ENDDO
       ENDDO
.c random number generator: warming up

       convran=2.**(-32)*(1.d0-1.d-15)
       CALL firstran(matseed)
       DO k=1,1000
        CALL ransi(nmax)
        CALL ransi(nmax/2)
        DO i=1,2*ns
         waste=irn(i)
        ENDDO
       ENDDO

 c now the interactions; a check of self-consistency is included;
 c here we have p=3, so +1 and -1 have the same probability

       DO i=1,ns
         CALL ransi(2*dim)
         count=0
         DO j=1,2*dim
           count=count+1
           jrea=irn(count)*convran+0.5
           IF (jrea.LT.concentr) THEN
             jint=1
           ELSE
             jint=-1
           ENDIF
           IF (coupling(j,i).EQ.1111) THEN
             coupling(j,i)=jint
             symm=neigh(j,i)
             DO k=1,2*dim
               IF (coupling(k,symm).EQ.1111) THEN
                 IF (neigh(k,symm).EQ.i) THEN
                   coupling(k,symm)=coupling(j,i)
                   check=1
                 ENDIF
               ELSE
                 check=1
               ENDIF
             ENDDO
```

```
            IF (check.EQ.0) THEN
              print*,'a problem with the n.n. list: the program stops'
              STOP
            ENDIF
          ENDIF
        ENDDO
      ENDDO

      RETURN
      END


c Definition of the botzmann factors for acceptance rates
      SUBROUTINE boltzw(temper,boltzfct)
c     ---------------------------------
c Description: the subroutine defines  the boltzmann factors that
c               depend on energy difference and temperature; this
c               routine works ONLY for plus/minus J interactions;
c               it needs as input the temperature (or a rescaled
c               temperature, depending on the definition of the
c               Hamiltonian and on the value of J; by default J=1,
c               so every other value must be included in a rescaled
c               temperature; it is valid ONLY for Potts models,
c               in which we have delta-like interactions.
c
c Input : the (rescaled) temperature temper
c Output: the array boltzfct containing the boltzmann weight for the
c         various energy difference; to the i-th element corresponds
c         the energy difference (i-2*dim-1) (with dim=3).
c
c History:
c Version   Date       Comment
c -------   ----       -------
c 1.0       04-10-00   working code   C.B.
c
c Declarations
      IMPLICIT NONE
      INTEGER*4 dim
      PARAMETER (dim=3)
      INTEGER*4 i
      REAL*8 boltzfct(4*dim+1)
      REAL*8 temper,invtemp,fact


      IF (temper.eq.0.) THEN
        print*,'the temperature is zero; the program stops'
        STOP
      ENDIF
      DO i=1,4*dim+1
         boltzfct(i)=0.
      ENDDO

      invtemp=1./temper
      DO i=1,4*dim+1
        fact=(i-2*dim-1)*invtemp
        boltzfct(i)=exp(-fact)
      ENDDO


      RETURN
      END


c Calculation of the total energy of a given configuration
      SUBROUTINE totaleng(stateall,neigh,coupling,engtot,totbond)
c     ----------------------------------------------------------
c Description: the subroutine calculates the total energy of the
c              spin configuration.
c engtot=-\sum_{<i,j>} (J_{ij}\delta_{\s_i,s_j})
c totbond=\sum_{<i,j>} (J_{ij})
c
c Input : stateall (=configuration), neigh (=n.n. list), coupling
c         (=interactions), the sum of
c Output: engtot (=the total energy)
c
c History:
c Version   Date       Comment
c -------   ----       -------
c 1.0       04-10-00   working code   C.B.
c
c Declarations
      IMPLICIT NONE

      INTEGER*4 boxlenght,ns,dim        ! lattice's dimensions
      INTEGER*4 nnnumber
      PARAMETER (dim=3,nnnumber=2*dim)
      PARAMETER (boxlenght=16)
      PARAMETER (ns=boxlenght**3)
      INTEGER*4 neigh(nnnumber,ns)      ! neighbors
      INTEGER*4 coupling(nnnumber,ns)   ! interactions
      INTEGER*4 stateall(ns)            ! configuration
      INTEGER*4 engtot,i,j,totbond

      totbond=0
      engtot=0
```

```
      DO i=1,ns
        DO j=1,nnnumber
          IF (stateall(i).eq.stateall(neigh(j,i))) THEN
            engtot=engtot-coupling(j,i)
          ENDIF
          totbond=totbond+coupling(j,i)
        ENDDO
      ENDDO

c Since I considered all the spin, I must divide by two

      engtot=engtot/2
      totbond=totbond/2

      RETURN
      END


c Random number generator: initialization
      SUBROUTINE firstran(iseed)
c     -------------------------
c setup for the random number generator
c sequential version
c shift register random generator with very long period
      implicit REAL*8 (a-h,o-z)

      save
      PARAMETER (mult=32781)
      PARAMETER (mod2=2796203,mul2=125)
c     PARAMETER (two=2d0,tm32=two**(-32))
      PARAMETER (len1=9689,ifd1=471)
      PARAMETER (len2=127,ifd2=30)
      INTEGER*2 inxt1(len1)
      INTEGER*2 inxt2(len2)
      INTEGER*4 ir1(len1)
      INTEGER*4 ir2(len2)
      INTEGER*4 ns,nmax
      PARAMETER (ns=4096,nmax=2*ns)
      INTEGER*4 irn(nmax)
c      PARAMETER (mxnx=500,mxny=500)
c      PARAMETER (mxsp=mxnx*mxny)
c      PARAMETER (mxrn=16*mxsp+1024)

c      INTEGER*4 iseed

      COMMON /nran/irn
      COMMON /rantool/ipnt1,ipnf1,ipnt2,ipnf2,inxt1,inxt2,ir1,ir2
      k=3**18+2*iseed
      k1=1313131*iseed
      k1=k1-(k1/mod2)*mod2
      DO i=1,len1
         k=k*mult
         k1=k1*mul2
         k1=k1-(k1/mod2)*mod2
         ir1(i)=k+k1*8193
c        write(6,*)i,k,k1,ir1(i)
      ENDDO
      DO i=1,len2
         k=k*mult
         k1=k1*mul2
         k1=k1-(k1/mod2)*mod2
         ir2(i)=k+k1*4099
c        write(6,*)i,k,k1,ir1(i)
      ENDDO
      DO i=1,len1
         inxt1(i)=i+1
      ENDDO
      inxt1(len1)=1
      ipnt1=1
      ipnf1=ifd1+1
      DO i=1,len2
         inxt2(i)=i+1
      ENDDO
      inxt2(len2)=1
      ipnt2=1
      ipnf2=ifd2+1
      return
      END


c Random number generator: production
      SUBROUTINE ransi(n)
c     -------------------
c random number generator
c sequential version
c shift register random generator with very long period
      implicit REAL*8 (a-h,o-z)
      save
      PARAMETER (mult=32781)
      PARAMETER (mod2=2796203,mul2=125)
c     PARAMETER (two=2d0,tm32=two**(-32))
      PARAMETER (len1=9689,ifd1=471)
      PARAMETER (len2=127,ifd2=30)
      INTEGER*2 inxt1(len1)
      INTEGER*2 inxt2(len2)
```

```
      INTEGER*4 ir1(len1)
      INTEGER*4 ir2(len2)
      INTEGER*4 ns,nmax,n
      PARAMETER (ns=4096,nmax=2*ns)
      INTEGER*4 irn(nmax)

c      PARAMETER (mxnx=500,mxny=500)
c      PARAMETER (mxsp=mxnx*mxny)
c      PARAMETER (mxrn=16*mxsp+1024)
      COMMON /nran/irn
      COMMON /rantool/ipnt1,ipnf1,ipnt2,ipnf2,inxt1,inxt2,ir1,ir2

c     calculate n random numbers
      DO i=1,n
         l=ieor(ir1(ipnt1),ir1(ipnf1))
         k=ieor(ir2(ipnt2),ir2(ipnf2))
c        write(6,*) i,ipnt1,ipnt2,l,k,ieor(k,l)
         irn(i)=ieor(k,l)
         ir1(ipnt1)=l
         ipnt1=inxt1(ipnt1)
         ipnf1=inxt1(ipnf1)
         ir2(ipnt2)=k
         ipnt2=inxt2(ipnt2)
         ipnf2=inxt2(ipnf2)
      ENDDO
      return

      END
```

# Bibliography


Adam, G. and Gibbs, J. H. (1965). On the temperature dependence of cooperative relaxation properties in glass-forming liquids. *J. Chem. Phys.*, 43:139–146.

Aizenmann, M. and Wehr, J. (1989). Rounding of first-order phase transitions in systems with quenched disorder. *Phys. Rev. Lett.*, 62:2503–2506.

Ballesteros, H. G., Cruz, A., Fernández, L. A., Martin-Mayor, V., Pech, J., Ruiz-Lorenzo, J. J., Tarancón, A., Téllez, P., Ullod, C. L., and Ungil, C. (2000). Critical behavior of the three-dimensional Ising spin glass. *Phys. Rev. B*, 62:14237–14245.

Barrat, A. and Zecchina, R. (1999). Time scale separation and heterogeneous off-equilibrium dynamics in spin models over random graphs. *Phys. Rev. E*, 59:R1299.

Baxter, R. J. (1982). Magnetisation discontinuity of the two-dimensional Potts model. *J. Phys. A*, 15:3329.

Benyoussef, A. and Loulidi, M. (1996). Short-range Potts spin-glass model:renormalization group method. *Phys. Rev. B*, 53:8215–8218.

Bhatt, R. N. and Young, A. P. (1988). Numerical studies of Ising spin glasses in two, three, and four dimensions. *Phys. Rev. B*, 37:5606–5614.

Bhatt, R. N. and Young, A. P. (1992). A new method for studying the dynamics of spin glasses. *Europhys. Lett.*, 20:59–64.

Billoire, A. and Marinari, E. (2001). Correlation time scales in the Sherrington-Kirkpatrick model. *J. Phys. A*, 34:L727–L734.

Binder, K. (1981). Finite size scaling analysis of Ising model block distribution functions. *Z. Phys. B*, 43:119–140.

Binder, K. (1992). Finite size effects at phase transitions. In Gausterer, H. and Lang, C. B., editors, *Computational methods in Field Theory*, pages 59–125. Springer-Verlag, Berlin.

Binder, K., Baschnagel, J., Kob, W., and Paul, W. (1999). Glass physics: still not transparent. *Physics World*, 12:54.

Binder, K. and Reger, J. D. (1992). Theory of orientational glasses: Models, concepts, simulations. *Adv. Phys.*, 41:547–627.

Binder, K. and Young, A. P. (1986). Spin glasses: Experimental facts, theoretical concepts, and open questions. *Rev. Mod. Phys.*, 58:801–976.

Blöte, H. W. J., Luijten, E., and Heringa, J. R. (1995). Ising universality in three dimensions: a Monte Carlo study. *Journal of Physics A: Mathematical and General*, 28:6289–6313.

Brout, R. (1959). Statistical mechanical theory of a random ferromagnetic system. *Phys. Rev.*, 115:824–835.

Cardy, J. (1996). *Scaling and Renormalization in Statistical Physics*. Cambridge University Press, Cambridge.

Chen, J.-H. and Lubensky, T. C. (1977). Mean field and $\epsilon$-expansion study of spin glasses. *Phys. Rev. B*, 16:2106–2114.

Crisanti, A., Horner, H., and Sommers, H.-J. (1993). The spherical $p$-spin interaction spin glass model: The dynamics. *Z. Phys. B*, 92:257–271.

Crisanti, A., Marinari, E., Ritort, F., and Rocco, A. (2001). A new method to compute the configurational entropy in spin glasses. preprint cond-mat/0105391.

Crisanti, A. and Ritort, F. (2000). Potential energy landscape of finite-size mean-field models for glasses. *Europhys. Lett.*, 51:147.

Crisanti, A. and Ritort, F. (2001). A real-space description of the glass transition based on heterogeneities and entropy barriers. preprint cond-mat/0102104.

Crisanti, A. and Sommers, H.-J. (1992). The spherical $p$-spin interaction spin glass model: The statics. *Z. Phys. B*, 87:341–354.

Cwilich, G. (1990). Mean-field theory and fluctuations in Potts spin glasses: II. *J. Phys. A*, 23:5029.

Cwilich, G. and Kirkpatrick, T. R. (1989). Mean-field theory and fluctuations in Potts spin glasses: I. *J. Phys. A*, 22:4971.

De Santis, E., Parisi, G., and Ritort, F. (1995). On the static and dynamical transition in the mean-field Potts glass. *J. Phys. A*, 28:3025–3041.

Debenedetti, P. G. (1996). *Metastable Liquids*. Princeton University Press, Princeton, New Jersey.

Dillmann, O., Janke, W., and Binder, K. (1998). Finite-size scaling in the *p*-state mean-field Potts glass: A Monte Carlo investigation. *J. Stat. Phys.*, 92:57–100.

Ediger, M. D. (2000). Spatially heterogeneous dynamics in supercooled liquids. *Ann. Rev. Phys. Chem.*, 51:99–128.

Edwards, S. F. and Anderson, P. W. (1975). Theory of spin glasses. *J. Phys. F.*, 5:965.

Elderfield, D. and Sherrington, D. (1983a). The curious case of the Potts spin glass. *J. Phys. C*, 16:L497–L503.

Elderfield, D. and Sherrington, D. (1983b). Novel non-ergodicity in the Potts spin glass. *J. Phys. C*, 16:L1169–L1175.

Erzan, A. and Lage, E. J. S. (1983). The infinite-ranged Potts spin glass model. *J. Phys. C*, 16:L555–L560.

Fisch, R. and Harris, A. B. (1977). Series study of a spin-glass model in continuous dimensionality. *Phys. Rev. Lett.*, 38:785–787.

Fischer, K. H. and Hertz, J. A. (1991). *Spin Glasses*. Cambridge University Press, Cambridge.

Franz, S. and Parisi, G. (2000). On non-linear susceptibilities in supercooled liquids. *J. Phys.: Condens. Matter*, 12:6335–6342.

Gardner, E. (1985). Spin glasses with $p$-spin interactions. *Nucl. Phys. B*, 257 [FS14]:747–765.

Gibbs, J. H. and DiMarzio, E. A. (1958). Nature of the glass transition and the glassy state. *J. Chem. Phys.*, 28:373–383.

Glotzer, S. C., Naeem, J., Lookman, T., MacIsaac, A. B., and Poole, P. H. (1998). Dynamical heterogeneity in the Ising spin glass. *Phys. Rev. E*, 57:7350–7353.

Goldbart, P. M. and Sherrington, D. (1985). Replica theory of the uniaxial quadrupolar glass. *J. Phys. C*, 18:1923–1940.

Goldschmidt, Y. Y. (1987). Dynamical relaxation in finite size systems. *Nucl. Phys. B*, 285 [FS19]:519–534.

Götze, W. (1989). Aspects of structural glass transitions. In Hansen, J. P., Levesque, D. L., and Zinn-Justin, J., editors, *Liquids, freezing and the glass transition*, page 287. North-Holland, Amsterdam.

Götze, W. (1999). Recent tests of the mode-coupling theory for glassy dynamics. *J. Phys.: Condens. Matter*, 11:A1–A45.

Grest, G. S., Anderson, M. P., and Srolovitz, D. J. (1988). Domain-growth kinetics for the q-state Potts model in two and three dimensions. *Phys. Rev. B*, 38:4752–4760.

Gross, D. J., Kanter, I., and Sompolinsky, H. (1985). Mean-field theory of the Potts glass. *Phys. Rev. Lett.*, 55:304–307.

Guerra, F. (1996). About the overlap distribution in mean field spin glass models. *Int. J. Mod. Phys. B*, 10:1675–1684.

Höchli, U. T., Knorr, K., and Loidl, A. (1990). Orientational glasses. *Adv. Phys.*, 39:405–615.

Hohenberg, P. C. and Halperin, B. I. (1977). Theory of dynamic critical phenomena. *Rev. Mod. Phys.*, 49:435.

Hukushima, K. and Kawamura, H. (2000). Replica-symmetry-breaking transitions in finite-size simulations. *Phys. Rev. E*, 62:3360.

Hukushima, K. and Nemoto, K. (1996). Exchange Monte Carlo method and application to spin glass simulations. *J. Phys. Soc. Jpn.*, 65:1604–1608.

Jäckle, J. (1986). Models of the glass transition. *Rep. Prog. Phys.*, 49:171–231.

Kauzmann, W. (1948). The nature of the glassy state and the behavior of liquids at low temperatures. *Chem. Rev.*, 43:219–256.

Kawashima, N. and Young, A. P. (1996). Phase transition in the three-dimensional $\pm J$ Ising spin glass. *Phys. Rev. B*, 53:R484–R487.

Kirkpatrick, T. R. and Thirumalai, D. (1988). Mean-field soft-spin Potts glass model: Statics and dynamics. *Phys. Rev. B*, 37:5342.

Kirkpatrick, T. R. and Thirumalai, D. (1995). Are disordered spin glass models relevant for the structural glass problem? *Transp. Theory Stat. Phys.*, 24(6-8):927.

Kirkpatrick, T. R., Thirumalai, D., and Wolynes, P. G. (1989). Scaling concepts for the dynamics of viscous liquids near an ideal glassy state. *Phys. Rev. A*, 40:1045–1054.

Kirkpatrick, T. R. and Wolynes, P. G. (1987). Stable and metastable states in mean-field Potts and structural glasses. *Phys. Rev. B*, 36:8552–8564.

Kob, W. (1997). The mode-coupling theory of the glass transition. In Fourkas, J., Kivelson, D., Mohanty, U., and Nelson, K., editors, *Experimental and Theoretical Approaches to Supercooled Liquids: Advances and Novel Applications*, page 28. ACS Books, Washington.

Kob, W. (1999). Computer simulations of supercooled liquids and glasses. *J. Phys.: Condens. Matter*, 11:R85.

Kondor, I. (1989). On chaos in spin glasses. *J. Phys. A*, 22:L163.

Landau, D. P. and Binder, K. (2000). *A Guide to Monte Carlo Simulations in Statistical Physics*. Cambridge University Press, Cambridge.

Ma, S.-K. (1976). *Modern Theory of Critical Phenomena*. Addison-Wesley, Redwood City, California.

Mackenzie, N. D. and Young, A. P. (1983). Statics and dynamics of the infinite-range Ising spin glass model. *J. Phys. C*, 16:5321–5337.

Marinari, E. (1996). Optimized Monte Carlo methods. In Kertész, J. and Kondor, I., editors, *Advances in Computer Simulations*, pages 50–81. Springer.

Marinari, E., Naitza, C., Zuliani, F., Parisi, G., Picco, M., and Ritort, F. (1998a). General method to determine replica symmetry breaking transitions. *Phys. Rev. Lett.*, 81:1698.

Marinari, E., Parisi, G., and Ruiz-Lorenzo, J. J. (1998b). Numerical simulations of spin glass systems. In (Young, 1998), pages 59–98.

Metropolis, N., Rosenbluth, A. W., Rosenbluth, M. N., Teller, A. H., and Teller, E. (1953). Equation of state calculations by fast computing machines. *J. Chem. Phys.*, 21:1087–1092.

Mézard, M., Parisi, G., Sourlas, N., Toulouse, G., and Virasoro, M. (1984). Nature of the spin glass phase. *Phys. Rev. Lett.*, 52:1156–1159.

Mézard, M., Parisi, G., and Virasoro, M. (1987). *Spin glass theory and beyond*. World Scientific, Singapore.

Monasson, R. (1995). Structural glass transition and the entropy of the metastable states. *Phys. Rev. Lett.*, 75:2847–2850.

Morgenstern, I. and Binder, K. (1980). Magnetic correlations in two-dimensional spin-glasses. *Phys. Rev. B*, 22:288–303.

Newman, M. E. J. and Barkema, G. T. (1999). *Monte Carlo Methods in Statistical Physics*. Oxford University Press, Oxford.

Ogielski, A. T. (1985). Dynamics of three-dimensional Ising spin glasses in thermal equilibrium. *Phys. Rev. B*, 32:7384–7398.

Olson, T. and Young, A. P. (1999). Monte Carlo study of the critical behavior of random bond Potts models. *Phys. Rev. B*, 60:3428–3434.

Palmer, R. G. (1982). Broken ergodicity. *Adv. Phys.*, 31:669–735.

Palmer, R. G. (1983). Broken ergodicity in spin glasses. In van Hemmen, J. L. and Morgenstern, I., editors, *Heidelberg Colloquium on Spin Glasses*, pages 234–251. Springer-Verlag, Berlin.

Parisi, G. (1992). *Field theory, disorder and simulations*. World Scientific, Singapore.

Parisi, G., Ricci-Tersenghi, F., and Ruiz-Lorenzo, J. J. (1999). Generalized off-equilibrium fluctuation-dissipation relations in random Ising systems. *Eur. Phys. J. B*, 11:317–325.

Parisi, G., Ritort, F., and Slanina, F. (1993a). Critical finite-size corrections for the Sherrington-Kirkpatrick spin glass. *J. Phys. A*, 26:247–259.

Parisi, G., Ritort, F., and Slanina, F. (1993b). Several results on the finite-size corrections in the Sherrington-Kirkpatrick spin glass model. *J. Phys. A*, 26:3775–3789.

Peters, B. O., Dünveg, B., Binder, K., d'Onorio de Meo, M., and Vollmayr, K. (1996). Finite-size scaling in the $p$-state mean-field potts glass: exact statistical mechanics for small samples. *J. Phys. A*, 29:3503–3519.

Picco, M., Ritort, F., and Sales, M. (2001). Order-parameter fluctuations (OPF) in spin glasses: Monte Carlo simulations and exact results for small sizes. *Eur. Phys. J. B*, 19:565.

Poole, P. H., Glotzer, S. C., Coniglio, A., and Naeem, J. (1997). Emergence of fast local dynamics on cooling toward the Ising spin glass transition. *Phys. Rev. Lett.*, 78:3394.

Privman, V., editor (1990). *Finite Size Scaling and Numerical Simulations of Statistical Systems*. World Scientific, Singapore.

Reuhl, M., Nielaba, P., and Binder, K. (1998). Slowing down in the three-dimensional three-state Potts glass with nearest neighbor exchange $\pm$ J: a Monte Carlo study. *Eur. Phys. J. B*, 2:225–232.

Ricci-Tersenghi, F. and Zecchina, R. (2000). Glassy dynamics near zero temperature. *Phys. Rev. E*, 62:R7567–R7570.

Rieger, H. (1994). Monte Carlo studies of Ising spin glasses and random field systems. In Stauffer, D., editor, *Annual Review of Computational Physics II*, pages 295–341. World Scientific, Singapore.

Ritort, F. (1994). Static chaos and scaling behavior in the spin-glass phase. *Phys. Rev. B*, 50:6844–6853.

Scheucher, M. and Reger, J. D. (1993). Critical behaviour of short range Potts glasses. *Z. Phys. B*, 91:383–396.

Sherrington, D. and Kirkpatrick, S. (1975). Solvable model of a spin glass. *Phys. Rev. Lett.*, 35:104–108.

Sillescu, H. (1999). Heterogeneity at the glass transition: a review. *J. Noncryst. Solids*, 243:81–108.

Stanley, H. E. (1971). *Introduction to phase transitions and critical phenomena*. Oxford University Press, Oxford.

Stein, D. S., editor (1992). *Spin glasses and biology*. World Scientific, Singapore.

Stühn, T. (2000). Methoden zur Equilibrierung unterkülter Flüssigkeiten. Diplomarbeit, Johannes Gutenberg Universität, Mainz.

Thouless, D. J., Anderson, P. W., and Palmer, R. G. (1977). Solution of "Solvable model of a spin glass". *Phil. Mag.*, 35:593–601.

Vollmayr, K., Reger, J. D., Scheucher, M., and Binder, K. (1993). Finite size effects at thermally-driven first order phase transitions: a phenomenological theory of the order parameter distribution. *Z. Phys. B*, 91:113–125.

Wang, J.-S. (1999). Is the broad histogram random walk dynamics correct? *Eur. Phys. J. B*, 8:287–291.

Wansleben, S. and Landau, D. P. (1991). Monte carlo investigation of critical dynamics in the three-dimensional Ising model. *Phys. Rev. B*, 43:6006–6014.

Wiseman, S. and Domany, E. (1998). Self-averaging, distribution of pseudocritical temperatures, and finite size scaling in critical disordered systems. *Phys. Rev. E*, 58:2938–2951.

Wolfgardt, M., Baschnagel, J., Paul, W., and Binder, K. (1996). Entropy of glassy polymer melts: Comparison between Gibbs-DiMarzio theory and simulation. *Phys. Rev. E*, 54:1535–1543.

Wu, F. Y. (1982). The Potts model. *Rev. Mod. Phys.*, 54:235.

Yamamoto, R. and Kob, W. (2000). Replica-exchange molecular dynamics simulation for supercooled liquids. *Phys. Rev. E*, 61:5473.

Young, A. P. (1983). Direct determination of the probability distribution for the spin-glass order parameter. *Phys. Rev. Lett.*, 51:195–198.

Young, A. P., editor (1998). *Spin glasses and random fields*. World Scientific, Singapore.

Young, A. P. and Kirkpatrick, S. (1982). Low-temperature behavior of the infinite-range Ising spin-glass: exact statistical mechanics for small samples. *Phys. Rev. B*, 25:440–451.

Zia, R. K. P. and Wallace, D. J. (1975). Critical behaviour of the continuous *n*-component Potts model. *J. Phys. A*, 8:1495–1507.

Zippelius, A. (1984). Critical dynamics of spin glasses. *Phys. Rev. B*, 29:2717–2723.